UNIVERSITÀ DEGLI STUDI DI MILANO

PhD in Chemistry, XXIX cycle

Faculty of Pharmacy

Department of Pharmaceutical Sciences (DISFARM)

ENZYME INHIBITORS AS POTENTIAL ANTIPARASITIC AGENTS

Supervisor: Prof. Paola CONTI

Co-supervisor: Dr. Lucia TAMBORINI

PhD student:

Gregorio CULLIA

R10447

Academic year 2016-2017

CONTENTS

List of used acronims and abbreviations 3

1. Parasitic diseases 7

2. Scope of the thesis 8

3. Protozoan parasitic diseases 9

3.1 Malaria 9

3.1.1 Treatment of malaria [7] 10

3.1.2 Drug resistance [9] 14

3.2 Human African trypanosomiasis (HAT) 17

3.2.1 Treatment of HAT [12] [7] 17

4. Bacterial parasitic diseases 21

4.1 *Chlamydia trachomatis* 21

4.1.1 Treatment of *C. trachomatis* infections [7] 21

5. Enzymes as drug targets 24

5.1 Enzyme reaction mechanism 24

5.2 Enzyme inhibitors 26

5.2.1 Competitive inhibitors 26

5.2.2 Covalent inhibitors 27

5.2.3 Re-evaluation of covalent inhibitors 29

5.3 Beyond the target 31

6. Inhibitors of *Plasmodium falciparum* glyceraldehyde-3-phosphate dehydrogenase (*Pf*GAPDH) 33

6.1 *Pf*GAPDH as target 33

6.2 *Pf*GAPDH structure 35

6.3 The first *Pf*GAPDH selective inhibitors 35

6.4 A useful biochemical tool 45

7. Inhibitors of *Trypanosoma brucei* cathepsin L-like protease (*Tb*CatL or rhodesain) 47

7.1 The multiple roles of *Tb*CatL [46] [47] 47

7.2 Peptide inhibitors of *Tb*CatL 48

7.2.1 Aldehyde and ketone derivatives 48

7.2.2 Michael acceptor derivatives 48

7.2.3 Constrained heterocycle derivatives 49

7.2.4 Nitrile derivatives 49

7.3 Design and synthesis of 3-bromoisoxazoline inhibitors [48] 49

7.4 Biological evaluation 50

7.5 Discussion 51

8. Inhibitors of *Trypanosoma brucei* N^5,N^{10}-methylenetetrahydrofolate dehydrogenase/cyclohydrolase (*Tb*DHCH or *Tb*FolD) [49] 52
8.1 The crucial role of DHCH in *T. brucei* folate metabolism 52
8.2 Reassignment of LY374571 structure 54
8.3 Design and synthesis of analogues of (*S*)-156 56
8.4 Biological assays 57
8.5 *Tb*DHCH crystal structure and computational docking studies 58
8.6 Conclusions 59
9. Human lysophosphatidic acid acyl transferase (*h*LPAAT) inhibitors as new anti-*Chlamydia* agents 60
9.1 Correlation of *h*LPAAT inhibition and *C. trachomatis* growth inhibition [55] 60
9.2 Design and synthesis of new CI-976 analogues 62
9.3 Biological investigation 68
9.4 Discussion 69
10. Conclusions 70
11. Appendix 71
11.1 Enzyme inhibitors 71
11.1.1 Non-competitive inhibitors 71
11.1.2 Uncompetitive inhibitors 72
11.1.3 Slow and tight binding inhibitors 73
11.2 The Hill coefficient 74
12. Experimental procedures 75
12.1 Materials and methods 75
12.2 Chemistry 76
12.3 Biology 202
13. Acknowledgments 203
14. References 205

List of used acronims and abbreviations

3BP: 3-bromopyruvate

*p*ABA: *para*-aminobenzoic acid

ACAT: acyl-CoA:cholesterol acyl transferase

ACT: artemisinin-based combination theraphy

ADP: adenosine diphosphate

ATP: adenosine triphosphate

BBB: blood-brain barrier

BTK: Bruton's tyrosine kinase

CatB: cathepsin B

CatL: cathepsin L

CDMT: 2-chloro-4,6-dimethoxy-1,3,5-triazine

CL: cardiolipin

CoA: coenzyme A

*m*CPBA: *m*-chloroperbenzoic acid

CTP: cytidine triphosphate

CTPS: cytidine triphosphate synthetase

DAPI: 4',6-diamidino-2-phenylindole

DBF: dibromoformaldoxyme

DBU: 1,8-diazabicyclo[5.4.0]undec-7-ene

DCM: dichloromethane

DFMO: α-difluoromethyl ornithine

DHFR: dihydrofolate reductase

DHPS: dihydropteroateate synthase

DIPEA: *N*,*N*-diisopropylethylamine

DMAP: 4-(dimethylamino)pyridine

DMF: *N*,*N*-dimethylformamide

DMP: Dess-Martin periodinane

DMSO: dimethyl sulfoxide

DNA: deoxyribonucleic acid

DTNB: 5,5'-dithiobis(2-nitrobenzoic acid)

EC_{50}/ED_{50}: half maximal effective concentration/dose

EDC (or EDAC): *N*-(3-dimethylaminopropyl)-*N′*-ethylcarbodiimide hydrochloride

EGFR: epidermal growth factor receptor

FMT: formyl methionyl transferase

G3P: glycerol-3-phosphate

GAPDH: glyceraldehyde 3-phosphate dehydrogenase

GCC: glycine cleavage complex

g-HAT: gambiense HAT

GMS: Greater Mekong Subregion

H_2F: dihydrofolate

H_4F: tetrahydrofolate

HAT: human African Trypanosomiasis

*h*ERG: human ether-à-go-go-related gene

HMEC: human microvascular endothelial cell

HOBt: hydroxybenzotriazole

HPLC:high performance liquid chromatography

IC_{50}: half maximal inhibitory concentration

i.m.: intramuscolar

i.v.: intravenous

KHMDS: potassium bis(trimethylsilyl)amide

LDA: lithium diisopropylamide

LiHMDS: lithium bis(trimethylsilyl)amide

LPA: lysophosphatidic acid

LPAAT: lysophosphatidic acid:acyl-CoA acyl transferase

MCT: monocarboxylate transporter

N^5,N^{10}-CH_2-H_4F: N^5,N^{10}-methylenetetrahydrofolate

N^5,N^{10}-CH^+-H_4F: N^5,N^{10}-methenyltetrahydrofolate

N^{10}-CHO-H_4F: N^{10}-formyltetrahydrofolate

$NAD(P)^+$: nicotinamide adenine dinucleotide (phosphate), oxidized state

NAD(P)H: nicotinamide adenine dinucleotide (phosphate), reduced state

NMM: *N*-methylmorpholine

NMR: nuclear magnetic resonance

NOE: nuclear Overhauser effect

NSAIDs: nonsteroidal anti-inflammatory drugs

NTD: neglected tropical disease

ODC: ornithine decarboxylase

PBS: phosphate-buffered saline

PA: phosphatidic acid

PC: phosphatidylcholine

PD: pharmacodynamics

PDB: protein data bank

PDC: pyridinium dichromate

PE: phosphatidylethanolamine

PG: phosphatidylglycerol

PI: phosphatidylinositol

PK: pharmacokinetics

PS: phosphatidylserine

PTR-1: pteridine reductase-1

PTSA: *p*-toluensulfonic acid

r-HAT: rhodesiense HAT

RNA: ribonucleic acid

mRNA: messenger RNA

rRNA: ribosomal RNA

tRNA: transfer RNA

ROS: radical oxygen species

SEM: scanning electron microscope

SHMT: serine hydroxymethyl transferase

TAG: triacylglycerol

TEA: triethylamine

TFA: trifluoroacetic acid

THF: tetrahydrofuran

dTMP: deoxythymidine monophosphate

TMS: trimethylsilyl

TS: thymidilate synthase

dUMP: deoxyuridine monophosphate

VSGs: variant surface glycoproteins

WHO: World Health Organization

XRD: X-ray diffraction

1. Parasitic diseases

A parasitic disease is an infection caused by a parasite, "an organism which lives in or on another organism (its host) and benefits by deriving nutrients at the other's expense". [1]

Parasitic diseases may be really different between them. A common characteristic is that they are mostly diffused in the tropical and subtropical areas of the world, where hygienic conditions are often poor. In these regions, parassitosis have a tremendous impact on population life and economy. Some of these diseases can be found in developed countries as well, but they represent serious treats just in particular circumstances, such as in immunodepressed patients and in pregnant women. However, because of migration flows, severe diseases could spread over their usual borders too.

For an easier discussion about the problem, parasites are classified according to two different criteria. The first one is based on Cavalier-Smith's classification of living beings in the six kingdoms of *Bacteria*, *Chromista*, *Fungi*, *Plantae*, *Protozoa* and *Animalia*. [2] Human parasites are found within *Bacteria*, *Fungi*, *Protozoa* and *Animalia* and, in addition, viruses can be included in this list. In a different classification, parasites are divided in different groups according to their localization in the host's body. Parasites which reside outside the human body (such as lice and fleas) are referred to as ectoparasites, while the ones which establish or inside the human body, such as many invertebrates, are named endoparasites. Moreover, among endoparasites we can distinguish facultative (e.g. *Listeria monocytogenes*, *Legionella*, *Yersinia*) and obligate (e.g. *Toxoplasma gondii*, *Rickettsia*, viruses) intracellular parasites.

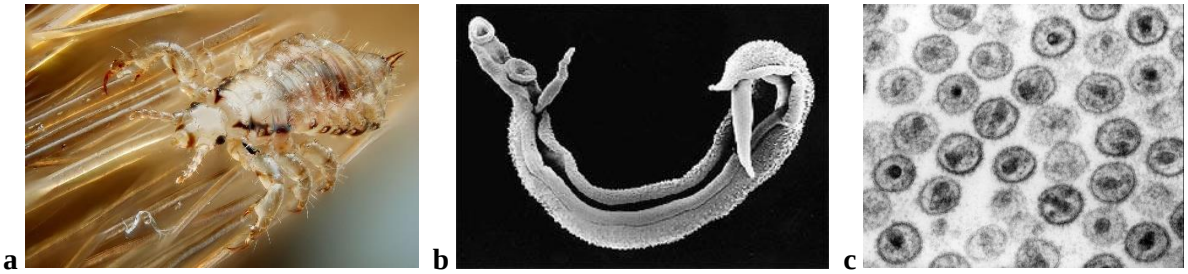

Figure 1. 1 Examples of parasites. **a.** Louse (Di Gilles San Martin - originally posted to Flickr as Male human head louse, CC BY-SA 2.0, https://commons.wikimedia.org/w/index.php?curid=11208622). **b.** SEM image of a male and female *Schistosoma mansoni* (http://www.cab.unimelb.edu.au/cab_schisto.htm) **c.** HIV-1 virions (http://emedicine.medscape.com/article/211316-overview).

The lack of systematic drug discovery programmes for these diseases in industries (for economic reasons) induced the World Healt Organization (WHO) to include some of these in the list of the Neglected Tropical Diseases (NTDs). [3]

2. Scope of the thesis

This work is related to the design and synthesis of new potential drugs for the treatment of parasitic diseases, mainly focusing on the protozoan infections. The development of agents for malaria and human African trypanosomiasis (HAT), two of the most prevalent protozoan parasitic diseases, represents the heart of this work. Enzymes have always been of primary interest in drug discovery, especially in the antimicrobial field. High druggability, ease of purification (which allows performing exhaustive structure-activity relationship studies) and chances for selective toxicity (due to the differences in enzyme isoforms or in metabolism) clearly explain their potential as pharmacological targets. Therefore, I selected crucial microbial enzymes to be exploited as new targets. During my PhD, I also spent ten months as visiting student at the Institute of Medical Sciences, University of Aberdeen, Scotland, under the supervion of Professor Matteo Zanda. Duting this period, my work concerned the development of new potential agents to treat *Chlamydia trachomatis* (an obliged intracellular bacterium) infections. The final goal of the present thesis is to describe drug-like molecules with a new mechanism of action and sufficiently active to prompt *in vivo* studies on animal models of the diseases.

3. Protozoan parasitic diseases

3.1 Malaria

Key points [4]

- Caused by 5 species of *Plasmodium*, transmitted by *Anopheles* mosquitoes;
- Mainly in sub-Saharan Africa but also in Asia, Latin America and Middle East;
- WHO estimates 214 million cases and 438000 deaths in 2015. Globally 3.2 billion people are at risk.

The parasite is transmitted to humans through the bites of female *Anopheles* mosquitoes (30 different species are major vectors) seeking for blood to nurture their eggs. *P. falciparum*, *P. vivax*, *P. malariae*, *P. ovale*, *P. knowlesi* are the agents of the diseases. The most important species are *P. falciparum*, the most prevalent in Africa and responsible for most malaria-related deaths globally, and *P. vivax*, diffused in other continents. After the injection, sporozoites reach host's liver. In the hepatocites they start dividing and differentiating into merozoites (an aploid form). Some species (*P. vivax* and *P. ovale*) also produce hypnozoites, a dormant form responsible of relapses after weeks or months. This first phase (pre-erythrocytic or hepatic stage) lasts for 5-16 days, then parasites enter in the bloodstream again and invade the erythrocytes (erythrocytic stage). Parasites undergo asexual replication differentiating in trophozoites and then in mature schizonts, which break releasing newly formed merozoites and starting a new cycle of infection (fig. 3.1). This stage is characterized by cyclic occurrence of flu-like symptoms every 24 hours (*P. knowlesi*), 48 hours (tertian fever, *P. falciparum*, *P. vivax* and *P. ovale*) or 72 hours (quartan fever, *P. malariae*). Some merzoites enter in the sexual cycle, developing in male and female gametocytes. When a mosquito bites an infected person it ingests the gametocytes. In the midgut, erythrocytes burst releasing gametocytes which mature in gametes that fuse to form diploid zygotes. Once differentiated in ookinetes, the parasites burrow in midgut wall and form oocysts. Aploid sporozoites are formed in the oocyst and relased upon burst (after 5-18 days). Sporozoites travel back to the salivary glands of the mosquito and the infection cycle starts again. [5]

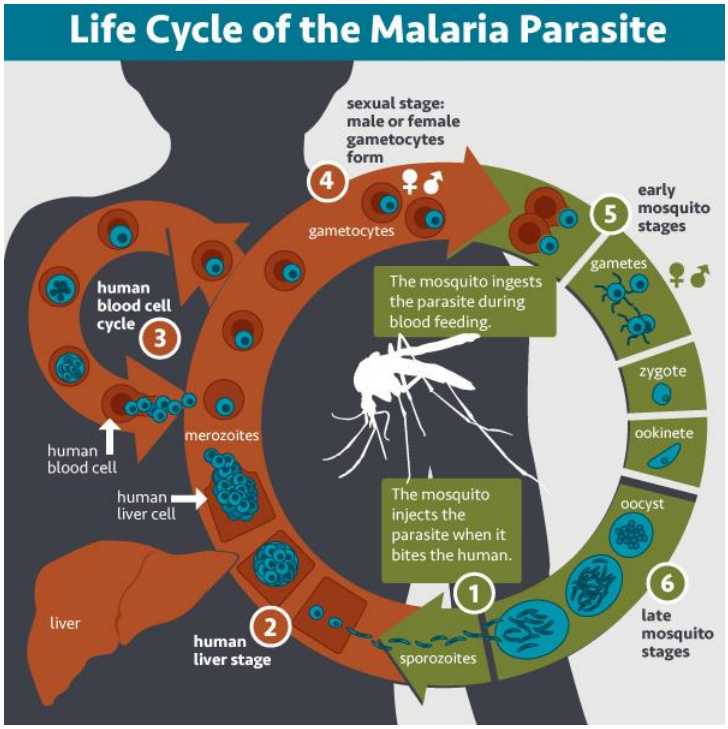

Figure 3. 1 Infection cycle of the malaria parasite (https://www.flickr.com/photos/niaid/20771605491).

As mentioned above, malaria is characterized by recurrent attacks, or paroxysms, including chills (along with headache, malaise, fatigue, muscular pain, occasional nausea, vomiting and diarrhoea) followed by fever and then sweating. While in *P. vivax* infections the person may feel well between attacks, in *P. falciparum* malaria the symptoms persist and, without treatment, death may occur. [6]

3.1.1 Treatment of malaria [7]

In July 2015 the European Medicines Agency expressed a positive opinion on the RTS,S/ASO1 malaria vaccine. However WHO underlined that further evaluations are needed prior to its wide introduction, and did not recommend its use in 6-12 week old children. [8] Hence, the treatment of malaria is still based on chemotheraphy.

Antimalarials are usually classified by their activity toward a specific stage of the parasite lifecycle, which will determine their potential application (prophylaxis versus acute treatment), and on their chemical structure. Because of a more homogeneous grouping, currently antimalarial drugs are here introduced in accordance with the second classification criterium.

Cinchona alkaloids

Quinine, derived from the bark of *Cinchona* tree, is the first known antimalarial. Its use was introduced in Europe in the seventeenth century by Spanish Jesuits returned from Peru, where Inca used cinchona bark to treat malaria. Quinine is a blood schizonticidal and, only for *P. vivax* and *P. malariae*, gametocydal as well. Its diastereoisomer, quinidine, is more potent and toxic. Three are the major adverse effects of quinine: cinchonism, a syndrome characterized by tinnitus, rashes, vertigo, nausea and vomiting, and abdominal pain; hypoglycaemia, caused by the stimulation of pancreatic β-cells; hypotension. Two peculiar toxic effects, probably due to direct neurotoxicity, are hearing and seeing impairments. Quinine has a short plasma half-life ($t_{1/2}$) that limits its use to acute treatments. Its major application is the parenteral treatment of chloroquine-resistant *P. falciparum* malaria.

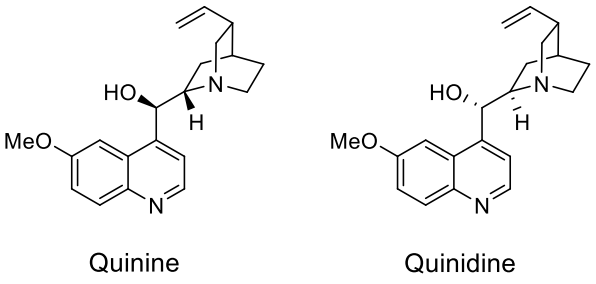

Figure 3. 2 Structures of quinine and quinidine.

9-Aminoacridines

Mepacrine, or quinacrine, was developed in 1934 as an analogue of 9-aminoacridine, which was known to possess antibacterial activity. This drug inspired the development of two other classes of quinolines, characterized by a similar structure.

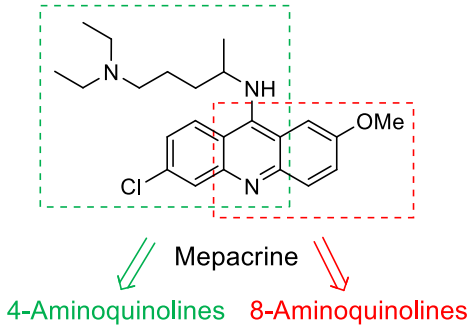

Figure 3. 3 Structure of mepacrine. The green and the red dashed boxes highlight the structural motives shared with 4-aminoquiinoline and 8-aminoquinoline antimalarials.

4-Aminoquinolines

Chloroquine is the main member of this class. It is the most potent derivative of the series and is usually considered a safe drug. Hydroxychloroquine is characterized by a better safety profile but is rarely used nowadays. As quinine, it is active toward circulating schizonts and gametocytes of *P. vivax*, *P. ovale* and *P. malariae*. Its toxicity is attributed the inhibition of heme aggregation, that leads to the presence of free and toxic heme in parasites, rather than DNA intercalation.

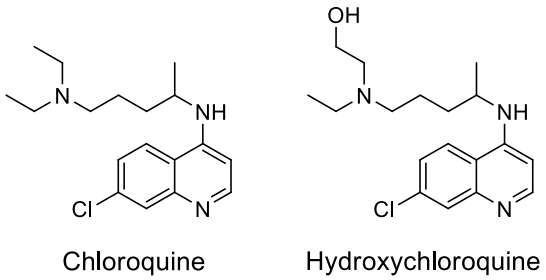

Figure 3. 4 Structures of chloroquine and of its derivative hydroxychloroquine.

8-Aminoquinolines

Pamaquine was introduced in 1926 but has been replaced by primaquine. This drug is a potent gametocydal for all the species of *Plasmodium* and acts towards the latent forms of *P. vivax* and *P. ovale* and the hepatic form of *P. falciparum*. It is believed that its action is related to the formation of radical oxygen species (ROS) via autoxidation of the 8-amino group. Primaquine is used to eradicate *P. vivax* and *P. ovale* infections, often in association with chloroquine. The drug is not given for long-term treatment due to potential toxicity and sensitization, which is common in people with glucose-6-phosphate dehydrogenase deficiency.

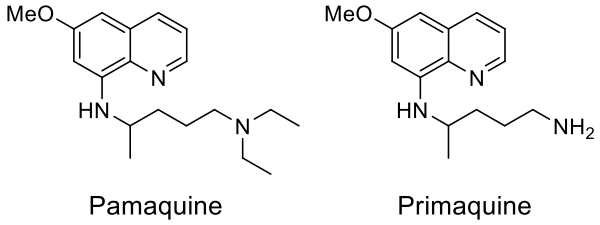

Figure 3. 5 Structures of pamaquine and primaquine.

Other quinolines derivatives

Mefloquine was synthesized with the idea of blocking metabolic sensible positions in quinine. It is used as prophylactic agent against *P. falciparum* and against chloroquine-resistant strains of *Plasmodium*. It is not effective toward the sexual forms of the parasites. High incidence of neuropsychiatric, gastrointestinal, dermatologic and cardiovascular side effects has been observed.

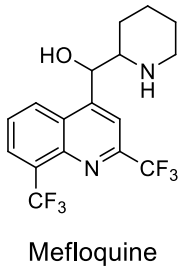

Figure 3. 6 Structure of mefloquine.

Halofantrine is a 9-phenanthrenemethanol derivative. It is effective against *P. falciparum*, also against chloroquine-resistant strains. Cross-resistance with mefloquine has been reported. CYP3A4 oxidizes the compound by *N*-dealkylation giving a more active compound, desbutylhalofantrine. The drug is not well absorbed but, because of side effects (gastrointestinal and cardiovascular), dosage must be limited.

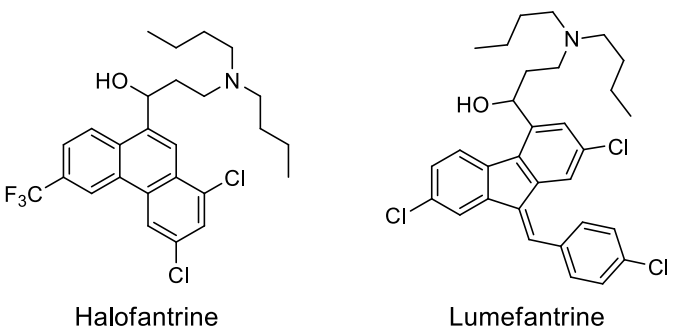

Figure 3. 7 Structures of halofantrine and lumefantrine.

Lumefantrine is a compound with a structure related to the one of halofantrine. It is used in combination with artemether to treat multi-resistant *P. falciparum* infections.

Pyrimidines/triazines

Pyrimethamine is a potent and selective *Plasmodium* dihydrofolate reductase (DHFR) inhibitor. The depletion of reduced cellular folates results in a slow blood schizonticidal action. Main toxic effects at therapeutic doses are occasional skin eruptions and haematopoiesis depression.

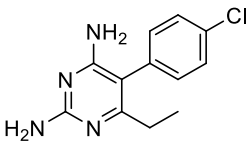

Pyrimethamine

Figure 3. 8 Structure of pyrimethamine.

Proguanil is a biguanide which is converted to cycloguanil (its active form) *in vivo*. This DHFR inhibitor is active against tissue and asexual blood forms of *P. falciparum* and *P. vivax* (but not toward hypnozoites). This drug has an optimal safety profile and, in contrast to pyrimethamine, can be administered during pregnancy.

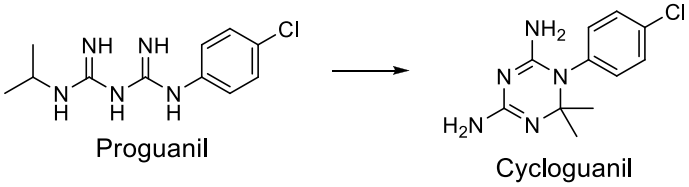

Proguanil Cycloguanil

Figure 3. 9 Structures of proguanil and of its active metabolite cycloguanil.

Sulfonamides and sulfones

Compounds of this class are inhibitors of dihydropteroate synthase (DHPS), an enzyme involved in the biosynthesis of folates. The success of this class of inhibitors is due to the fact that humans, in contrast to some microbes, do not possess the ability to synthesize folates. DHPS inhibitors compete with *p*-aminobenzoic acid (*p*ABA), one of the two substrates of the enzyme, blocking the synthesis of dihydropteroate or alternatively, they can be also incorporated in a false metabolite. Both the situations lead to blood schizonticidal effect, especially marked toward *P. falciparum*. Due to synergic mechanisms of action, these compounds are often co-administered with DHFR inhibitors (e.g. pyrimethamine and sulfadoxine, a long-acting sulfonamide) to treat malaria attacks.

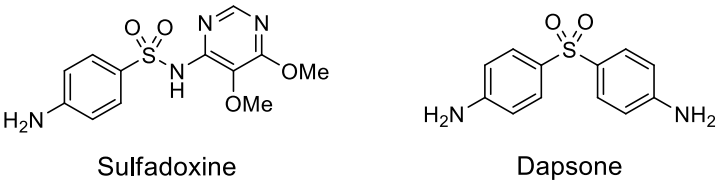

Sulfadoxine Dapsone

Figure 3. 10 Structures of sulfadoxine and dapsone.

Endoperoxides

Artemisinin has been isolated from the Chinese plant *Artemisia annua*. Synthetic and semisynthetic derivatives, with improved stability (artemether) and water solubility (artesunate), have also been developed. All these molecules are active in virtue of the presence of the endoperoxide group. It is believed that artemisinins are activated by the intervention of the heme iron resulting in the production of a free radical. This targets sarcoplasmic reticulum Ca^{2+}-ATPase (*Pf*ATP6) altering calcium stores and may also form covalent adducts to specific membrane associated proteins. These drugs are active on gametocytes and on the all the asexual stages of *Plasmodium*, with the exception of the primary or latent hepatic forms. For these reasons, and because of a short plasma $t_{1/2}$, artemisinins are not used in prophylaxis. In order to prevent development of resistance, these drugs are often administered in a combination therapy (artemisinin-based combination therapies, ACTs) with other drugs (e.g. artemether-lumefantrine, artesunate-amodiaquine, and artesunate-sulfadoxine-pyrimethamine).

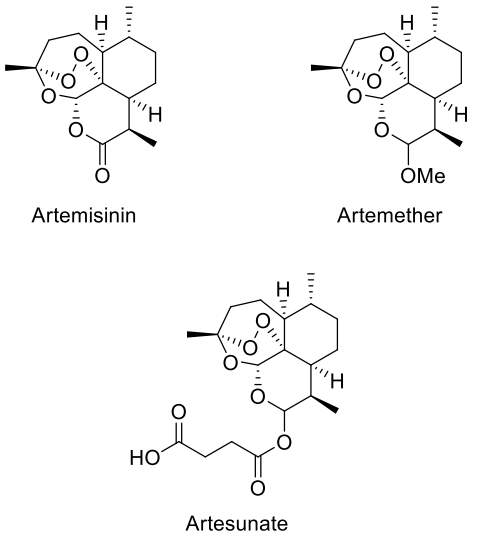

Figure 3. 11 Structures of artemisinin and of its derivatives artemether and artesunate.

Tetracyclines

Tetracycline and doxycycline, in particular, are used to treat quinine-resistant infections. They interact with the rRNA in the minor ribosomal subunit affecting protein synthesis. These drugs are effective toward hematic schizonts and tissue primary form of *P. falciparum* but with slow action. Toxicity limits their use: they can easily cause photosensitization reaction and they are not suitable for pregnant women and children.

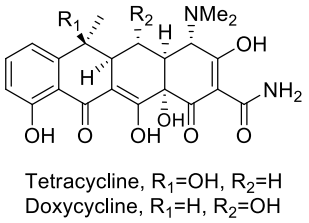

Figure 3. 12 Structures of tetracycline and doxycycline.

Naphthoquinones

Atovaquone is active toward hepatic forms of the parasites (but not toward the hypnozoites of *P. vivax*). Its action is based on the interference with the generation of mitochondrial membrane potential. It is usually administered together with proguanil in order to enhance efficacy.

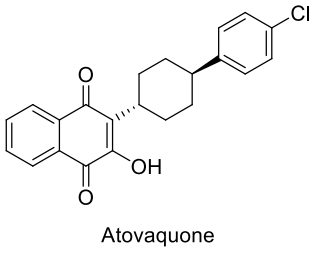

Figure 3. 13 Structure of atovaquone.

Currently, WHO recommends a 3 days ACT treatment (artemether-lumefantrine, artesunate-lumefantrine, artesunate-mefloquine, dihydroartemisinin-piperaquine, and artesunate-sulfadoxine-pyrimethamine) for uncomplicated *P. falciparum* malaria, except pregnant women in the first trimester (in this case a 7 days with quinine-clindamycin is suggested). When malaria is caused by other species, chloroquine can be used (if effective) alternatively to ACT. Primaquine should be used to prevent relapses of *P. vivax* or *P. ovale* but glyceraldehyde 6-phosphate dehydrogenase status must be carefully evaluated. In case of pregnancy or

breastfeeding, the use of chloroquine should be preferred. In the case of severe infection, artesunate should be administered i.v. or i.m. until the patient can tolerate oral medication (the parenteral treatment must last 24 hours, at least), at this point a 3 days treatment with ACT must complete the cycle. [11]

3.1.2 Drug resistance [9]

Resistance to antimalarials is a major problem at date. To have a general knowledge of the extension of the phenomenon, I here briefly report some of the data collected by WHO, focusing on the two major species of *Plasmodium*. For a detailed view, references and corresponding updates should be consulted.

Plasmodium falciparum

Monotherapy is no longer recommended, even for uncomplicated infections. Withdrawal of chloroquine has already started years ago. It presented high to extremely high treatment failure rate in all regions with the exception of Central America. Resistance diminished in some areas but there is still caution about worldwide reintroduction of this drug. Amodiaquine is more effective than chloroquine, despite cross-resistance. However, treatment failure rate is very high in South America, Middle East and Africa (slightly lower in Western Africa). It has been chosen as first-line drug in combination with artesunate; the efficacy of this combination was correlated with the efficacy of amodiaquine alone (where artesunate resistance is absent or low). Acting on the same metabolic pathway, the combination sulfadoxine-pyrimethamine is considered as a monotherapy. The failure rate is low in South America, Middle East and Central Asia but high in Africa (very high in Eastern Africa). Resistance rapidly develops and reduction in resistance has been rarely documented. The efficacy for the ACT, as for amodiaquine, is correlated with the efficacy of sulfadoxine-pyrimethamine alone. Because of low cost, long half-life and safety in pregnant women and children, this association is still used with success for intermittent preventive treatment, even in areas with moderate resistance. Mefloquine resistance was reported few years after its introduction at the Cambodia-Thailand border, probably because of an improper use (i.e. low doses). It still is a great concern in the Greater Mekong subregion (GMS), while low treatment failure rates have been reported in Africa and South America (even if mutations related to quinolones resistance have been detected in the parasite). The efficacy of quinine is not clear: it remains a second-line treatment (especially in association with other antibiotics) and its adverse effects appear in most of the patients. The association of atovaquone and pyrimethamine remains effective in different areas but, because of its cost, it remains limited to travellers from industrialized countries. Fatty food lowers the adsorption of atovaquone.

Plasmodium vivax

When ACTs are not used, chloroquine remains the drug of choice for *P. vivax* infections. Resistance is confirmed in South America, Southeast Asia and Ethiopia. Mefloquine is highly effective against chloroquine resistant infections. Pyrimethamine is only effective toward wild-type *P. vivax* and key mutations related to resistance have been found in many countries. *P. vivax* shows some degree of "innate resistance" to sulfadoxine. Primaquine is highly active toward hypnozoites. Despite several reports of resistance, the data are affected by many confounding factors and then must be interpreted with caution.

Resistance toward artemisinin and derivatives [10]

The importance of artemisinin could be perceived by the motivations for the conferment of the 2015 Nobel Prize in Physiology or Medicine to Youyou Tu, who firstly isolated the molecule:

"The Nobel Assembly at Karolinska Institutet has today decided to award the 2015 Nobel Prize in Physiology or Medicine with one half jointly to William C. Campbell and Satoshi Ōmura […] and the other half to Youyou Tu for her discoveries concerning a novel therapy against malaria. Diseases caused by parasites have plagued humankind for millennia and constitute a major global health problem. […] Youyou Tu discovered Artemisinin, a drug that has significantly reduced the mortality rates for patients suffering from malaria. These two discoveries have provided humankind with powerful new means to combat these debilitating diseases that affect hundreds of millions of people annually. The consequences in terms of improved human health and reduced suffering are immeasurable." [11]

Being such important drugs, the analysis of resistance to artemisinins deserve a separate discussion. Artemisinin resistance is defined as a delayed parasite clearance, and actually affects only ring-stage parasites. It is, shortly, a partial resistance and at the date no evidences of full resistance have emerged. Several non-synonymous mutations in the Kelch 13 (K13)-propeller domain were associated with delayed parasite clearance *in vitro* and *in vivo* and are currently monitored as marker for resistance. The success of ACTs therapy is however not compromised as long as the partner drug remains effective. The major concerns regard Southeast Asia, in particular the GMS, where resistant falciparum malaria have emerged independently in many areas (fig. 3.14). In Cambodia, the combination artesunate-mefloquine was reintroduced as first-line treatment in 2014 and gives a 100% success rate; in 2008 it was replaced by dihydroartemisinin-piperaquine but, because of high failure rates due to increasing piperaquine resistance, this last association was abandoned. In Lao, the association of artemether and lumefantrine is losing efficacy while in Myanmar a delayed clearance has been observed for the three major ACTs (artesunate-mefloquine, dihydroartemisinin-piperaquine, and artemether-lumefantrine). Dihydroartemisinin-piperaquine is currently used as first-line treatment in Thailand (artesunate-mefloquine and artemether-lumefantrine showed high failure rates) while resistance to the same ACT developed in Viet Nam. K13 mutations and delays in parasites clearance have been also observed in Africa and South America.

Figure 3. 14 Diffusion of artemisinins resistance in the GMS (http://apps.who.int/iris/bitstream/10665/250294/1/WHO-HTM-GMP-2016.11-eng.pdf?ua=1).

Humans are rapidly losing their position of strength against *Plasmodium* parasites. The forced selection conditions created and the inappropriate use of available drugs led to the appearance of stronger parasites that often require carefully therapy evaluation to provide a complete eradication. Keeping in mind the objective of this tough battle (the complete eradication of malaria), it is evident that we urgently need new agents to be used against these parasites, since the older ones are losing efficacy (if not already ineffective).

3.2 Human African trypanosomiasis (HAT)

Key points [12]

- Caused by two subspecies of *Trypanosoma brucei*, transmitted by *Glossina* flies (tsetse flies);
- Spread in 36 sub-Saharan Africa countries;
- 3796 cases recorded and 20000 estimated in 2014. 65 million people at risk.

T. brucei is transmitted to humans by the bites of tsetse flies which have acquired the parasite from infected human beings or animals. Two different forms may develop: *T. b. gambiense* causes western HAT (g-HAT), the chronic form (found in 24 countries of western and central Africa, 98% of the reported cases), while *T. b. rhodesiense* causes eastern HAT (r-HAT), the acute form (found in 13 countries of eastern and southern Africa, 2% of the reported cases). The subspecies *T. b. brucei* is only infectious to animals, causing Nagana disease, and is hence used for biological studies. Other ways of infection are possible: in particular, mother-to-child transmission, mechanical transmission through other blood-sucking insects and sexual transmission have been reported. Injected metacyclic trypomastigotes mature in bloodstream trypomastigotes and start dividing in subcutaneous tissues, blood and lymph. This is the haemo-lymphatic stage of the disease, characterized by headaches, itches, joint pains and bouts of fever, due to fluctuations of parasite levels in the blood. The immune system recognises *T. brucei* and destroys most of the cells. However, some of the parasites modify their variant surface glycoproteins (VSGs) and this allows them to escape the immune response. The ability of *T. brucei* of constantly evading the immune system renders the development of a vaccine for HAT impossible. A peculiar symptom of this phase of the disease is the Winterbottom's sign, which is due to tremendous swollen lymph nodes along the back of the neck. When the parasites invade the central nervous system, the neurological (or meningo-encephalic) phase begins. It is accompanied by more specific symptoms, like changes of behaviour, confusion, sensory disturbances and poor coordination, which make the disease to be commonly known as "sleeping sickness". In contrast to *Plasmodium* parasites, the life cycle of *T. brucei* is completely extracellular. When untreated, the infection invariantly ends with the death of the human host. In the case of r-HAT, the neurological phase develop early, compromising any possible intervention; this is the reason that underlies the little number of reported case of eastern HAT.

3.2.1 Treatment of HAT [12] [7]

The outcome of HAT treatment is strictly dependent on the moment of the diagnosis, with earlier treated patients having higher cure rate. Giving the different localization of the parasites during the two phases of the disease, drugs with different physicochemical properties are needed. In particular, the treatment of the neurological phase absolutely requires agents able to cross the blood-brain barrier (BBB). At the date, only five drugs are approved for the treatment of HAT, two (suramin and pentamidine) for the first stage, and three (melarsoprol, nifurtimox, eflornithine) for the second stage.

Suramin

This drug was developed by Bayer in 1920 and has been sold with the brand name Germanin. This molecule is a polisulfone naphtylamine, formulated as hexa sodium salt. The mechanism of action is still unknown but the negative charges of the molecule seem to be involved. The drug is administered through slow endovenous infusion to treat first stage *T. b. rhodesiense* infections. It presents serious adverse effects, in particular high neurotoxicity and nephrotoxicity. Asthenia, nausea and fatigue are common acute reactions while a more severe reaction, which leads to shock and loss of consciousness, is rarer.

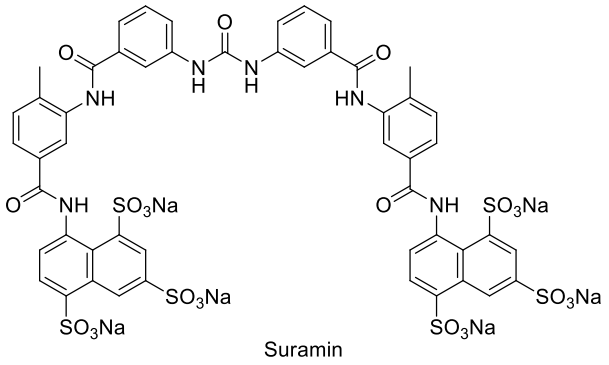

Figure 3. 15 Structure of suramin.

Pentamidine

This drug, developed in the 1930s, is mainly used for the treatment of first stage *T. b. gambiense* infection. The mechanism of action is still unclear but, after concentration in the cell (P2 transporter, among others, is involved), it may interact with negatively charged macromolecules leading to toxic effects. It is administered by intramuscular injections for 7 days. Due to high tissue distribution and high plasma $t_{1/2}$, pentamidine has been successfully employed in prophylaxis. It presents moderate toxicity: hypoglycemia and hypertension are common; nephrotoxicity and leukopenia have been also linked to its use.

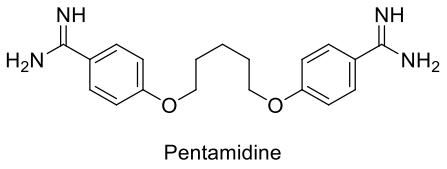

Figure 3. 16 Structure of pentamidine.

Melarsoprol

The story that led to this drug starts in the XIX century, when David Livingston observed the efficacy of Fowler's solution (1% aqueous KH_2AsO_4) in the treatment of HAT. Later, Friedheim, a Swiss chemist, synthesized melarsen, an organic form of As(V). Melarsen oxide, a reduced form of melarsen, showed higher activity and toxicity. Lastly, melarsen oxide was conjugated with the British anti-lewisite, an arsenic detoxifier, obtaining the pro-drug melarsoprol. This is the drug of choice for the treatment of neurological stage of r-HAT. It is rapidly metabolized in melarsen oxide. Its cellular effects are linked to the presence of the As, which causes inhibition of glycolysis and that forms covalent bonds with various cellular thiols. In addition, melarsen oxide is able to form an adduct with

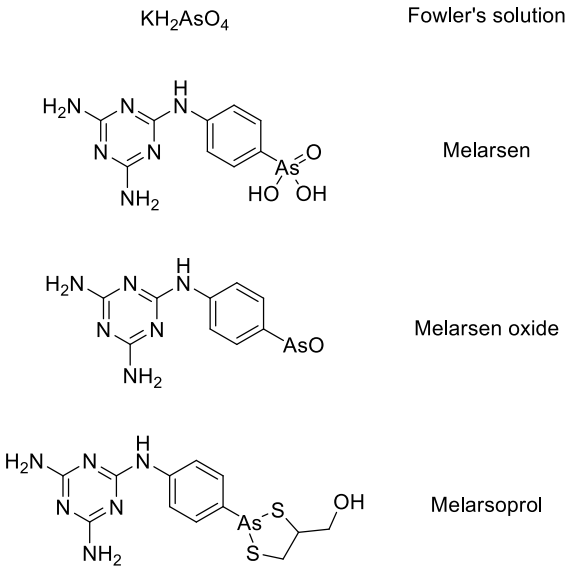

Figure 3. 17 Steps in the development of melarsoprol.

trypanothione, resulting in a potent competitive inhibitor of trypanothione reductase. These two effects probably contribute to the antiparasitic activity. Toxicity of this drug is extremely high, with 5% to 10% of the patients developing reactive haemorrhagic thrombocytopenia that, in half of them, leads to death. When possible, glucocorticoids are co-administered to reduce this risk. Thrombocytopenia and cardiac insufficiency also appear in some cases. Some strains of the parasite developed a reduced sensitivity to melarsoprol, probably due to transport defects (P2 adenine/adenosine transporter is able to bind melarsoprol).

Nifurtimox

Nifurtimox is effective in both early and late infections. It is activated to anionic nitroradicals that, in turn, promote the formation of ROS, leading to oxidative stress (lipids peroxidation, enzyme inactivation, DNA damage). Because of a shared mechanism of action, it is commonly administered in combination with eflornithine for the treatment of the second stage of g-HAT. Its adverse effects include hypersensitivity reactions, nausea, vomit, peripheral neuropathy and gastrointestinal symptoms.

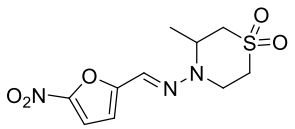

Nifurtimox

Figure 3. 18 Structure of nifurtimox.

Eflornithine

Eflornithine, or α-difluoromethyl ornithine (DFMO), has been initially developed as antineoplastic. Later on it showed activity toward g-HAT. DFMO is a suicide inhibitor of the enzyme ornithine decarboxylase (ODC), which catalyses the limiting step in the synthesis of polyamines (mainly putrescine and spermidine), which are essential for cellular differentiation and division. Moreover, spermidine is together with glutathione a constituent of trypanothione, the main cellular antioxidant in the parasite. Thus, depleting *T. b. gambiense* of polyamines also exposes it to oxidative stress. The selective toxicity of DMFO toward *T. b. gambiense* is due to a more rapid ODC turnover in humans. Eflornithine is administered through slow intravenous infusion over a 14 days treatment.

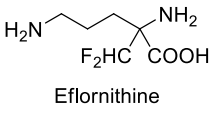

Eflornithine

Figure 3. 19 Structure of eflornithine.

With these informations in hand, it can be easily concluded that the treatment of HAT is rather complex. Drugs present severe adverse effects and must be administered through parenteral routes following complicated therapeutic schemes. Hospitalization and a 24 months follow-up are also required. During this period body fluids, as cerebrospinal fluid, must be examined to assess a complete cure. In order to ease the suffering of the poor people menaced by HAT, manufacturers donate drugs to WHO, which treats patients in the disease endemic areas for free.

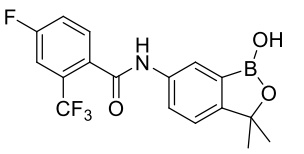

SCYX-7158

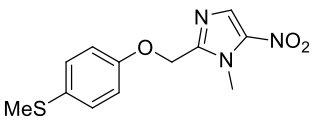

Fexinidazole

Figure 3. 20 SCYX-7158 and fexinidazole, two compounds under clinical investigation.

Despite the drawbacks of existing agents, only two drugs are currently under clinical investigation. The benzoxaborole SCYX-7158 successfully concluded phase I clinical studies in March 2015 in France and a phase II/III trial started in 2016 in the Democratic Republic of the Congo. [13] Fexinidazole entered a phase II/III clinical trial for the

second stage g-HAT and for both the stages of r-HAT in 2012. Results of these studies are still to be disclosed. [14]

4. Bacterial parasitic diseases

4.1 *Chlamydia trachomatis*

Key points [15]

- Caused by three biovars of the Gram negative bacteria *Chlamydia trachomatis*;
- Diffused worldwide. Higher prevalence in the Americas and in the Western Pacific region;
- Incidence rate of 38 and 33 per 1000 for women and men, respectively; WHO estimates an overall prevalence of 4.2% for females and 2.7% for males.

C. trachomatis is the agent of the most common bacterial sexually transmitted infection. It causes three major diseases: genital infections, lymphogranuloma venereum (genital ulcer disease) and trachoma (eye infection). The infection is often asymptomatic (in the 70% of women and the 50% of men). Abnormal vaginal discharge, dysuria and post-coital and intermenstrual bleeding are common symptoms in women, who also show cervical friability and discharge. In men dysuria and urethral discharge are sometimes accompanied by testicular pain. Infection often resolves spontaneously but it can ascend the reproductive tract causing pelvic inflammatory disease, ectopic pregnancy, salpingitis, tubal factor infertility in women, and epididymitis in men. Rectal and oropharyngeal infections are also common. Infection in pregnancy is associated with preterm birth and low birth weight. Infants can be also infected at delivery, resulting in neonatal conjunctivitis and/or nasopharyngeal infection.

Trachoma is common in the rural areas of Africa, Central and South America, Asia, Australia and Middle-East, where hygienic conditions are low. Infection occurs through personal contact and by flies that have touched infected people. After several infections, the inside of the eyelid becomes scarred (trachomatous conjunctival scarring) at the point that it turns inward (trachomatous trichiasis). Eyelashes rub the eyeball causing constant pain and light intolerance. If untreated, irreversible opacities form, resulting in visual impairment and blindness. The sight of 1.9 million people is impaired by *C. trachomatis* (1.4% of the total of blind individuals), making it the leading infectious cause of blindness. [16]

4.1.1 Treatment of *C. trachomatis* infections [7]

Azithromycin and doxycycline are the drugs of election in uncomplicated case and the first can be used during pregnancy and for the treatment of neonates conjunctivitis as well. Lymphogranuloma venereum and anorectal infections are preferentially treated with doxycycline. [15]

Macrolides (azithromycin, erythromycin)

Macrolides are antibiotics that work blocking protein synthesis. They bind to the ribosomal 50S subunit, close to chloramphenicol binding site, inhibiting the translocation of the growing peptide. They are absorbed from the gastrointestinal tract and rapidly reach effective concentration in all the tissues. These drugs are better accumulated in Gram positive bacteria. Azithromycin is more active than erythromycin toward *C. trachomatis*. Several mechanisms of resistance have been described. They include: efflux pumps; expression of methylases that modify ribosomes, reducing affinity for the drugs; hydrolysis by esterases (*Enterobacteriaceae*); mutations that alter a protein in 50S ribosome subunit. Cross resistance has been described as well. These drugs are macro lactones bound to two deoxysugars. Azithromycin presents a cyclic amine which improves acid stability, tissue penetration and broaden the activity spectra of the drug. Adverse effects to these drugs are little; the major concern regards the development of cholestatic hepatitis, since these drugs are mainly eliminated with the bile. They might interfere with other drugs because they cause inhibition of CYP3A4.

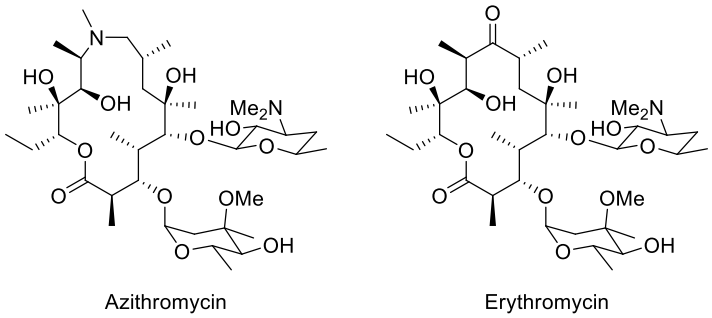

Figure 4. 1 Structures of azithromycin and erythromycin.

Tetracyclines (doxycycline, tetracycline)

Tetracyclines, as mentioned in paragraph 3.1.1, inhibit protein synthesis binding to the 30S ribosomal subunit. They can be given either by oral or by parenteral (intravenous) administration. Since these molecules are avid chelators of divalent cations, oral administration with concomitant ingestion of high quantities of metal cations causes a reduction in adsorption. For the same reason, they accumulate in bones, leading to reduction of growth in children and teeth spotting. Other adverse effects include hepatotoxicity, photosensitization, renal toxicity and, in fewer cases, hypersensitivity. Resistance is diffused and occurs through the following mechanisms: reduced accumulation (combination of reduced penetration and improved efflux); synthesis of a ribosomal protein that displaces tetracyclines; enzyme inactivation.

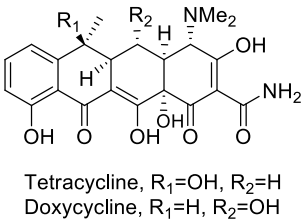

Figure 4. 2 Structures of tetracycline and doxycycline.

Ofloxacin

Ofloxacin is a member of the class of the fluoroquinolones antibiotics. 6-Fluoroquinol-4-ones act inhibiting DNA supercoiling. In many Gram negative bacteria they inhibit DNA gyrase, while in Gram positive the principal macromolecular target is represented by topoisomerase IV. They can be assumed by oral administration, but these drugs should be avoided during pregnancy. They distribute well in the body and are excreted with urine. Most common adverse

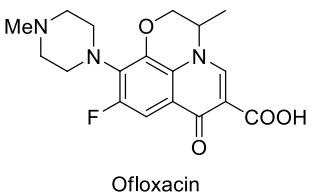

Figure 4. 3 Structure of ofloxacin.

reactions involve the gastrointestinal system (nausea, vomiting, abdominal pain, diarrhoea), while other severe reactions are rare.

5. Enzymes as drug targets

Enzymes are proteins that act as catalysts in cells. The substrate(s) of the enzyme binds to the active site, a binding pocket with a unique three dimensional structure. The stereo-electronic properties, resulting from the tertiary structure of the whole protein, are optimized to establish a specific network of interactions with the substrate, giving a stabilized transition state. The active site must not be consider as a fixed structure, but as a flexible architecture, which exists in different microstates with different affinities for ligands (e.g. substrate, product, inhibitors). In the following section, I will give descriptive and analytical information of enzyme catalysis and inhibition. This chapter is thought as a practical guide for the interpretation of the results presented in this thesis and thus is just focused on few relevant aspects. Additional information on enzymes are provided in the appendix (chapter 11).

5.1 Enzyme reaction mechanism

Enzyme catalyzed reactions is characterized by the transition through different states (fig. 5.1), which are connected by a set of micro-reversible equilibria. The first step in enzyme catalysis is represented by the formation of the enzyme-substrate binary complex *ES*. In most of the cases, this is a reversible equilibrium process that can be described by a pseudo-first-order association constant (k_{on}) and a first-order dissociation constant (k_{off}). The formation of the *ES* complex represents a thermodynamic equilibrium, quantifiable in terms of an enzyme-substrate dissociation constant (K_s), defined as the ratio of reactant and product concentrations, and as the ratio of the constants k_{off} and k_{on} (eq. 1). The value of K_s in inversely proportional to the affinity of the substrate to the enzyme.

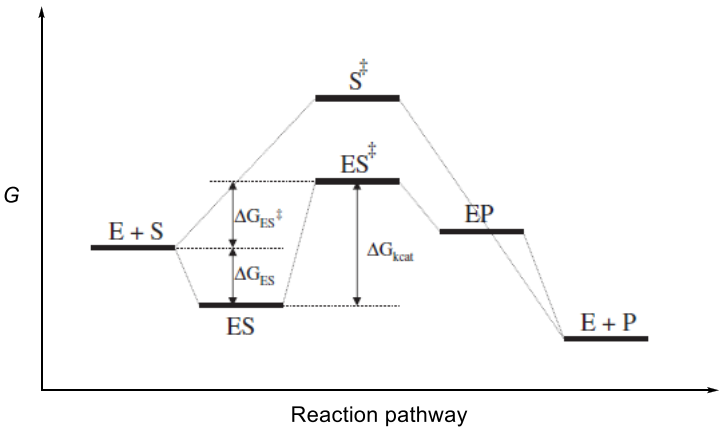

Figure 5. 1 The course of enzyme-catalyzed reaction compared to the one of uncatalyzed reaction.

$$E + S \underset{k_{off}}{\overset{k_{on}}{\rightleftharpoons}} ES$$

Figure 5. 2 Equilibrium of the formation of *ES*.

$$K_s = \frac{[E][S]}{[ES]} = \frac{k_{off}}{k_{on}} \qquad \text{(eq. 1)}$$

Along the reaction course, the complex proceeds to the formation of a bound transition state ($ES^{‡}$), which has a lower energy compared to the transition state for uncatalyzed reaction ($S^{‡}$). Enzymes stabilize the transition state with different mechanisms: approximation of the substrates, the formation of covalent intermediates, acid or basic catalysis and the distortion of the substrate(s). $ES^{‡}$ evolves in a product-enzyme complex (*EP*) and, finally, the product is released. The overall rate of conversion of *ES* to *E+P* is quantified in terms of a composite rate constant (k_{cat}). However, since the formation of $ES^{‡}$ is the rate-limiting step in the process (due to its high thermodynamic barrier) we can consider k_{cat} to be a first-order constant for the transition from *ES* to $ES^{‡}$.

Commonly, enzyme reaction studies are performed under steady state conditions: working with a high molar excess of *S*, compared to *E*, the concentration of *ES* will be constant. Since the reaction rate depends on [*ES*], it will also be constant over time (it can be defined by the slope of the plot of [*S*] or [*P*] as a function of time). Once [*S*] decreases, reaction rate slows down until an equilibrium between the forward and the reverse reactions is established. Independently, Henri, and Michealis and Menten studied the variation of the reaction rate as a function of [*S*] in a rapid equilibrium model (k_{off}>>k_{cat}), leading to the mathematical expression reported in equation 2. The term V_{max} refers to the maximum velocity obtained at infinite [*S*] and is equal to the product of k_{cat} and [*E*] (eq. 3).

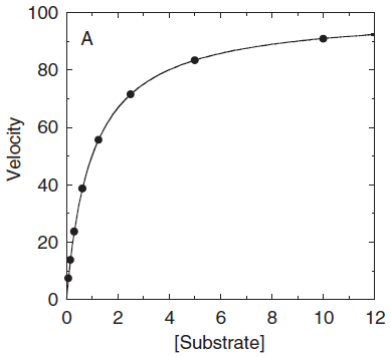

Figure 5. 1 Plot of reaction velocity as a function of [*S*].

$$v = \frac{V_{max}[S]}{K_s + [S]} \quad \text{(eq. 2)} \qquad V_{max} = k_{cat}[E] \quad \text{(eq. 3)}$$

Later, Briggs and Haldane demonstrated that equation 2 can be used in the case of steady state with the substitution of K_s with the kinetic constant K_M (eq. 4, the Michaelis-Menten equation).

$$v = \frac{V_{max}[S]}{K_M + [S]} \text{ (eq. 4)}$$

K_M (as K_s) has the unit of molarity. When [*S*] is fixed to be equivalent to K_M we obtain that $v = \frac{1}{2}V_{max}$. We can consider K_M as a measure of the relative affinity of the *ES* complex under steady state conditions. K_M and k_{cat} can be determined from the plot of *v* over [*S*], which can also be displayed on a semilog scale. The Michaelis-Menten equation can be linearized (eq. 5) and data displayed on plot of 1/*v* as a function of 1/[*S*]: the slope of the obtained line is equal to K_M/V_{max}, the y-intercept to $1/V_{max}$ and the x-intercept to $-1/K_M$. However, because of the need of algebraic manipulation, double reciprocal (or Lineweaver-Burk) plots are not used to determine kinetic constants. On the other hand, they are highly predictive of the inhibition modality of assayed inhibitors.

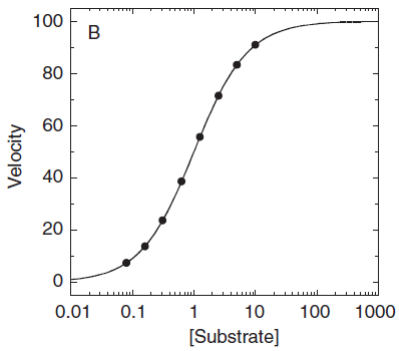

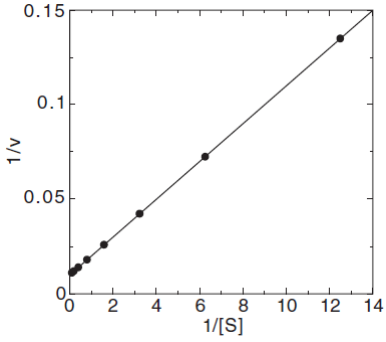

Figure 5. 2 The semilog plot and the Lineweaver-Burk plot are reported on the left. Up in the page is reported the direct fit plot.

$$\frac{1}{v} = \left(\frac{K_M}{V_{max}} \cdot \frac{1}{[S]}\right) + \frac{1}{V_{max}} \quad \text{(eq. 5)}$$

5.2 Enzyme inhibitors

For enzyme inhibitors the affinity for the enzyme is described by the dissociation constant K_i. Inhibitors can bind to the binary complex *ES* or to the free enzyme, causing a variation of the affinity of the enzyme for the substrate of a factor α. For reversible enzyme inhibitors, three different modalities of inhibition are distinguished, basing on the different behaviour in relation with the substrate. In this chapter, only competitive inhibition is examined, while non-competitive and uncompetitive inhibition are presented in the appendix. Inhibition of the catalytic activity could be partial, in the case of partial inhibitors, or complete, for dead-end inhibitors.

5.2.1 Competitive inhibitors

Competitive inhibitors bind exclusively to the free enzyme (α= ∞). The value of V_{max} will be unaffected but the apparent K_M [defined as $K_M(1+[I]/K_i)$] will increase with increasing inhibitor concentration. The steady-state velocity equation in this situation is represented by equation 6 and plots for this situation are reported in figure 5.3

$$v = \frac{V_{\max}[S]}{[S] + K_{\mathrm{M}}\left(1 + \frac{[I]}{K_{\mathrm{i}}}\right)} \qquad (\mathrm{eq.}\,6)$$

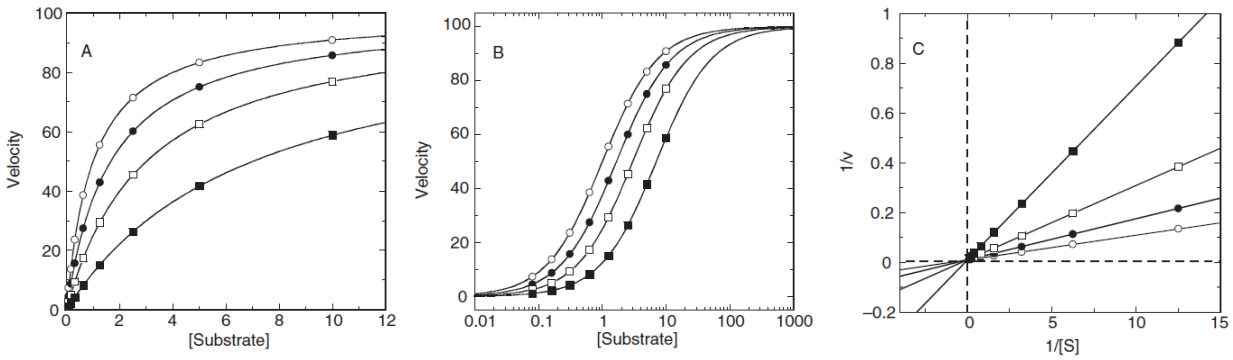

Figure 5. 3 Direct fit, semilog and double reciprocal plots for competitive inhibition. In the plots here reporterd, highest [*I*] situation is represented by the filled square curve while empty circle curve is for lowest [*I*].

A saturable binding is expected for reversible inhibitors. The fraction of free enzyme is equal to the fractional activity (v_i/v_0), while the fraction of enzyme bound to the inhibitor is equal to 1-(v_i/v_0), so % inhibition is defined as 100(1-(v_i/v_0)). Fractional activity can be plotted as a function of [*I*]. The concentration of the inhibitor corresponding to the [*I*] needed to reach 50% inhibition is referred to as the IC_{50},. The isotherm equations that link fractional activity or % inhibition to [*I*] are described below (eq. 7 and 8, respectively).

$$\frac{v_{\mathrm{i}}}{v_0} = \frac{1}{1 + ([I]/\mathrm{IC}_{50})} \qquad (\mathrm{eq.}\,7)$$

$$\%\ \mathrm{Inhibition} = \frac{100}{1 + ([I]/\mathrm{IC}_{50})} \qquad (\mathrm{eq.}\,8)$$

IC_{50} is a measure of relative inhibitory potency, being influenced by solution conditions (pH, ionic strength, temperature) and, especially, by [*S*]. In particular, with increasing [*S*], IC_{50} will increase curvilinearly for competitive inhibitors. Nevertheless, giving the convenience of their determination, IC_{50} values are widely

used to compare the activities of inhibitors with the same inhibition modality and assayed under the same conditions.

Reversibility of inhibition is usually determined by a large dilution of the enzyme-inhibitor complex ("jump-dilution"). The target is incubated at a concentration 100-fold over the concentration required for the assay and with [*I*] equivalent to 10-fold the IC_{50}. After an equilibration time, the mixture is diluted 100-fold in reaction buffer containing the substrate to initiate the reaction. In this way, [*I*] rapidly change from 10 IC_{50} to 0.1 IC_{50}, which correspond to approximately 91% and 9% inhibition, respectively. Following the reaction progress curve we aspect a straight line in the cases of fully reversible inhibition and of irreversible (or very slow reversible) inhibition: in the latter case, residual activity will reach a value close to 9%. If the inhibition is slowly reversible we will instead obtain a curve in which the linear phase follows a curvilinear lag phase. The inhibition modality is then determined observing the effects of the variation of both $[S]/K_M$ and $[I]/IC_{50}$ on activity.

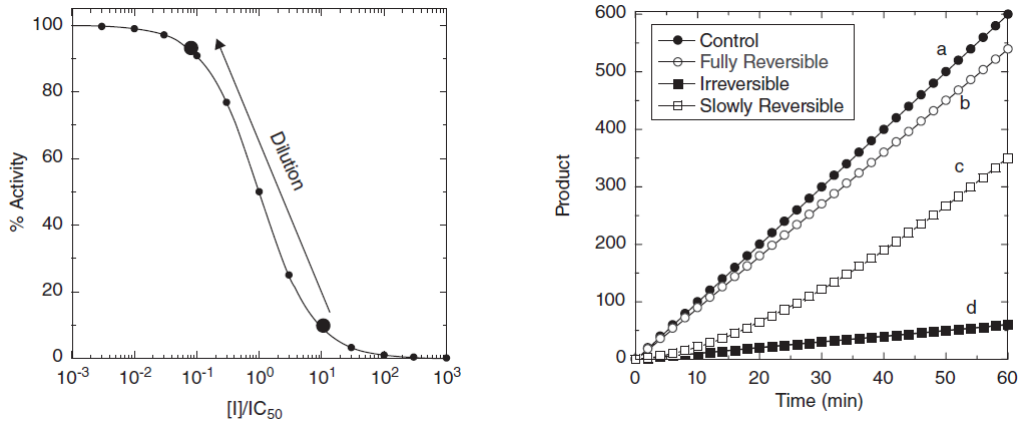

Figure 5. 4 Determination of inhibition reversibility with a rapid dilution approach. Effect of dilution on % activity (left) and observed recovery of activity for different inhibition behaviours (right).

For an accurate comparison of inhibitory potencies of different inhibitors, only K_i values should be taken in account. Cheng and Prusoff derived equations that, knowing the IC_{50}, [*S*], K_M and the inhibition modality, allow to derive K_i.The relationship of IC_{50} and K_i for competitive inhibitors is described by equation 9.

$$IC_{50} = K_i\left(1 + \frac{[S]}{K_M}\right) \quad (\text{eq. } 9)$$

Cheng-Prusoff equations also represent an alternative method for determining the inhibition modality.

5.2.2 Covalent inhibitors

Covalent inhibitors irreversibly bind to a critical amino acidic residue of the enzyme abolishing its activity. Other inactivators (without the potential application as drugs) are protein denaturants, as detergents, urea, guanidine and some oxidants. All irreversible covalent inhibitors will display a slow binding behaviour, with k_{obs} describing the rate of inactivation. Given $[I]>[E]_T$, equation 10 describes the reaction curve (where v_i is the highest observed reaction rate).

$$[P] = \frac{v_i}{k_{obs}}[1 - \exp(-k_{obs}t)] \qquad \text{(eq. 10)}$$

Depending on the mechanism of irreversible inhibition (considering the cases of a one-step reaction), the relationship between k_{obs} and [*I*] will change. For nonspecific affinity labels the plot will be linear, with a slope with the unity of a second-rate constant (usually expressed as $k_{obs}/[I]$ or k_{inact}/K_I), and will pass through the origin. For quiescent affinity labels and mechanism-based inhibitors (with a two-step mechanism) the curve will pass through the origin but, at high values of [*I*] will reach a plateau. The maximum rate of inactivation (reached at infinite value of [*I*]) is referred to as k_{inact}. In this case the relationship between of k_{obs} and [*I*] is expressed by equation 11, similar to Michaelis-Menten equation, and the inhibitory efficiency is usually measured as the half-life for inactivation at infinite [*I*], $t_{1/2}^{\infty}$ (equal to $0.693/k_{inact}$). K_I (which should not be confused with the dissociation constant for the initial complex) has a meaning for inactivators similar to the meaning of K_M for substrates. When $[I] << K_I$, the plot of k_{obs} as a function of [*I*] will be linear, with a slope equal to k_{inact}/K_I. This parameter is then used during SAR for the comparison of inactivation efficacy for all enzyme inhibitors.

$$k_{obs} = \frac{k_{inact}[I]}{K_I + [I]} \qquad \text{(eq. 11)}$$

We can distinguish three different mechanisms of action for irreversible inhibitors:

a. *Nonspecific affinity labelling*

   Affinity labels are reactive molecules, generally containing an electrophile, that form covalent bonds with cellular macromolecules without specificity. The only some drugs antineoplastic, as nitrogen mustards and nitrosoureas act with this mechanism. For other therapeutic areas such general reactivity is not acceptable.

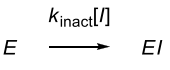

b. *Quiescent affinity labelling*

   This kind of inactivators present a weak electrophile and this allows then to selectively react with catalytic residues after a proper orientation in the enzyme active site (during the reversible binding step). Acetil salicylic acid and omeprazole are two examples of quiescent affinity labels.

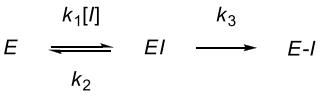

c. *Mechanism-based inactivators*

   Mechanism-based inactivators, commonly known as suicide inhibitors, are molecules that are recognised by the enzyme and are converted into an affinity label, a transition state analogue or a very tight binding reversible inhibitor, prior to release from the active site. Because of their mechanism, they can be very specific for a family of enzymes that catalyse a common reaction. The activated species (*A*) can be released from the enzyme, reducing the fraction of inhibitor that goes directly from the isolated form (*I*) to the covalent adduct *E*-*A*. The ratio k_6/k_7 (the partition ratio, *r*) is then used as a measurement of efficiency

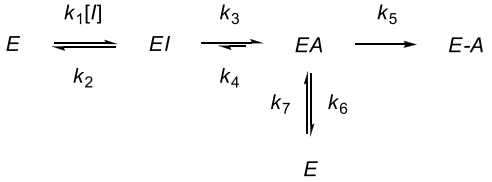

of mechanism-based inhibition (with higher efficiency for values of *r* close to zero). For this type of inhibitors k_{inact} and K_I have the form described in equations 12 and 13.

$$k_{\text{inact}} = \frac{k_3 k_5}{k_3 + k_5 + k_6} \quad \text{(eq. 12)} \qquad K_I = \left(\frac{k_1 + k_3}{k_2}\right)\left(\frac{k_6 + k_5}{k_3 + k_5 + k_6}\right) \quad \text{(eq. 13)}$$

Only in situation of rapid equilibrium (when k_1 and k_2 are very large and k_3 is rate-limiting) K_I will be equal to K_i, while in other situations the two constants will have different meanings.

5.2.3 Re-evaluation of covalent inhibitors

Covalent inhibitors have always been considered with suspect. Only suicide inhibitors are generally considered considerably safe, because of the need of activation by a specific enzyme. The concerns regarding off target reactions, which can result in toxic effects, in particular idiosyncrasic reactions (after protein haptenization) make people working in the drug discovery area to abandon molecules containing electrophiles in their structure. This caution is absolutely legitimate. Some of the approved covalent inhibitors (or, more generally, covalent approach-based drugs), as nitrogen mustards and nitrosoureas, are only used in critical acute states because their intrinsic very high toxicity. Even when targeting non-human enzymes, covalent drugs can lead to severe allergic reactions in sensible patients, as in the case of β-lactam antimicrobials. However, several covalent inhibitors are approved for the human use from a long time and they are assumed almost every day without the need of any medical prescription. Two examples are the NSAIDs acetylsalicylic acid and acetaminophen. Other covalent approach-based drugs are used for chronic therapies: dutasteride and finasteride (5α-reductase inhibitors) are used in the treatment of benign prostatic hyperplasia, clopidogrel ($P2Y_{12}$ receptor inhibitor) is an antiplatelet used to prevent heart attacks and strokes in patient at risk and orlistat (pancreatic lipases inhibitor) is used to treat obesity. When properly used, these drugs do not present serious adverse effects. Many scientists, both from industry and academia, have underlined the underestimated role that covalent inhibitors already play in therapy and all their unexploited potential. [17] [18] [19] [20] Targeted covalent inhibitors (quiescent affinity labels), in particular, are gaining more and more attention. The success in this field is granted through the optimization of the two portion of the inhibitors: the warhead, the electrophilic portion of the molecule, must possess a balanced reactivity (low enough to avoid off target reactions but still able to form covalent bond with the targeted nucleophile); the recognition moiety, instead, must be properly designed in order to establish a specific network of non-covalent interactions with the macromolecule of interest with the aim to enhance selectivity of action and, at the same time, to properly orientate the warhead for a faster reaction. The advantages that target covalent inhibitors present are notable. The non-equilibrium condition that underlie covalent inhibition lead to a greater biochemical efficiency (escaping competition with the substrate). For the same reason, PD and PK effects are dissociated, prolonging the efficacy of drugs with low plasma $t_{1/2}$ and allowing to administer the drugs less frequently and at lower doses. This also greatly reduces the risk of idiosyncrasic reactions, which have been correlated with daily dose

more rather than the mechanism of inhibition (the same kind of toxicity is caused by several non-covalent drugs as halothane, carbamazepine, and felbamate). The growing interest in the field is testified by the number of recently approved drugs that acts through a covalent modification of their biological target (e.g. afatinib, osimertinib, ibrutinib, dimethyl fumarate).

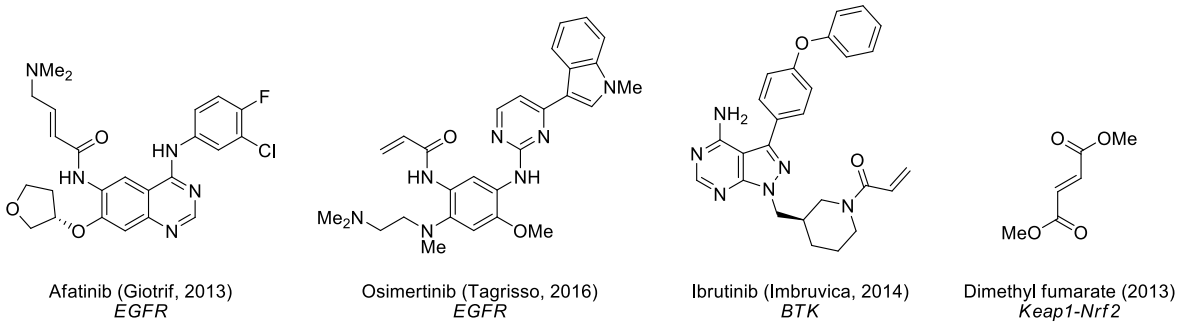

Figure 5. 5 Recently approved drugs (the brand name and the year of approval are reported in brackets) that act alkylating target enzymes (reported below).

This approach is then absolutely valuable but, as general recommendations, it should be applied this strategy only toward targets with high $t_{1/2}$ using warheads with moderate reactivity. To further improve opportunities in this field, Taunton and co-workers described that the introduction of an electron-withdrawing substituent at the α-position of acrylamide Michael acceptors results in a reversibile electrophile. The reason behind this is that the stronger acidity of the α-proton in the adduct favours the retro-Michael reaction. [21] [22] This approach has been applied in the design and synthesis of the reversible inhibitors bardoxolone methyl (EGFR inhibitor, fig. 5.6). In principle, the development of prodrug of covalent inhibitors could be considered as well. This approach has been just little exploited, but it demonstrated great effectiveness as in the case of proton pump inhibitors (e.g. omeprazole, lansoprazole, pantoprazole, fig. 5.7), which revolutionised the treatment of peptic ulcer. These molecules are converted to reactive sulfenic acids/sulfenamides only in the acidic environment of the stomach, where they covalently bind to their target, the H^+/K^+-ATPase in parietal cells, granting a selective action.

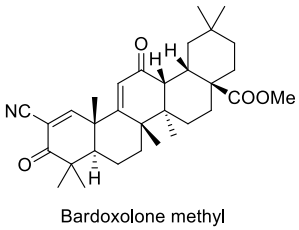

Figure 5. 6 Structure of the α-cyano enone bardoxolone methyl.

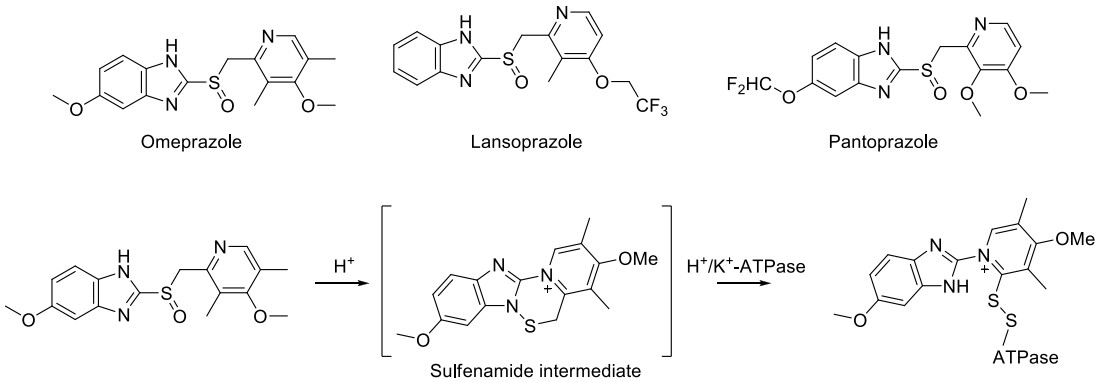

Figure 5. 7 Examples of proton pump inhibitors (above) and mechanism of activation of omeprazole (below).

5.3 Beyond the target

Knowing the molecular target is, nowadays, an essential requirement in the drug discovery process. However, the quality of the hits (the chemical starting points) is ultimately assessed by cellular assays. In a quite recent perspective [23], different partnerships involved in the discovery of new drugs for infectious tropical diseases proposed disease-specific criteria for the progression from hit to lead and for reliable early leads.

Good hits must be characterized by:

- Adequate *in vitro* potency: for antimalarials EC_{50}< 1 μM, for *Trypanosomatidae* disease EC_{50}< 10 μM;
- Limited cytotoxicity toward mammalian cell lines (>10-fold selectivity window);
- Acceptable *in vitro* response (concentration-growth inhibition correlation);
- Tractable chemotype: no instable moieties, amenable to structural variation, and must pass drug-like filters (such as the pan-assay interference filters, PAINS). [24] Conformity to Lipinski's rule of five [25] is preferred;
- Selectivity in biochemical counter-assay (e.g. mammalian homologous), where relevant;
- No major synthesis or formulation issues (≤ 5 synthetic steps, acceptable yields, acceptable solubility).

For lead compounds, the requirements become more and more stringent:

- Adequate *in vitro* potency: for antimalarials compounds must show EC_{50}< 100 nM;
- A selective toxicity 100-fold higher for pathogens compared to mammalian cells (a tighter selectivity window could be accepted in particularly challenging fields);
- Oral efficacy in the appropriate disease model;
- Series expansion should be amenable;
- No detrimental chemical feature associated with the pharmacophore;
- Acceptable physicochemical properties: solubility in PBS> 10 μM and acceptable lipophilicity (logP< 5);
- At least, good oral bioavailability in rodents (F> 25%);
- Manageable drug metabolism and pharmacokinetic profiles (i.e. liver microsomal and hepatocyte stability; good membrane permeability; manageable CYP450 inhibition);
- Acceptable early safety assessment based on target (orthologue) and compound liabilities, *in vivo* observations, *in vitro* studies (e.g. genotoxicity, mini-Ames test), cytotoxicity, cardiac safety (e.g. *h*ERG interaction), and *in silico* approaches. Selectivity, based on the assay on human orthologues and paralogues of the targeted enzyme, should be reached;
- No acute *in vivo* toxicity (derived from of the observation of the efficacy studies, particularly at high and repeated doses).

These guidelines are based on the experience and delined to increase the success rate in drug discovery. However, every therapeutic area involves different demands that should be kept in consideration. For example, antimalarial agents should ideally display efficacy toward the different stages of the parasite (since most of the

available drugs are only active on the asexuate form of *Plasmodium*) and toward a panel of resistant strains; on the other hand, antitrypanosomal agents should be able to cross the BBB. In addition, the existence of intellectual properties conflicts should be evaluated in each case.

These recommendations highlight the advantages of a rational drug discovery process, which will anticipate liabilities connected with the followed approach (from chemistry and biology points of view). Moreover, it is once again recalled the importance of optimizing biopharmaceutical properties together with potency.

6. Inhibitors of *Plasmodium falciparum* glyceraldehyde-3-phosphate dehydrogenase (*Pf*GAPDH)

6.1 *Pf*GAPDH as target

Glyceraldehyde 3-phosphate dehydrogenase (GAPDH, EC 1.2.1.12) is a homotetrameric enzyme involved in glycolysis. [26] It catalyses the conversion of glyceraldehyde 3-phosphate in 1,3-biphosphoglycerate with the concomitant reduction of the NAD^+ cofactor: remarkably, the reaction catalysed by GAPDH is the first in which energy is produced (as NADH) within glycolysis (while in the previous steps energy is consumed). Since it represents the bottleneck for the production of high energy containing cofactors (NADH and ATP), GAPDH is considered a valuable target to inhibit the growth of those cells that only rely on glycolysis for energy production, as *P. falciparum* [27] and cancer cells. [28] [29]

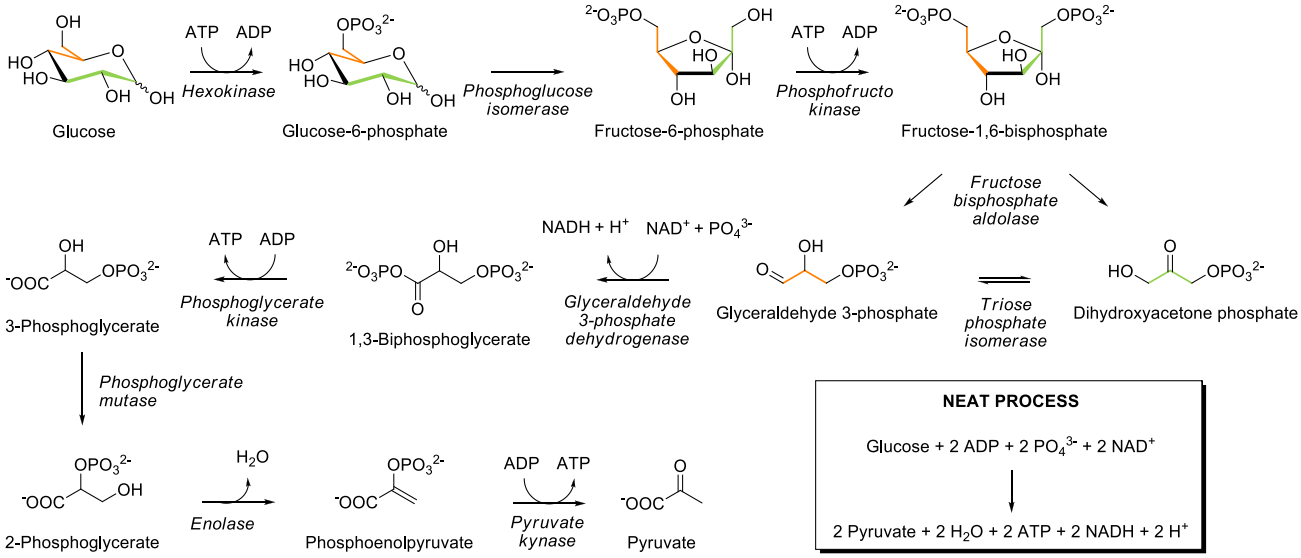

Scheme 6. 1 Glycolysis sequence. Glucose is partially oxidized to two molecules of pyruvate with production of two molecules of ATP and two molecules of NADH. GAPDH occupies a central role in the whole process.

The catalytic mechanism (scheme 6. 2) involves the intervention of a cysteine residue, activated by a proximal histidine residue (Cys153 and His180 in *Pf*GAPDH): the generated thiolate reacts with glyceraldehyde 3-phosphate giving a thioester intermediate and reducing the NAD^+ cofactor; subsequent phosphorolysis releases 1,3-biphosphoglycerate and the catalytic thiolate.

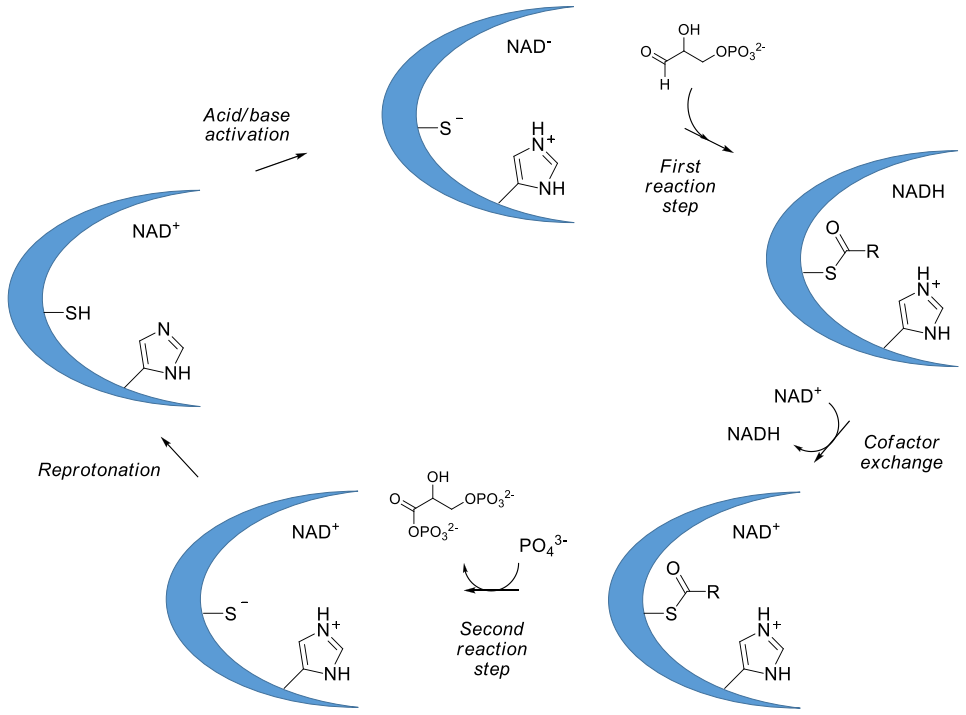

Scheme 6. 2 Schematic representation of GAPDH catalysis.

GAPDH possesses additional functions from its key position within anaerobic catabolism. [30] In parasites, bacteria and humans, its involvement in other cellular processes, such as DNA repair, control of gene expression, membrane trafficking, cell signalling, interaction with RNA and other proteins (particularly in neurodegenerative disease) has been postulated. [31] *Pf*GAPDH was found to be able to interact with *Pf*enolase, plasminogen, α-tubulin and lysozyme in a specific way. [32] In addition, surface-expressed *Plasmodium* GAPDH is involved in Kupffer cells traversing through interaction with CD68 receptors and, because of this, is a promising candidate for the development of preerythrocytic vaccine. [33] All these aspects highlight the enormous potential of *Pf*GAPDH as a target for the treatment of malaria.

6.2 *Pf*GAPDH structure

The structure of *Pf*GAPDH, coded by the PF14_0598 gene, has been independently determined at high resolutions (2.25 Å and 2.6 Å) by two different groups. [34] [35] The protein has a mass of 36.6 kDa and a pI of 7.6. The enzyme does not present any targeting signal, hence the different cell localization is probably due to post translational modifications. Each monomer is composed by 334 amino acid residues organized in the following way: residues 4-152 and 320-337 constitute the NAD^+ binding domain, adopting a classical Rossmann fold (NAD^+ is found in every monomer); residues 153-319 constitute the catalytic domain; residues 181-209 are arranged in a feature known as S-loop that connects the two domins. NAD^+ binds in extended conformation bringing the nicotinamide ring in proximity of the active site, located at the interface of the two domains. Parasite and human GAPDHs show a relatively high sequence identity (63%). The major difference from the human isoform is found in the S-loop, where a Lys-Gly dipeptide, absent in *h*GAPDH, is inserted. This creates a bulge that reduces the opening of the solvent accessible channel that spans close to the NAD^+ cofactor.

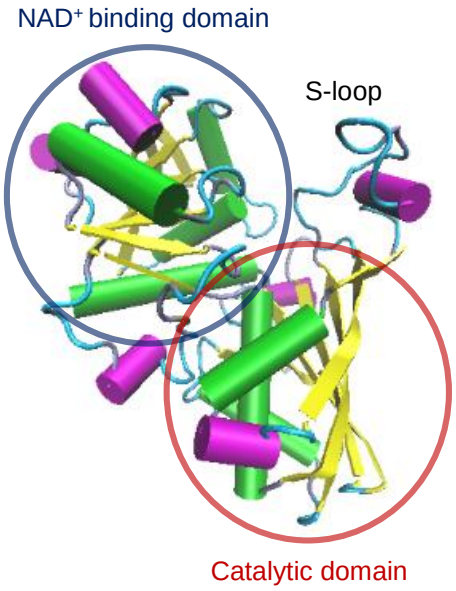

Figure 6. 1 GAPDH monomer (PDB 2B4R). The domains are highlighted and different secondary structures are depicted in different colours.

6.3 The first *Pf*GAPDH selective inhibitors

Know inhibitors of *Pf*GAPDH, 3-bromopyruvate (3BP) and iodoacetamide, are alkylating agents that react with the catalytic cysteine abolishing the enzyme activity, but these molecules are not selective and do not possess drug-like properties. Iodoacetamide is an alkylating reagent able to form covalent bonds with cysteine residues and, more slowly, with histidine residues in an aspecific way. 3BP has emerged in the last years as a potential anticancer agent. [36] Its preferential action toward cancer cells depends on several factors, as higher glycolytic rate (the "Warburg effect"), acidic microenvironment and overexpression of monocarboxylate transporters (MCTs) MTC-1 and MCT-4. However, GAPDH is just one of the number of proteins that this molecule is able to alkylate (its principal target is hexokinase-2). The high reactivity of this molecule is reflected as well by its low $t_{1/2}$ (77 min at physiological temperature and pH). This property, together with the lack of documentation of safety in humans (no clinical studies were performed), tells that 3BP could not be seriously considered for the employment as antimalarial agent. Indeed some of the patients may be healthy and just need a prophylactic treatment, so a high safety profile and the possibility of enteral administration are required (requirements are very different from cancer therapy). In order to obtain selective GAPDH inhibitors, I decided to exploit the 3-

Figure 6. 2 Two known inactivators of GAPDH.

bromo-Δ^2-isoxazoline ring, which was recently proposed as a novel warhead for the design of inhibitors of reactive cysteine containing enzymes. [37] In a recent research, 3-bromoacivicin [(*S*,*S*)-**1**] [a synthetic analogue of the natural compound acivicin, (*S*,*S*)-**2**] was described as a potent inhibitor of the enzyme cytidine triphosphate synthetase of *T. brucei* (*Tb*CTPS). [38]

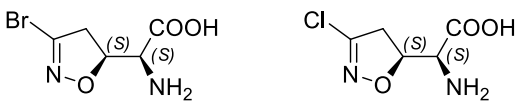

(*S*,*S*)-**1** (*S*,*S*)-**2**

Figure 6. 3 Structures of 3-bromoacivicin [(*S*,*S*)-**1**], an analogue of the natural antibiotic acivicin [(*S*,*S*)-**2**], from *Streptomyces sviceus*.

This enzyme is a glutamine amido-transferase that catalyses the *de novo* synthesis of CTP in the parasite. Both (*S*,*S*)-**1** and (*S*,*S*)-**2** are able to bind the glutaminase domain of the enzyme, due to the fact that their structures mimic L-glutamine, and to react with the catalytic Cys residue forming a covalent adduct. Because of higher reactivity in the proposed addition-elimination mechanism, (*S*,*S*)-**1** turned out to be three times more potent than (*S*,*S*)-**2** (*Tb*CTPS IC_{50}= 98 nM vs 320 nM); this difference was even greater for *T. brucei* cultures (ED_{50}= 38 nM vs 450 nM). The most important feature of the 3-bromoisoxazoline warhead is that its reactivity seems to be moderate enough to avoid a catastrophic aspecific effect: indeed, when assayed *in vitro* against human cells, the compound showed 300 fold higher IC_{50} [12.91 μM; for (*S*,*S*)-**2** IC_{50} was 15.65 μM]. [39] Starting from these promising results, I synthesized compound (*S*,*S*)-**1** to be assayed against *Pf*GAPDH. This compound showed complete irreversible inhibition of *Pf*GAPDH enzymatic activity but with low potency (k_{inact}/K_i = 0.7 $s^{-1}M^{-1}$). A characteristic of the inhibition kinetic is that the rate was very high in the initial phase and then reduced during the second phase. The values of k_{inact}/K_i were obtained from the slow phase of this biphasic inhibition. In order to understand the role of the amino and carboxyl groups, I synthesized analogues of (*S*,*S*)-**1** following a simplification strategy. At the same time I wanted to obtain inhibitors able to bind *Pf*GAPDH more tightly while losing affinity toward *Tb*CTPS. To pursue these objectives, I introduced in the molecules additional functionalization (e.g. carbamate, ester) that might establish additional interaction with the target enzyme while removing the amino acidic function, responsible for the recognition by glutamine-dependent enzymes such as CTPS (fig. 6.4).

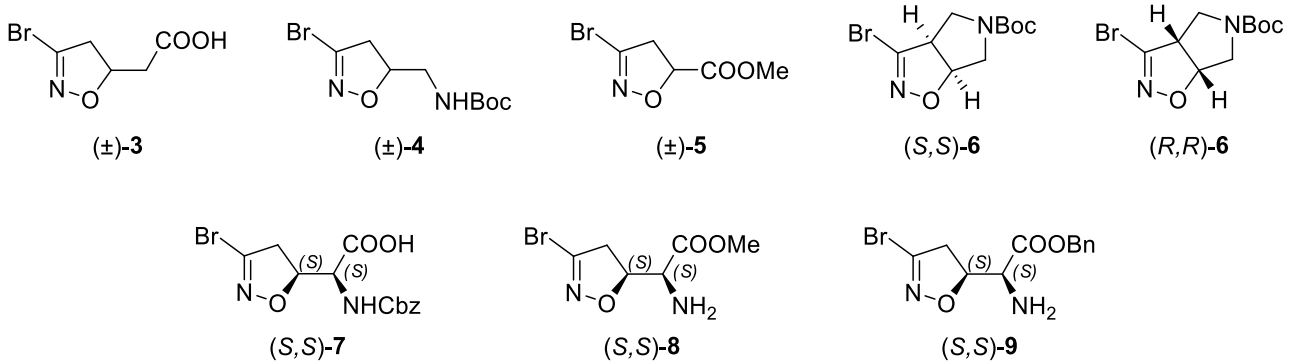

Figure 6. 4 Analogues of (*S*,*S*)-**1**.

In parallel, I synthesized a series of inhibitors in which the amino acidic recognition moiety was replaced by a phenyl ring, so to obtain a very simple model molecule easy to be further decorated. The position 4 of the ring was differently functionalized with substituents able to tune the electronic properties or that can be exploited for further functionalization (fig. 6.5).

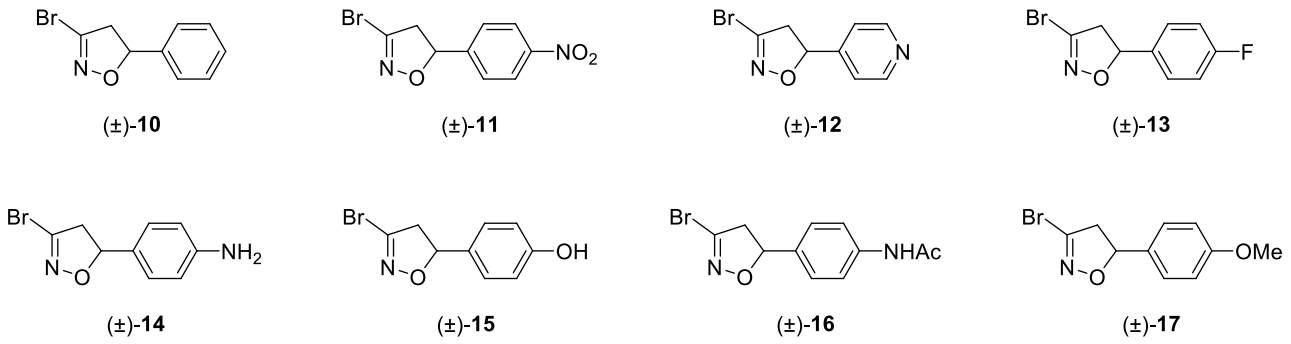

Figure 6. 5 3-Bromo-5-phenyl-isoxazoline analogues.

The key step in the synthesis of these compounds was the 1,3-dipolar cycloaddition between bromonitrile oxide, generated *in situ* from dibromoformaldoxyme (DBF) in presence of a base through the loss of HBr, and the required alkene, which acts as a dipolarophile (scheme 6.3). To prevent the side reaction which produces furoxane, reactions were performed in organic solvents using an inorganic base, which allowed a slow formation of bromonitrile oxide. As known, because of relative frontier molecular orbitals energies, the 1,3-dipolar cycloaddition gave as a major product (≥ 90%) the 5-substituted bromoisoxazoline over the 4-substituted bromoisoxazoline.

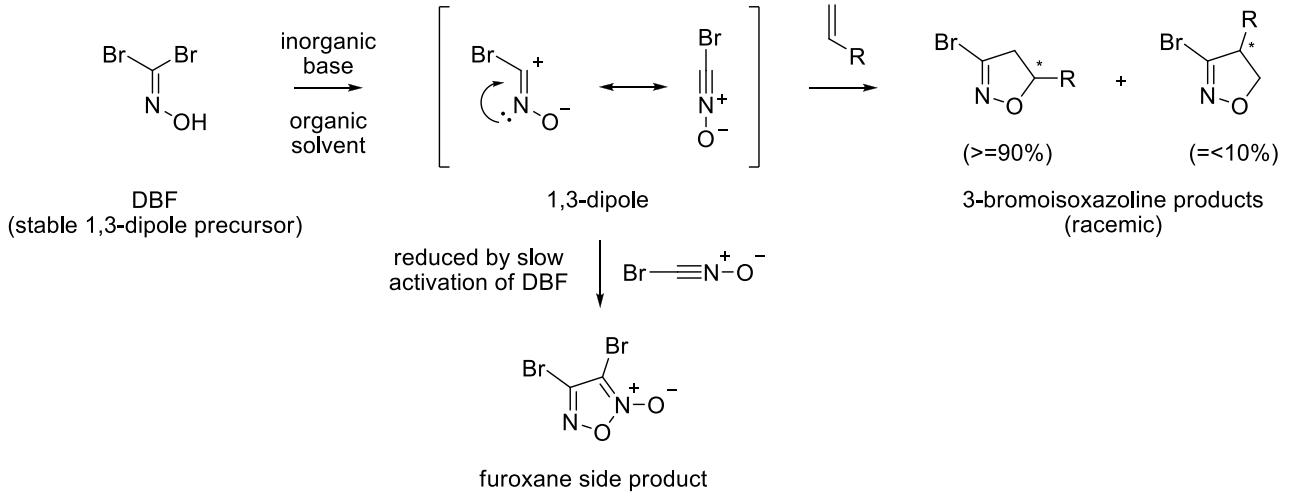

Scheme 6. 3 Overview of 1,3-dipolar cycloaddition reaction of bromonitriloxide and alkenes.

Some alkene were commercially available, while others were synthesized through Wittig olefination of commercial aldehydes. The alkene used for the synthesis of compound (±)-**6** was synthesized starting from *cis*-1,4-dichloro-2-butene, following a published procedure. [40] The racemate was resolved by mean of preparative HPLC on chiral stationary phase. (*S,S*)-**6** was crystallized and its absolute configuration was determined by X-ray crystallography (by Dr. Leonardo Lo Presti, University of Milan), thanks to anomalous scattering due to the heavy bromine atom. Enantiopure analogues of (*S,S*)-**1** were obtained starting from a chiral alkene derived from D-serine. The synthetic strategy exploited the intrinsic stability of Garner's aldehyde [(*R*)-**22**], which is olefinated and used in the 1,3-dipolar cycloaddition (scheme 6.4). The two resulting cycloadducts could be separated as well as their deprotected analogues (scheme 6.5). Mainly because of an easier purification (due to lower lipophilicity of the compounds), I preferred to perform diastereoisomers

separation on the two alcohols. The chance of inverting the order of the cycloaddition and deprotection stepw was also took in consideration but, because of a lower (*S*,*R*)/(*R*,*R*) diastereoisomeric ratio, it was discarded.

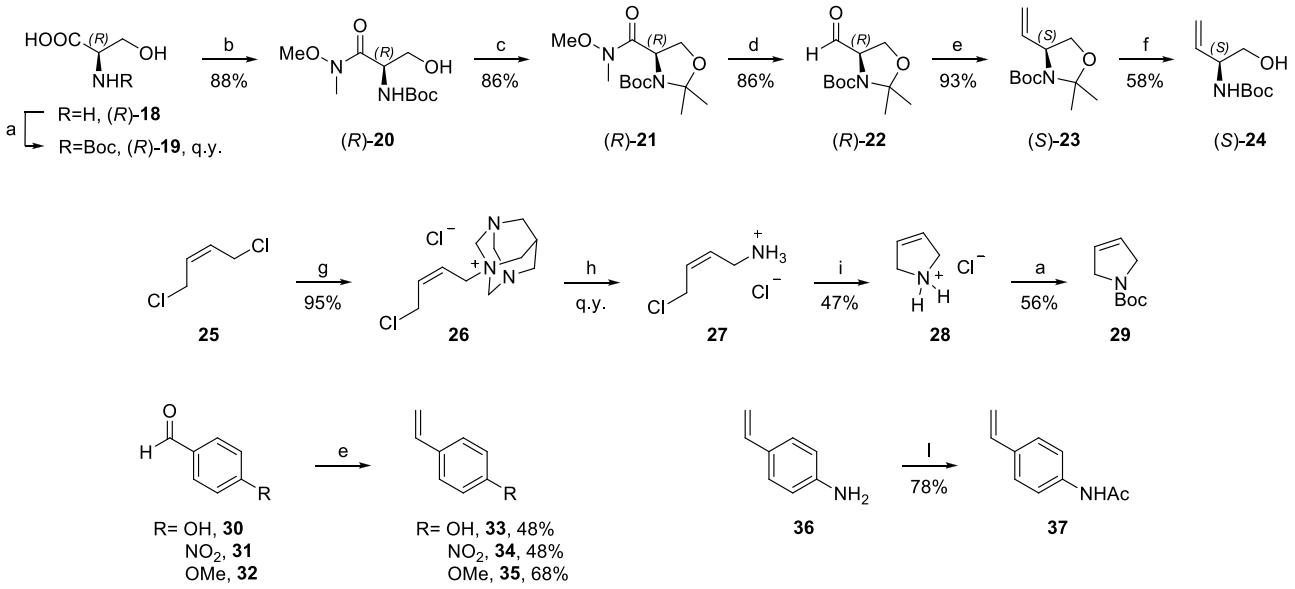

Reagents and conditions: a) Boc_2O, $NaHCO_3$, THF/w, o.n.; b) NHMeOMe*HCl, EDC, TEA, dry DCM, -15 °C; c) acetone dimethyl acetal, PTSA, benzene, reflux; d) $LiAlH_4$, dry THF, 2h; e) $MePPh_3Br$, 0.5 M KHMDS in PhMe, dry THF; f) PTSA, MeOH, 6h; g) 5:1 AcOH/w, 40 °C; h) PDC, DMF; i) 33% HBr/AcOH

Scheme 6. 4 Synthesis of alkenes to be uses as dipolarophiles in 1,3-dipolar cycloaddition reaction.

Synthesized compounds were assayed on the isolated enzyme and the results are reported in the following table, only showing the potencies of compounds able to produce inhibition. The biochemical assays were performed by Professor Stefano Bruno and co-workers, at the University of Parma.

Table 6. 1 Relative potencies of active *Pf*GAPDH inhibitors. Compounds that are not able to inhibit the enzyme are not reported.

Compound	(*S*,*S*)-**8**	(±)-**10**	(*S*,*S*)-**9**	(±)-**6**	(±)-**15**	(±)-**4**	(*S*,*S*)-**7**	(*S*,*S*)-**1**	(±)-**3**	(±)-**12**	(±)-**17**
*Pf*GAPDH k_{inact}/K_i ($s^{-1}M^{-1}$)	10.7	10.3	6.6	4.8	3.1	2.9	2.6	0.7	0.7	0.47	0.34

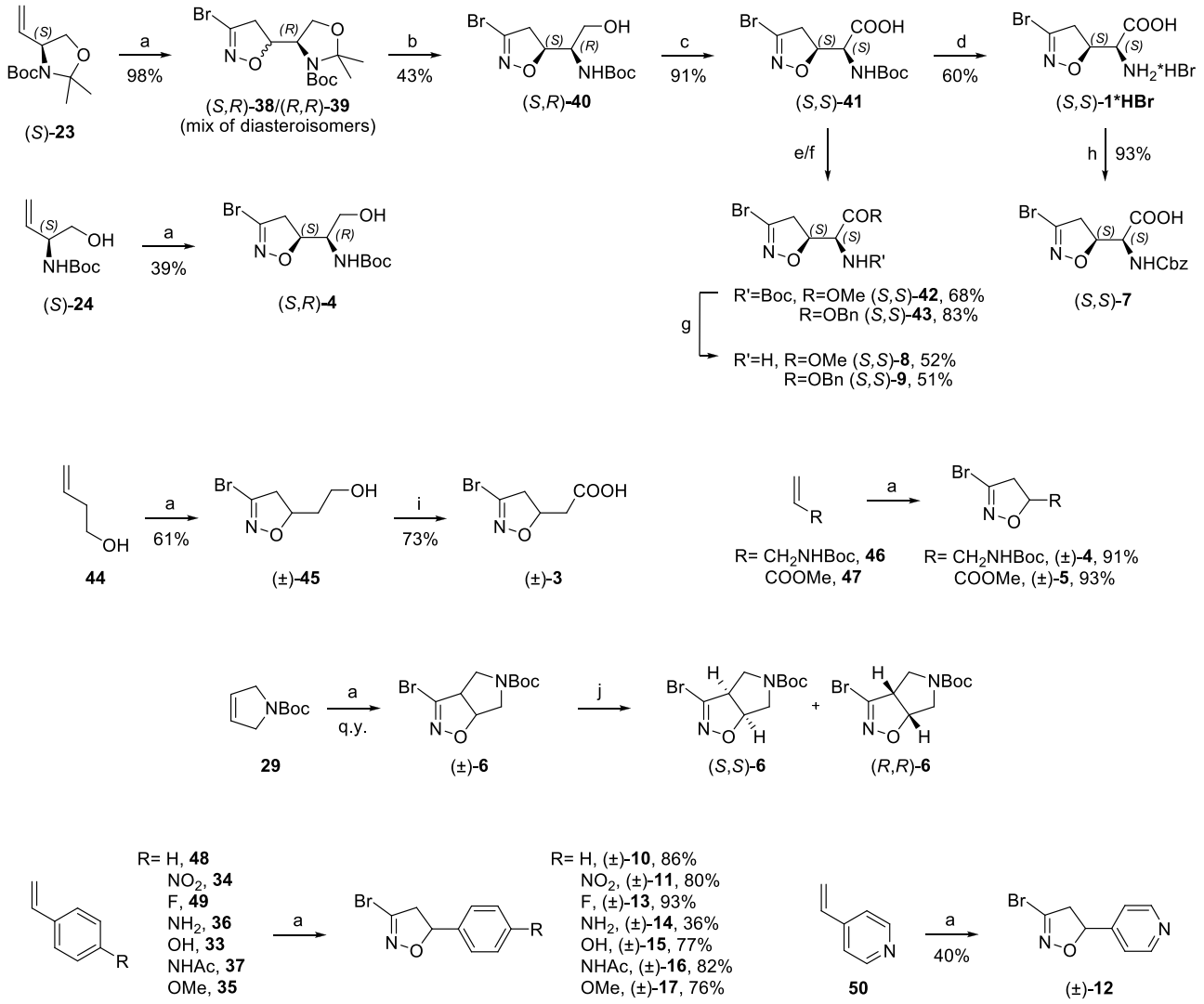

Reagents and conditions: a) DBF, $NaHCO_3$, EtOAc or DMC, r.t.; b) 5:1 AcOH/w, 40 °C, 48h, flash chromatography; c) PDC, DMF, r.t., 4h; d) 33% HBr/AcOH, r.t., 5min; e) $TMSCHN_2$, MeOH/PhMe, r.t., 1h; f) BnBr, NaI, K_2CO_3, DMF, 50 °C, 1h; g) 15% TFA/DCM, r.t., 4h; h) CbzCl, $NaHCO_3$, THF/w, r.t., 1h; i) $NaIO_4$, $RuO_2{*}H_2O$, CCl_2/w/MeCN, r.t., 45min; j) prep HPLC (*n*-hexane/*i*-PrOH), Kromasil 5-Amycoat

Scheme 6. 5 Synthetic scheme of 3-bromoisoxazoline compounds.

Several analogues from both series showed greater potency compared to (*S*,*S*)-**1**. The most active compounds were characterized by an amino ester moiety, showing that the free carboxylate is not implicated in any key interaction. Only few compounds of the 5-phenyl series showed inhibitory activity, but, notably, compound (±)-**10** was among the most potent compounds, unequivocally demonstrating the the amino acidic portion is not necessary for the recognition by *Pf*GAPDH. A subset of compounds was submitted to a computational study in order to rationalize the obtained range of potency. Covalent docking studies of the two most potent compounds were performed by the group of Professor Ettore Novellino. For (*S*,*S*)-**8**, two hydrogen bonds were observed between the isoxazoline nitrogen and Cys153 backbone NH, and between the carbonyl oxygen and a NAD^+ ribose hydroxyl. The methoxy group establishes a hydrophobic interaction with Ala184 side chain and a weak hydrogen bond with Thr183 hydroxy group; the protonated amine is not involved in any interaction. When compound (±)-**10** was docked into the *Pf*GAPDH-NAD^+ binary complex, both the isoxazoline and the nicotinamide rings adopted a different orientation from the one observed for (*S*,*S*)-**8**. This allows the phenyl ring two establish two π-cation interactions on its two faces, one with the protonated pyridinium of NAD^+ and the other with Arg237 side chain.

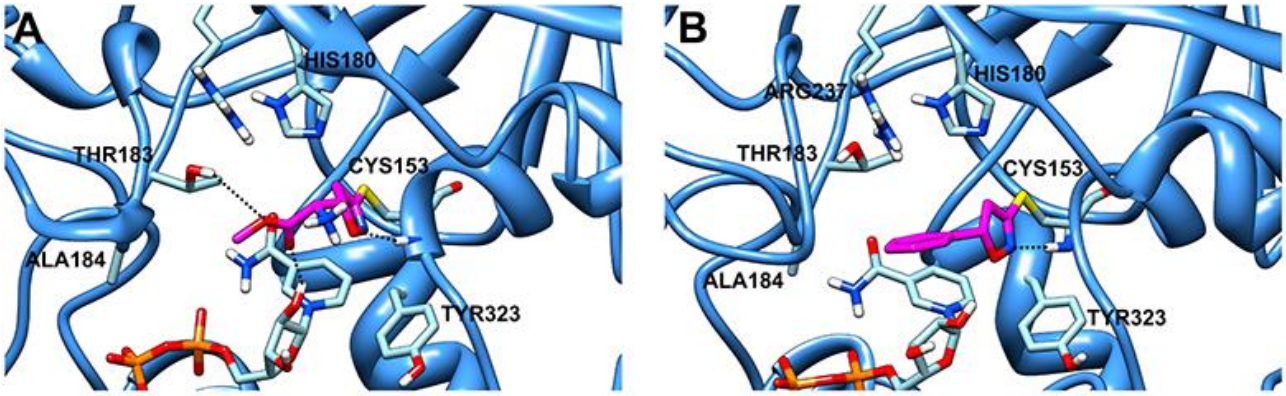

Figure 6. 6 Binding modes of (*S*,*S*)-**8** and (±)-**10** (**A** and **B**, respectively). The enzyme structure is depicted in blue. The inhibitors, the NAD^+, and the interacting residues are depicted as sticks with atomic positions colored red O, blue N, orange P, yellow S, and C magenta for the inhibitors and cyan for the cofactor and for the enzyme residues in the active site.

However, these findings were not sufficient to explain the great differences in observed activity despite similar binding modes. An exhausting answer to this discrepancy was obtained through the analysis of the electronic properties of the inhibitors. In the series related to (*S*,*S*)-**1**, activity was proportional to the ability of the 5-substituent to withdraw electrons from the electrophilic carbon, while for the 5-phenyl substituted analogues activity was correlated to the electron density of the aromatic ring. Noticing the proximity of the side chain of Tyr323 to the oxygen atom of the 3-bromoisoxazoline, I thought that introducing a group able to establish interactions in that position could be positive in terms of efficacy. Due to chemical accessibility of compound (±)-**10**, I used it as model compound to replace the 3-bromoisoxazoline warhead with other electrophiles.

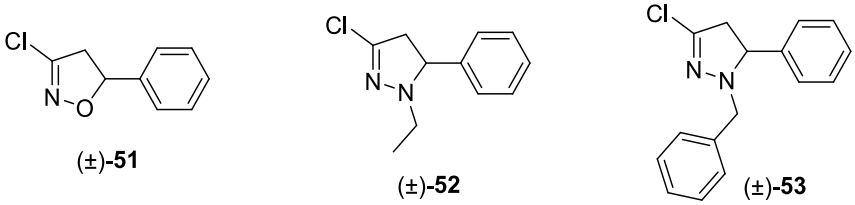

Figure 6. 7 Structures of compounds (±)-**51**, (±)-**52** and (±)-**53**.

In compound (±)-**51** I introduced a 3-chloroisoxazoline, while in compounds (±)-**52** and (±)-**53** a 1-alkyl-3-chloro-pyrazoline, which allowed to introduce an additional position of diversification (fig. 6.7). Compound (±)-**51** was obtained treating (±)-**10** with a 10 M solution of HCl in THF leading to bromine/chlorine exchange. In order to obtain pyrazolines (±)-**52** and (±)-**53**, a one-pot condensation/cyclization reaction between methyl *E*-cinnamate (**54**) and hydrazine was performed, obtaining the key intermediate 5-phenylpyrazolin-3-one [(±)-**55**]. This intermediate was alkylated through reductive amination or nucleophilic substitution obtaining intermediates (±)-**56** and (±)-**57**, which were chlorinated using $POCl_3$ (scheme 6.6). None of these three compounds were able to inhibit *Pf*GAPDH. While for (±)-**51** this confirmed that 3-chloroisoxazoline is less reactive than 3-bromoisoxazoline, compounds (±)-**52** and (±)-**53** inactivities were in contrast with the results obtained during the screening against *Tb*CTPS [39], when some 1-alkyl-3-chloropyrazoline analogues of (*S*,*S*)-**1** showed good inhibition potency toward the isolated CTPS.

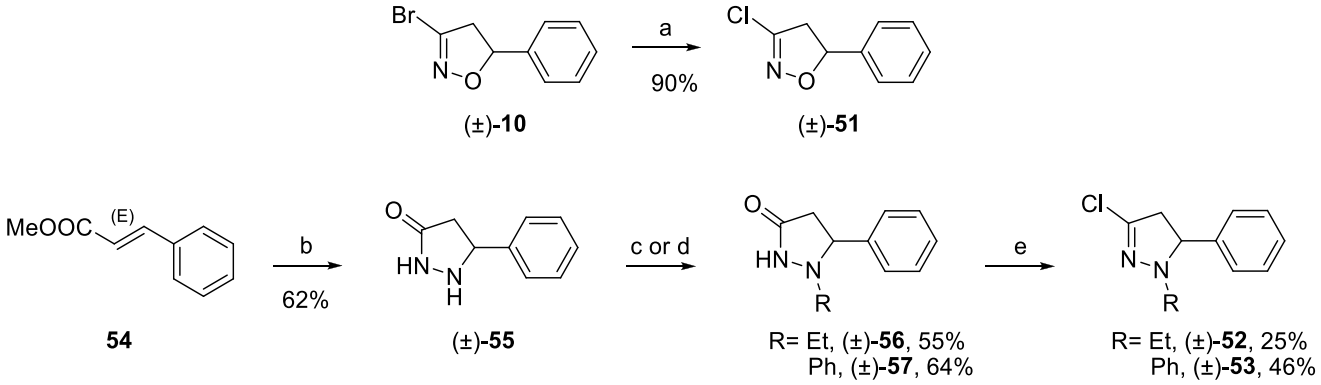

Scheme 6. 6 Synthesis of 3-chloroisoxazoline and 1-alkyl-3-chloro-pyrazoline analogues.

In order to demonstrate that the inhibition of *Pf*GAPDH is due to the alkylation of catalytic Cys residue, an additional study was necessary. Indeed, beside the one involved in catalysis, each monomer of GAPDH possesses 4 reactive cysteine residues (determined upon reaction with iodoacetamide and DTNB) which might, at least in principle, react with the 3-bromoisoxazoline. The enzyme was then incubated with inhibitors and, after extensive dialysis, MS studies of the undigested and digested protein were performed. In the first case, the obtained *m*/*z* values were consistent with alkylation of one cysteine residue for each monomer. MS analysis of the trypsin-digested enzyme, with comparison of predicted fragments, allowed assessing that the alkylated residue was really the catalytic one. This amazing result strengthen the value of 3-bromoisoxazoline as warhead, showing in a very clear way how its balanced reactivity is optimal in the design of covalent targeted inhibitors. [41] Another important question to be sorted out regarded the ability of inhibitors to discriminate between *Pf*GAPDH and *h*GAPDH. Compounds were then assayed on the isolated human isoform and, in this case, a maximum 25% inhibition was observed. This result was, after a careful analysis of all the possible explanations, rationalized by a negative cooperativity effect happening after the binding of the first molecule of inhibitor to GAPDH. While in *P. falciparum* isoform this just reduces the binding affinity (explaining the bifasic rate of inhibition), in the human enzyme it completely prevents further alkylation. Despite a very fast initial phase of inhibition of *h*GAPDH (faster than the one observed for *Pf*GAPDH), the inhibitors I synthesized showed thus a selective action toward the parasitic enzyme. [42] Having a reasonable number of active

compounds in hand, inhibitors were submitted for *in vitro* activity evaluation toward *P. falciparum* cultures. These biological assays were performed by the group of Professor Donatella Taramelli at the University of Milan. D10 and W2 strains of the parasite (chloroquine-sensitive and chloroquine-resistant, respectively) were employed. Some compounds showed submicromolar EC_{50} for both the strains. Without keeping (*S*,*S*)-**1** in consideration, because this compound is likely to exhibit toxic effects through multiple mechanisms, compounds (*S*,*S*)-**8** and (*S*,*S*)-**9** were the other two active compounds. In particular, (*S*,*S*)-**9** showed the highest activity, even greater on the W2 strain. Toxicity toward human cell lines (HMEC-1) was sensibly lower (selectivity index in the range of 10^4).

Table 6. 2 Summary of biological assay for the presented compounds. Please note the different dimensions for IC_{50}.

Compound	***Pf*GAPDH** k_{inact}/K_i **($s^{-1}M^{-1}$)**	***P.falciparum*** **D10 IC_{50} (µM)**	***P.falciparum*** **W2 IC_{50} (µM)**	**HMEC-1** **IC_{50} (mM)**	**Selectivity index**
(*S*,*S*)-**8**	10.7	0.792±0.211	0.880±0.231	34.8±10.4	3.9(10^4)
(±)-**10**	10.3	inact.	inact.		
(*S*,*S*)-**9**	6.6	0.368±0.116	0.259±0.048	>63.9	>17.4(10^4)
(±)-**6**	4.8	inact.	inact.		
(±)-**15**	3.1	inact.	inact.		
(±)-**4**	2.9	/	/		
(*S*,*R*)-**58**	2.6	inact.	inact.		
(*S*,*S*)-**7**	2.6	/	/		
(*S*,*S*)-**1**	0.7	0.346±.079	0.341±0.119	19.7±6.9	5.7(10^4)
(±)-**3**	0.7	/	/		
(*S*,*S*)-**59**	0.63	0.365±0.110	0.476±0.177	14.9±4.3	3.1(10^4)
(±)-**12**	0.47	/	/		
(±)-**17**	0.34	inact.	inact.		
Chloroquine	/	0.0186±0.0057	0.486±0.053		

With the aim of generating more active analogues with improved stability, in view of future development, I synthesized compounds (*S,R*)-**58** and (*S,S*)-**59**, in which the potentially liable benzyl ester is replaced by a benzyl ether or by a benzyl amide, respectively. (*S,R*)-**58** was obtained alkylating (*S,R*)-**40** with benzyl bromide in presence of Ag_2O and deprotecting the obtained product. These conditions proved to be the most effective, among the explored ones (not reported here) for this reaction. Yields were low still acceptable from a drug discovery point of view. Coupling (*S,S*)-**41** to benzylamide using the classical EDC/HOBt procedure and removing the protective group gave compound (*S,S*)-**59** in good overall yield (scheme 6.7).

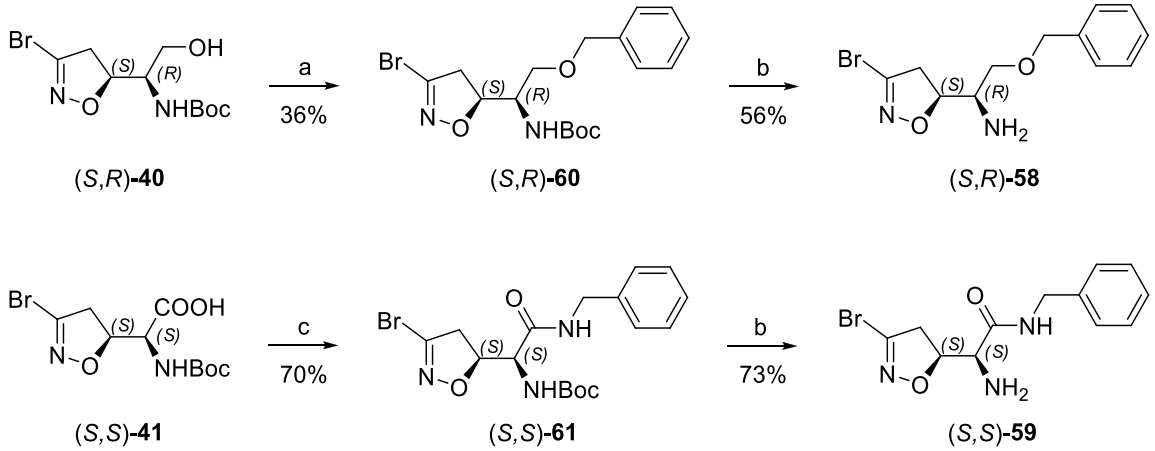

Reagents and conditions: a) BnBr, Ag_2O, dry DMC, r.t., o.n.; b) i. 15% TFA/DCM, r.t., 4h; ii. sat. $NaHCO_3$; c) $BnNH_2$, EDC, HOBt, dry THF, r.t., 2h

Scheme 6. 7 Synthesis of compouds (*S,R*)-**58** and (*S,S*)-**59**.

Following the same synthetic approach, I synthesized amino ethers (*S,R*)-**62**-**64** and amino amides (*S,S*)-**65**-**68** in which the position 4 of the phenyl ring was differently substituted (scheme 6.8). For the synthesis of these compounds, commercial benzyl bromides and benzyl amines were employed. Notably, it was not possible to obtain the compound that derives from the 4-methoxybenzyl bromide. Indeed the 4-methoxybenzyl radical is employed as protective group of alcohols, phenols and carboxylates, and is removed in presence of Ag_2O or strong acids (e.g. TFA), making it unsuitable for the synthesis of a derivative following the above described strategy. Compounds (*S,R*)-**58** and (*S,S*)-**59** were assayed on the isolated enzyme and toward *P. falciparum* cultures. The obtained results were conflicting: while (*S,R*)-**58** displayed higher enzyme inhibition activity toward *Pf*GAPDH, it was inactive *in vitro*, instead (*S,S*)-**59** showed growth inhibition activity comparable to compound (*S,S*)-**9**. I speculated that this discrepancy could be related to a different grade of penetration in parasite cells. Looking at calculated physicochemical properties of the two molecules, I noticed that the calculated pK_a of (*S,R*)-**58** (pK_a 8.5) is greater than the one of (*S,S*)-**59** and (*S,S*)-**9** (pK_a 7.2 and 6.2, respectively). [43] Thus, at physiological pH (7.4) the penetration of (*S,R*)-**57** by simple diffusion is greatly reduced by its higher degree of protonation, although different mechanism of penetration (e.g. active transport) cannot be ruled out at this moment. In vitro studies to assess the membrane penetration properties of (*S,R*)-**58** and (*S,S*)-**59** are currently on going, using the PAMPA assay.

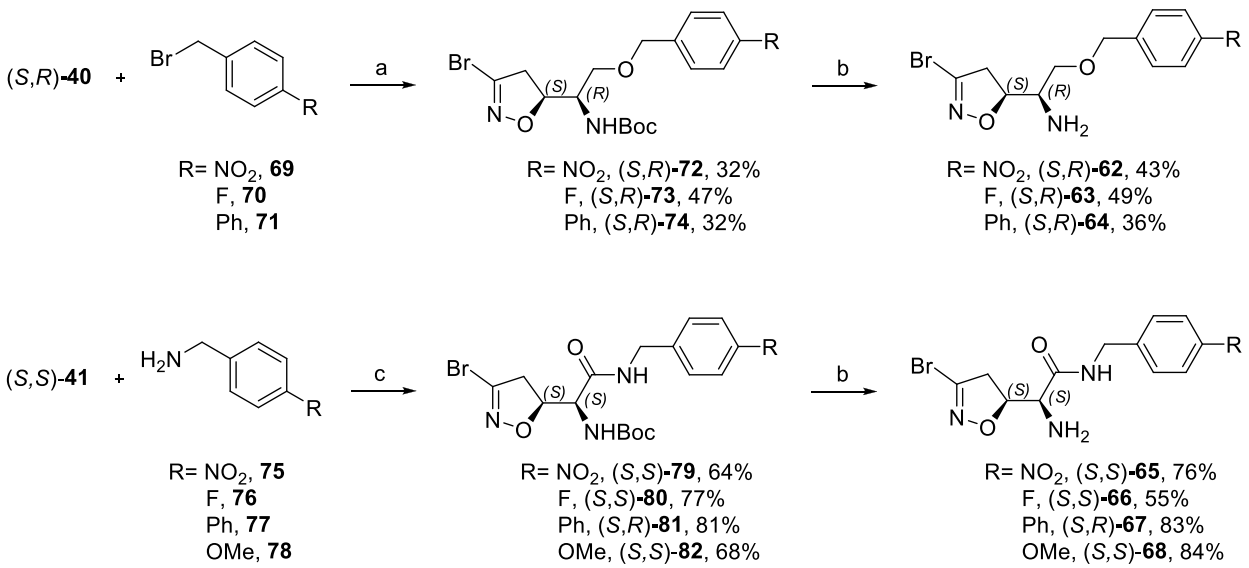

Reagents and conditions: a) Ag_2O, dry DMC, r.t., o.n.; b) i. 15% TFA/DCM, r.t., 4h; ii. sat. $NaHCO_3$; c) EDC, HOBt, dry THF, r.t., 2h

Scheme 6. 8 Synthesis of compounds (*S*,*R*)-**62**-**64** and (*S*,*S*)-**65**-**68**.

Since the most active molecules possessed the benzyl group and a weakly basic amino group, I synthesized compounds (*R*,*S*)-**83** and (*S*,*S*)-**84** in which a sulfone group was introduced between the two functionalities, working as a linker while reducing the basicity of the amine (calc. p*K*a 7.4). To obtain them, alcohol (*S*)-**24** was converted into mesilate (*S*)-**85** and substituted with commercial benzyl mercaptan in presence of a strong base (DBU). The obtained intermediate (*S*)-**86** was used as dipolarophile in the 1,3-dipolar cycloaddition with bromonitrile oxide obtaining the two separable diastereoisomers (*R*,*S*)-**87** and (*R*,*S*)-**88**. Oxidation and deprotection reactions finally allowed me to obtain the desired compounds (scheme 6.9).

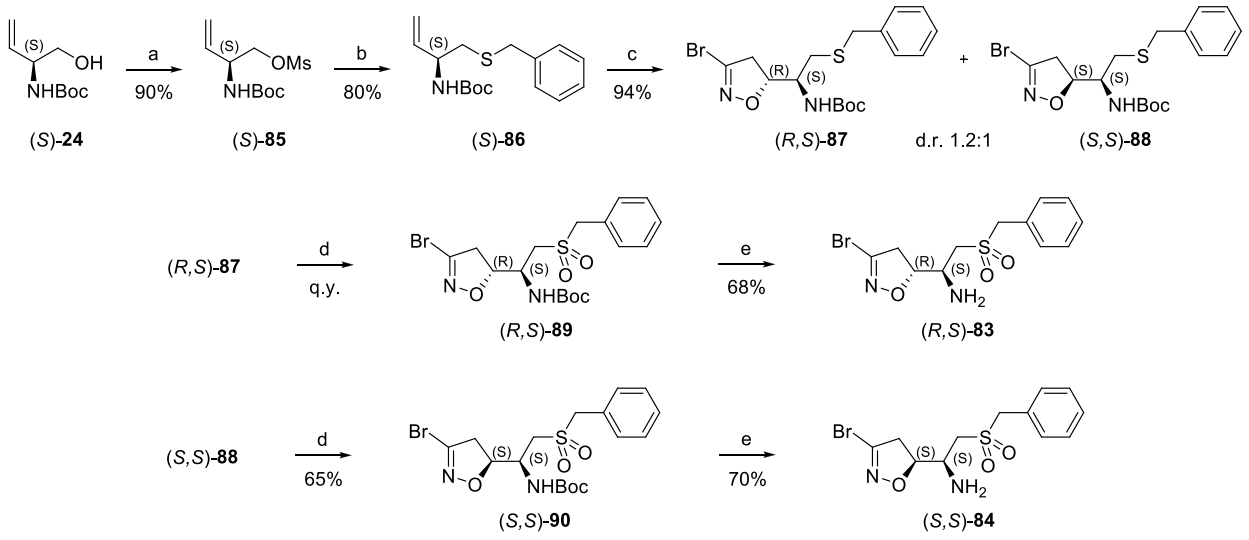

Reagents and conditions: a) MsCl, TEA, DMAP, dry DCM, 0 °C, 10min; b) BnSH, DBU, benzene, r.t., 30min; c) DBF, $NaHCO_3$, EtOAc, r.t., o.n., flash chromatography; d) *m*CPBA, $CHCl_3$, r.t., 10min; e) i. 15% TFA/DCM, r.t., 1h; ii. sat. aq. $NaHCO_3$

Scheme 6. 9 Synthesis of the 1,2-(benzylsulfonyl)amines (*R*,*S*)-**83** and (*S*,*S*)-**84**.

Compounds (*R*,*S*)-**83** and (*R*,*S*)-**84** are currently under evaluation for their activity on isolated *Pf*GAPDH and on parasite cultures.

6.4 A useful biochemical tool

Despite the good results obtained with the described compounds, it cannot be assumed that the observed antiparasitic activity is related (or is only related) to *Pf*GAPDH inhibition. In order to prove it, there are two possible approaches:

- using GAPDH knockout *P. falciparum* strains the antiparasitic activity of the compounds should be abolished; if instead cells are not viable, they should present similar cellular effects to the one observed during the exposure to compounds;
- since described inhibitors showed irreversible binding, isolating bound enzymes after incubation and performing a proteomic study would allow to identify all the inactivated molecules, which may underlie cell death.

The second strategy represents a more convenient way to assess the hypothesis that active compounds killed *P. falciparum* cell through GAPDH inhibition. The major problem is associated with purification of the enzyme-compound adducts from a complex mixture. Therefore, I decided to link the 3-Br-isoxazoline scaffold, present in all the active compounds, to biotin, which is a molecule well-known for its very high affinity to streptavidin. I synthesized molecule (*S*,*S*,*S*,*S*,R)-**91** in which a 1,5-pentyldiamine spacer links biotin to the carboxylate of (*S*,*S*)-**1**. In this way I obtained three desired effects:

- the distance between biotin and the inhibitor is long enough to expect no perturbation of the binding with *Pf*GAPDH;
- the two moieties are linked through stable (at least for *in-vitro* conditions) amide bonds which will prevent dissociation;
- the absence of an amino acidic group, due to conversion of the carboxylate into an amide, prevents binding to CTPS and other glutamine-dependent enzymes known to interact with Br-Acivicin.

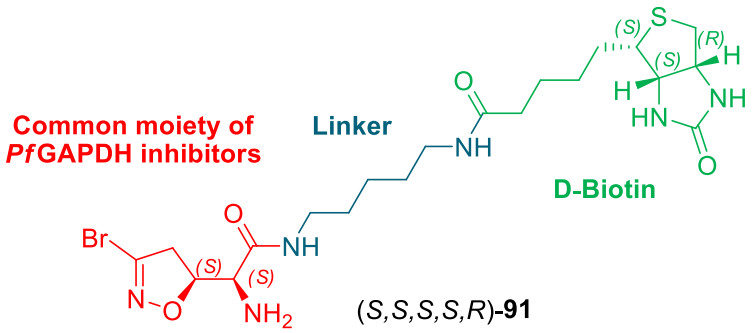

(*S*,*S*,*S*,*S*,*R*)-**91**

As minor drawback, this way of linking biotin to compounds is known to reduce cell permeation; working on cell lysates is then necessary to obtain reliable results. [44] The synthesis of this molecule started from the coupling of commercial *N*-Boc cadaverine (**92**) and biotin ((*S*,*S*,R)-**93**) using the common EDAC/HOBt chemistry. Deprotection of (*S*,*S*,R)-**94** gave the pure amine (*S*,*S*,R)-**95** which was coupled to (*S*,*S*)-**41** with the above reported reagents. *tert*-Butoxycarbonyl protective group of **96** was finally removed under acidic conditions and (*S*,*S*,*S*,*S*,R)-**91** obtained and used as a trifluoroacetate salt (scheme 6.10).

The compound showed inhibition toward *Pf*GAPDH and the planned biochemical studies are still in progress at the University of Parma (in collaboration with the group of Prof. Stefano Bruno), therefore I cannot report the results of this investigation.

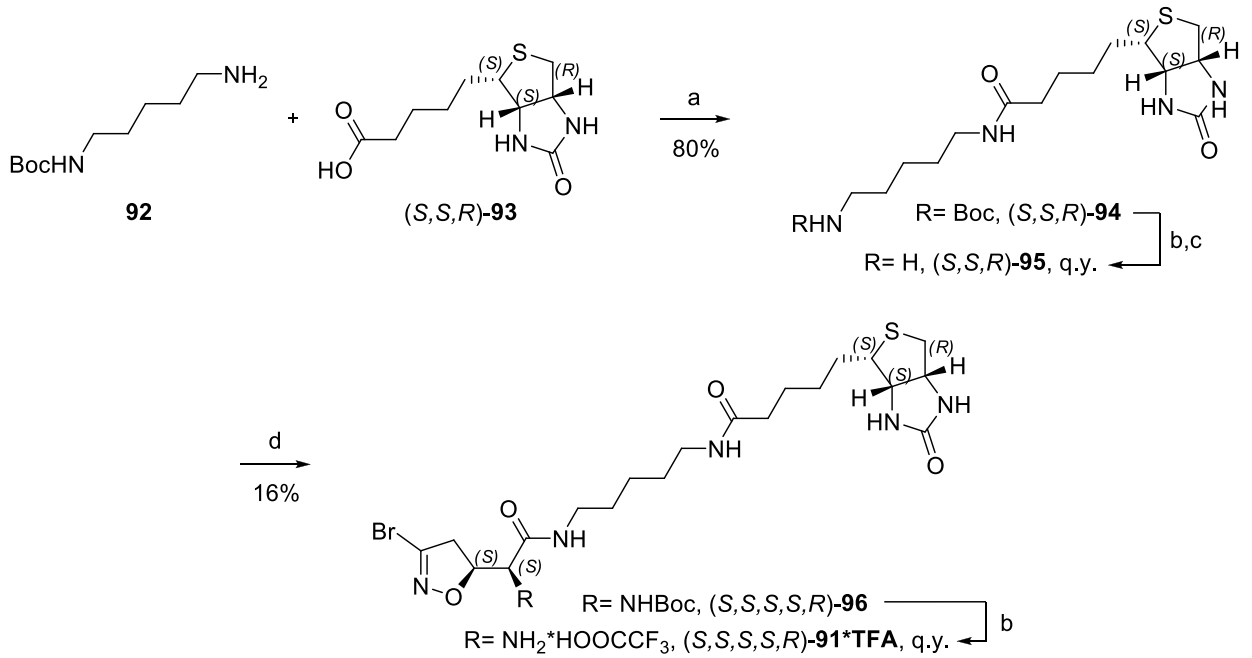

Reagents and conditions: a) EDAC, HOBt, TEA, DMF, r.t., o.n.; b) 30% TFA/DCM, r.t., o.n.; c) K_2HCO_3, 1:1 $CHCl_3$/MeOH, r.t., 30min; d) (*S*,*S*)-**41**, EDAC, HOBt, TEA, DCM, DMF, r.t., o.n.

Scheme 6. 8 Synthesis of compound (*S*,*S*,*S*,*S*,*R*)-**91*TFA**

7. Inhibitors of *Trypanosoma brucei* cathepsin L-like protease (*Tb*CatL or rhodesain)

Rhodesain is the major cysteine protease in *T. brucei*. [45] In addition to proteolytic activity, it participates to several other functions which are essential for the virulence and defense of the parasite. In the past, several covalent inhibitors have been described; among the most potent, are the ones characterized by a peptidic recognition moiety mimicking the natural substrate coupled to an electrophilic warhead. In this chapter I describe the synthesis of new *Tb*CatL inhibitors inspired by known azadipeptide nitriles and containing the promising 3-bromoisoxazoline warhead. This project was performed in collaboration with Dr. Roberta Ettari from University of Messina. My major role in this work was the synthesis of the warhead in racemic and enantiopure form.

7.1 The multiple roles of *Tb*CatL [46] [47]

Rhodesain consists of a single peptide chain (215 amino acid residues in total) which folds creating two distinct domains. Between them, located in a cleft, is the catalytic triad Cys25/His162/Asn182. As seen in other proteases, the catalytic Cys residue is activated by His, which works as a base catalyst; Asn, through a hydrogen bond, stabilizes the correct tautomer of the His imidazole ring for catalysis. In addition to proteolysis, the activity of *Tb*CatL has been linked to the ability of the parasite to cross the BBB and to variant surface glycoproteins (VSGs) turnover. As mentioned before, invasion of the CNS by *T. brucei* represents the critical point of HAT: this phase presents indeed the most severe symptomatology and often resolves with the death of the patient. It seems that this BBB penetration is facilitated by the activation of G_q-protein-coupled receptors (known as protease activated receptors) by rhodesain. Variant surface glycoproteins coat the cell membrane of the parasites preventing the host's immune system to reach surface epitopes. VSGs are themselves antigenic but their periodic modification allows the parasite to evade immune response, rendering also the development of a vaccine impossible. Another hypothesized role of *Tb*CatL is the extracellular degradation of host's immunoglobulins, further reducing the efficacy of immune response. Keeping all this in mind, rhodesain clearly appears a central tool of the parasite and its inhibition may be a successful approach for the treatment of such harsh disease.

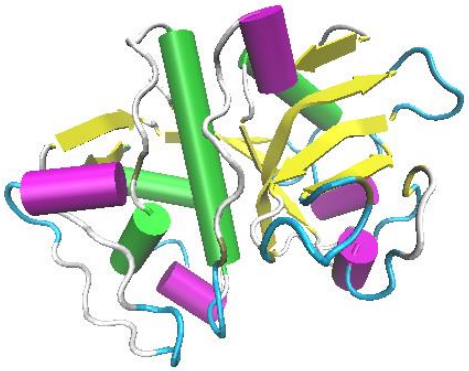

Figure 7. 1 Cartoon representation of rhodesain (PDB 2P86). The different secondary structures are depicted in different colours.

7.2 Peptide inhibitors of *Tb*CatL

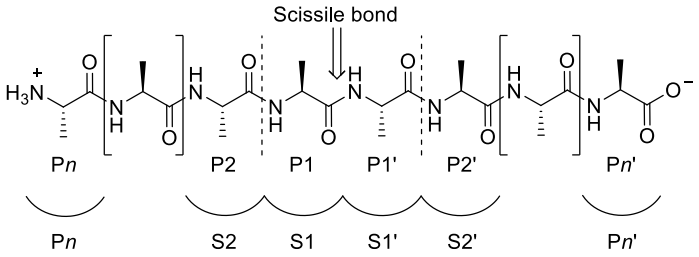

Figure 7. 2 Numbering method used for substrate residues and binding sites of proteases.

Before describing some examples of peptide-based inhibitors, it is necessary to introduce some nomenclature. Both the enzyme pocket and the substrate residues (indicated with letters S and P, respectively) are numbered according to their position with regards to the scissile bond. Numbering goes from 1 to *n* toward the *N*-terminus of the substrate and from 1' to *n*' toward the *C*-terminus of the substrate (fig. 7.2). This way of indicating inhibitor subunits greatly helps the discussion of the structure-activity relationships. I will now describe some class of peptide inhibitors following a classification based on the chemical properties of their warheads.

7.2.1 Aldehyde and ketone derivatives

These inhibitors possess an aldehyde or an alkylmethyl-/diazomethyl-ketone as reversible or irreversible warhead, respectively. Their recognition moiety is represented by a dipeptide containing lipophilic residues in the P1 and P2 sites. k_{inact}/K_i values of these inhibitors are in the 10^8-10^7 $min^{-1}M^{-1}$ range; some of them also showed trypanocidal activity *in vitro*. Cbz-Phe-Ala-CHN_2 (**89**), Cbz-Phe-Phe-CHN_2 (**90**) and Cbz-Phe-Phe-CH_2Cl (**91**) are ketone derivatives that showed potent enzyme inhibition and growth inhibition of *T. b. brucei* (a subspecies non infective for humans) in the micromolar range (6.1, 4.8 and 3.6 µM, respectively). Two peptidyl aldehydes, Cbz-Phe-Tyr-CHO (**92**) and 1-NapSO_2-Ile-Trp-CHO (**93**), showed higher potency on the enzyme and **93** showed great antiproliferative activity (ED_{50}= 18 nM).

7.2.2 Michael acceptor derivatives

In this group, we find the well characterized vinyl sulfone irreversible inhibitors (fig. 7.3). The structure of these inhibitors allowed to investigate the preference for S1' occupancy, showing that the introduction of a phenyl ring with a short linker is positive for enzyme inhibition (R= OPh, CH_2Ph, Ph), while a longer linker (R= CH_2CH_2Ph) or the modification of the sulfone in a sulphonamide (R= NHPh) reduces the activity. Regarding the S2 pocket, it showed preference for large hydrophobic residues (R'= *i*Bu, Bn). In addition to Cbz (R''= OBn), other groups have been introduced in the P3 site. Despite lower enzyme inhibition, introduction of groups such as morpholine or 4-methyl-pyperazine through a urea linker improve pharmacokinetic properties of the inhibitors, such as oral bioavailability. Another group of inhibitors reported in literature are polypeptides characterized by the presence of fumaric acid acting as electrophile. The most potent ones bear hydrophobic residues (Ile, Phe, Chg) at the P2 position and Asn or Glu at the P1 site. Unfortunately, these compounds were not active on *T. b. brucei* cultures, probably because of stability or cell penetration problems. Other acrylic and crotonic acid derivatives have been described but some of them behave as non covalent inhibitors.

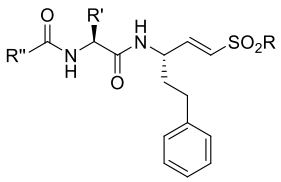

Figure 7. 3 General structure of vinyl sulfone inhibitors.

7.2.3 Constrained heterocycle derivatives

In this class of inhibitors the warhead is represented by an electrophilic 3-term heterocycle (α,β-epoxyester, aziridine *trans*-2,3-dicarboxylate). The epoxide derivatives were linked to the CbzPhe-HPhe recognition moiety and showed good enzyme inhibition and promising *in vitro* activity (micromolar *T. b. brucei* IC_{50} and significant selectivity toxicity, compared to human cell lines growth inhibition). Aziridines, instead, were characterized by a dipeptide, containing a cyclic α or β amino acid, linked to the heterocyclic nitrogen. The two esters, usually benzyl esters, should be in *trans* configuration for covalent inhibition. Despite promising activity toward isolated *Tb*CatL, trypanocidal activity of these compounds is just modest.

7.2.4 Nitrile derivatives

In these compounds, the Cα of the amino acid residue in the P1 position is replaced by a tertiary nitrogen, which binds an alkyl residue and the reactive nitrile. These inhibitors react with Cys giving, in a reversible way, an isothiosemicarbazide adduct. The occupancy preferences are a methyl group at P1 and, confirming precedent observations, a large hydrophobic Phe or Leu residue at P2. At the enzyme level, strong inhibition was observed for compounds carrying at the P3 position a *tert*-butyl carbamate (IC_{50}= 0.06 nM, the most potent inhibitor, fig. 7.4), a benzyl carbamate and a benzodioxane Some inhibitors showed good inhibition of the parasites *in vitro* with a good correlation with the enzyme inhibitory activity. This might be due to optimal penetration into cells and to an increased proteolytic stability, because of the presence of the methylated nitrogen at the peptide bond between the P1 and P2 residue.

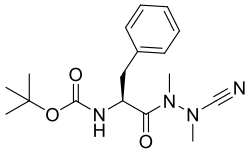

Figure 7. 4 Structure of the most potent *Tb*CatL inhibitor, characterized by the azadipeptide nitrile warhead.

7.3 Design and synthesis of 3-bromoisoxazoline inhibitors [48]

Despite the great number of different warhead used in the development of peptidic covalent *Tb*CatL inhibitors, 3-bromoisoxazoline was never exploited in any series. Because of the interesting properties of this electrophile, I planned to couple this warhead to known recognition moieties. In particular, I noticed a similarity between the azanitrile and the bicyclic compound (±)-**6** (fig. 7.5). In particular, the CH_2 of the pyrrolidine ring nicely mimics the methyl bound to the nitrogen involved in the peptidic bond and the distances between the nitrogen and the electrophilic carbon are comparable. The designed inhibitors are then characterized by the presence of the bicyclic scaffold containing the 3-bromoisoxazoline at the P1 site, different amino acid residues at the P2 site (Leu, Phe, homoPhe, given the above discussed preferences of the S2 binding pocket of rhodesain) and different carbamates at the P3 site (fig. 7.6). The planned synthetic scheme involves the carbamoylation of the desired enantiopure aminoester, followed by ester hydrolysis. The obtained acid is then coupled to amine (±)-**148**, obtained from the deprotection of (±)-**6**, using EDC/HOBt to prevent

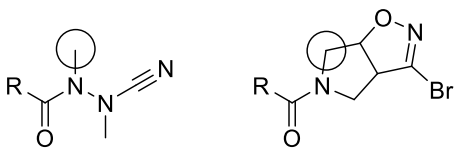

Figure 7. 5 Comparison of the azanitrile warhead and the bicyclic compound **6**.

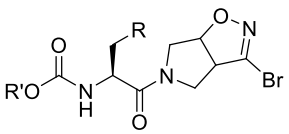

R= *i*Pr, Phe, Bn
R'= *n*Pr, allyl, *t*Bu, Bn,

Figure 7. 6 Structure of designed inhibitors.

racemization (scheme 7.1). Compounds were initially obtained and assayed as diastereoisomeric mixtures because of the impossibility of purification using conventional methods. For some of the more interesting pairs, the single diastereoisomers were synthesized starting from enantiopure (*R,R*)-**6** and (*S,S*)-**6**, in turn obtained after chiral HPLC resolution [see schemes 6.4 and 6.5 for the synthesis of (±)-**6**]. In particular, compounds synthesized as single enantiomers are (*S,S,S*)-**126**, (*S,R,R*)-**127**, (*S,S,S*)-**134**, (*S,R,R*)-**135**, (*S,S,S*)-**142** and (*S,R,R*)-**143**.

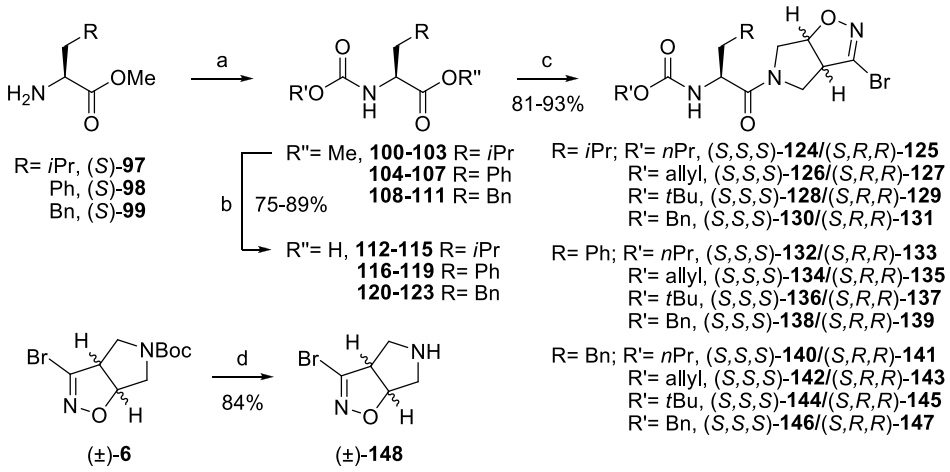

Reagents and conditions: a) R'OCOCl, aq. $NaHCO_3$/dioxane (7:3), r.t., 12h or Boc_2O, TEA, DCM, r.t., 12h; b) LiOH, MeOH/H_2O (1:1), r.t., 8h; c) (±)-**148**, EDCI, HOBt, DIPEA, DMF/DCM, r.t., 12h; d) 30% TFA/DCM, r.t., 4h

Scheme 7. 1 Synthetic scheme for the 3-bromoisoxazoline inhibitors.

7.4 Biological evaluation

The new compounds were assayed on the isolated enzyme (table 7.1). The most active mixture was the one bearing the allyl carbamate at the P3 site and the homoPhe at the P2 site [(*S,S,S*)-**142**/(*S,R,R*)-**143**]. The activity decreased when the homoPhe was replaced by other residues, while it was completely lost varying the carbamate substituent. When Phe is present at the P2 site, both allyl and benzyl carbamates are tolerated, while only allyl and *tert*-butyl carbamates are compatible with Leu at the P2 site. The single diastereoisomers assayed displayed similar enzyme inhibition, indicating that the configuration of the two bridging carbons in the warhead plays a marginal role.

The same compounds were assayed on *h*CatB and *h*CatL and none of them showed inhibition up to a concentration of 100 µM, highlighting great selectivity. Active compounds were also evaluated *in vitro* against *T. b. brucei* cultures and J774.1 mouse macrophages. The active compounds, although with modest potency, were the diastereoisomeric mixture (*S,S,S*)-**138**/(*S,R,R*)-**139** (IC_{50}= 16.45 µM) and (*S,R,R*)-**143** (IC_{50}= 32.04 µM). Interestingly none of the compounds exerted toxic effects toward mammalian cells (IC_{50}> 100 µM).

Table 7. 1 Inhibitory data of the presented compounds against rhodesain.

Compound	*Tb*CatL K_i (μM) or % inhibition at 100 μM	Compound	*Tb*CatL K_i (μM) or % inhibition at 100 μM
(*S*,*S*,*S*)-**124**/(*S*,*R*,*R*)-**125**	11.3%	(*S*,*R*,*R*)-**135**	15.14 ± 0.16
(*S*,*S*,*S*)-**126**/(*S*,*R*,*R*)-**127**	8.36 ± 0.63	(*S*,*S*,*S*)-**136**/(*S*,*R*,*R*)-**137**	17.73 ± 1.19
(*S*,*S*,*S*)-**126**	8.52 ± 0.57	(*S*,*S*,*S*)-**138**/(*S*,*R*,*R*)-**139**	8.41 ± 0.09
(*S*,*R*,*R*)-**127**	9.05 ± 0.08	(*S*,*S*,*S*)-**140**/(*S*,*R*,*R*)-**141**	15.3%
(*S*,*S*,*S*)-**128**/(*S*,*R*,*R*)-**129**	13.6 ± 0.35	(*S*,*S*,*S*)-**142**/(*S*,*R*,*R*)-**143**	2.62 ± 0.21
(*S*,*S*,*S*)-**130**/(*S*,*R*,*R*)-**131**	8.3%	(*S*,*S*,*S*)-**142**	3.35 ± 0.12
(*S*,*S*,*S*)-**132**/(*S*,*R*,*R*)-**133**	13.1%	(*S*,*R*,*R*)-**143**	2.73 ± 0.29
(*S*,*S*,*S*)-**134**/(*S*,*R*,*R*)-**135**	16.78 ± 0.09	(*S*,*S*,*S*)-**144**/(*S*,*R*,*R*)-**145**	5.8%
(*S*,*S*,*S*)-**134**	16.58 ± 0.59	(*S*,*S*,*S*)-**146**/(*S*,*R*,*R*)-**147**	No inhibition

7.5 Discussion

As often seen in the development of new antiparasitic drugs, promising activity against the target is not always reflected in antiparasitic activity, probably because of poor cell penetration. Covalent docking studies allowed to understand the relationships between P2 and P3 substituents. In particular, in the case of bulky P2 substituent (homoPhe), a small group (e.g. allyl carbamate) at P3 is preferred; when the P2 residue is less bulky (Phe), an aromatic substituent at P3 (e.g. benzyl carbamate) is instead preferred. This demand is very likely due to the relative sizes of the S2 and S3 pockets. Interestingly, this was confirmed by the observation that inhibitors having the Leu residue at the P2 site place the side chain in the S2 or in the S3 pocket depending on the different P3 substituent. The ability of the P2 and P3 substituents to exchange the binding with their relative binding pockets may be also the reason for the similar activities of the single diastereoisomers. These results represent the basis for future development of 3-bromoisoxazoline based covalent inhibitors of rhodesain. The moderate activity could be enhanced with proper modifications suggested by the performed docking studies, obtaining more potent compounds while preserving the already remarkable high selectivity.

8. Inhibitors of *Trypanosoma brucei* N^5,N^{10}-methylenetetrahydrofolate dehydrogenase/cyclohydrolase (*Tb*DHCH or *Tb*FolD) [49]

In this chapter I describe the synthesis of *Tb*DHCH inhibitors. Despite the importance of this enzyme in *T-brucei* metabolism, it has never been taken in consideration as a target by medicinal chemists.

8.1 The crucial role of DHCH in *T. brucei* folate metabolism

Folates are versatile molecules which are widely exploited from living beings as cofactors that carry monocarbon units. In medicinal chemistry, folate pathway has always represented an amazing source of biological targets, ranging from biosynthetic to reductive enzymes. Successful examples of drugs are sulphonamides (DHPS inhibitors) and trimethoprim and methotrexate (DHFR inhibitors). The great diversities in the pathway and in enzyme isoforms from different organisms are at the basis of the achievements obtained in this field. For example, sulphonamides are not toxic to humans because we do not possess the enzymes, such as DHPS, necessary for the synthesis of folates, while selectivity of DHFR inhibitors is due to the differences in structure among microbial and human orthologs. In contrast to different organisms, in *T. brucei* the folate pathway is relatively simple (scheme 8.1). The parasite assumes folates from the environment and reduces it mainly through DHFR activity (in *T. brucei* this enzyme is fused with a thymidilate synthase, TS) to dihydrofolate (H_2F) and tetrahydrofolate (H_4F). Another enzyme, pteridine reductase-1 (PTR-1), offers an alternative to DHFR-TS for the reduction of folates. H_4F is the central point of the folate cofactor network. It can be modified by different enzymes generating derivatives bringing a monocarbon unit at different states of oxidation. By intervention of the glycine cleavage complex (GCC; *T. brucei* do not possess any serine hydroxymethyl transferase, SHMT), it is converted to N^5,N^{10}-methylenetetrahydrofolate (N^5,N^{10}-CH_2-H_4F). This cofactor can be used from TS for the conversion of deoxyuridine monophosphate (dUMP) to deoxythymidine monophosphate (dTMP) regenerating H_2F. Another destiny of N^5,N^{10}-CH_2-H_4F is its oxidation to N^{10}-formyltetrahydrofolate (N^{10}-CHO-H_4F). In human, this cofactor can be synthesized by the intervention of different enzymes: a cytoplasmatic C1-tetrahydrofolate synthase (MTHFD1) possesses methylenetetrahydrofolate dehydrogenase, methylenetetrahydrofolate cyclohydrolase and formate-tetrahydrofolate ligase activities, while in mitochondrial two bifunctional enzymes with dehydrogenase/cyclohydrolase activity (MTHFD2 and MTHFD2L) and a monofunctional

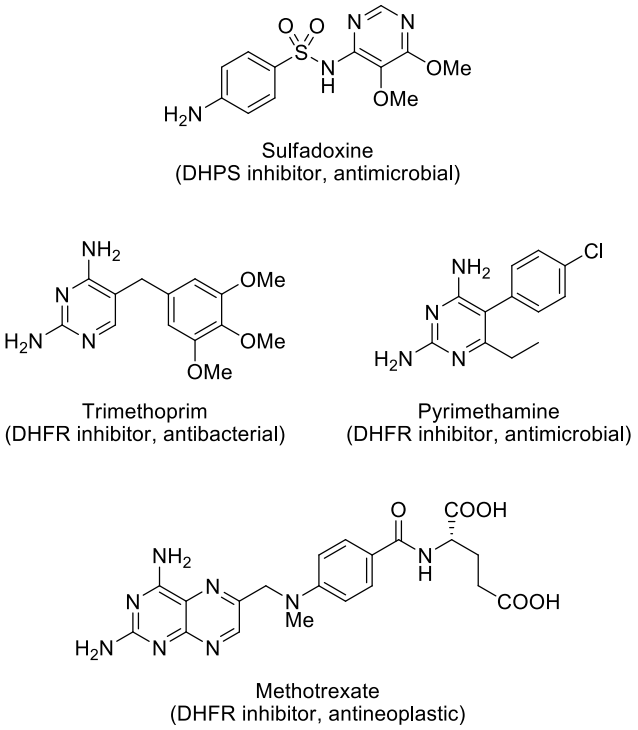

Figure 8. 1 Antifolates in clinical use. The target and the application of each compound are reported in brackets.

formate-tetrahydrofolate ligase (MTHFD1L) are present. [50] In *T. brucei*, in contrast, only N^5,N^{10}-methylenetetrahydrofolate dehydrogenase/cyclohydrolase (DHCH or FolD) possesses this activity. *Tb*DHCH is a bifunctional enzyme, it catalyzes two subsequently reaction in the same catalytic site. The first reaction is the oxidation of N^5,N^{10}-CH_2-H_4F to N^5,N^{10}-methenyltetrahydrofolate (N^5,N^{10}-CH^+-H_4F), with reduction of $NADP^+$. Following, N^5,N^{10}-CH^+-H_4F is hydrolysed to the final product N^{10}-CHO-H_4F. This cofactor is essential for the methylation of the initial methionyl-$tRNA^{Met}$ in the fMet-$tRNA^{Met}$, the initiator amino acyl-tRNA in the mRNA translation process. This reaction is catalysed by formyl methionyl transferase (FMT) and the cofactor is released as H_4F. Any involvement of N^{10}-CHO-H_4F in purines biosynthesis, differently from many organisms, is discarded since *T. brucei* only depends of foreign sources of purines. Interestingly, DHCH has been validated as target for the treatment of bacterial infections [51] and, through genetic and chemical approaches, for the treatment or *L. major* infections, [52] a protozoan parasite related to *T. brucei*. Because of these evidences, I decided to investigate *Tb*DHCH as a target. I selected molecule LY374571 [(*S*)-**149**], developed as a potential antineoplastic from Ely Lilly researchers, [53] as model compound for the development of a new series of inhibitors.

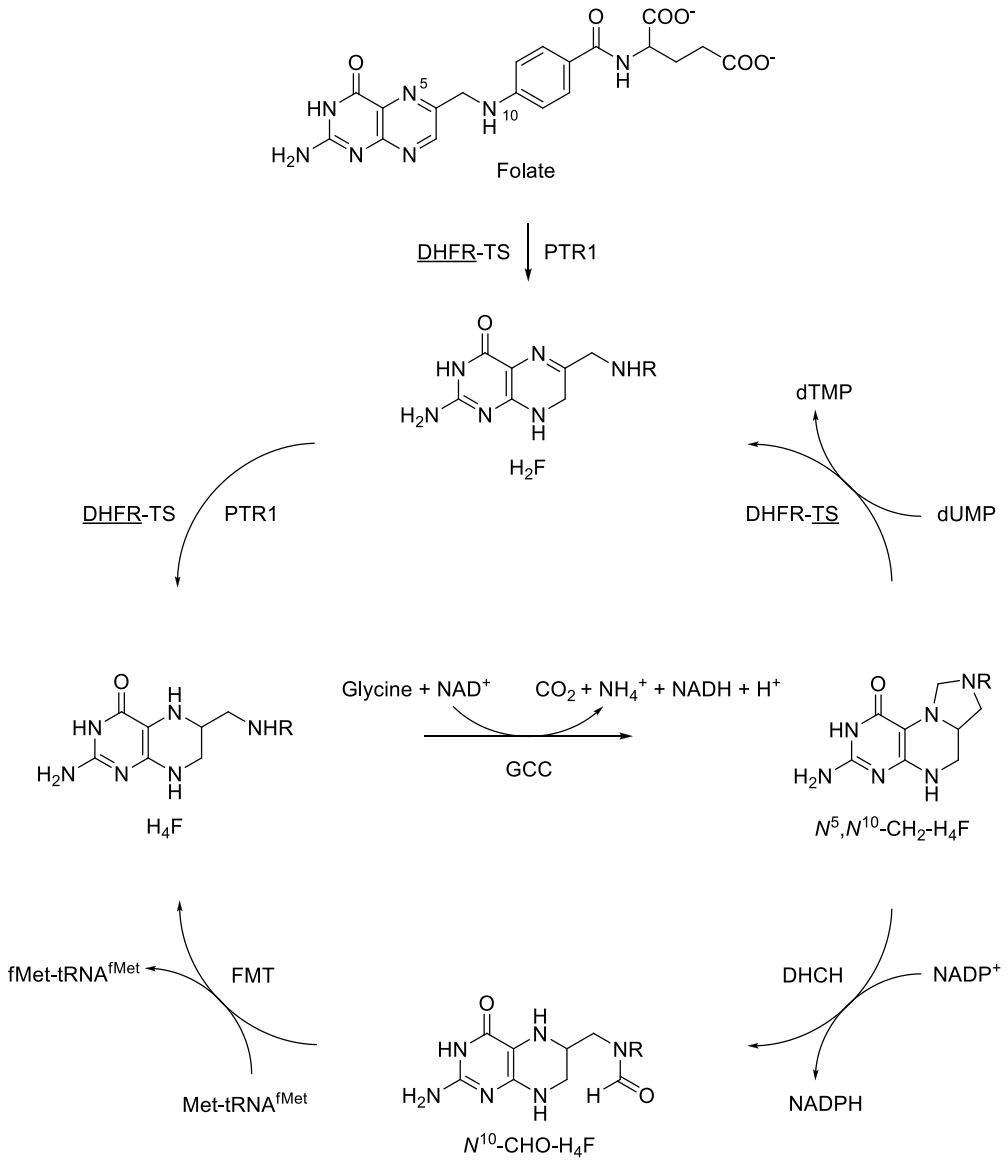

Scheme 8. 1 Folate pathway in *Trypanosoma brucei*.

8.2 Reassignment of LY374571 structure

I started this project synthesizing compound (*S*)-**149**, following the reported synthetic procedure. [53] The first step in the synthesis was the reaction of the 2,5,6-triaminopyrimidin-4-ol (**150**) with the ethyl 4-isocyanatebenzoate (**151**) forming the urea derivative **152**. Although, as described, I obtained a single product, I found out that it possessed a different connectivity from the one of described in the literature for this intermediate. The obtained structure observed by NOE NMR experiments, corresponded to that of intermediate **153** instead of **152**. Indeed, the predicted nucleophilicity of the nitrogens anticipates the formation of **153** rather than **152**, supporting my result. To unequivocally confirm the new structural assignment, I submitted the compound to X-ray crystallography. In collaboration with Dr. Leonardo Lo Presti (University of Milan), I was thus able to unambiguously determine the structure of the intermediate, which indeed possessed the connectivity described by the chemical strucutre **153** (fig. 8.1).

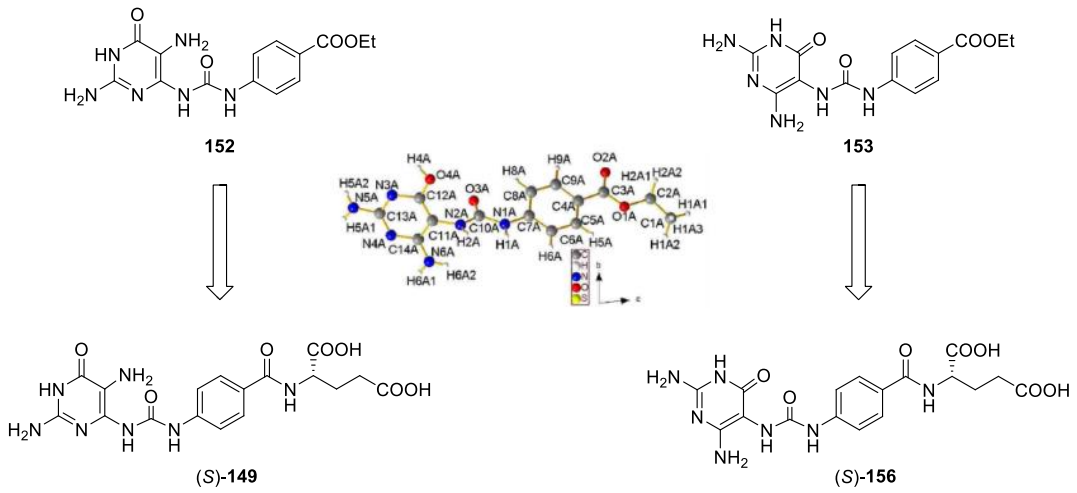

Figure 8. 2 XRD of the crystal of the product of the first reaction in the synthetic procedure revealed connectivity of intermediate **153** (different from described intermediate **152**). This will ultimately lead to product (*S*)-**156**.

The ester was then hydrolysed and the resulting acid (**154**) was coupled with (*S*)-glutamate diethylester hydrochloride [(*S*)-**158**] following a procedure based on the use of CDMT and NMM. Intermediate (*S*)-**155** was finally hydrolysed obtaining the desired product (*S*)-**156**, which describes the actual structure of LY374571 (scheme 8.2). In a previous study, a strange electronic density was observed from the X-ray co-crystal structure of (*S*)-**149** with the DHCH of *Acinetobacter baumanii*. [54] In particular, the researchers observed a structure similar to (*S*)-**156** rather than (*S*)-**149**; with my work I have corroborated the hypothesis that the structure attributed to LY374571 was not correct.

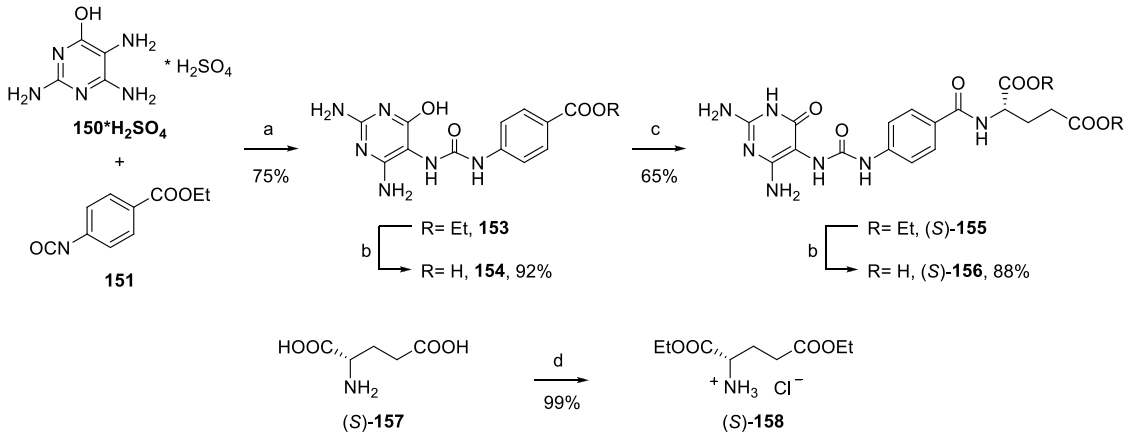

Reagents and conditions: a) 1M aq NaOH, MeCN; b) i. 1M aq NaOH; ii. 1M aq HCl; c) NMM, CDMT, (*S*)-**137**, dry DMF; d) $SOCl_2$, EtOH

Scheme 8. 2 Synthetic scheme for compound (*S*)-**156**.

8.3 Design and synthesis of analogues of (*S*)-156

Based on the observation that the synthetic intermediate **154** showed a notable enzyme inhibition (60% at 100 μM), I hypothesized that the glutamate residue of (*S*)-**156** could be replaced by other groups. I then decided to perform a structure activity relationship study of this compound focusing on the amino acid tail. In the design of new inhibitors, I exploited classical medicinal chemistry strategies such as simplification, homologation and addition of aromatic rings that can establish additional interactions with the target. Some of the used amino esters were commercially available while others were synthesized from the corresponding amino acid (scheme 8.3). With the aim of understanding the optimal distance between the two carboxylates, I synthesized the derivative coupled with (*S*)-aspartic acid [(*S*)-**175**] and with (*S*)-2-aminoadipate [(*S*)-**176**], the lower and the higher homologs of (*S*)-glutamate, respectively. I also synthesized analogues in which the proximal or the distal carboxylate is removed: this was achieved using γ-amino butyrate and (*S*)-alanine as amino acid tails [compounds **177** and (*S*)-**178**, respectively]. Among this subset of analogues, I synthesized a derivative in which only the distal group is present but only two methylenes separate it from the amino group (β-alanine residue, compound **179**). Lastly, (*S*)-phenylalanine and (*S*)-tyrosine were exploited as amino acidic tails [compounds (*S*)-**180** and (*S*)-**181**, respectively]. The phenyl ring of these derivatives may establish interactions with the amino acid residues present in the active site, such as π-π interactions or π-cation interactions, giving a stronger binding to the enzyme. Moreover, (*S*)-**181** presents a hydroxyl group, able to form hydrogen bonds with the amino acid residues or with the NH or CO groups of the enzyme backbone. The synthesis of these analogues followed the one described for (*S*)-**156** with the use of the desired amino ester (ethyl or methyl ester) in the coupling step with **154**.

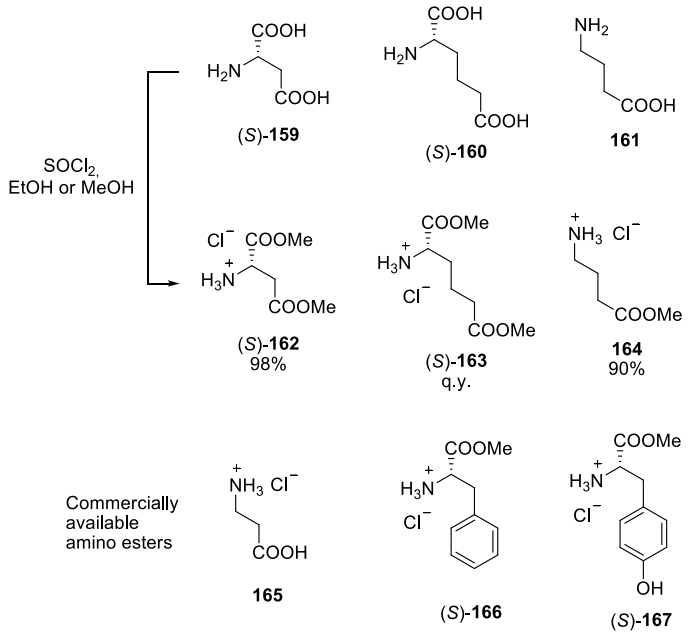

Scheme 8. 3 Amino esters hydrochloride employed in the SAR study. Above: synthesized ones; below: purchased ones.

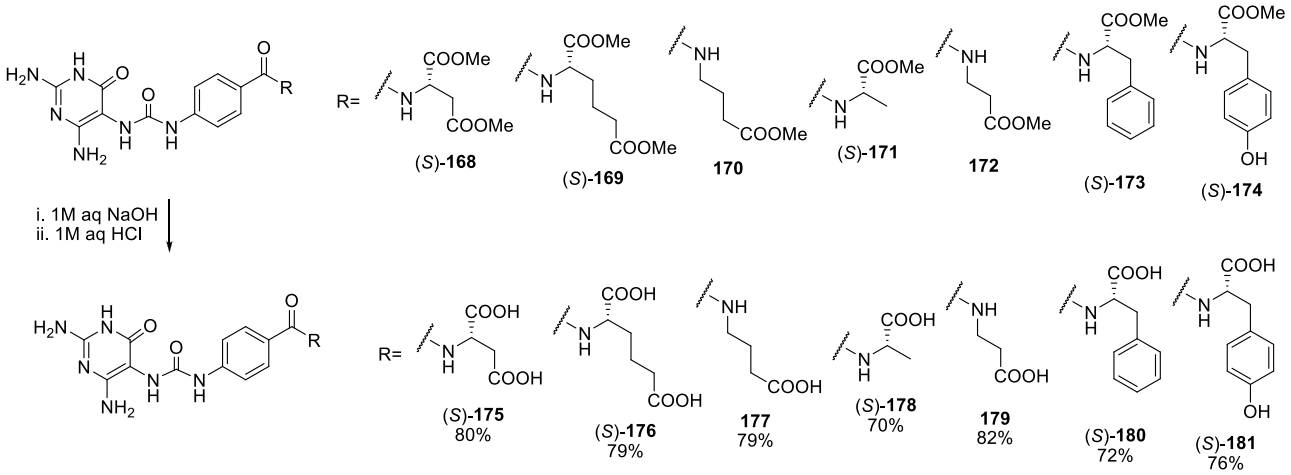

Scheme 8. 4 Synthesis of analogues of (*S*)-**156**.

8.4 Biological assays

A subset of the presented compounds [(*S*)-**156**, (*S*)-**176**, **177**, (*S*)-**178**, (*S*)-**180** and (*S*)-**181**] were assayed on isolated *Tb*DHCH. With the exception of **177**, all showed a competitive micro/submicromolar inhibition of the enzyme, remarking the importance of the proximal carboxylate for activity. Compounds (*S*)-**176** and (*S*)-**180** were about two times more potent than the model compound (*S*)-**156**, indicating that the distal carboxyl group can be moved to a different distance or it can be removed. The difference in activity between (*S*)-**180** and (*S*)-**181** could be due to a steric clash between the hydroxyl group of (*S*)-**181** and a residue in the active site. The compounds were assayed on *T. brucei* cultures and only (*S*)-**156** showed a weak growth inhibition. This result was very disappointing considering the promising activities of the analogues towards the enzyme. A good result is the relative low toxicity of these compounds toward human cell cultures (THP1 macrophages were used).

Table 8. 1 Resume of the biological assays (against isolated enzyme, *T. brucei* and human macrophages cultures).

Compound	*Tb*DHCH K_i (μM)	*T. brucei* IC_{50} (μM)	THP1 IC_{50} (μM)
(*S*)-**156**	1.1 ± 0.8	49 ± 3.2	194 ± 8.2
(*S*)-**176**	0.48 ± 0.7	No inhibition	90 ± 16
177	168 ± 8.5	No inhibition	98 ± 12
(*S*)-**178**	3.2 ± 0.3	No inhibition	113 ± 17
(*S*)-**180**	0.54 ± 0.08	No inhibition	94 ± 8
(*S*)-**181**	7.3 ± 0.7	No inhibition	77 ± 7

8.5 *Tb*DHCH crystal structure and computational docking studies

The group of Professor William N. Hunter determined the structure of *Tb*DHCH in ternary complex with compound (*S*)-**156** and $NADP^+$ cofactor (at 2.05 Å resolution, PDB 4CJX). (fig. 8.3 A). The enzyme is a dimer of two subunits of 297 amino acid residues. Each subunity consists in 11 α-helices and 11 β-sheet organized in a C-terminal $NADP^+$-binding domain (with the characteristic Rossmann fold) and an N-terminal substrate binding domain. The pyrimidine is stacked between Lys56 and Gln100 residues (which are in contact through a hydrogen bond) one one side and Ile174 on the other side. Asp123 side chain, backbone carbonyls of Leu101 and Val99, and the backbone amide of Leu101 are also involved in interaction with the pyrimidine head of (*S*)-**156**. Moreover, solvent mediated interactions link the pyrimidine oxygen to the side chains of Lys56 and Asp123; this last residue also binds the urea carbonyl. The phenyl ring of (*S*)-**156** establish a π-π interaction with Tyr52 side chain, on one face, and van der Waals interactions with the side chains of Gly276, Pro277 and Thr279. The side chains of Thr, Leu, Leu and Pro form a hydrophobic channel in which the tail of the inhibitor is positioned. The α-carboxylate establishes a hydrogen bond with the side chain nitrogen of Gly273 and a long-range ionic interaction with Arg10; the γ-carboxylate similarly interacts with Arg54. Bindings of (*S*)-**176** and (*S*)-**180** were predicted by means of docking studies. The homologation of the glutamate tail allows the γ-carboxylate to establish an ionic interaction with Arg54 or Arg10 (in two different plausible binding modes) at a closer distance and this may cause the observed increase in affinity. Two different binding modes were also described for (*S*)-**180**. In the first one the phenyl ring establishes a π-cation interaction with Arg10, while in the other the same group establishes hydrophobic

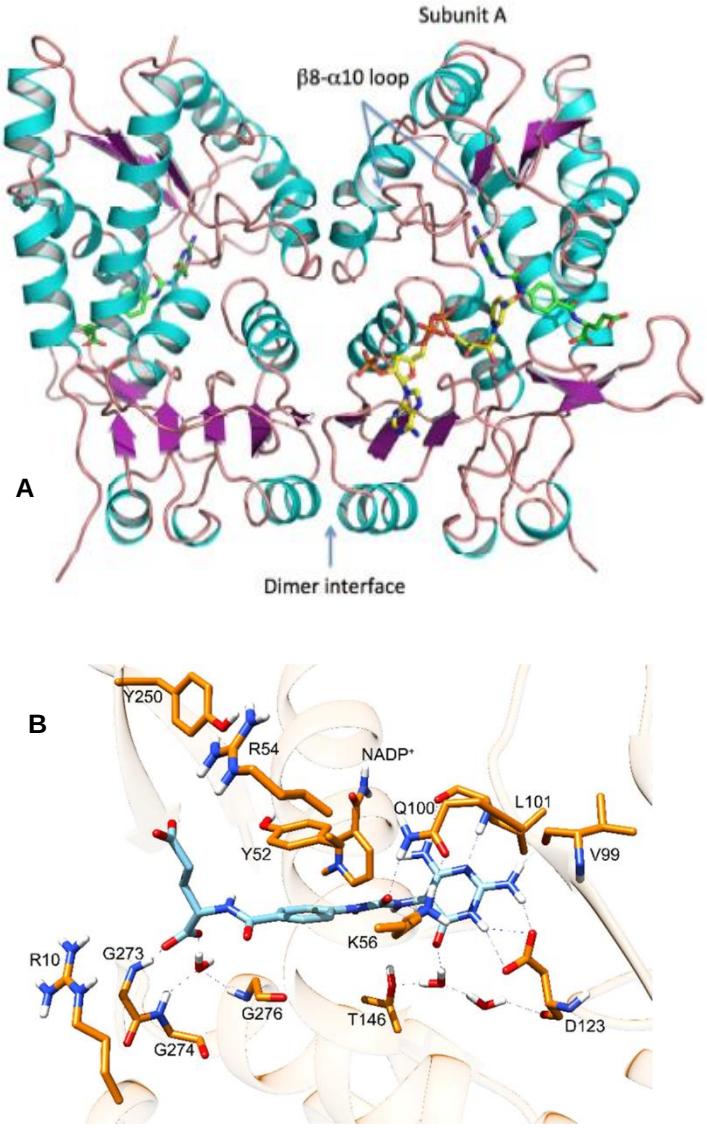

Figure 8. 3 **A** The dimer of *Tb*FolD. Secondary structure is depicted as helices colored cyan, β-strands red, and loops and coils brown. $NADP^+$ and (*S*)-**156** are depicted as sticks with atomic positions colored red O, blue N, orange P and C yellow for the co-factor, green for the inhibitor; **B** (*S*)-**156** bound in the active site of *Tb*FolD. The polypeptide is depicted as off-white ribbon, the interacting residues, and the nicotinate moiety of the cofactor, which was modeled, are represented with C atoms as orange sticks, the ligand as cyan sticks. All O, N, and H atom positions are red, blue, and white, respectively. Blue dashed lines represent potential hydrogen bonding interactions.

contacts with Tyr52, Tyr250 and Leu252. Because of the loss of activity with the introduction of a hydroxyl group in compound (*S*)-**181**, it is likely that only the second pose is relevant.

8.6 Conclusions

In this project I described the first series of *Tb*DHCH inhibitors, selecting (*S*)-**156** as the reference compound and performing a study of the structure activity relationships around the amino acidic tail. In particular, I showed how the replacement of the glutamate residue with a 2-amino adipate [(*S*)-**176**] or a phenylalanine [(*S*)-**180**] residues generates a sensible improvement in the inhibitory potency of these analogues. The obtained results were explained through docking studies using the X-ray crystal structure of the ternary complex (*S*)-**156**-$NADP^+$-*Tb*FolD. Considering the similarities in the physicochemical properties of these compounds, I speculate that modifications in the amino acidic tail, while improving potency, may reduce the affinity towards transporters, possibly involved in the active transport of the inhibitors through the parasite membrane. Giving the low lipophilicity of these compounds it is indeed unlikely that they can penetrate into cells through simple diffusion. Results obtained in this study represent a solid base for the future development of effective inhibitors of *Tb*DHCH.

9. Human lysophosphatidic acid acyl transferase (*h*LPAAT) inhibitors as new anti-*Chlamydia* agents

In a previous work, CI-976 (**182**), a molecule able to inhibit the enzymes acyl-CoA:cholesterol acyl transferase (ACAT) and lysophosphatidic acid:acyl-CoA acyl transferase (LPAAT) was found able to inhibit the growth of *C. trachomatis* in human cells. Herein, I describe the design and synthesis of analogues of **182** with the aim of generating a more potent and safe compound.

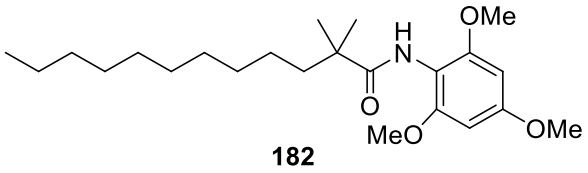

182

Figure 9. 1 Structure of the dual LPAAT and ACAT inhibitor CI-976.

9.1 Correlation of *h*LPAAT inhibition and *C. trachomatis* growth inhibition [55]

182 is a long chain saturated aryl amide that was firstly described as an ACAT inhibitor during a SAR campaign of related compounds. [56] Later on, this molecule showed the additional ability of inhibiting a human specific Golgi-associated LPAAT. [57] This membrane-associated enzyme is widely expressed and is involved in the Kennedy pathway (the *de novo* synthesis of glycerophosholipids). In humans, six isoforms (α-ζ) of this enzyme are known. [58] LPAAT catalyzes the conversion of lysophosphatidic acid (LPA) in phosphatidic acid (PA), which can be further modified to other lipids (TAG, PE, PC, PS, PI, PG, CL; scheme 9.1). [59]

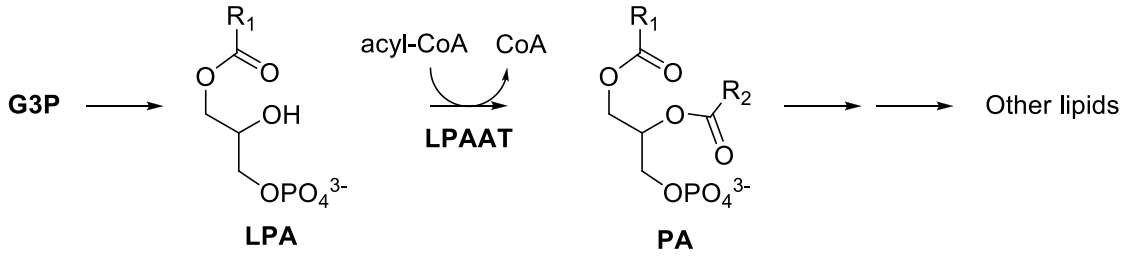

Scheme 9. 1 LPAAT catalyzes the conversion of LPA to PA, the key intermediate of the *de novo* biosynthesis of lipids.

Compound **182** showed also to cause an accumulation of transferrin (Tf) in the Rab11-positive compartment (specific for the slow recycling pathway of Tf) in human cells. [60] The inhibition of *h*LPAAT was correlated to the ability of **182** to hamper the development of *Chlamydia* inclusions in human cells, observed in another work. Rab11 vescicles were found to be intimately associated with chlamydial inclusion, and they probably represent the source of iron for the parasite; the delay in the recycling pathway caused by **182** led to the accumulation of iron-laden vescicles around *Chlamydia* inclusions, with inhibition of chlamydial growth (probably due to iron overload, fig. 9.2). Since another dual ACAT/LPAAT inhibitor (FR179254) showed the

same anti-chlamydial effect, while a specific ACAT inhibitor (Sandoz 58-035) turned out to be inactive, LPAAT inhibition was linked with the antibacterial properties of **182**, despite the biological connection between enzyme inhibition and Tf recycling delay are still to be elucidated. [55]

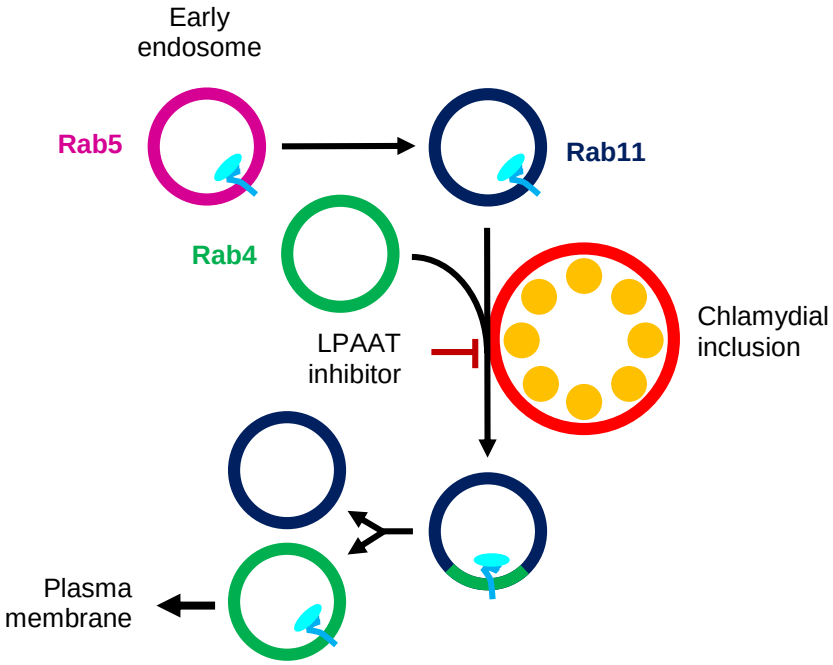

Figure 9. 2 Slow recycling pathway of Tf and its relationship with *C. trachomatis* inclusion. Rab5 positive early endosomes mature to Rab11 comparts that fuse with Rab4 for recycling back to the plasma membrane. Approximately the 20% of Tf is recycled by this pathway, which is probably used by *C. trachomatis* for iron supply. Several evidences linked LPAAT inhibition with a delay in this pathway, which results in iron overload and, lastly, growth abrogation. *[55]*

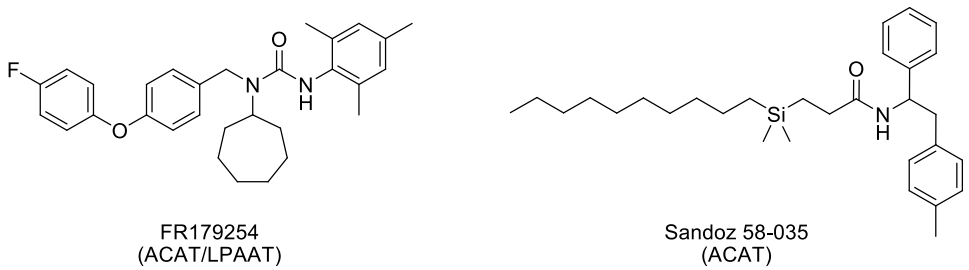

Figure 9. 3 Structures of compounds used to assess the correlation of LPAAT inhibition and anti-chlamydial activity.

9.2 Design and synthesis of new CI-976 analogues

The structure of **182** is quite simple, nevertheless peculiar features could be idenfied, in particular: the amide group, the α-methyl groups, the electron rich aromatic ring and the long saturated aliphatic chain. In order to generate more potent analogues, my strategy was to introduce little modifications at the groups listed above and then to proceed with a deeper study around the most promising compounds. Initially, I focused on the substitution of the α position of **182**. I investigated the role of the methyl groups synthesizing analogues (±)-**183** and **184**, in which one or both groups were removed. Another modification I introduced was the replacement of the two methyl groups with two fluorine atoms (compound **185**). The CF_2 group is known to behave as an oxygen atom, therefore compound **185** should possess properties similar to a carbamate; moreover, the fluorine atoms might establish an intramolecular hydrogen bond with the amide proton, resulting in a stable five member ring-like structure

In order to obtain (±)-**183**, ethyl laurate (**186**) was methylated to give intermediate (±)-**187** and then hydrolized. The resulting acid (±)-**188** was condensed with aniline **189**, obtained reducing the commercially available nitrobenzene **190**. Condensation of the same aniline with lauric acid (**191**) gave compound **184** (scheme 9.2).

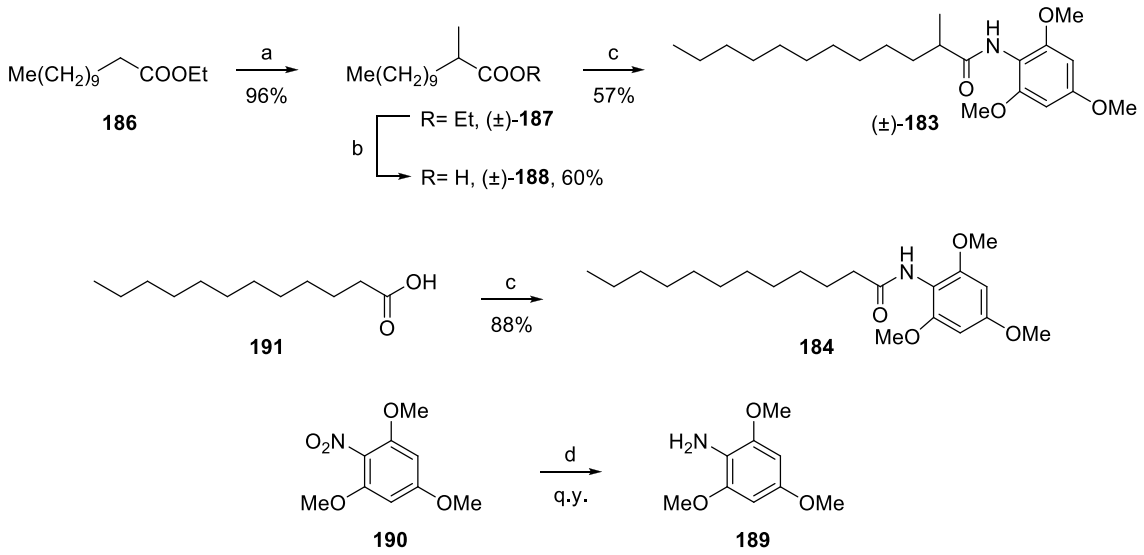

Reagents and conditions: a) LDA, MeI, THF, -78 °C to r.t., o.n.; b) LiOH, H_2O, reflux, 24h; c) **189**, 1,1'-carbonyldiimidazole, THF, 45 °C, o.n.; d) Zn, AcOH, EtOH, r.t., o.n.

Scheme 9. 2 Synthesis of (±)-**183** and **184**.

The strategy for the synthesis of **185** involved, as first step, the Reformatzky reaction between decyl aldehyde (**192**) and the bromo acetate **193** obtaining intermediate (±)-**194**. This reaction was already reported in literature [61] and allowed to efficiently introduce the 2,2-difluoro functionality. Compound (±)-**194** was then deoxygenated following the Barton-McCombie procedure, which exploits the ability of imidazolyl thionocarbonates to form radicals. Tributyltin hydride, activated by exposure to high temperatures (refluxing toluene), was used as a source of radicals. Compound (±)-**195**, obtained treating (±)-**194** with 1,1'-thiocarbonyldiimidazole, was slowly added to the reaction mixture in order to prevent side reactions of the radical intermediates. The convertion to the α-gemdifluoro ester **196** was fast and very efficient. Rather than submitting ester **196** to a hydrolysis/coupling sequence, I performed a direct convertion to amide. Taking advantage of the absence of acidic protons in **196**, I could treat it with the anion of aniline **189**, generated in presence of a strong base (LiHMDS, specifically) obtaining the target compound **185** (scheme 9.3).

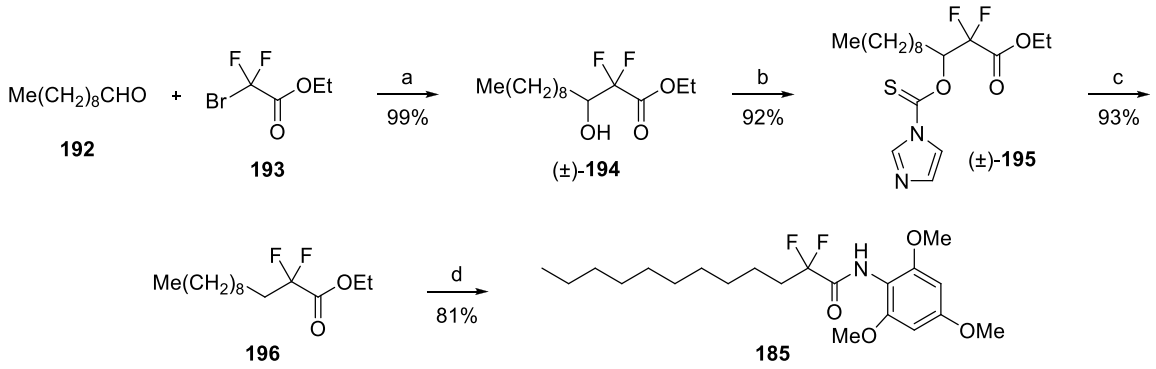

Reagents and conditions: a) Zn, TMSCl, THF, r.t., 3h; b) 1,1'-thiocarbonyldiimidazole, DMAP, DCM, r.t., 1.5h; c) Bu_3SnH, PhMe, reflux, 30min; d) **189**, LiHMDS, THF, r.t., 1h.

Scheme 9. 3 Synthesis of the α-gemdifluoro compound **185**.

Another approach that I followed, was the inclusion of the methyls into carbocyclic rings of variable size, introducing a certain degree of rigidification to the structure. In particular, I synthesized the α-carbocyclic derivatives **197**, **198** and **199**, characterized by the presence of a 4, 5 and 6-terms ring. The varying ring size allows the tuning of the bond angle between the alkyl chain and the aryl amide with a potential influence on the activity. To obtain these derivatives, different cycloalkane esters [(±)-**200**, (±)-**201** and (±)-**202**] were alkylated with 1-bromodecane (**203**). The obtained esters (**204-206**) were converted to amides **197**, **198** and **199** following the same strategy used for the synthesis of **185**. The initially designed compounds also included the α-cyclopropane derivative, as this represents the direct analogue of **182**. Surprisingly, when **207** was submitted for alkylation under the same conditions used for the synthesis of the carbocyclic esters (±)-**204-206**, I only obtained a product which was completely different from the expected one. After a thorough analysis, I concluded that the product obtained possessed the structure of **208**. Indeed, it has been already reported in the literature that **207** characteristically undergoes subsequent Claisen-aldol reactions when exposed to LDA, giving the tricyclic diester product **208** (scheme 9.4). [62] Although the desired α-

cyclopropane analogue of **182** might been obtained following other approaches, further attempts were not performed, mainly because of time restraints.

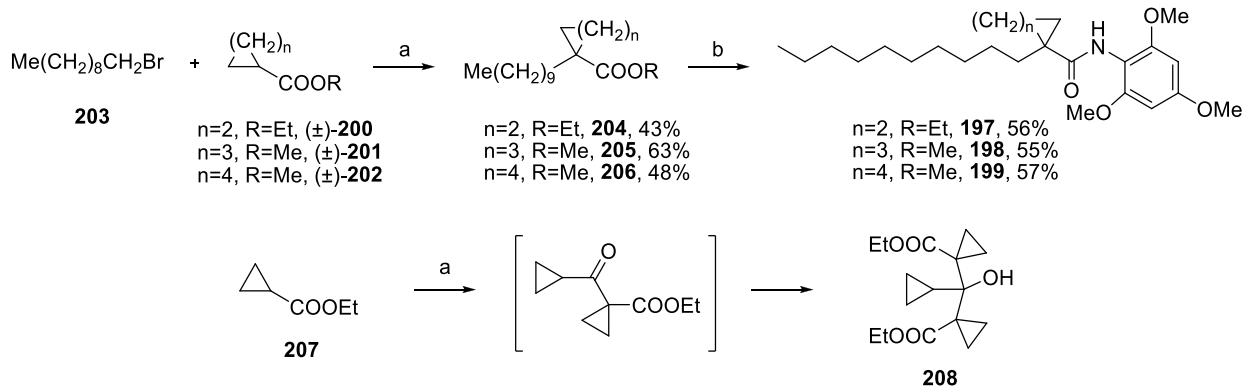

Reagents and conditions: a) LDA, THF, -78 °C to r.t., o.n.; b) **189**, LiHMDS, THF, r.t., o.n.

Scheme 9. 4 Synthesis of the α-carbocyclic compounds **197**, **198** and **199**.

I then turned my attention to the properties of the aromatic ring of compounds **182**, **184** and **185**. A common approach in medicinal chemistry is to synthesize analogues with different substituents that modify the electronic properties of the ring or introduce steric biases that force the molecule to assume the desired conformation. Thus, I synthesized analogues in which the strongly electron rich 2,4,6-trimethoxyphenyl is replaced by electron deficient, neutral or electron rich phenyl rings. Methyl isobutyrate (**209**) was alkylated with **203** and the resulting intermediate **210** was converted to amides **211**-**213** using the desired aniline and LiHMDS (this strategy was possible due to the lack of acidic protons). Following the same strategy, the gemdifluoro ester **196** was used to obtain products **214**-**219**. Remarkably, the phenyl rings of compounds **217** and **219** possess *ortho* substituents that might have an influence on the conformation of the molecules. In particular, the two *ortho iso*-propyls of **217**, due to steric strain, should force the phenyl ring to assume a perpendicular position in regards to the carbonyl. In compound **195**, instead, the *ortho* methoxy group might establish an intramolecular hydrogen bond with the amide proton creating a stable network of 5 atoms. Lastly, the acid **191** was converted in the corresponding acyl chloride which was treated with the desired aniline obtaining compounds **220**-**225**, analogues of **184** (scheme 9.5).

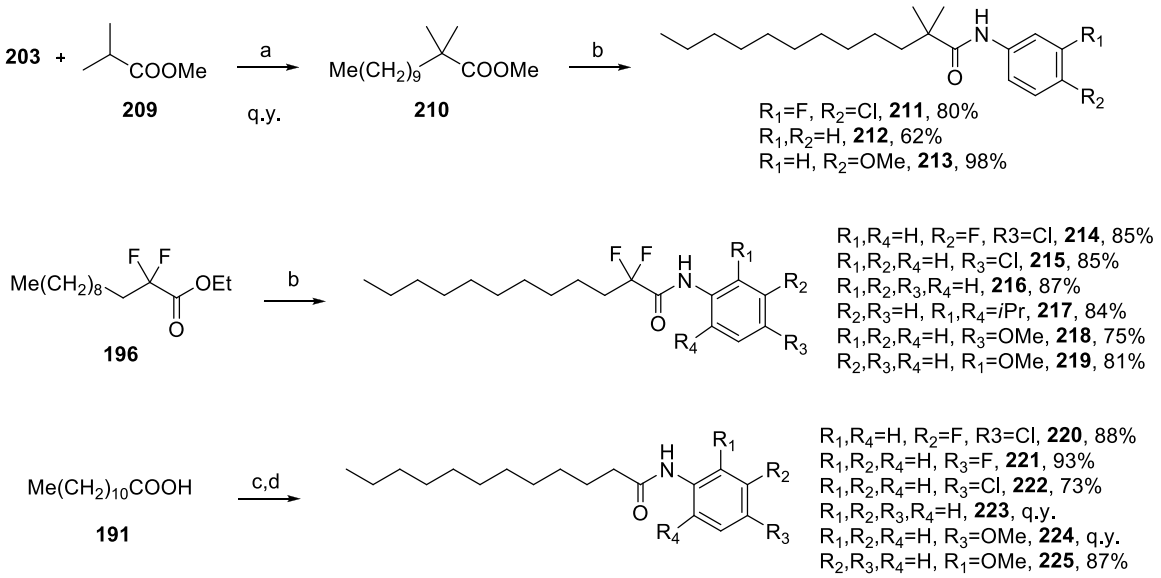

Reagents and conditions: a) LDA, THF, -78 °C to r.t., overnight; b) substituted aniline, LiHMDS, THF, r.t.,1h; oxalyl chloride, DMC, r.t., 4h; d) substituted aniline, TEA, DMAP, DCM, r.t., o.n.

Scheme 9. 5 Synthesis of analogues of compounds **182**, **184** and **185** with differently decorated phenyl rings.

For the synthesis of compounds **211**-**225**, commercially available anilines **226**-**232** were used.

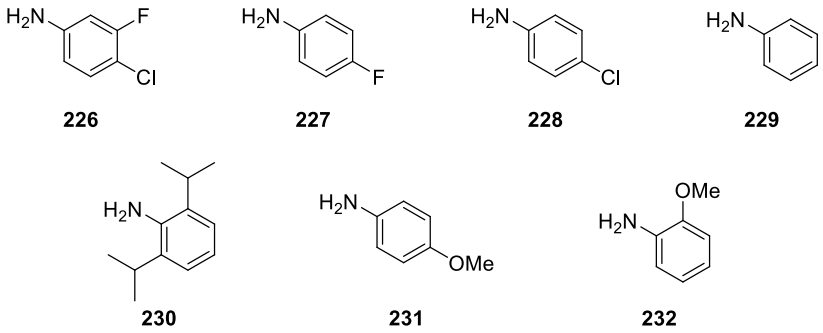

Figure 9. 4 Anilines used for the synthesis of compounds **211**-**225**.

Since compound **185** showed promising activity in the cellular assay (see paragraph 9.3), I focused my attention on the synthesis of new analogues in which additional modifications were introduced while preserving both the α-gemdifluoro group and the 2,4,6-trimethoxyaniline. A first, sintetically convenient, modification was the introduction of a group able to establish a hydrogen bond in the β position of **185**. Intermediate (±)-**194** was converted into the β-hydroxy (H-bond donor) derivatives [(±)-**233** and (±)-**234**] upon treatment with anilines **229** and **189**, respectively, and LiHMDS. The two new analogues were also converted into β-keto derivatives upon facile oxidation with DMP (scheme 9.6). The ketone introduced in compounds **235** and 236 may act as H-bond acceptor.

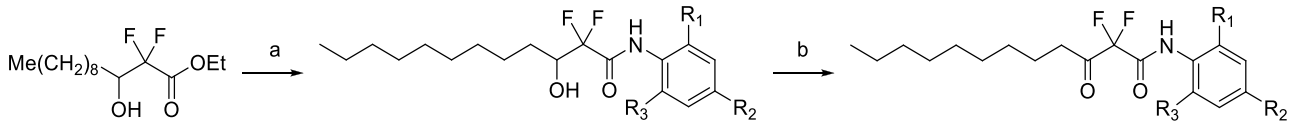

(±)-**194**

R_1,R_2,R_3=H, (±)-**233**, 78%
R_1,R_2,R_3=OMe, (±)-**234**, 77%

R_1,R_2,R_3=H, **235**, q.y.
R_1,R_2,R_3=OMe, **236**, q.y.

Reagents and conditions: a) **229** or **189**, LiHMDS, THF, r.t., 1h; b) DMP, DCM, r.t., 30min.

Scheme 9. 6 Synthesis of β-functionalized analogues of compounds **185** and **216**.

In order to investigate the role of the amide proton for the activity, I synthesized compound **237**, the *N*-methylated analogue of **185**. This modification abrogate the ability of the molecule to donate a hydrogen bond in that position and also the possibility of tautomerization of the amide is eliminated. This modification is of particular interest since the amide nitrogen of **185** could be easily exploited to install additional groups which might positively contribute to the activity, as it was done in compound **238**, in which I introduced a benzyl group (scheme 9.7).

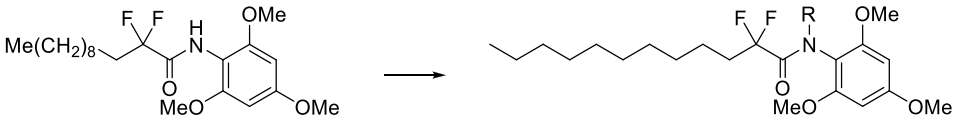

185

R=Me, **237**, q.y.
R=Bn, **238**, 93%

Reagents and conditions: NaH, MeI or BnBr, THF, r.t., o.n.

Scheme 9. 7 Synthesis of *N*-alkylated derivatives of **185**.

Assuming that **185** might function as a false substrate of LPAAT (due to structural similarity with the acyl groups found in the natural substrates), I designed one analogue in which the saturated alkyl chain of **185** is replaced by a benzyl residue. This modification was inspired by the α-aryl-propionic acid NSAIDs (e.g. ibruprofen, ketoprofen), in which variously substituted phenyl rings effectively mimic the chain of arachidonic acid, the pro-inflammatory messenger that can be also found in one of the substrates of LPAAT (arachidonoyl-CoA). It is indeed common that unsaturated fatty acids are linked to the 2-OH of glycerol in fatty acids. The synthetic strategy was analog to the one described for compound **185**, but in this case benzaldehyde (**239**) was used as starting material. Compound **243** was obtained in low overall yields but still acceptable for the scope of the work (scheme 9.8). Distillation of benzaldehyde prior to reaction would provide a starting material of higher purity and potentially higher yields for the Reformatzky reaction (scheme 9.8, step a), while a possible explanation for the low yields of the deoxygenation reaction (scheme 9.8, step c) is the increased stability of the benzyl radical intermediate compared to the secondary alkyl radical generated from (±)-**195**.

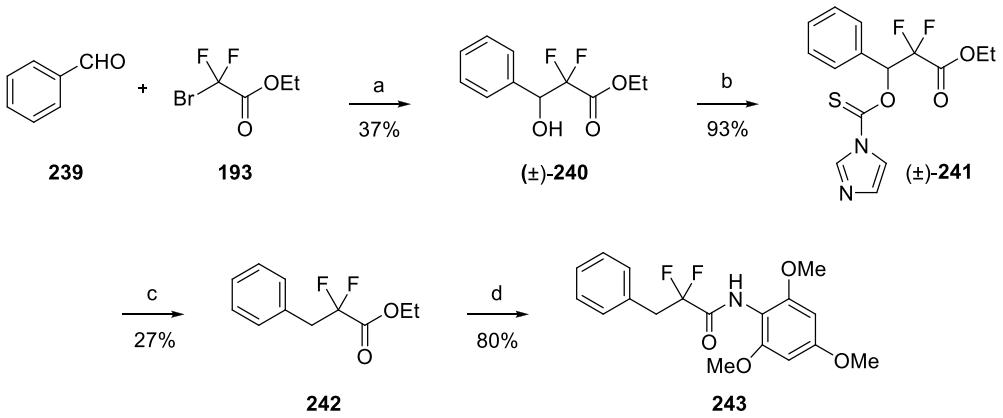

Reagents and conditions: a) Zn, TMSCl, THF, r.t., 3h; b) 1,1'-thiocarbonyldiimidazole, DMAP, DCM, r.t., 1.5h; c) Bu_3SnH, PhMe, reflux, 30min; d) **189**, LiHMDS, THF, r.t., 1h.

Scheme 9. 8 Synthesis of compound **243**.

9.3 Biological investigation

The compounds were tested for the ability to halt the growth of *C. trachomatis* in human cells in a phenotypic screening. HeLa cultures were infected with *C. trachomatis* serovar L2 and then treated with different inhibitors at a 100 µM final concentration. After appropriate staining, the culture were observed with a confocal microscope. Some of the compounds showed cytotoxic effects on human cells and these were discarded from evaluation, since the bacteria needs healthy cells to develop. The only compound that showed similar activity to **182** (evaluating the mean inclusion size) was **185**, in which the methyl groups are replaced by two fluorine atoms. Figure 9.5 shows the similar anti-chlamydial effect of the two compounds.

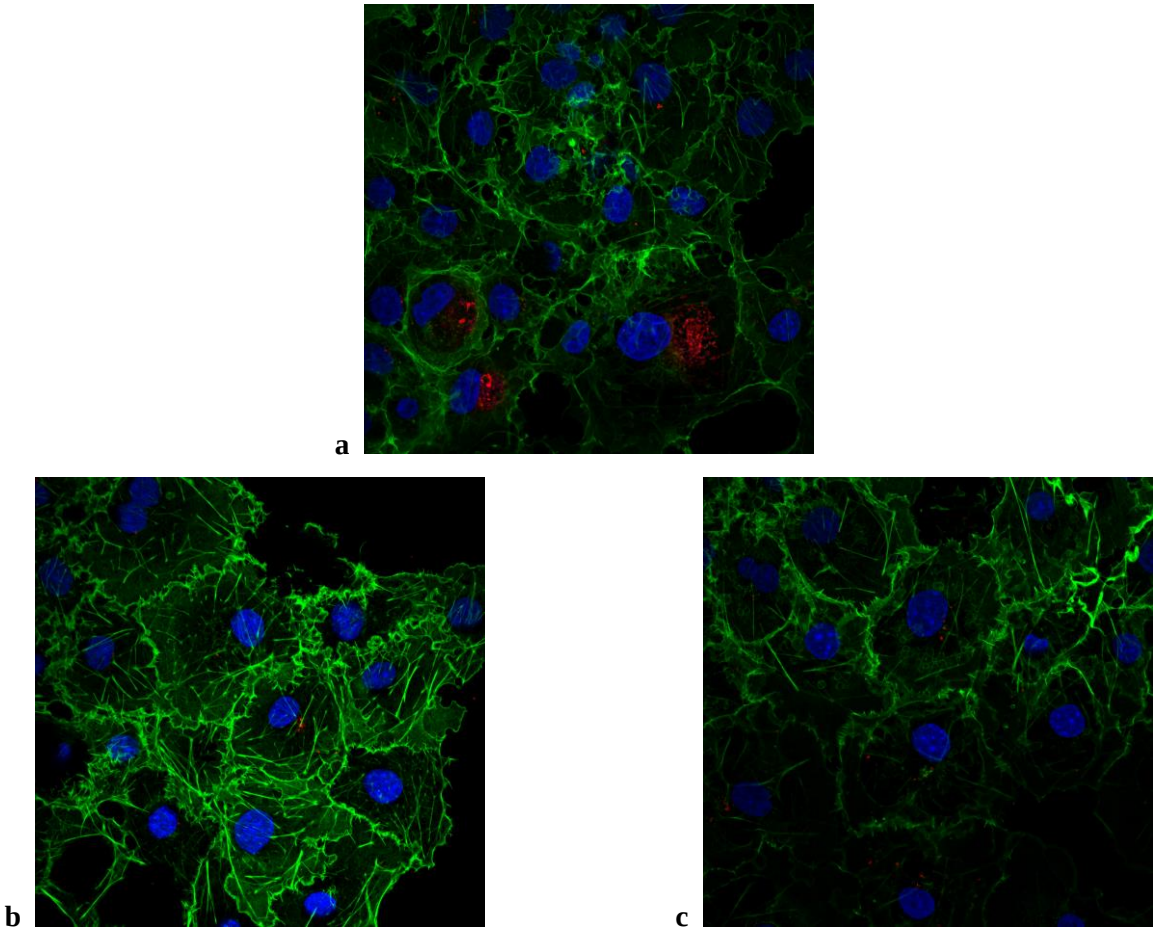

Figure 9. 5 Images of HeLa cells cultures treated infected with *C. trachomatis* after preincubation with DMSO (**a**), **182** (**b**) and **185** (**c**). DAPI is depicted in blue, phalloidin in green and *C. trachomatis* in red.

To evaluate if the observed activity was due, as hypothesized, to an interaction with *h*LPAAT and not to a direct effect on the parasite, I used *Escherichia. coli* as a model bacterium, since *Chlamydia trachomatis* could not be object of many biological investigations because of its intrinsic fragility. *E. coli* possesses a unique form of LPAAT, commonly referred to as *pls*C. In a previous work, it was observed that non-functional mutation of *pls*C results in growth defects of the bacterium when incubated at 42 °C. [63] I then evaluated the growth of *E. coli* cultures under these conditions in presence of representing compounds at a 100 µM concentration. For all of them, I just recorded a non significant reduction in the optical dispersion of the cultures, which

excludes any involvement of the bacterial isoform. As additional confirmation, enzyme inhibition assay on *E. coli* lysates, performed published procedures, [57] [58] [64] gave negative results.

9.4 Discussion

In this part of my thesis, I confirmed the importance that the transferrin pathway has for the *C. trachomatis* inclusion process. However, a proper target deconvolution and the identification of the interaction between *h*LPAAT and the transferrin slow recycling pathway are still required. Unfortunately, only one of the synthesized analogues (**185**) presented significant activity, but these results may serve as guide for future studies, which might be aided by structural informations. These molecules may represent the starting point for the development of novel antibacterial or, even more generally, novel antimicrobials acting toward obligate intracellular parasites that exploit the transferrin pathway for iron acquisition. This approach represents a different strategy in the treatment of infections: rather than acting on microbial targets, the inhibition of host's trafficking pathways that are fundamental for the infection but dispensable for the host will result in antimicrobial activity.

10. Conclusions

In the present thesis, I described the rational design of new inhibitors of enzymes that play a critical role for parasite survival and for virulence.

For two enzymes, *Pf*GAPDH and *Tb*CatL, both containing a catalytic cysteine residue, I designed covalent inhibitors exploiting the new 3-bromoisoxazoline warhead. This electrophilic moiety showed very interesting properties, most notably a balanced reactivity toward nucleophiles that results in selective reaction with activated cysteines. I propose that this warhead can be employed in the design of covalent inhibitors of other enzymes by linking it to a properly designed recognition moiety.

Describing the first *Tb*FolD inhibitors, I filled a gap in the pharmacological investigation of the reduced folate pathway of *Trypanosoma brucei*. Moreover, the first X-ray structure of *Tb*FolD in the presence of $NADP^+$ and an inhibitor was obtained using compound (*S*)-**156**. The obtained structural informations can certainly give a significant boost to the rational design of new potent *Tb*FolD inhibitors. Further advances in this field might probably result in the first effective antifolates acting toward this parasite.

Despite the low efficacy and the limited number of active compounds presented in the last chapter of this thesis, inhibition of LPAAT (which should be further confirmed) was confirmed to represent a general approach for the inhibition of the growth of different obliged intracellular parasites, more than *Chlamydia trachomatis*. More studies, such as isolation and structure determination, could prompt the description of more effective analogues.

This thesis represents thus a contribution in the antiparasitic field, with a particular focus on neglected tropical diseases (human African trypanosomiasis, trachoma).

Moreover, all the presented compounds could be exploited to perform structure-activity relationships studies on different enzyme isoforms, covering therapeutic areas currently of great interest (e.g. treatment of cancer). Some of the GAPDH inhibitors described in my thesis are already under valuation for their antiproliferative activity against tumor cell lines.

As a general final comment, I can conclude that although the selection of a proper molecular target and the development of highly potent inhibitors are essential prerequisites, the development of truly effective antiparasitic agents is hampered by the difficulty in obtaining compounds able to efficiently permeate the parasite cell membrane. Therefore, phisico-chemical properties such as solubility, pKa and logP must be always considered and properly tuned. As an alternative, pro-drug approaches could be taken into consideration to improve cell penetration, and consequently the efficacy of highly potent enzymatic inhibitors characterized by low antiparasitic activity.

11. Appendix

This appendix is an integration to chapter 5. Although a bit out of context from the whole thesis, I decided to include a more exhaustive analysis in order to provide a complete sight of the mechanisms of enzyme inhibition. Please note that the numbering of the equations follows the one started in chapter 5.

11.1 Enzyme inhibitors

Description of competitive mechanism of inhibition is reported in paragraph 5.2.1.

11.1.1 Non-competitive inhibitors

Non-competitive inhibitors binds equally to the free enzyme (with dissociation constant K_i) and to the binary complex *ES*. In the latter case the dissociation constant is modified by a factor α (αK_i): when α> 1 the affinity is greater for the free enzyme while when α< 1 the affinity is greater for the complex *ES*. The effect of this kind of inhibitors is to lower V_{max}, as we can see from the velocity equation 14 (and its simplified version, eq. 15).

$$v = \frac{\frac{V_{\max}}{\left(1+\frac{[I]}{\alpha K_i}\right)}[S]}{[S] + K_M\left(\frac{\left(1+\frac{[I]}{K_i}\right)}{\left(1+\frac{[I]}{\alpha K_i}\right)}\right)} \qquad \text{(eq. 14)}$$

$$v = \frac{V_{\max}[S]}{[S]\left(1+\frac{[I]}{\alpha K_i}\right) + K_M\left(1+\frac{[I]}{K_i}\right)} \qquad \text{(eq. 15)}$$

In the case of α= 1 (when the affinity of the inhibitor is the same for *E* and *ES*) equation 15 can be further modified, giving equation 16.

$$v = \frac{V_{\max}[S]}{([S] + K_M)\left(1+\frac{[I]}{K_i}\right)} \qquad \text{(eq. 16)}$$

The effect of non-competitive inhibitors on the apparent value of K_M depends on the value of the correction factor α: for α> 1 it is increased, for α< 1 it is decreased and, finally, it is unaffected for α= 1.

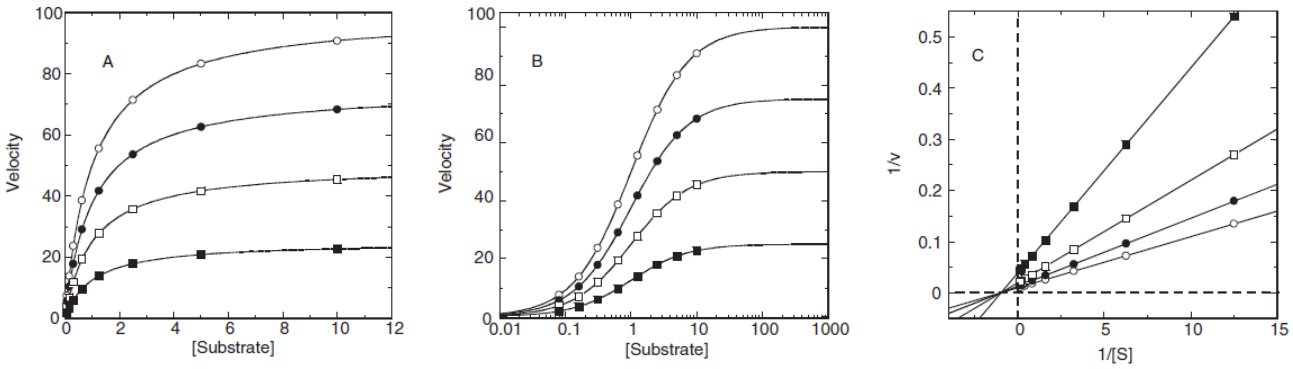

Figure 11. 1 Direct fit, semilog and double reciprocal plots for non-competitive inhibitors with α= 1 (highest [*I*] for the filled square curve, lowest [*I*] for the empty circle curve).

For non-competitive inhibitors a diagnostic feature of the double-reciprocal plot is that lines obtained at different [*I*] intersect at a point other than the *y*-axis. For α= 1, the intersection point is on the *x*-axis, while for α> 1 and α< 1 it is above or below, respectively, the *x*-axis. Equation 17 is the Cheng-Prusoff equation for non-competitive inhibitors.

$$\mathrm{IC}_{50} = \frac{[S] + K_\mathrm{M}}{\frac{K_\mathrm{M}}{K_\mathrm{i}} + \frac{[S]}{\alpha K_\mathrm{i}}} \quad (\text{eq. } 17)$$

11.1.2 Uncompetitive inhibitors

Uncompetitive inhibitors bind exclusively to the binary *ES* complex. We can then expect a decrease of the apparent V_{max} and, because of the thermodynamic equilibrium between *ES*, *EI* and *ESI*, also the apparent K_M is decreased. The reaction rate equation is then described by equation 18 that can be simplified giving equation 19.

$$v = \frac{\frac{V_\mathrm{max}}{\left(1 + \frac{[I]}{\alpha K_\mathrm{i}}\right)}[S]}{[S] + \frac{K_\mathrm{M}}{\left(1 + \frac{[I]}{\alpha K_\mathrm{i}}\right)}} \quad (\text{eq. } 18) \qquad v = \frac{V_\mathrm{max}[S]}{[S]\left(1 + \frac{[I]}{\alpha K_\mathrm{i}}\right) + K_\mathrm{M}} \quad (\text{eq. } 19)$$

From a double reciprocal plot of an uncompetitive inhibitor at different concentrations we will obtain a series of parallel lines with different *y*-intercept values (because of different V_{max}). Recalling that the slope of the line in such plot is given by K_M/V_{max} and that both the values are equally affected by the term $(1+[I]/\alpha K_i)$ (see eq. 18), we can understand why the slope do not vary with different [*I*].

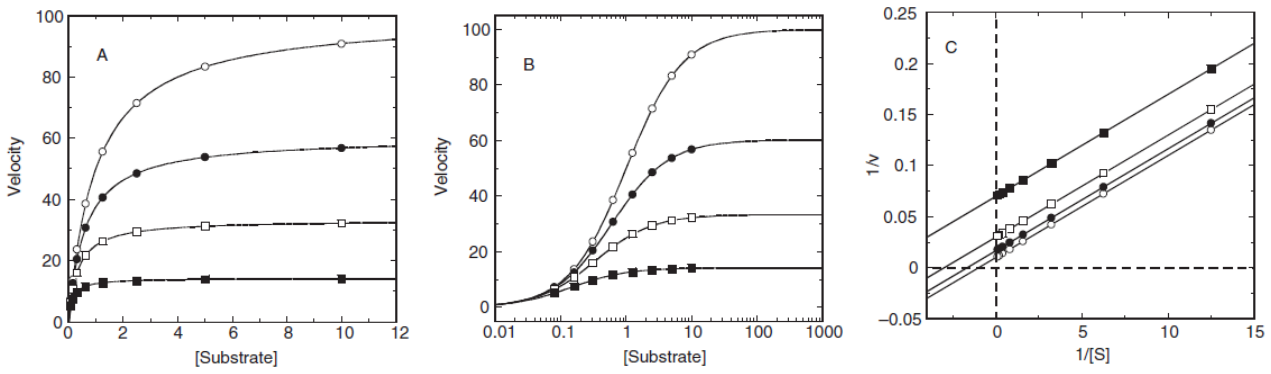

Figure 11. 2 Direct fit, semilog and double reciprocal plots for non-competitive inhibitors with α= 1 (highest [*I*] for the filled square curve, lowest [*I*] for the empty circle curve).

Equation 20 is the Cheng-Prusoff equation for uncompetitive inhibitors.

$$\mathrm{IC}_{50} = \alpha K_\mathrm{i}\left(1 + \frac{K_\mathrm{M}}{[S]}\right) \quad (\text{eq. } 20)$$

A recapitulatory table for the effect on enzyme parameters for different inhibition modalities is reported below.

Table 11. 1 Effect of inhibitors on apparent steady-state kinetic constant and on catalytic steps.

Parameter	Inhibition modality				
	Competitive	Non-competitive α> 1	Non-competitive α= 1	Non-competitive α< 1	Uncompetitive
K_M	Increase linearly with increasing [I]	Increase linearly with increasing [I]	No effect	Decrease curvilinearly with increasing [I]	Decrease curvilinearly with increasing [I]
V_{max}	No effect	Decrease curvilinearly with increasing [I]	Decrease curvilinearly with increasing [I]	Decrease curvilinearly with increasing [I]	Decrease curvilinearly with increasing [I]
V_{max}/K_M	Decrease curvilinearly with increasing [I]	Decrease curvilinearly with increasing [I]	Decrease curvilinearly with increasing [I]	Decrease curvilinearly with increasing [I]	No effect
Step affected	$E + S \rightarrow ES$	$E + S \rightarrow ES^{\ddagger}$	$E + S \rightarrow ES^{\ddagger}$	$E + S \rightarrow ES^{\ddagger}$	$ES \rightarrow ES^{\ddagger}$

11.1.3 Slow and tight binding inhibitors

Slow binding inhibitors need considerable time to reach the equilibrium between their dissociated and enzyme-bound forms. Tight binding inhibitors, which often display slow binding behaviour, associate to enzyme with a very slow dissociation rate (the equilibrium assumption is not more valid). In both the cases, only apparent values of inhibition could be determined and a different analytical treatment is necessary.

11.2 The Hill coefficient

In reality, enzymes might possess multiple binding sites and the binding of one ligand may influence the affinity of the same ligand for other binding site (as process referred to as cooperativity). When affinity is enhanced we have positive cooperativity while when it is decreased we have negative cooperativity. Moreover, it might be that inhibitor/enzyme stoichiometry is different from 1-to-1: the binding of two or more inhibitor molecules to one enzyme may be required for inhibition or the binding of one molecule to a binding site of an enzyme dimer could be sufficient for the inhibition of both the active sites in the dimer. Equations 7 and 8 are thus modified as equations 21 and 22 to take into account these mechanisms.

$$\frac{v_i}{v_0} = \frac{1}{1 + ([I]/\mathrm{IC}_{50})^h} \quad (\mathrm{eq.}\,21) \qquad \% \text{ Inhibition} = \frac{100}{1 + ([I]/\mathrm{IC}_{50})^h} \quad (\mathrm{eq.}\,22)$$

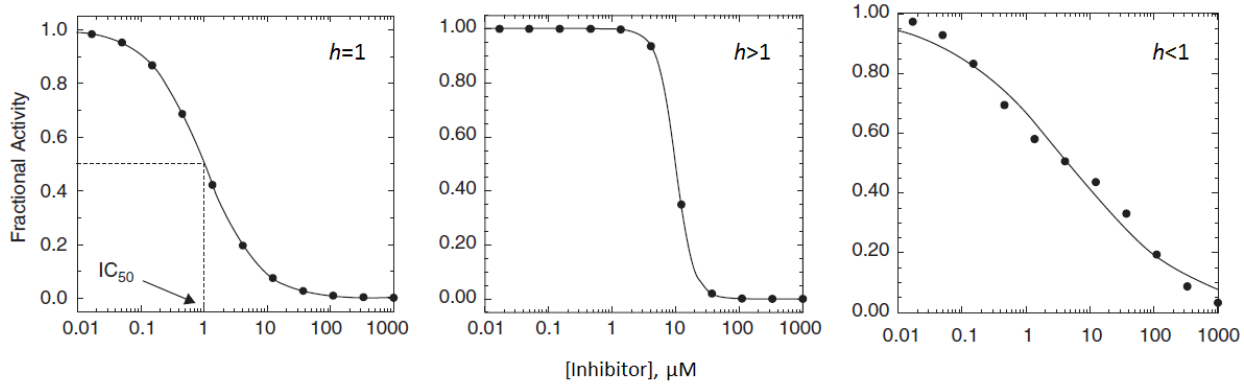

Figure 11. 3 Effect of Hill coefficient on curve shape.

The exponential term *h* is referred to as the Hill coefficient or Hill slope: it is related to the stoichiometry of inhibition and it also represents the steepness of the concentration-inhibition relationship. For a 1-to-1 stoichiometry we have *h*= 1, which is the normality for the majority of the small molecule inhibitors. Situations in which *h* is significantly different from 1 may also reflect a non-ideal behaviour of the inhibitor. *h*>> 1 (sharp reduction of activity) can be seen for nonspecific inhibition (e.g. protein denaturants), compounds that inhibits the enzyme as micelle (and thus IC_{50} will be reflective of the critical micellar concentration) or tight binding/irreversible inhibitors. *h*<< 1 (very smooth reduction of activity) may be due to the presence non-equivalent binding pockets in the same enzyme molecule (or an equilibrium of more forms of a single enzyme with a binding pocket with different affinity for *I*) or on separate enzyme molecules that contribute to activity (e.g. in the case of insufficient purification). Another reason may be compound aggregation or insolubility at high concentration, leading to a less than expected % inhibition at higher concentrations. The following plots represent enzyme inhibition with different Hill coefficients.

12. Experimental procedures

12.1 Materials and methods

All reagents and solvents were obtained from commercial suppliers and used without further purification. Merck silica gel 60 F_{245} plates were used as analytical TLC; flash column chromatography was performed on Merck silica gel (200-400 mesh). TLC were monitored at 254 nm and 365 nm and developed with a $KMnO_4$ or a ninhydrin solutions. NMR analysis were performed with a Varian Mercury 300 MHz or a Bruker 400 MHz spectrometers. ^{1}H, ^{13}C and ^{19}F chemical shifts (δ) are expressed in parts per million (ppm) and coupling costants (*J*) in hertz (Hz). Signal multiplicity is espressed as s (singlet), d (doublet), t (triplet), q (quartet), qui (quintet), sex (sextet), sep (septet), or m (multiplet). MW reactions were performed in a CEM Discover apparatus. MS analyses were performed on a Varian 320-MS triple quadrupole spectrometer with an electron spray ionization (ESI) source. Specific rotatory power was determined with a Jasco P1010 polarimeter. Melting points were obtained with a Büchi Melting Point B-540 apparatus. Analytical HPLC was performed using Jasco PU-980 pumps and a Jasco UV-975 detector. Preparative HPLC was performed with a Waters 1525 Binary HPLC pump connected to a Waters 2489 UV/Visible detector. The wavelength used for detection was 245 nm.

12.2 Chemistry

Synthesis of dibromoformaldoxime (DBF)

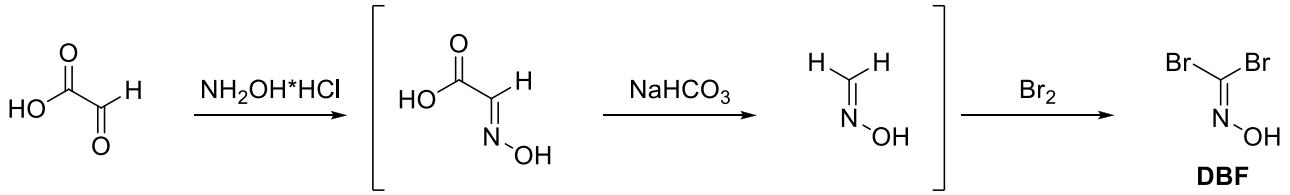

The synthesis of DBF was performed following a one-pot published procedure [65] with some modifications.

Glyoxylic acid monohydrate (31 g, 338 mmol) was dissolved in water (200 mL). Hydroxylamine hydrochloride (25 g, 338 mmol) was added and the reaction mixture was stirred at room temperature for 20 h. $NaHCO_3$ (58.8 g, 700 mmol) was then added portionwise. Subsequently, keeping the temperature of the reaction mixture below 10 °C, a solution of bromine (24.1 mL, 396 mml) in DCM (125 mL) was added dropwise. Reaction mixture was stirred at room temperature for 3 h. Phases were separated and the aqueous phase extracted with DCM (4x60 mL). The pooled organic layers were dried over Na_2SO_4, filtered and the solvent was removed under reduced pressure keeping the temperature below 40 °C. Crystallization with petroleum ether afforded the desired product (tipical yields around 25%) as a white solid (m.p.= 67-68 °C) (lit. m.p.= 65-66 °C) [65] which was used without further characterization.

Synthesis of (*R*)-*tert*-butyl 3-hydroxy-1-(methoxy(methyl)amino)-1-oxopropan-2-ylcarbamate [(*R*)-20]

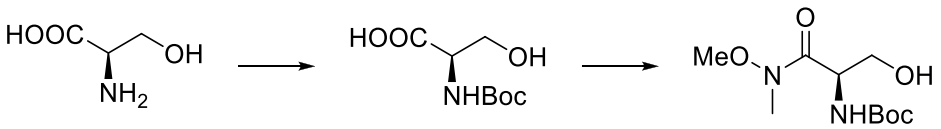

(*R*)-**18** (*R*)-**19** (*R*)-**20**

A solution of Boc_2O (12.5 g, 57.1 mmol) in THF (25 mL) was added dropwise at 0 °C to a solution of (*R*)-**18** (5.00 g, 47.6 mmol) and $NaHCO_3$ (11.2 g, 133.3 mmol) in water (50 mL). Reaction was stirred at room temperature until consumption of (*R*)-**18**. Reaction mixture was washed with Et_2O (x2), the aqueous phase was made acid with 1 M aq. HCl and extracted with EtOAc. The organic phase was dried over anhydrous Na_2SO_4, filtered and the solvent was removed under vacuum obtaining (*R*)-2-(tert-butoxycarbonylamino)-3-hydroxypropanoic acid [(*R*)-**19**] as a grey oil (9.56 g, quantitative yield) that was used in the following step without characterization.

R_f= 0.39 (DCM/MeOH, 9:1)

NMM (2.95 g, 26.8 mmol) and *N,O*-dimethylhydroxylamine hydrochloride (2.61 g, 26.8 mmol) were added at -15 °C to a solution of (*R*)-**19** (5.00 g, 24.4 mmol) in dry DCM (95 mL). Reaction mixture was stirred at -15 °C for 3 h then it was poured into 1 M aq. HCl and ice solution (30 mL). Phases were separated and the aqueous extracted with DCM (3x50 mL). The pooled organic layers were washed with brine, dried over anhydrous Na_2SO_4, filtered and the solvent was removed under vacuum obtaining (*R*)-*tert*-butyl 3-hydroxy-1-(methoxy(methyl)amino)-1-oxopropan-2-ylcarbamate [(*R*)-**20**] as a white solid (5.30 g, 88% yield).

R_f= 0.54 (EtOAc, 100%).

^{1}H-NMR (300 MHz, $CDCl_3$): δ= 5.60 (d, *J*= 6.0 Hz, 1H), 4.78 (m, 1H), 3.81 (m, 2H), 3.77 (s, 3H), 3.22 (s, 3H), 2.67 (m, 1H), 1.44 (s, 9H).

These NMR data are in keeping with the literature. [66]

Synthesis of (*R*)-*tert*-butyl 4-(methoxy(methyl)carbamoyl)-2,2-dimethyloxazolidine-3-carboxylate [(*R*)-21]

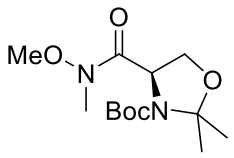

(*R*)-**21**

PTSA*H_2O (202 mg, 1.06 mmol) and 2,2-dimethoxypropane (7.86 mL, 63.9 mmol) were added to a suspension of (*R*)-**20** (5.30 g, 21.3 mmol) in benzene (115 mL). The reaction mixture was stirred under reflux for 30 min, then the MeOH-benzene azeotrope was distilled over 1 h. Additional 2,2-dimethoxypropane (2.88 mL, 23.4 mmol) was added and distillation of the azeotrope was continued for 3 h. Benzene was removed under reduced pressure, Et_2O was added and washed with 5% aq. $NaHCO_3$ and brine. The organic layer was dried over anhydrous Na_2SO_4, filtered and the solvent was removed under vacuum. The crude product was purified by flash chromatography on silica gel (cyclohexane/EtOAc, 8:2 to 1:1) obtaining (*R*)-*tert*-butyl 4-(methoxy(methyl)carbamoyl)-2,2-dimethyloxazolidine-3-carboxylate [(*R*)-**21**] as a yellow oil (5.29 g, 86% yield).

R_f= 0.25 (cyclohexane/EtOAc, 7:3).

^{1}H-NMR (300 MHz, $CDCl_3$, 1:1 mixture of rotamers): δ= 4.80 (m, 1H), 4.72 (m, 1H), 4.18 (m, 2H), 3.94 (m, 2H), 3.74 (s, 3H), 3.69 (s, 3H), 3.21 (s, 6H), 1.70 (s, 3H), 1.68 (s, 3H), 1.56 (s, 3H), 1.52 (s, 3H), 1.49 (s, 9H), 1.41 (s, 9H). Spectroscopic data were consistent with the literature data for this compound. [67]

Synthesis of (*R*)-*tert*-butyl 4-formyl-2,2-dimethyloxazolidine-3-carboxylate [(*R*)-22]

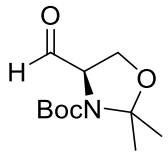

(*R*)-**22**

$LiAlH_4$ (347 mg, 9.15 mmol) was added portionwise at 0 °C to a solution of (*R*)-**21** (5.29 g, 18.3 mmol) in dry THF (130 mL). The reaction was stirred at 0 °C for 2 h, then sat. aq. $KHSO_4$ (100 mL) and Et_2O were added and the mixture was stirred at room temperature for 30 min. Phases were separated and the aqueous phase was extracted with Et_2O (2x75 mL). The pooled organic layers were dried over anhydrous Na_2SO_4, filtered and the solvent was removed under reduced pressure. The crude product was purified by flash chromatography on silica gel (cyclohexane/EtOAc, 8:2) obtaining (*R*)-*tert*-butyl 4-formyl-2,2-dimethyloxazolidine-3-carboxylate [(*R*)-**22**] as a yellow oil (3.62 g, 86% yield).

R_f= 0.25 (cyclohexane/EtOAc, 7:3).

^{1}H-NMR (300 MHz, $CDCl_3$, major rotamer): δ= 9.54 (d, *J*= 2.1 Hz, 1H), 4.19 (m, 1H), 4.08 (m, 2H), 1.59 (s, 3H), 1.51 (s, 3H), 1.43 (s, 9H).

These NMR data are in keeping with the literature. [68]

Synthesis of (*S*)-*tert*-butyl 2,2-dimethyl-4-vinyloxazolidine-3-carboxylate [(*S*)-23]

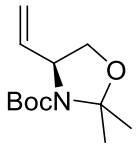

(*S*)-**23**

KHMDS (36.4 mL, 0.5 M in toluene, 18.2 mmol) was added to a suspension of methyltriphenylphosphonium bromide (6.97 g, 19.5 mmol) in dry THF (30 mL). After stirring at room temperature for 30 min, the reaction mixture was cooled at -78 °C and a solution of (*R*)-**22** (3.00 g, 13.0 mmol) in dry THF (15.5 mL) was added. The reaction was stirred at room temperature for 3 h. Et_2O (60 mL) and water (10 mL) were added, phases were separated and the aqueous phase was extracted with Et_2O. The pooled organic layers were washed with brine, dried over anhydrous Na_2SO_4, filtered and the solvent was removed under vacuum. The crude product was purified by flash chromatography on silica gel (cyclohexane/EtOAc, 9:1) obtaining (*S*)-*tert*-butyl 2,2-dimethyl-4-vinyloxazolidine-3-carboxylate [(*S*)-**23**] as a yellow oil (2.74 g, 93% yield).

R_f= 0.41 (cyclohexane/EtOAc, 8:2).

^{1}H-NMR (300 MHz, $CDCl_3$, major rotamer): δ= 5.81 (m, 1H), 5.30-5.18 (m, 2H), 4.45-4.20 (m, 1H), 4.04 (dd, *J*= 6.3, 8.7 Hz, 2H), 3.74 (dd, *J*= 2.2, 8.7 Hz, 2H), 1.60 (s, 3H), 1.51 (s, 3H), 1.44 (s, 9H).

These NMR data are in keeping with the literature. [69]

Synthesis of (*S*)-*tert*-butyl 1-hydroxybut-3-en-2-ylcarbamate [(*S*)-24]

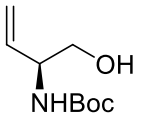

(*S*)-**24**

PTSA*H_2O (339 mg, 1.78 mmol) was added at 0 °C to a solution of (*S*)-**23** (811 mg, 3.57 mmol) in MeOH (35 mL). The reaction mixture was stirred at room temperature for 6 h, then the volume was reduced under vacuum and EtOAc was added and washed with sat. aq. $NaHCO_3$. The organic phase was dried over Na_2SO_4, filtered and the solvent was removed under reduced pressure obtaining (*S*)-*tert*-butyl 1-hydroxybut-3-en-2-ylcarbamate [(*S*)-**24**] was obtained as a pale yellow oil (387 mg, 58% yield).

R_f= 0.29 (cyclohexane/EtOAc, 6:4).

^{1}H-NMR (300 MHz, $CDCl_3$): δ= 5.79 (ddd, *J*= 5.4, 10.5, 17.1 Hz, 1H), 5.24 (dd, *J*= 1.2, 17.1 Hz, 1H), 5.19 (dd, *J*= 1.2, 10.5 Hz, 1H), 5.00 (d, *J*= 7.2 Hz, 1H), 4.20 (m, 1H), 3.68 (dd, *J*= 4.7, 11.3 Hz, 1H), 3.59 (dd, *J*= 5.9, 11.3 Hz, 1H), 2.62 (m, 1H), 1.43 (s, 9H).

^{13}C-NMR (75 MHz, $CDCl_3$): δ= 156.0, 135.5, 116.4, 79.8, 65.0, 54.6, 28.3.

NMR data are in keeping with the literature. [70]

$[\alpha]_D^{20}$= - 22.4° (c= 0.55, $CHCl_3$). (lit. – 22.4°) [70]

Synthesis of *tert*-butyl (*R*)-1-((*S*)-3-bromo-4,5-dihydroisoxazol-5-yl)-2-hydroxyethylcarbamate [(*S*,*R*)-40]

Method A

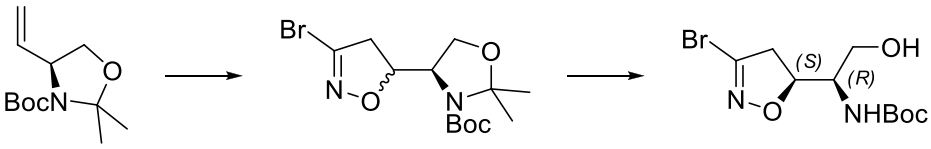

(*S*)-**23** (*S*,*R*)-**38**/(*R*,*R*)-**39** (*S*,*R*)-**40**

DBF (2.13 g, 10.5 mmol) and $NaHCO_3$ (4.41 g, 52.5 mmol) were added to a solution of (*S*)-**23** (2.38 g, 2.00 mmol) in EtOAc (45 mL). The reaction mixture was stirred at room temperature until consumption of (*S*)-**23**. EtOAc was added and washed with water, dried over anhydrous Na_2SO_4 and the solvent was removed under reduced pressure. The crude product was purified by flash chromatography on silica gel (cyclohexane/EtOAc, 9:1) obtaining the cycloadducts (*S*,*R*)-**38** and (*R*,*R*)-**39** in a diastereoisomeric mixture as yellow oil (3.59 g, 98% yield).

The mixture of (*S*,*R*)-**38** and (*R*,*R*)-**39** (4.36 g, 11.3 mmol) was dissolved in 5:1 AcOH/water (100 mL). The reaction mixture was stirred at 40 °C for 48 h. The solvent was removed under reduced pressure, EtOAc (100 mL) was added and washed with water (2x60 mL). The crude was purified by flash chromatography on silica gel (cyclohexane/EtOAc, 9:1 to 1:1) obtaining *tert*-butyl (*R*)-1-((*S*)-3-bromo-4,5-dihydroisoxazol-5-yl)-2-hydroxyethylcarbamate [(*S*,*R*)-**40**] as a white solid (1.50 g, 43% yield). The calculated diastereoisomeric ratio for the 1,3-cycloaddition step was indirectly quantified as 1.4:1 (*S*,*R*)-**38**/(*R*,*R*)-**39**.

Method B

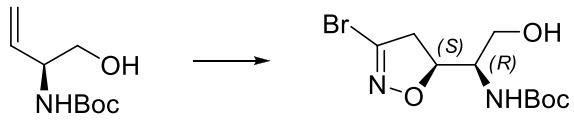

(*S*)-**24** (*S*,*R*)-**40**

DBF (2.07 g, 10.2 mmol) and $NaHCO_3$ (3.59 g, 42.7 mmol) were added to a solution of (*S*)-**24** (1.6 g, 8.54 mmol) in EtOAc (30 mL). The reaction mixture was stirred at room temperature until consumption of (*S*)-**24**. EtOAc was added and washed with water, dried over anhydrous Na_2SO_4 and evaporated under reduced pressure. The crude product was purified by flash chromatography on silica gel (cyclohexane/EtOAc, 7:3) obtaining *tert*-butyl (*R*)-1-((*S*)-3-bromo-4,5-dihydroisoxazol-5-yl)-2-hydroxyethylcarbamate [(*S*,*R*)-**40**] as a white solid (1.01 g, 39% yield). This 1,3-cycloaddition step showed a diastereoisomeric ratio of 1:1.

R_f= 0.37 (cyclohexane/EtOAc, 6:4).

^{1}H-NMR (300 MHz, $CDCl_3$): δ= 5.11 (bs, 1H), 4.77 (ddd, *J*= 8.7, 8.7, 8.7 Hz, 1H), 3.99-3.88 (m, 1H), 3.82-3.67 (m, 2H), 3.38-3.25 (m, 2H), 1.89 (bs, 1 H), 1.45 (s, 9 H).

NMR data are in keeping with the literature. [38]

Synthesis of (*S*)-2-((*S*)-3-bromo-4,5-dihydroisoxazol-5-yl)-2-(*tert*-butoxycarbonylamino)acetic acid [(*S*,*S*)-41]

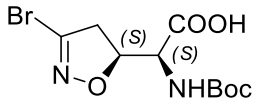

(*S*,*S*)-**41**

PDC (10.9 g, 29.1 mmol) was added to a solution of (*S*,*R*)-**40** (600 mg, 1.94 mmol) in DMF (11 mL). The reaction mixture was stirred at room temperature for 6 h, then water (34 mL) was added and it was extracted with EtOAc (3x25 mL). The organic phase was extracted with 1 M aq. NaOH (4x20 mL), then the organic extracts were made acid with 2 M aq. HCl and extracted with EtOAc (3x60 mL). The pooled organic extracts were dried over anhydrous Na_2SO_4 and the solvent was removed under reduced pressure obtaining (*S*)-2-((*S*)-3-bromo-4,5-dihydroisoxazol-5-yl)-2-(*tert*-butoxycarbonylamino)acetic acid [(*S*,*S*)-**41**] as a green solid (574 mg, 91% yield).

R_f= 0.60 (DCM/MeOH, 9:1 + 1% AcOH).

^{1}H-NMR (300 MHz, $CDCl_3$): δ= 5.45 (bs, 1H), 5.00 (ddd, *J*= 3.9, 7.7, 11.0 Hz, 1H), 4.52 (dd, *J*= 3.9, 8.0 Hz, 1H), 3.60–3.30 (m, 2H), 1.45 (s, 9H).

These NMR data are in keeping with the literature. [38]

Synthesis of (*S*)-2-amino-2-((*S*)-3-bromo-4,5-dihydroisoxazol-5-yl)acetic acid hydrobromide [(*S*,*S*)-1*HBr]

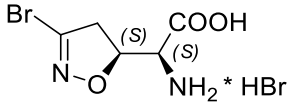

(*S*,*S*)-**1*HBr**

33% HBr/AcOH (7 mL) was added to (*S*,*S*)-**41** (200 mg, 0.619 mmol). The reaction mixture was stirred at room temperature for 5 min, then the solvent was removed under reduced pressure. The obtained solid was crystallized with *i*PrOH/Et_2O. (*S*)-2-amino-2-((*S*)-3-bromo-4,5-dihydroisoxazol-5-yl)acetic acid hydrobromide [(*S*,*S*)-**1*HBr**] was obtained as a grey solid (112 mg, 60% yield).

^{1}H-NMR (300 MHz, D_2O): δ= 5.10 (ddd, *J*= 3.3, 7.5, 11.1 Hz, 1H), 4.06 (d, *J*= 3.3 Hz, 1H), 3.51 (dd, *J*= 11.1, 18.0 Hz, 1H), 3.39 (dd, *J*= 7.5, 18.0 Hz, 1H).

^{13}C-NMR (75 MHz, D_2O): δ= 169.1, 141.0, 79.3, 55.5, 43.1.

MS(ESI): *m*/*z* calcd for $C_5H_8{}^{79}Br_2N_2O_3$: 222.0 (M-HBr); found: 223.0 $[M\text{-}HBr+H]^+$.

Synthesis of (±)-2-(3-bromo-4,5-dihydroisoxazol-5-yl)acetic acid [(±)-3]

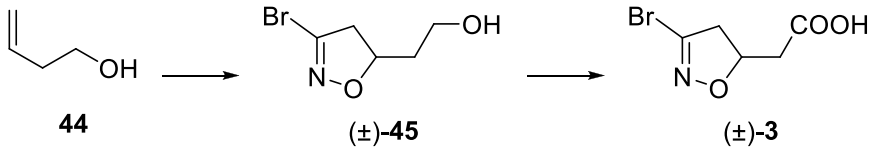

44 (±)-**45** (±)-**3**

DBF (0.40 g, 2.0 mmol) and $NaHCO_3$ (0.84 g, 10.0 mmol) were added to a solution of 3-buten-1-ol (**44**) (167 µL, 2.00 mmol) in EtOAc (2.8 mL). The reaction mixture was heated in microwave reactor at 80 °C for 1 h. Few drops of water were added and the solvent was decanted. The organic phase was washed with water (2x10 mL), dried over anhydrous Na_2SO_4 and the solvent was removed under reduced pressure. The crude product was purified by flash chromatography on silica gel (cyclohexane/EtOAc, 1:1) obtaining (±)-2-(3-bromo-4,5-dihydroisoxazol-5-yl)ethanol [(±)-**45**] as a yellow oil (237 mg, 61% yield).

R_f= 0.26 (cyclohexane/EtOAc, 1:1)

^{1}H-NMR (300 MHz, $CDCl_3$): δ= 4.84 (dddd, *J*= 5.2, 8.5, 8.5, 10.2 Hz, 1H), 3.79-3.72 (m, 2H), 3.32 (dd, *J*= 10.2, 17.3 Hz, 1H), 2.94 (dd, *J*= 8.5, 17.3 Hz, 1H), 2.59 (bs, 1H), 2.03-1.80 (m, 2H).

^{13}C-NMR (75 MHz, $CDCl_3$): δ= 138.1, 80.2, 59.2, 47.0, 37.5.

$NaIO_4$ (1.04 g, 4.88 mmol) and a catalytic amount of $Ru_2O{\cdot}H_2O$ (2.5 mg) were added to a solution of (±)-**45** (237 mg, 1.22 mmol) in 1.5:1:1 H_2O/MeCN/CCl_4 (9.2 mL). The suspension was vigorously stirred at room temperature for 45 min, then DCM (10 mL) and water (10 mL) were added. The organic layer was separated and the solvent was removed under reduced pressure. The residue was dissolved in EtOAc (5 mL), extracted with 10% aq. K_2CO_3 (3x5 mL). The aqueous phase was made acidic with 2 M aq. HCl and newly extracted with EtOAc (3x5 mL). The organic extracts were washed with brine, dried over anhydrous Na_2SO_4, and the solvent removed under vacuum obtaining (±)-2-(3-bromo-4,5-dihydroisoxazol-5-yl)acetic acid [(±)-**3**] as a white solid (185 mg, 73% yield) which recrystallizes from *n*-hexane/EtOAc as white prisms (m.p.= 82-83 °C) (lit. m.p.= 82-83 °C). [39]

R_f= 0.40 (DCM/MeOH, 95:5 + 1% AcOH)

^{1}H-NMR (300 MHz, $CDCl_3$): δ= 5.05 (dddd, *J*= 6.0, 7.3, 7.3, 10.4 Hz, 1H), 3.45 (dd, *J*=10.4, 17.4 Hz, 1H), 3.00 (dd, *J*= 7.3, 17.4 Hz, 1H), 2.90 (dd, *J*= 6.0, 16.8 Hz, 1 H), 2.54 (dd, *J*= 7.3, 16.8 Hz, 1H).

^{13}C-NMR (75 MHz, $CDCl_3$): δ= 175.3, 137.6, 77.5, 46.8, 39.2.

MS(ESI): *m*/*z* calcd for $C_5H_6{}^{79}BrNO_3$: 206.9; found: 205.8 $[M-H]^-$.

Synthesis of (±)-*tert*-butyl (3-bromo-4,5-dihydroisoxazol-5-yl)methylcarbamate [(±)-4]

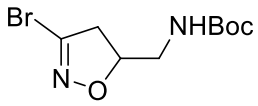

(±)-**4**

tert-Butyl allylcarbamate (**44**) was synthesized following published synthetic procedure. [71]

DBF (2.7 g, 13.0 mmol) and $NaHCO_3$ (4.2 g, 50.0 mmol) were added to a solution of **44** (1.8 g, 11.5 mmol) in EtOAc (50 mL). The reaction mixture was stirred at room temperature until consumption of **44**. Water was added, phases were separated and the aqueous phase was extracted with EtOAc (3x15 mL). The organic extracts were dried over anhydrous Na_2SO_4 and the solvent was removed under vacuum. The crude product was purified by flash chromatography on silica gel (cyclohexane/EtOAc, 85:15) obtaining (±)-*tert*-butyl (3-bromo-4,5-dihydroisoxazol-5-yl)methylcarbamate [(±)-**4**] as a white solid (2.92 g, 91% yield) which recrystallizes as colourless prisms from petroleum ether/EtOAc (m.p.= 69-70 °C) (lit. m.p.= 69-70 °C). [71]

R_f= 0.29 (cyclohexane/EtOAc, 8:2).

^{1}H-NMR (300 MHz, $CDCl_3$): δ= 4.88 (bs, 1H), 4.83-4.74 (m, 1H), 3.44-3.38 (m, 2H), 3.27 (dd, *J*=10.8, 17.4 Hz, 1H), 3.04 (dd, *J*= 7.5, 17.4 Hz, 1H), 1.45 (s, 9H).

^{13}C-NMR (75 MHz, $CDCl_3$): δ= 156.3, 137.7, 80.9, 80.0, 43.8, 43.2, 28.4.

MS(ESI): *m*/*z* calcd for $C_9H_{15}{}^{79}BrN_2O_3$: 278.0; found: 279.1 $[M+H]^+$.

Synthesis of (±)-methyl 3-bromo-4,5-dihydroisoxazole-5-carboxylate [(±)-5]

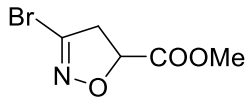

(±)-**5**

DBF (200 mg, 0.986 mmol) and $NaHCO_3$ (414 mg, 4.93 mmol) were added to a solution of methyl acrylate (133 µL, 1.48 mmol) in EtOAc (2.5 mL). The reaction mixture was vigorously stirred at room temperature for 30 h. EtOAc (10 mL) was added and the organic phase was washed with water (7 mL), dried over anhydrous Na_2SO_4, filtered and evaporated to afford (±)-methyl 3-bromo-4,5-dihydroisoxazole-5-carboxylate [(±)-**5**] as a yellow oil (190 mg, 93% yield).

R_f= 0.37 (cyclohexane/EtOAc, 8:2).

^{1}H-NMR (300 MHz, $CDCl_3$): δ= 5.10 (dd, *J*= 8.2, 10.2 Hz, 1H), 3.83 (s, 3H), 3.55-3.47 (m, 2H).

^{13}C-NMR (75 MHz, $CDCl_3$): δ= 169.6, 137.0, 78.4, 53.3, 45.0.

MS(ESI): *m*/*z* calcd for $C_5H_6{}^{79}BrNO_3$: 206.9; found: 207.8 $[M+H]^+$.

Synthesis of (±)-*tert*-butyl 3-bromo-6,6a-dihydro-3a*H*-pyrrolo[3,4-*d*]isoxazole-5(4*H*)-carboxylate [(±)-6] and HPLC resolution of the racemate

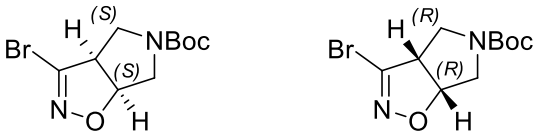

(*S,S*)-**6** (*R,R*)-**6**

tert-Butyl 2,5-dihydro-1*H*-pyrrole-1-carboxylate (**29**) was obtained following published synthetic procedure. [40]

DBF (3.6 g, 17.7 mmol) and $NaHCO_3$ (3.81 g, 44.3 mmol) were added to a solution of **29** (1.5 g, 11.5 mmol) in EtOAc (30 mL). The reaction mixture was stirred at room temperature until consumption of **29**. Water was added, phases were separated and the aqueous phase was extracted with EtOAc. The organic extracts were dried over anhydrous Na_2SO_4 and the solvent was removed under vacuum. The crude product was purified by flash chromatography on silica gel (cyclohexane/EtOAc, 9:1 to 8:2) obtaining (±)-*tert*-butyl 3-bromo-6,6a-dihydro-3a*H*-pyrrolo[3,4-*d*]isoxazole-5(4*H*)-carboxylate [(±)-**6**] as a white solid (2.58 g, quantitative yield) which recrystallizes from *i*PrOH as white prisms (m.p.= 50-52 °C) (lit. m.p.= 50-52 °C). [72]

R_f= 0.43 (cyclohexane/AcOEt, 7:3).

^{1}H-NMR (300 MHz, $CDCl_3$): δ= 5.24 (ddd, *J*= 1.4, 5.8, 8.8 Hz, 1H), 4.02-3.86 (m, 3H), 3.52 (dd, *J*= 5.8, 13.2 Hz, 1H), 3.41 (dd, *J*= 8.0, 12.1 Hz, 1 H), 1.45 (s, 9H).

^{13}C-NMR (75 MHz, $CDCl_3$): δ= 154.2, 139.6, 85.0, 80.8, 57.4, 54.0, 48.6, 28.5.

MS(ESI): *m*/*z* calcd for $C_{10}H_{15}{}^{79}BrN_2O_3$: 290.0; found: 291.0 $[M+H]^+$.

The racemic mixture was resolved by HPLC using a Kromasil 5-AmyCoat 21.2x250 mm column and *n*-hexane/*i*PrOH 9:1 as eluent (flux= 15 mL, λ= 220 nm, $V_{injection}$= 1 mL; c= 100 mg/mL).

(-)-**6** t_R= 8.99 min; $[\alpha]_D^{20}$= - 100.5° (c= 0.60, $CHCl_3$).

(+)-**6** t_R= 10.81 min; $[\alpha]_D^{20}$= + 101.0° (c= 0.64, $CHCl_3$).

(+)-**6** was crystallized from EtOAc/*n*-hexane 1:20 as colourless prisms and its absolute configuration was determined by X-ray crystallography analysis exploiting anomalous scattering due to the presence of the heavy bromine atom. (+)-(*S,S*)-**6**; (-)-(*R,R*)-**6**.

Synthesis of (*S*)-2-(benzyloxycarbonylamino)-2-((*S*)-3-bromo-4,5-dihydroisoxazol-5-yl)acetic acid [(*S*,*S*)-7]

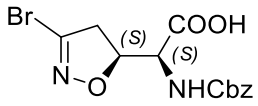

(*S*,*S*)-**7**

$NaHCO_3$ (84 mg, 1.00 mmol) was added to a solution of (*S*,*S*)-**1*HBr** (76 mg, 0.250 mmol) in 1:1 water/THF (8 mL). The reaction mixture was stirred at room temperature for 5 min, then benzyl chloroformate (39 mL, 0.28 mmol) was added dropwise and the reaction was stirred at room temperature for 1 h. After disappearance of the starting material, the organic solvent was removed under reduced pressure and the aqueous phase was washed with Et_2O (1x4 mL), made acidic with 2 M HCl and extracted with EtOAc (3x5 mL). The pooled organic extracts were dried over anhydrous Na_2SO_4, and the solvent evaporated obtaining (*S*)-2-(benzyloxycarbonylamino)-2-((*S*)-3-bromo-4,5-dihydroisoxazol-5-yl)acetic acid [(*S*,*S*)-**7**] as an hygroscopic white foam (83 mg, 93% yield).

R_f= 0.35 (DCM/MeOH, 95:5 + 1% AcOH).

^{1}H -NMR (300 MHz, $CDCl_3$): δ= 8.90 (bs, 1H), 7.40–7.25 (m, 5H), 5.92 (d, *J*=7.7 Hz, 1H), 5.12 (s, 2H), 4.98–4.85 (m, 1H), 4.58 (dd, *J*=3.6, 8.2 Hz, 1H), 3.58–3.18 (m, 2H).

^{13}C-NMR (75 MHz, $CDCl_3$): δ= 171.7, 156.4, 138.7, 135.9, 128.9, 128.7, 128.4, 81.9, 67.9, 56.6, 44.2.

$[\alpha]_D^{20}$= + 167° (c= 0.20, H_2O).

MS(ESI): *m/z* calcd for $C_{13}H_{13}{}^{79}BrN_2O_5$: 356.0; found: 357.0 $[M+H]^+$.

Synthesis of (*S*)-methyl 2-((*S*)-3-bromo-4,5-dihydroisoxazol-5-yl)-2-(*tert*-butoxycarbonylamino)acetate [(*S*,*S*)-42]

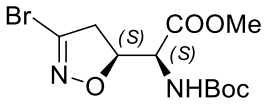

(*S*,*S*)-**42**

Trimethylsilyl diazomethane (155 µL, 2.0 M in hexanes, 0.310 mmol) was added at 0 °C to a solution of (*S*,*S*)-**41** (100 mg, 0.310 mmol) in 7:3 toluene/MeOH (2.0 mL). Reaction mixture was stirred at room temperature for 1 h, then it was quenched with few drops of AcOH. The solvent was removed under reduced pressure and the crude product was purified by flash chromatography on silica gel (cyclohexane/EtOAc, 8:2 to 7:3) obtaining (*S*)-methyl 2-((*S*)-3-bromo-4,5-dihydroisoxazol-5-yl)-2-(*tert*-butoxycarbonylamino)acetate [(*S*,*S*)-**42**] as a yellow oil (71 mg, 68% yield).

R_f= 0.44 (cyclohexane/EtOAc, 7:3).

^{1}H-NMR (300 MHz, $CDCl_3$): δ= 5.50 (d, *J*= 8.0, 1H), 4.92 (ddd, *J*= 3.3, 7.2, 10.5 Hz, 1H), 4.42 (dd, *J*= 3.3, 8.0 Hz, 1H), 3.78 (s, 3H), 3.44 (dd, *J*= 7.2, 17.3 Hz, 1H), 3.36 (dd, *J*= 10.5, 17.3 Hz, 1H), 1.42 (s, 9H).

^{13}C-NMR (75 MHz, $CDCl_3$): δ= 169.3, 155.3, 138.2, 82.2, 80.9, 56.6, 53.2, 44.5, 28.4.

$[\alpha]_D^{20}$= + 158.1° (c= 0.50, $CHCl_3$).

Synthesis of (*S*)-methyl 2-amino-2-((*S*)-3-bromo-4,5-dihydroisoxazol-5-yl)acetate [(*S*,*S*)-8]

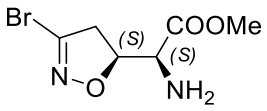

(*S*,*S*)-**8**

TFA (163 µL, 2.11 mmol) was added at 0 °C to a solution of (*S*,*S*)-**42** (71 mg, 0.211 mmol) in DCM (380 µL). Reaction mixture was stirred at room temperature for 4 h, then DCM was added and the acid was quenched with 5% aq. $NaHCO_3$. Phases were separated and the aqueous phase was extracted with DCM. The pooled organic layers were dried over anhydrous Na_2SO_4, filtered and the solvent was removed under reduced pressure. The crude product was purified by flash chromatography on silica gel using 100% EtOAc as eluent, obtaining (*S*)-methyl 2-amino-2-((*S*)-3-bromo-4,5-dihydroisoxazol-5-yl)acetate [(*S*,*S*)-**8**] as a red oil (26 mg, 52% yield).

R_f= 0.40 (EtOAc, 100%).

^{1}H-NMR (300 MHz, $CDCl_3$): δ= 5.00 (ddd, *J*= 3.5, 8.0, 10.7 Hz, 1H), 3.92 (d, *J* = 3.5 Hz, 1H), 3.75 (s, 3H), 3.33 (dd, *J*= 8.0, 17.3 Hz, 1H), 3.20 (dd, *J*= 10.7, 17.3 Hz, 1H), 1.90 (bs, 2H).

^{13}C-NMR (75 MHz, $CDCl_3$): δ= 172.0, 138.2, 82.7, 56.2, 52.8, 42.5.

$[\alpha]_D^{20}$= + 95.7° (c= 0.34, $CHCl_3$).

MS(ESI): *m*/*z* calcd for $C_6H_9{}^{79}BrN_2O_3$: 236.0; found: 236.9 $[M+H]^+$.

Synthesis of (*S*)-benzyl 2-((*S*)-3-bromo-4,5-dihydroisoxazol-5-yl)-2-(*tert*-butoxycarbonylamino)acetate [(*S*,*S*)-43]

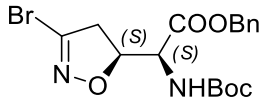

(*S*,*S*)-**41**

Benzyl bromide (66.2 µL, 0.557 mmol) was added to a solution of (*S*,*S*)-**41** (150 mg, 0.464 mmol) in DMF (1.5 mL). Reaction mixture was stirred at 50 °C for 1 h, then EtOAc was added and washed with 1 M aq. HCl, 5% aq. $NaHCO_3$ and brine. The organic phase was dried over anhydrous Na_2SO_4, filtered and the solvent was removed under reduced pressure. The crude product was purified by flash chromatography on silica gel (cyclohexane/EtOAc, 95:5 to 8:2) obtaining (*S*)-benzyl 2-((*S*)-3-bromo-4,5-dihydroisoxazol-5-yl)-2-(*tert*-butoxycarbonylamino)acetate [(*S*,*S*)-**43**] as a yellow oil (160 mg, 83% yield).

R_f= 0.51 (cyclohexane/EtOAc, 3:1).

^{1}H-NMR (300 MHz, $CDCl_3$): δ= 7.40−7.30 (m, 5H), 5.55 (d, *J*= 6.0 Hz, 1H), 5.22 (d, *J* = 12.0 Hz, 1H), 5.14 (d, *J*= 12.0 Hz, 1H), 4.83 (ddd, *J* = 3.6, 7.4, 11.0 Hz, 1H), 4.50 (m, 1H), 3.42 (dd, *J* = 6.9, 17.6 Hz, 1H), 3.30 (dd, *J* = 11.3, 17.6 Hz, 1H), 1.42 (s, 9H).

^{13}C-NMR (75 MHz, $CDCl_3$): δ= 168.7, 155.3, 138.1, 134.9, 128.9, 128.9, 82.3, 80.9, 68.3, 56.6, 44.4, 28.5.

$[\alpha]_D^{20}$= + 132.0° (c= 0.50, $CHCl_3$).

Synthesis of (*S*)-benzyl 2-amino-2-((*S*)-3-bromo-4,5-dihydroisoxazol-5-yl)acetate [(*S*,*S*)-9]

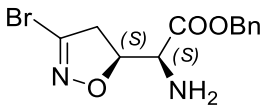

(*S*,*S*)-**9**

TFA (300 µL, 13.7 mmol) was added at 0 °C to a solution of (*S*,*S*)-**43** (116 mg, 0.281 mmol) in DCM (1.0 mL). Reaction mixture was stirred at room temperature for 4 h, then DCM was added and the acid was quenched with 5% aq. $NaHCO_3$. Phases were separated and the aqueous phase was extracted with DCM. The pooled organic layers were dried over anhydrous Na_2SO_4, filtered and the solvent was removed under reduced pressure. The crude product was purified by flash chromatography on silica gel using 100% EtOAc as eluent, obtaining (*S*)-benzyl 2-amino-2-((*S*)-3-bromo-4,5-dihydroisoxazol-5-yl)acetate [(*S*,*S*)-**9**] as an orange oil (45 mg, 51% yield).

R_f= 0.65 (EtOAc, 100%).

^{1}H-NMR (300 MHz, $CDCl_3$): δ= 7.40−7.30 (m, 5H), 5.21 (d, *J* = 12.0 Hz, 1H), 5.16 (d, *J* = 12.0 Hz, 1H), 4.98 (ddd, *J* = 3.9, 8.0, 10.7 Hz, 1H), 3.94 (d, *J* = 3.9 Hz, 1H), 3.33 (dd, *J*= 8.0, 17.3 Hz, 1H), 3.10 (dd, *J*= 10.7, 17.3 Hz, 1H), 1.70 (bs, 2H).

^{13}C-NMR (75 MHz, $CDCl_3$): δ= 171.4, 138.1, 135.3, 129.0, 128.9, 128.7, 82.8, 67.6, 56.3, 42.4.

$[\alpha]_D^{20}$= + 63.4° (c= 0.72, $CHCl_3$).

MS(ESI): *m*/*z* calcd for $C_{12}H_{13}{}^{79}BrN_2O_3$: 312.0; found: 312.9 $[M+H]^+$.

Synthesis of (±)-3-bromo-5-phenyl-4,5-dihydroisoxazole [(±)-10]

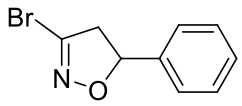

(±)-**10**

DBF (1.00 g, 4.93 mmol) and $NaHCO_3$ (2.07 g, 24.6 mmol) were added to a solution of styrene (**48**) (0.85 mL, 7.40 mmol) in EtOAc (16 mL). The reaction mixture was vigorously stirred at room temperature until consumption of DBF. EtOAc was added and the organic phase was washed with water, dried over anhydrous Na_2SO_4, filtered and evaporated. The crude product was purified by flash chromatography on silica gel (cyclohexane/EtOAc, 95:5) obtaining (±)-3-bromo-5-phenyl-4,5-dihydroisoxazole [(±)-**10**] as a colorless oil (960 mg, 86% yield).

R_f= 0.50 (cyclohexane/EtOAc, 9:1).

^{1}H-NMR (300 MHz, $CDCl_3$): δ= 7.42-7.31 (m, 5H), 5.67 (dd, *J*= 8.9, 11.0 Hz, 1H), 3.62 (dd, *J*= 11.0, 17.3 Hz, 1H), 3.21 (dd, *J*= 8.9, 17.3, 1H).

^{13}C-NMR (75 MHz, $CDCl_3$): δ= 139.5, 137.0, 129.2, 129.0, 126.2, 83.5, 49.4.

MS(ESI): *m*/*z* calcd for $C_9H_8{}^{79}BrNO$: 225.0; found: 225.9 $[M+H]^+$.

Synthesis of 1-nitro-4-vinylbenzene (34)

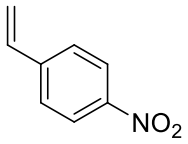

32

KHMDS (5.46 mL, 0.5 M in toluene, 2.73 mmol) was added to a suspension of methyltriphenylphosphonium bromide (1.06 g, 2.98 mmol) in dry THF (6 mL). The reaction mixture was vigorously stirred at room temperature for 30 min, then a solution of 4-nitrobenzaldehyde (**31**) (300 µL, 1.95 mmol) in dry THF (2 mL) was added. The reaction mixture was stirred at room temperature for 2.5 h, then it was quenched with 25% aq NH_4Cl (10 mL), phases were separated and the aqueous phase was extracted with Et_2O (2x15 mL). The combined organic phases were washed with brine (15 mL), dried over anhydrous Na_2SO_4, filtered and evaporated. The crude product was purified by flash chromatography on silica gel (cyclohexane/EtOAc, 99:1 to 9:1) obtaining 1-nitro-4-vinylbenzene (**34**) as a yellow oil (130 mg, 48% yield).

R_f= 0.51 (cyclohexane/EtOAc, 95:5).

^{1}H-NMR (300 MHz, $CDCl_3$): δ= 8.19 (m, 2H), 7.54 (m, 2H), 6.68 (dd, *J*= 8.4, 13.2 Hz, 1H), 5.93 (d, *J*= 13.2 Hz, 1H), 5.50 (d, *J*= 8.4 Hz, 1H).

^{13}C-NMR (75 MHz, $CDCl_3$): δ= 147.1, 143.8, 134.9, 126.8, 123.9, 118.6.

Synthesis of (±)-3-bromo-5-(4-nitrophenyl)-4,5-dihydroisoxazole [(±)-11]

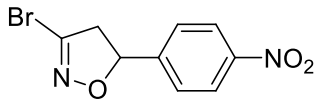

(±)-**11**

DBF (176 mg, 0.872 mmol) and $NaHCO_3$ (366 mg, 4.36 mmol) were added to a solution of **34** (130 mg, 0.872 mmol) in EtOAc (2.6 mL). The reaction mixture was vigorously stirred at room temperature until consumption of **34**. EtOAc (10 mL) was added and the organic phase was washed with water (7 mL), dried over anhydrous Na_2SO_4, filtered and evaporated. The crude product was purified by flash chromatography on silica gel (cyclohexane/EtOAc, 9:1) obtaining (±)-3-bromo-5-(4-nitrophenyl)-4,5-dihydroisoxazole [(±)-**11**] as a white solid (190 mg, 80 % yield) which recrystallizes as white needles (m.p.= 101.1-101.5 °C).

R_f= 0.41 (cyclohexane/EtOAc, 8:2).

^{1}H-NMR (300 MHz, $CDCl_3$): δ= 8.26 (m, 2H), 7.53 (m, 2H), 5.78 (dd, *J*= 8.2, 11.1 Hz, 1H), 3.74 (dd, *J*= 11.1, 17.3 Hz, 1H), 3.17 (dd, *J*= 8.2, 17.3 Hz, 1H).

^{13}C-NMR (75 MHz, $CDCl_3$): δ= 148.2, 146.8, 136.9, 126.9, 124.4, 81.9, 49.6.

MS(ESI): *m/z* calcd for $C_9H_7{}^{79}BrN_2O_3$: 270.0; found: 270.8 $[M+H]^+$.

Synthesis of (±)-3-bromo-5-(pyridin-4-yl)-4,5-dihydroisoxazole [(±)-12]

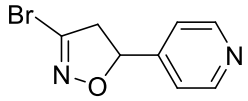

(±)-**12**

DBF (194 mg, 0.955 mmol) and $NaHCO_3$ (160 mg, 1.91 mmol) were added to a solution of 4-vinylpyridine (**50**) (103 µL, 0.955 mmol) in EtOAc (1.9 mL). The reaction mixture was vigorously stirred at room temperature until consumption of **50**. EtOAc was added and the organic phase was washed with water, dried over anhydrous Na_2SO_4, filtered and evaporated. The crude product was purified by flash chromatography on silica gel (cyclohexane/EtOAc, 2:8) obtaining (±)-3-bromo-5-(pyridin-4-yl)-4,5-dihydroisoxazole [(±)-**12**] as a white solid (87 mg, 40% yield) which recrystallizes as colorless prisms from *n*-hexane/EtOAc (decomposes at T> 72 °C).

R_f= 0.40 (EtOAc).

^{1}H-NMR (300 MHz, $CDCl_3$): δ= 8.60 (d, *J*= 6.0 Hz, 2H), 7.22 (d, *J*= 6.0 Hz, 2H), 5.65 (dd, *J*= 8.0, 11.0 Hz, 1H), 3.70 (dd, *J*= 11.0, 17.3 Hz, 1H), 3.12 (dd, *J*= 8.0, 17.3 Hz, 1H).

^{13}C-NMR (75 MHz, $CDCl_3$): δ= 150.5, 148.7, 137.0, 120.6, 81.3, 49.2.

MS(ESI): *m/z* calcd for $C_8H_7{}^{79}BrN_2O$ 226.0; found 227.1 $[M+H]^+$.

Synthesis of (±)-3-bromo-5-(4-fluorophenyl)-4,5-dihydroisoxazole [(±)-13]

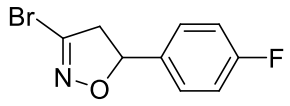

(±)-**13**

DBF (150 mg, 0.739 mmol) and $NaHCO_3$ (310 mg, 3.69 mmol) were added to a solution of 4-fluorostyrene (**49**) (132 µL, 1.11 mmol) in EtOAc (3 mL). The reaction mixture was vigorously stirred at room temperature for 24 h. EtOAc (10 mL) was added and the organic phase was washed with water (7 mL), dried over anhydrous Na_2SO_4, filtered and evaporated. The crude product was purified by flash chromatography on silica gel (cyclohexane/EtOAc, 98:2) obtaining (±)-3-bromo-5-(4-fluorophenyl)-4,5-dihydroisoxazole [(±)-**13**] as a white solid (154 mg, 93% yield) which recrystallizes as white needles from *n*-hexane (m.p.= 59.2-59.9 °C).

R_f= 0.37 (cyclohexane/EtOAc, 9:1).

^{1}H-NMR (300 MHz, $CDCl_3$): δ= 7.33 (m, 2H), 7.08 (m, 2H), 5.66 (dd, *J*= 9.1, 10.7 Hz, 1H), 3.61 (dd, *J*= 10.7, 17.3 Hz, 1H), 3.18 (dd, *J*= 9.1, 17.3 Hz, 1H).

^{13}C-NMR (75 MHz, $CDCl_3$): δ= 163.1 (d, $J_{C\text{-}F}$= 247.9 Hz), 136.9, 135.3 (d, $J_{C\text{-}F}$= 3.1 Hz), 128.1 (d, $J_{C\text{-}F}$= 8.3 Hz), 116.1 (d, $J_{C\text{-}F}$= 21.7 Hz), 82.8, 49.4.

MS(ESI): *m/z* calcd for $C_9H_7{}^{79}BrFNO$: 243.0; found: 243.9 $[M+H]^+$.

Synthesis of (±)-4-(3-bromo-4,5-dihydroisoxazol-5-yl)aniline [(±)-14]

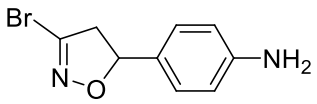

(±)-**14**

DBF (200 mg, 0.986 mmol) and $NaHCO_3$ (414 mg, 4.93 mmol) were added to a solution of 4-vinylaniline (**36**) (115 µL, 0.986 mmol) in EtOAc (2.3 mL). The reaction mixture was vigorously stirred at room temperature for 20 h. EtOAc (10 mL) was added and the organic phase was washed with water, dried over anhydrous Na_2SO_4, filtered and evaporated. The crude product was purified by flash chromatography on silica gel (cyclohexane/EtOAc, 8:2 to 7:3) obtaining (±)-4-(3-bromo-4,5-dihydroisoxazol-5-yl)aniline [(±)-**14**] as a brown oil (85 mg, 36% yield).

R_f= 0.26 (cyclohexane/EtOAc, 7:3).

^{1}H-NMR (300 MHz, $CDCl_3$): δ= 7.15 (m, 2H), 6.71 (m, 2H), 5.56 (dd, *J*= 9.6, 10.7 Hz, 1H), 3.51 (dd, *J*= 10.7, 17.3 Hz, 1H), 3.18 (dd, *J*= 9.6, 17.3 Hz, 1H).

^{13}C-NMR (75 MHz, $CDCl_3$): δ= 147.3, 137.0, 128.6, 127.9, 115.4, 83.9, 48.9.

MS(ESI): *m/z* calcd for $C_9H_9{}^{79}BrN_2O$: 240.0; found: 241.0 $[M+H]^+$.

Synthesis of 4-vinylphenol (33)

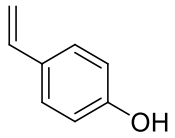

33

KHMDS (6.9 mL, 0.5 M in toluene, 3.44 mmol) was added to a suspension of methyltriphenylphosphonium bromide (1.32 g, 3.69 mmol) in dry THF (9 mL). The reaction mixture was vigorously stirred at room temperature for 30 min, then a solution of 4-hydroxybenzaldehyde (**30**) (300 mg, 2.46 mmol) in dry THF (3 mL) was added. The reaction mixture was stirred at room temperature for 2.5 h, then it was quenched with 25% aq. NH_4Cl (10 mL), phases were separated and the aqueous phase was extracted with Et_2O. The pooled organic phases were washed with brine (15 mL), dried over anhydrous Na_2SO_4, filtered and evaporated. The crude product was purified by flash chromatography on silica gel (cyclohexane/EtOAc, 85:5) obtaining 4-vinylphenol (**33**) as a grey solid (140 mg, 48% yield) (m.p.= 71.9-72.6 °C) (lit. m.p.= 71-72 °C). [73]

R_f= 0.59 (cyclohexane/EtOAc, 7:3)

^{1}H-NMR (300 MHz, CD_3OD): δ= 7.25 (m, 2H), 6.72 (m, 2H), 6.68 (dd, *J*= 10.8, 17.8 Hz, 1H), 5.55 (dd, *J*= 0.9, 17.8 Hz, 1H), 5.02 (dd, *J*= 0.9, 10.8 Hz, 1H).

These NMR data are in keeping with the literature. [73]

Synthesis of (±)-4-(3-bromo-4,5-dihydroisoxazol-5-yl)phenol [(±)-15]

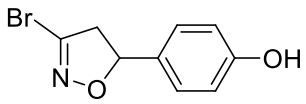

(±)**-15**

DBF (108 mg, 0.530 mmol) and $NaHCO_3$ (223 mg, 2.65 mmol) were added to a solution of **33** (63 mg, 0.530 mmol) in EtOAc (2.0 mL). The reaction mixture was vigorously stirred at room temperature until consumption of **33**. EtOAc (10 mL) was added and the organic phase was washed with water, dried over anhydrous Na_2SO_4, filtered and evaporated. The crude product was purified by flash chromatography on silica gel (cyclohexane/EtOAc, 8:2) obtaining (±)-4-(3-bromo-4,5-dihydroisoxazol-5-yl)phenol [(±)-**15**] as a yellow oil (99 mg, 77% yield).

R_f= 0.44 (cyclohexane/EtOAc, 7:3).

^{1}H-NMR (300 MHz, $CDCl_3$): δ= 7.18 (m, 2H), 6.84 (m, 2H), 6.51 (bs, 1H) 5.59 (dd, *J*= 9.6, 10.7 Hz, 1H), 3.55 (dd, *J*= 10.7, 17.4 Hz, 1H), 3.19 (dd, *J*= 9.6, 17.4 Hz, 1H).

^{13}C-NMR (75 MHz, $CDCl_3$): δ= 156.8, 137.5, 130.7, 128.1, 116.1, 83.7, 49.0.

MS(ESI): *m/z* calcd for $C_9H_8{}^{79}BrNO_2$: 241.0; found: 241.8 $[M+H]^+$.

Synthesis of *N*-(4-vinylphenyl)acetamide (37)

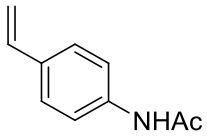

37

Sodium acetate (34 mg, 0.513 mmol) and acetic anhydride (157 µL, 1.76 mmol) were added to a solution of 4-vinylaniline (**36**) (200 µL, 1.71 mmol) in glacial acetic acid (0.5 mL). The reaction mixture was stirred at room temperature for 30 min, then it was cooled, filtered on a hirsch and washed with water. *N*-(4-Vinylphenyl)acetamide (**37**) was obtained as a white solid (215 mg, 78% yield) (m.p.= 132.3-133.8 °C). [74]

R_f= 0.21 (cyclohexane/EtOAc, 7:3).

^{1}H-NMR (300 MHz, $CDCl_3$): δ= 7.46 (m, 2H), 7.36 (m, 2H), 7.25 (bs, 1H), 6.66 (dd, *J*= 10.7, 17.6 Hz, 1H), 5.67 (d, *J*= 17.6 Hz, 1H), 5.02 (d, *J*= 10.7 Hz, 1H), 2.17 (s, 3H).

These NMR data are in keeping with the literature. [74]

Synthesis of (±)-*N*-(4-(3-bromo-4,5-dihydroisoxazol-5-yl)phenyl)acetamide [(±)-16]

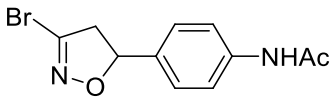

(±)-16

DBF (201 mg, 0.993 mmol) and $NaHCO_3$ (417 mg, 5.10 mmol) were added to a solution of **37** (160 mg, 0.993 mmol) in DCM (4.2 mL). The reaction mixture was vigorously stirred at room temperature until consumption of **37**. 5% MeOH/DCM was added and solid $NaHCO_3$ was filtered off. The crude product was purified by flash chromatography on silica gel (cyclohexane/EtOAc, 6:4 to 4:6) obtaining (±)-*N*-(4-(3-bromo-4,5-dihydroisoxazol-5-yl)phenyl)acetamide [(±)-**16**] as a white solid (232 mg, 82% yield) (m.p.= 165.5-166.1 °C then decomposes).

R_f= 0.27 (cyclohexane/EtOAc, 1:1).

^{1}H-NMR (300 MHz, $CDCl_3$): δ= 7.52 (m, 2H), 7.30 (m, 2H), 7.21 (bs, 1H), 5.63 (dd, *J*= Hz, 2H), 4.77 (ddd, *J*= 9.2, 10.7 Hz, 1H), 3.59 (dd, *J*= 10.7, 17.3 Hz, 1H), 3.18 (dd, *J*= 9.2, 17.3 Hz, 1H), 2.18 (s, 3H).

^{13}C-NMR (75 MHz, $CDCl_3$): δ= 168.8, 138.7, 137.1, 135.0, 127.0, 120.4, 83.2, 49.2 24.8.

MS(ESI): *m/z* calcd for $C_{11}H_{11}{}^{79}BrN_2O_2$: 282.0; found: 282.8 $[M+H]^+$.

Synthesis of 1-methoxy-4-vinylbenzene (35)

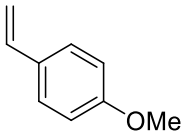

35

KHMDS (6.16 mL, 0.5 M in toluene, 3.08 mmol) was added to a suspension of methyltriphenylphosphonium bromide (1.18 g, 3.30 mmol) in dry THF (6 mL).The reaction mixture was stirred at room temperature for 30 min, then a solution of 4-methoxybenzaldehyde (**32**) (268 µL, 2.20 mmol) in dry THF (2 mL) was added. The reaction mixture was stirred at room temperature for 2.5 h, it was quenched with 25% aq. NH_4Cl (10 mL), phases were separated and the aqueous phase was extracted with Et_2O (2 x 15 mL). The combined organic phases were washed with brine (15 mL), dried over anhydrous Na_2SO_4, filtered and evaporated. The crude product was purified by flash chromatography on silica gel (cyclohexane/EtOAc, 99:1) obtaining 1-methoxy-4-vinylbenzene (**35**) as a yellow oil (200 mg, 68% yield).

R_f= 0.72 (cyclohexane/EtOAc, 95:5).

^{1}H-NMR (300 MHz, $CDCl_3$): δ= 7.35 (m, 2H), 6.86 (m, 2H), 6.67 (dd, *J*= 10.8, 17.7 Hz, 1H), 5.62 (d, *J*= 17.7, 1H), 5.13 (d, *J*= 10.8, 1H), 3.82 (s, 3H).

^{13}C-NMR (75 MHz, $CDCl_3$): δ= 159.3, 136.2, 130.4, 127.3, 113.9, 111.5, 55.3.

Synthesis of (±)-3-bromo-5-(4-methoxyphenyl)-4,5-dihydroisoxazole [(±)-17]

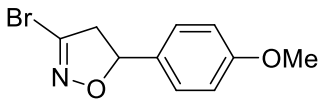

(±)-**17**

DBF (287 mg, 1.42 mmol) and $NaHCO_3$ (596 mg, 7.10 mmol) were added to a solution of **35** (190 mg, 1.41 mmol) in EtOAc (3.8 mL). The reaction mixture was vigorously stirred at room temperature until consumption of **35**. EtOAc (10 mL) was added and the organic phase was washed with water (7 mL), dried over anhydrous Na_2SO_4, filtered and the solvent was removed under vacuum. The crude product was purified by flash chromatography on silica gel (cyclohexane/EtOAc, 9:1) obtaining (±)-3-bromo-5-(4-methoxyphenyl)-4,5-dihydroisoxazole [(±)-**17**] as a yellow solid (276 mg, 76% yield) which recrystallizes from diisopropylether as yellow scales (m.p.= 59.4-60.8 °C) (lit. m.p.= 62-63 °C). [75]

R_f= 0.49 (cyclohexane/EtOAc, 9:1).

^{1}H-NMR (300 MHz, $CDCl_3$): δ= 7.28 (m, 2H), 6.91 (m, 2H), 5.62 (dd, *J*= 9.4, 10.7 Hz, 1H), 3.81 (s, 3H), 3.56 (dd, *J*= 10.7, 17.3 Hz, 1H), 3.20 (dd, *J*= 9.4, 17.3 Hz, 1H).

^{13}C-NMR (75 MHz, $CDCl_3$): δ= 160.2, 137.0, 131.2, 127.8, 114.5, 83.4, 55.6, 49.1.

MS(ESI): *m/z* calcd for $C_{10}H_{10}{}^{79}BrNO_2$: 255.0; found: 255.8 $[M+H]^+$.

Synthesis of (±)-3-chloro-5-phenyl-4,5-dihydroisoxazole [(±)-51]

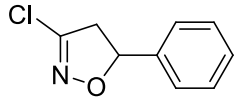

(±)-**51**

(±)-**10** (452 mg, 2.0 mmol) was dissolved in 10 M HCl in THF (5 mL). The reaction mixture was stirred at room temperature for 4 h, then the solvent was evaporated, water (5 mL) added, and the aqueous phase extracted with EtOAc (2x5 mL). The pooled organic layers were dried over anhydrous Na_2SO_4, filtered and the solvent was removed under reduced pressure. The crude product was purified by flash chromatography on silica gel (cyclohexane/EtOAc, 95:5) obtaining (±)-3-chloro-5-phenyl-4,5-dihydroisoxazole [(±)-**51**] as a colorless oil (327 mg, 90% yield).

R_f= 0.46 (cyclohexane/EtOAc, 9:1).

^{1}H-NMR (300 MHz, $CDCl_3$): δ= 7.42-7.35 (m, 5H), 5.67 (dd, *J*= 9.1, 10.7 Hz, 1H), 3.62 (dd, *J*= 10.7, 17.0 Hz, 1H), 3.18 (dd, *J*= 9.1, 17.0 Hz, 1H).

^{13}C-NMR (75 MHz, $CDCl_3$): δ= 148.8, 139.5, 129.2, 129.0, 126.2, 84.1, 46.4.

MS(ESI): *m/z* calcd for $C_9H_8{}^{35}ClNO$: 181.0; found: 182.0 $[M+H]^+$.

Synthesis of (±)-5-phenylpyrazolidin-3-one [(±)-55]

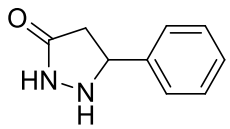

(±)-**55**

Methyl (*E*)-cinnamate (**54**) (1.00 g, 6.17 mmol) was added to a solution of hydrazine monohydrate (329 µL, 6.79 mmol) in EtOH (6.2 mL). Reaction mixture was stirred under reflux for 50 h. The solvent was removed under vacuum and the crude product was purified by flash chromatography on silica gel ($CHCl_3$/MeOH, 15:1) obtaining (±)-5-phenylpyrazolidin-3-one [(±)-**55**] as a white solid (620 mg, 62% yield) (m.p.= 100.8-101.7 °C) (lit. m.p.= 100-102 °C). [76]

R_f= 0.32 (DCM/MeOH, 95:5).

^{1}H-NMR (300 MHz, $CDCl_3$): δ= 7.43-7.30 (m, 5H), 4.83 (dd, *J*= 7.7, 9.2 Hz, 1H), 2.84 (dd, *J*= 7.7, 16.2 Hz, 1H), 2.76 (dd, *J*= 9.2, 16.2 Hz, 1H).

^{13}C-NMR (75 MHz, $CDCl_3$): δ= 176.9, 138.9, 129.1, 128.5, 126.8, 61.8, 38.7.

Synthesis of (±)-1-ethyl-5-phenylpyrazolidin-3-one [(±)-56]

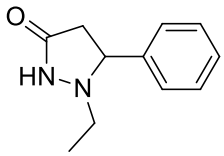

(±)-**56**

Acetaldehyde (108 µL, 1.91 mmol) was added to a solution of (±)-**55** (200 mg, 1.23 mmol) in MeOH (28 mL). Reaction mixture was stirred at room temperature for 30 min, then $NaBH_4$ (84 mg, 1.85 mmol) was added and the reaction mixture was stirred for 1 h. The solvent was removed under vacuum, the residue was dissolved in EtOAc (15 mL) and washed with 10% aq. NH_4Cl (3x15 mL). The organic phase was dried over anhydrous Na_2SO_4, filtered and the solvent was removed under reduced pressure. The crude product was purified by flash chromatography on silica gel (cyclohexane/EtOAc, 3:8) obtaining (±)-1-ethyl-5-phenylpyrazolidin-3-one [(±)-**56**] as a white solid (130 mg, 55% yield) which recrystallizes from diisopropyl ether as white needles (m.p.= 113.0-113.6 °C).

R_f= 0.39 (cyclohexane/EtOAc, 2:8).

^{1}H-NMR (300 MHz, $CDCl_3$): δ= 8.25 (bs, 1H), 7.46-7.26 (m, 5H), 4.12 (dd, *J*= 8.4, 8.7 Hz, 1H), 3.02 (dd, *J*= 8.4, 16.8 Hz, 1H), 2.86 (dq, *J*= 7.3, 12.0 Hz, 1H), 2.67 (dq, *J*= 6.9, 12.0 Hz, 1H), 2.56 (dd, *J*= 8.7, 16.8 Hz, 1H), 1.14 (dd, *J*= 6.9, 7.3 Hz, 3H).

^{13}C-NMR (75 MHz, $CDCl_3$): δ= 173.1, 140.3, 128.9, 128.2, 127.3, 67.8, 53.0, 39.9, 13.1.

Synthesis of (±)-3-chloro-1-ethyl-5-phenyl-4,5-dihydro-1*H*-pyrazole [(±)-52]

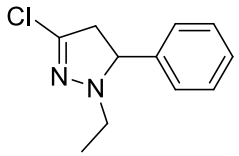

(±)-**52**

$POCl_3$ (1.25 mL, 12.5 mmol) was added to a solution of (±)-**56** (237 mg, 1.25 mmol) in MeCN (60 mL).The reaction was stirred under reflux for 3 h. The solvent was removed under vacuum, the residue was dissolved in EtOAc (50 mL) and the solution was added dropwise to an ice and water solution (30 mL). The organic layer was separated and washed with H_2O (50 mL) and brine (50 mL). The organic phase was dried over anhydrous Na_2SO_4, filtered and the solvent was removed under reduced pressure. The crude product was purified by flash chromatography on silica gel (cyclohexane/EtOAc, 98:2) obtaining (±)-3-chloro-1-ethyl-5-phenyl-4,5-dihydro-1*H*-pyrazole [(±)-**52**] as a yellow oil (64 mg, 25% yield).

R_f= 0.48 (cyclohexane/EtOAc, 95:5).

^{1}H-NMR (300 MHz, $CDCl_3$): δ= 7.45-7.28 (m, 5H), 4.28 (dd, *J*= 10.2, 14.3 Hz, 1H), 3.15 (dd, *J*= 10.2, 16.6 Hz, 1H), 2.94 (dd, *J*= 14.3, 16.6 Hz, 1H), 2.90 (dq, *J*= 7.3, 12.6 Hz, 1H), 2.80 (dd, *J*= 7.0, 12.6 Hz, 1H), 1.17 (dt, *J*= 7.0, 7.3 Hz, 3H).

^{13}C-NMR (75 MHz, $CDCl_3$): δ= 141.2, 139.7, 128.9, 128.4, 127.8, 72.1, 49.1, 47.6, 12.9, 10.3

MS(ESI): *m/z* calcd for $C_{11}H_{13}{}^{35}ClN_2$: 208.1; found: 209.0 $[M+H]^+$.

Synthesis of (±)-1-benzyl-5-phenylpyrazolidin-3-one [(±)-57]

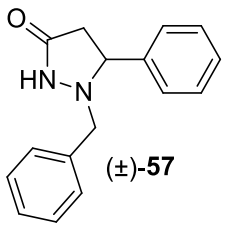

(±)-**57**

Benzyl bromide (147 µL, 1.23 mmol), K_2CO_3 (170 mg, 1.23 mmol) and NaI (18 mg, 0.12 mmol) were added to a solution of (±)-**55** (200 mg, 1.23 mmol) in MeCN (23 mL). The reaction mixture was stirred under reflux for 3 h. The solvent was removed under vacuum and the residue was diluted with EtOAc (25 mL). The organic layer was washed with 3% aq. NH_4Cl (25 mL), dried over anhydrous Na_2SO_4, filtered and the solvent was removed under reduced pressure. The crude product was purified by flash chromatography on silica gel (cyclohexane/EtOAc, 6:4 to 1:1) obtaining (±)-1-benzyl-5-phenylpyrazolidin-3-one [(±)-**57**] as a white solid (200 mg, 64% yield) which recrystallizes from diisopropyl ether as white needles (m.p.= 110.8-112.4 °C).

R_f= 0.46 (cyclohexane/EtOAc, 4:6).

^{1}H-NMR (300 MHz, $CDCl_3$): δ= 7.51-7.27 (m, 10H), 6.76 (bs, 1H), 4.23 (dd, *J*= 8.2, 9.6 Hz, 1H), 4.04 (d, *J*= 12.8 Hz, 1H), 3.58 (d, *J*= 12.8 Hz, 1H), 2.98 (dd, *J*= 8.2, 16.8 Hz, 1H), 2.58 (dd, *J*= 9.6, 9.6 Hz, 1H).

^{13}C-NMR (75 MHz, $CDCl_3$): δ= 172.9, 139.8, 136.4, 129.3, 129.1, 129.0, 128.3, 128.3, 127.4, 67.3, 62.3, 39.7.

Synthesis of (±)-1-benzyl-3-chloro-5-phenyl-4,5-dihydro-1*H*-pyrazole [(±)-53]

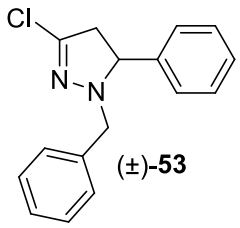

(±)-**53**

$POCl_3$ (793 µL, 7.93 mmol) was added to a solution of (±)-**57** (200 mg, 0.793 mmol) in MeCN (34 mL).The reaction mixture was stirred under reflux for 3 h. The solvent was removed under vacuum, the residue was dissolved in EtOAc (50 mL) and the solution was added dropwise to an ice and water solution (30 mL). The organic layer was separated and washed with H_2O (50 mL) and brine (50 mL). The organic phase was dried over anhydrous Na_2SO_4, filtered and the solvent was removed under reduced pressure. The crude product was purified by flash chromatography on silica gel (cyclohexane/EtOAc, 99:1) obtaining (±)-1-benzyl-3-chloro-5-phenyl-4,5-dihydro-1*H*-pyrazole [(±)-**53**] as a yellow oil (100 mg, 46% yield).

R_f= 0.54 (cyclohexane/EtOAc, 95:5).

^{1}H-NMR (300 MHz, $CDCl_3$): δ= 7.47-7.22 (m, 10H), 4.30 (dd, *J*= 10.2, 14.3 Hz, 1H), 4.28 (d, *J*= 14.0 Hz, 1H), 3.83 (d, *J*= 14.0 Hz, 1H), 3.09 (dd, *J*= 10.2, 16.5 Hz, 1H), 2.94 (dd, *J*= 14.3, 16.5 Hz, 1H).

^{13}C-NMR (75 MHz, $CDCl_3$): δ= 141.3, 139.2, 136.4, 129.7, 129.0, 128.5, 128.0, 127.6, 70.5, 57.4, 47.6.

MS(ESI): *m/z* calcd for $C_{16}H_{15}{}^{35}ClN_2$: 270.1; found: 271.5 $[M+H]^+$.

Synthesis of *tert*-butyl (*R*)-2-(benzyloxy)-1-((*S*)-3-bromo-4,5-dihydroisoxazol-5-yl)ethylcarbamate [(*S,R*)-60]

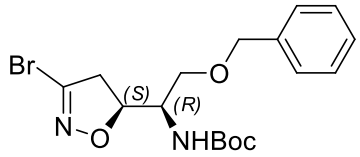

(*S,R*)-**60**

Freshly prepared Ag_2O (115 mg, 0.498 mmol) and benzyl bromide (395 µL, 3.32 mmol) were added to a solution of (*S,R*)-**40** (100 mg, 0.332 mmol) in DCM (4.0 mL). Reaction mixture was stirred at room temperature overnight, then it was filtered over celite and the solvent was removed under reduced pressure. The crude product was purified by flash chromatography on silica gel (cyclohexane/EtOAc, 9:1 to 8:2) obtaining *tert*-butyl (*R*)-2-(benzyloxy)-1-((*S*)-3-bromo-4,5-dihydroisoxazol-5-yl)ethylcarbamate [(*S,R*)-**60**] as a yellow oil (48 mg, 36% yield).

R_f= 0.50 (cyclohexane/EtOAc, 8:2).

^{1}H-NMR (300 MHz, $CDCl_3$): δ= 7.41-7.25 (m, 5H), 5.06 (d, *J*= 7.1 Hz, 2H), 4.77 (ddd, *J*= 7.2, 8.4, 10.2 Hz, 1H), 4.52 (s, 2H), 3.85 (m, 1H), 3.79 (dd, *J*= 2.5, 9.6 Hz, 1H), 3.55 (dd, *J*= 3.7, 9.6 Hz, 1H), 3.34 (dd, *J*= 7.2, 17.7 Hz, 1H), 3.22 (dd, *J*= 10.2, 17.7 Hz, 1H), 1.44 (s, 9H).

^{13}C-NMR (75 MHz, $CDCl_3$): δ= 155.6, 138.0, 137.7, 128.5, 127.9, 127.7, 80.6, 80.1, 73.5, 68.6, 52.4, 44.3, 28.3.

$[\alpha]_D^{20}$= + 48.0° (c= 0.95, $CHCl_3$).

Synthesis of (*R*)-2-(benzyloxy)-1-((*S*)-3-bromo-4,5-dihydroisoxazol-5-yl)ethanamine [(*S*,*R*)-58]

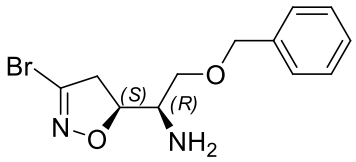

(*S*,*R*)-**58**

TFA (86 µL, 1.13 mmol) was added at 0 °C to a solution of (*S*,*R*)-**60** (45 mg, 0.113 mmol) in DCM (487 µL). The reaction mixture was stirred at room temperature for 4 h, then DCM was added and the acid was quenched with 5% aq. $NaHCO_3$. Phases were separated and the aqueous phase was extracted with DCM. The pooled organic layers were dried over anhydrous Na_2SO_4, filtered and the solvent was removed under reduced pressure. The crude product was purified by flash chromatography on silica gel (DCM/MeOH, 96:4) obtaining (*R*)-2-(benzyloxy)-1-((*S*)-3-bromo-4,5-dihydroisoxazol-5-yl)ethanamine [(*S*,*R*)-**58**] as a yellow oil (19 mg, 56% yield).

R_f= 0.32 (DCM/MeOH, 96:4).

^{1}H-NMR (300 MHz, $CDCl_3$): δ= 7.40-7.25 (m, 5H), 4.69 (ddd, *J*= 5.3, 8.7, 10.8 Hz, 1H), 4.51 (s, 2H), 3.50 (dd, *J*= 4.5, 9.3 Hz, 1H), 3.40 (dd, *J*= 5.7, 9.3 Hz, 1H), 3.34 (dd, *J*= 8.7, 17.7 Hz, 1H), 3.28 (ddd, *J*= 4.5, 5.3, 5.7 Hz, 1H), 3.10 (dd, *J*= 10.8, 17.7 Hz, 1H), 1.38 (bs, 2H).

^{13}C-NMR (75 MHz, $CDCl_3$): δ= 138.0, 137.8, 128.5, 127.8, 127.7, 83.3, 73.5, 71.3, 52.5, 42.3.

$[\alpha]_D^{20}$= + 58.3° (c= 0.75, $CHCl_3$).

MS(ESI): *m/z* calcd for $C_{12}H_{15}{}^{79}BrN_2O_2$: 298.0; found: 298.8 $[M+H]^+$.

Synthesis of *tert*-butyl (*S*)-2-(benzylamino)-1-((*S*)-3-bromo-4,5-dihydroisoxazol-5-yl)-2-oxoethylcarbamate [(*S*,*S*)-61]

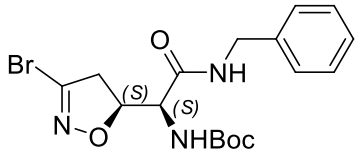

(*S*,*R*)-**61**

Benzylamine (18.2 µL, 0.167 mmol), EDC hydrochloride (32 mg, 0.167 mmol) and HOBt (11 mg, 0.0835 mmol) were added to a solution of (*S*,*S*)-**41** (54 mg, 0.167 mmol) in dry THF (6 mL). The reaction mixture was stirred at room temperature for 2 h, then the solvent was removed under reduced pressure and the crude product was purified by flash chromatography on silica gel (cyclohexane/EtOAc, 7:3) obtaining *tert*-butyl (*S*)-2-(benzylamino)-1-((*S*)-3-bromo-4,5-dihydroisoxazol-5-yl)-2-oxoethylcarbamate [(*S*,*S*)-**61**] as a colourless oil (48 mg, 70% yield).

R_f= 0.32 (cyclohexane/EtOAc, 7:3).

^{1}H-NMR (300 MHz, $CDCl_3$): δ= 7.38-7.22 (m, 5H), 6.54 (t, *J*= 5.7 Hz, 1H), 5.48 (d, *J*= 7.8 Hz, 1H), 4.74 (ddd, *J*= 6.6, 8.3, 10.5 Hz, 1H), 4.48 (d, *J*= 5.7 Hz, 2H), 4.26 (dd, *J*= 7.8, 8.3 Hz, 1H), 3.52 (dd, *J*= 6.6, 17.7 Hz, 1H), 3.32 (dd, *J*= 10.5, 17.7 Hz, 1H), 1.44 (s, 9H).

^{13}C-NMR (75 MHz, $CDCl_3$): δ= 168.4, 155.9, 138.8, 137.4, 128.7, 127.6, 127.6, 81.8, 80.8, 55.7, 44.3, 43.8, 28.2.

$[\alpha]_D^{20}$= + 141.3° (c= 1.0, $CHCl_3$).

Synthesis of (*S*)-2-amino-*N*-benzyl-2-((*S*)-3-bromo-4,5-dihydroisoxazol-5-yl)acetamide [(*S*,*S*)-59]

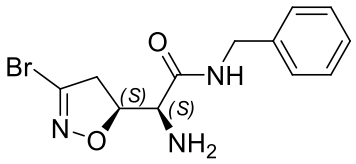

(*S*,*S*)-**59**

TFA (185 µL, 2.42 mmol) was added at 0 °C to a solution of (*S*,*S*)-**61** (100 mg, 0.242 mmol) in DCM (1 mL). The reaction mixture was stirred at room temperature for 4 h, then it was diluted with DCM and the acid was quenched with 5% aq. $NaHCO_3$. Phases were separated and the aqueous phase was extracted with DCM. The pooled organic layers were dried over anhydrous Na_2SO_4, filtered and the solvent was removed under reduced pressure. The crude product was purified by flash chromatography on silica gel (EtOAc, 100%) obtaining (*S*)-2-amino-*N*-benzyl-2-((*S*)-3-bromo-4,5-dihydroisoxazol-5-yl)acetamide [(*S*,*S*)-**59**] as a colourless solid (55 mg, 73% yield) which recrystallizes from 1:3 *i*PrOH/*n*-hexane as colourless needles (m.p.= 90.6-91.3 °C).

R_f= 0.28 (EtOAc, 100%).

^{1}H-NMR (300 MHz, $CDCl_3$): δ= 7.41-7.23 (m, 6H), 5.09 (dt, *J*= 4.8, 9.6 Hz, 1H), 4.44 (d, *J*= 6.3 Hz, 2H), 3.80 (d, *J*= 4.8 Hz, 1H), 3.22 (d, *J*= 9.6 Hz, 2H), 1.49 (bs, 2H).

^{13}C-NMR (75 MHz, $CDCl_3$): δ= 170.5, 138.1, 137.8, 128.8, 127.7, 127.6, 82.8, 56.4, 43.3, 41.8.

$[\alpha]_D^{20}$= + 80.9° (c= 1.0, $CHCl_3$).

MS(ESI): *m/z* calcd for $C_{12}H_{14}{}^{79}BrN_3O_2$: 311.0; found: 311.9 $[M+H]^+$.

Synthesis of *tert*-butyl (*R*)-1-((*S*)-3-bromo-4,5-dihydroisoxazol-5-yl)-2-(4-nitrobenzyloxy)ethylcarbamate [(*S,R*)-72]

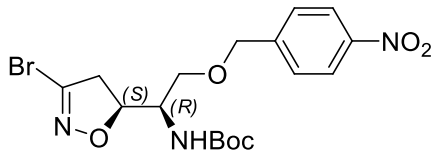

(*S,R*)-**72**

Freshly prepared Ag_2O (749 mg, 3.23 mmol) and 4-nitrobenzyl bromide (**69**) (1.40 g, 6.47 mmol) were added to a solution of (*S,R*)-**40** (200 mg, 0.647 mmol) in DCM (6.7 mL). Reaction mixture was stirred at room temperature overnight, then it was filtered over celite and the solvent was removed under reduced pressure. The crude product was purified by flash chromatography on silica gel (cyclohexane/EtOAc, 9:1 to 8:2) obtaining *tert*-butyl (*R*)-1-((*S*)-3-bromo-4,5-dihydroisoxazol-5-yl)-2-(4-nitrobenzyloxy)ethylcarbamate [(*S,R*)-**72**] as a brown oil (98 mg, 32% yield).

R_f= 0.25 (cyclohexane/EtOAc, 8:2).

^{1}H-NMR (300 MHz, $CDCl_3$): δ= 8.21 (d, *J*= 8.7 Hz, 2H), 7.47 (d, *J*= 8.7 Hz, 2H), 5.00 (d, *J*= 8.1 Hz, 1H), 4.78 (q, *J*= 8.7 Hz, 1H), 4.63 (m, 2H), 3.89 (m, 1H), 3.84 (dd, *J*= 2.6, 9.3 Hz, 1H), 3.61 (dd, *J*= 3.6, 9.3 Hz, 1H), 3.35 (dd, *J*= 7.5, 17.6 Hz, 1H), 3.27 (dd, *J*= 10.6, 17.6 Hz, 1H), 1.45 (s, 9H).

^{13}C-NMR (75 MHz, $CDCl_3$): δ= 155.5, 147.5, 145.1, 138.1, 127.8, 123.7, 80.5, 80.4, 72.2, 69.3, 52.4, 44.5, 28.3.

$[\alpha]_D^{20}$= + 48.9° (c= 0.112, $CHCl_3$).

Synthesis of (*R*)-1-((*S*)-3-bromo-4,5-dihydroisoxazol-5-yl)-2-(4-nitrobenzyloxy)ethanamine [(*S*,*R*)-62]

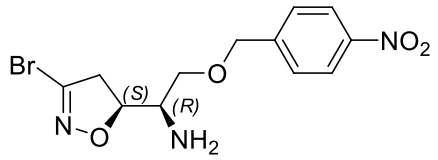

(*S*,*R*)-**61**

TFA (132 µL, 1.73 mmol) was added at 0 °C to a solution of (*S*,*R*)-**72** (77 mg, 0.173 mmol) in DCM (0.8 mL). The reaction mixture was stirred at room temperature for 4 h, then DCM was added and the acid was quenched with 5% aq. $NaHCO_3$. Phases were separated and the aqueous phase was extracted with DCM. The pooled organic layers were dried over anhydrous Na_2SO_4, filtered and the solvent was removed under reduced pressure. The crude product was purified by flash chromatography on silica gel (EtOAc, 100%) obtaining (*R*)-1-((*S*)-3-bromo-4,5-dihydroisoxazol-5-yl)-2-(4-nitrobenzyloxy)ethanamine [(*S*,*R*)-**62**] as a white solid (26 mg, 43% yield) which recrystallizes from 1:3 *i*PrOH/*n*-hexane as colourless needles (m.p.= 86.8-87.5 °C).

R_f= 0.30 (EtOAc, 100%).

^{1}H-NMR (300 MHz, $CDCl_3$): δ= 8.20 (m, 2H), 7.47 (m, 2H), 4.70 (ddd, *J*= 5.7, 8.4, 10.8 Hz, 1H), 4.62 (s, 2H), 3.58 (dd, *J*= 4.5, 9.5 Hz, 1H), 3.52 (dd, *J*= 5.7, 9.5 Hz, 1H), 3.34 (dd, *J*= 8.4, 17.1 Hz, 1H), 3.28 (m, 1H), 3.17 (dd, *J*= 10.8, 17.1 Hz, 1H), 1.66 (bs, 2H).

^{13}C-NMR (75 MHz, $CDCl_3$): δ= 147.5, 145.3, 137.9, 127.7, 123.7, 82.9, 72.2, 72.0, 52.7, 42.8.

$[\alpha]_D^{20}$= + 54.5° (c= 0.326, $CHCl_3$).

MS(ESI): *m/z* calcd for $C_{12}H_{14}{}^{79}BrN_3O_4$: 343.0; found 344.0 $[M+H]^+$.

Synthesis of *tert*-butyl (*R*)-1-((*S*)-3-bromo-4,5-dihydroisoxazol-5-yl)-2-(4-fluorobenzyloxy)ethylcarbamate [(*S,R*)-73]

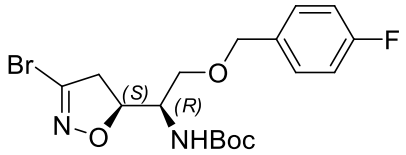

(*S,R*)-**73**

Freshly prepared Ag_2O (749 mg, 3.23 mmol) and 4-fluorobenzyl bromide (**70**) (722 µL, 6.47 mmol) were added to a solution of (*S,R*)-**40** (100 mg, 0.332 mmol) in DCM (6.7 mL). Reaction mixture was stirred at room temperature overnight, then it was filtered over celite and the solvent was removed under reduced pressure. The crude product was purified by flash chromatography on silica gel (cyclohexane/EtOAc, 9:1 to 8:2) obtaining *tert*-butyl (*R*)-1-((*S*)-3-bromo-4,5-dihydroisoxazol-5-yl)-2-(4-fluorobenzyloxy)ethylcarbamate [(*S,R*)-**73**] as a yellow oil (127 mg, 47% yield).

R_f= 0.55 (cyclohexane/EtOAc, 7:3).

^{1}H-NMR (300 MHz, $CDCl_3$): δ= 7.28 (m, 2H), 7.03 (t, *J*= 9.0 Hz, 2H), 5.01 (d, *J*= 6.9 Hz, 1H), 4.76 (dd, *J*= 8.6, 17.6 Hz, 1H), 4.47 (s, 2H), 3.85 (m, 1H), 3.77 (dd, *J*= 2.3, 9.6 Hz, 1H), 3.53 (dd, *J*= 3.7, 9.6 Hz, 1H), 3.33 (dd, *J*= 7.2, 17.7 Hz, 1H), 3.23 (dd, *J*= 10.5, 17.7 Hz, 1H), 1.44 (s, 9H).

^{13}C-NMR (75 MHz, $CDCl_3$): δ= 162.4 (d, $J_{C\text{-}F}$= 245.1 Hz), 155.6, 138.1, 133.4, 129.5 (d, $J_{C\text{-}F}$= 8.0 Hz), 115.4 (d, $J_{C\text{-}F}$= 21.7 Hz), 80.6, 80.2, 72.8, 68.6, 52.4, 44.4, 28.3.

This intermediate was not pure enough to provide an accurate absolute value of specific optical rotation.

Synthesis of (*R*)-1-((*S*)-3-bromo-4,5-dihydroisoxazol-5-yl)-2-(4-fluorobenzyloxy)ethanamine [(*S*,*R*)-63]

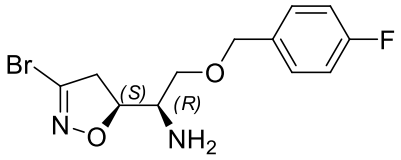

(*S*,*R*)-**63**

TFA (187 µL, 2.44 mmol) was added at 0 °C to a solution of (*S*,*R*)-**73** (102 mg, 0.244 mmol) in DCM (1.1 mL). The reaction mixture was stirred at room temperature for 4 h, then DCM was added and the acid was quenched with 5% aq. $NaHCO_3$. Phases were separated and the aqueous phase was extracted with DCM. The pooled organic layers were dried over anhydrous Na_2SO_4, filtered and the solvent was removed under reduced pressure. The crude product was purified by flash chromatography on silica gel (EtOAc, 100%) obtaining (*R*)-1-((*S*)-3-bromo-4,5-dihydroisoxazol-5-yl)-2-(4-fluorobenzyloxy)ethanamine [(*S*,*R*)-**63**] as a yellow oil (38 mg, 49% yield).

R_f= 0.35 (EtOAc, 100%).

^{1}H-NMR (300 MHz, $CDCl_3$): δ= 7.30 (m, 2H), 7.04 (m, 2H), 4.76 (ddd, *J*= 5.1, 8.7, 11.1 Hz, 1H), 4.49 (s, 2H), 3.56 (dd, *J*= 4.6, 9.6 Hz, 1H), 3.49 (dd, *J*= 5.5, 9.6 Hz, 1H), 3.38 (dd, *J*= 8.7, 17.7 Hz, 1H), 3.34 (ddd, *J*= 4.6, 5.1, 5.5 Hz, 1H), 3.17 (dd, *J*= 11.1, 17.7 Hz, 1H).

^{13}C-NMR (75 MHz, $CDCl_3$): δ= 162.4 (d, $J_{C\text{-}F}$= 245.0 Hz), 138.0, 133.5 (d, $J_{C\text{-}F}$= 2.6 Hz), 129.5 (d, $J_{C\text{-}F}$= 8.0 Hz), 115.4 (d, $J_{C\text{-}F}$= 20.6 Hz), 80.0, 72.8, 71.1, 52.6, 42.5.

$[\alpha]_D^{20}$= + 59.0° (c= 0.50, $CHCl_3$).

MS(ESI): *m/z* calcd for $C_{12}H_{14}{}^{79}BrFN_2O_2$: 316.0; found 316.9 $[M+H]^+$.

Synthesis of *tert*-butyl (*R*)-2-(biphenyl-4-ylmethoxy)-1-((*S*)-3-bromo-4,5-dihydroisoxazol-5-yl)ethylcarbamate [(*S*,*R*)-74]

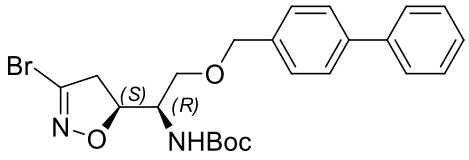

(*S*,*R*)-**74**

Freshly prepared Ag_2O (749 mg, 3.23 mmol) and 4-bromomethylbiphenyl bromide (**71**) (1.60 g, 6.47 mmol) were added to a solution of (*S*,*R*)-**40** (200 mg, 0.647 mmol) in DCM (6.7 mL). Reaction mixture was stirred at room temperature overnight, then it was filtered over celite and the solvent was removed under reduced pressure. The crude product was purified by flash chromatography on silica gel (cyclohexane/EtOAc, 9:1 to 8:2) obtaining *tert*-butyl (*R*)-2-(biphenyl-4-ylmethoxy)-1-((*S*)-3-bromo-4,5-dihydroisoxazol-5-yl)ethylcarbamate [(*S*,*R*)-**74**] as a yellow oil (98 mg, 32% yield).

R_f= 0.47 (cyclohexane/EtOAc, 8:2).

^{1}H-NMR (300 MHz, $CDCl_3$): δ= 7.59 (m, 4H), 7.48-7.32 (m, 5H), 5.06 (d, *J*= 8.1 Hz, 1H), 4.80 (m, 1H), 4.57 (s, 2H), 3.88 (m, 1H), 3.83 (dd, *J*= 2.5, 9.4 Hz, 1H), 3.59 (dd, *J*= 3.7, 9.4 Hz, 1H), 3.36 (dd, *J*= 7.2, 17.2 Hz, 1H), 3.24 (dd, *J*= 10.5, 17.2 Hz, 1H), 1.45 (s, 9H).

^{13}C-NMR (75 MHz, $CDCl_3$): δ= 155.6, 140.9, 140.8, 138.1, 136.7, 128.8, 128.2, 127.4, 127.2, 127.1, 80.6, 80.1, 73.3, 68.7, 52.4, 44.4, 28.3.

$[\alpha]_D^{20}$= + 34.1° (c= 0.90, $CHCl_3$).

Synthesis of (*R*)-2-(biphenyl-4-ylmethoxy)-1-((*S*)-3-bromo-4,5-dihydroisoxazol-5-yl)ethanamine [(*S,R*)-64]

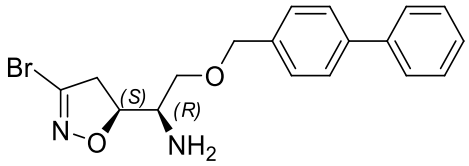

(*S,R*)-**64**

TFA (157 µL, 2.06 mmol) was added at 0 °C to a solution of (*S,R*)-**74** (98 mg, 0.206 mmol) in DCM (0.9 mL). The reaction mixture was stirred at room temperature for 4 h, then DCM was added and the acid was quenched with 5% aq. $NaHCO_3$. Phases were separated and the aqueous phase was extracted with DCM. The pooled organic layers were dried over anhydrous Na_2SO_4, filtered and the solvent was removed under reduced pressure. The crude product was purified by flash chromatography on silica gel (cyclohexane/EtOAc, 2:8 to EtOAc, 100%) obtaining (*R*)-2-(biphenyl-4-ylmethoxy)-1-((*S*)-3-bromo-4,5-dihydroisoxazol-5-yl)ethanamine [(*S,R*)-**64**] as a yellow oil (28 mg, 36% yield).

R_f= 0.39 (cyclohexane/EtOAc, 2:8).

^{1}H-NMR (300 MHz, $CDCl_3$): δ= 7.58 (m, 4H), 7.48-7.32 (m, 5H), 4.73 (ddd, *J*= 5.1, 8.7, 11.1 Hz, 1H), 4.56 (s, 2H), 3.56 (dd, *J*= 4.2, 9.4 Hz, 1H), 3.49 (dd, *J*= 6.0, 9.4 Hz, 1H), 3.37 (dd, *J*= 8.7, 17.7 Hz, 1H), 3.33 (ddd, *J*= 4.2, 5.1, 6.0 Hz, 1H), 3.14 (dd, *J*= 11.1, 17.7 Hz, 1H), 1.77 (bs, 2H).

^{13}C-NMR (75 MHz, $CDCl_3$): δ= 140.8, 140.7, 138.0, 136.8, 128.8, 128.2, 127.4, 127.2, 127.1, 83.3, 73.2, 71.4, 52.6, 42.4.

$[\alpha]_D^{20}$= + 189.9° (c= 0.35, $CHCl_3$).

MS(ESI): *m/z* calcd for $C_{18}H_{19}{}^{79}BrN_2O_2$: 374.1; found: 375.1 $[M+H]^+$.

Synthesis of *tert*-butyl (*S*)-1-((*S*)-3-bromo-4,5-dihydroisoxazol-5-yl)-2-(4-nitrobenzylamino)-2-oxoethylcarbamate [(*S,S*)-79]

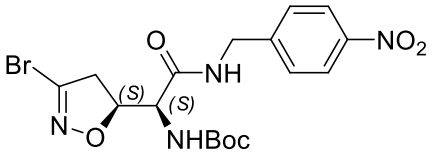

(*S,S*)-**79**

4-Nitrobenzylamine hydrochloride (**75**) (58 mg, 0.309 mmol), triethylamine (43 µL, 0.309 mmol), EDC hydrochloride (59 mg, 0.309 mmol) and HOBt (21 mg, 0.154 mmol) were added to a solution of (*S,S*)-**41** (100 mg, 0.309 mmol) in dry THF (12 mL). The reaction mixture was stirred at room temperature for 2 h, then the solvent was removed under reduced pressure and the crude product was purified by flash chromatography on silica gel (cyclohexane/EtOAc, 7:3) obtaining *tert*-butyl (*S*)-1-((*S*)-3-bromo-4,5-dihydroisoxazol-5-yl)-2-(4-nitrobenzylamino)-2-oxoethylcarbamate [(*S,S*)-**79**]as a yellow solid (90 mg, 64% yield) which recrystallizes from 1:4 *i*PrOH/*n*-hexane as colorless needles (m.p.= 140.8-141.5 °C).

R_f= 0.26 (cyclohexane/EtOAc, 7:3).

^{1}H-NMR (300 MHz, $CDCl_3$): δ= 8.18 (d, *J*= 8.5 Hz, 2H), 7.45 (d, *J*= 8.5 Hz, 2H), 6.92 (t, *J*= 5.7 Hz, 1H), 5.48 (d, *J*= 7.5 Hz, 1H), 4.77 (ddd, *J*= 6.0, 6.3, 10.5 Hz, 1H), 4.61 (dd, *J*= 6.6, 15.9 Hz, 1H), 4.54 (dd, *J*= 6.0, 15.9 Hz, 1H), 4.33 (dd, *J*= 6.0, 7.5 Hz, 1H), 3.52 (dd, *J*= 6.3, 18.1 Hz, 1H), 3.34 (dd, *J*= 10.5, 18.1 Hz, 1H), 1.44 (s, 9H).

^{13}C-NMR (75 MHz, $CDCl_3$): δ= 169.1, 155.9, 147.2, 145.2, 138.8, 128.0, 123.8, 81.6, 81.0, 55.8, 44.2, 42.9, 28.2.

$[\alpha]_D^{20}$= + 102.6° (c= 0.50, $CHCl_3$).

Synthesis of (*S*)-2-amino-2-((*S*)-3-bromo-4,5-dihydroisoxazol-5-yl)-*N*-(4-nitrobenzyl)acetamide [(*S,R*)-65]

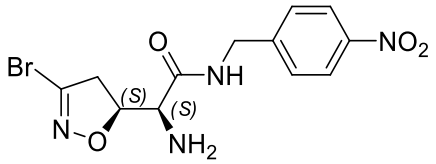

(*S,S*)-**65**

TFA (150 µL, 1.96 mmol) was added at 0 °C to a solution of (*S,R*)-**79** (87 mg, 0.196 mmol) in DCM (0.85 mL). The reaction mixture was stirred at room temperature for 4 h, then DCM was added and the acid was quenched with 5% aq. $NaHCO_3$. Phases were separated and the aqueous phase was extracted with DCM. The pooled organic layers were dried over anhydrous Na_2SO_4, filtered and the solvent was removed under reduced pressure. The crude product was purified by flash chromatography on silica gel (EtOAc, 100%) obtaining (*S*)-2-amino-2-((*S*)-3-bromo-4,5-dihydroisoxazol-5-yl)-*N*-(4-nitrobenzyl)acetamide [(*S,S*)-**65**] as a colourless solid (51 mg, 76% yield) which recrystallizes from 1:3 *i*PrOH/*n*-hexane as white needles (m.p.= 138.8-139.3 °C).

R_f= 0.30 (EtOAc, 100%).

^{1}H-NMR (300 MHz, CD_3OD): δ= 8.18 (m, 2H), 7.54 (m, 2H), 4.85 (dt, *J*= 6.0, 9.6 Hz, 1H), 4.56 (d, *J*= 16.0 Hz, 1H), 4.48 (d, *J*= 16.0 Hz, 1H), 3.57 (d, *J*= 6.0 Hz, 1H), 3.36 (d, *J*= 9.6 Hz, 1H).

^{13}C-NMR (75 MHz, CD_3OD): δ= 172.7, 147.1, 146.2, 138.1, 127.9, 123.2, 83.1, 56.8, 42.6, 42.0.

$[\alpha]_D^{20}$= + 112.0° (c= 0.33, MeOH).

MS(ESI): *m/z* calcd for $C_{12}H_{13}{}^{79}BrN_4O_4$: 356.0; found: 357.0 $[M+H]^+$.

Synthesis of *tert*-butyl (*S*)-1-((*S*)-3-bromo-4,5-dihydroisoxazol-5-yl)-2-(4-fluorobenzylamino)-2-oxoethylcarbamate [(*S*,*S*)-80]

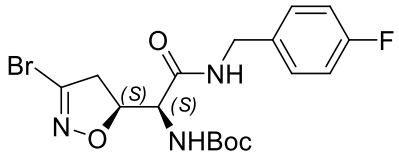

(*S*,*S*)-**80**

4-Fluorobenzylamine (**76**) (35 µL, 0.309 mmol), EDC hydrochloride (59 mg, 0.309 mmol) and HOBt (21 mg, 0.154 mmol) were added to a solution of (*S*,*S*)-**41** (100 mg, 0.309 mmol) in dry THF (12 mL). The reaction mixture was stirred at room temperature for 2 h, then the solvent was removed under reduced pressure and the crude product was purified by flash chromatography on silica gel (cyclohexane/EtOAc, 7:3) obtaining *tert*-butyl (*S*)-1-((*S*)-3-bromo-4,5-dihydroisoxazol-5-yl)-2-(4-fluorobenzylamino)-2-oxoethylcarbamate [(*S*,*S*)-**80**] as a brown oil (103 mg, 77% yield).

R_f= 0.27 (cyclohexane/EtOAc, 7:3).

^{1}H-NMR (300 MHz, $CDCl_3$): δ= 7.24 (m, 2H), 7.01 (m, 2H), 6.55 (t, *J*= 5.7 Hz, 1H), 5.46 (d, *J*= 6.6 Hz, 1H), 4.73 (m, 1H), 4.44 (d, *J*= 5.7 Hz, 2H), 4.25 (t, *J*= 7.9 Hz, 1H), 3.52 (dd, *J*= 5.8, 17.7 Hz, 1H), 3.32 (dd, *J*= 10.9, 17.7 Hz, 1H), 1.44 (s, 9H).

^{13}C-NMR (75 MHz, $CDCl_3$): δ= 168.5, 162.2 (d, $J_{C\text{-}F}$= 243.9 Hz), 155.8, 138.7, 133.3 (d, $J_{C\text{-}F}$= 2.8 Hz), 129.3 (d, $J_{C\text{-}F}$= 9.1 Hz), 115.5 (d, $J_{C\text{-}F}$= 21.7 Hz), 81.7, 80.8, 55.7, 44.2, 43.0, 28.2.

$[\alpha]_D^{20}$= + 94.9° (c= 0.50, $CHCl_3$).

Synthesis of (*S*)-2-amino-2-((*S*)-3-bromo-4,5-dihydroisoxazol-5-yl)-*N*-(4-fluorobenzyl)acetamide [(*S*,*S*)-66]

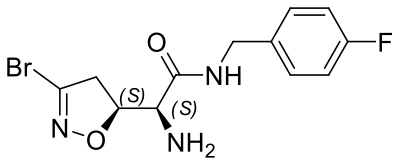

(*S*,*S*)-**66**

TFA (192 µL, 2.51 mmol) was added at 0 °C to a solution of (*S*,*S*)-**80** (108 mg, 0.251 mmol) in DCM (1.1 mL). The reaction mixture was stirred at room temperature for 4 h, then DCM was added and the acid was quenched with 5% aq. $NaHCO_3$. Phases were separated and the aqueous phase was extracted with DCM. The pooled organic layers were dried over anhydrous Na_2SO_4, filtered and the solvent was removed under reduced pressure. The crude product was purified by flash chromatography on silica gel (EtOAc, 100%) obtaining (*S*)-2-amino-2-((*S*)-3-bromo-4,5-dihydroisoxazol-5-yl)-*N*-(4-fluorobenzyl)acetamide [(*S*,*S*)-**66**] as colourless solid (46 mg, 55% yield) which recrystallizes from 1:4 *i*PrOH/*n*-hexane as white needles (m.p.= 86.2-86.6 °C).

R_f= 0.44 (EtOAc, 100%).

^{1}H-NMR (300 MHz, $CDCl_3$): δ= 7.38, (t, *J*= 6.0 Hz, 1H), 7.24 (m, 2H), 7.02 (m, 2H), 5.07 (dt, *J*= 4.5, 10.0 Hz, 1H), 4.41 (d, *J*= 6.0 Hz, 2H), 3.80 (d, *J*= 4.5 Hz, 1H), 3.23 (d, *J*= 10.0 Hz, 1H), 1.73 (bs, 2H).

^{13}C-NMR (75 MHz, $CDCl_3$): δ= 170.7, 162.2 (d, $J_{C\text{-}F}$= 245.0 Hz), 138.1, 133.7 (d, $J_{C\text{-}F}$= 3.0 Hz), 129.4 (d, $J_{C\text{-}F}$= 8.0 Hz), 115.6 (d, $J_{C\text{-}F}$= 20.6 Hz), 82.7, 56.4, 42.6, 42.0.

$[\alpha]_D^{20}$= + 86.1° (c= 0.50, $CHCl_3$).

MS(ESI): *m/z* calcd for $C_{12}H_{13}{}^{79}BrFN_3O_2$: 329.0; found: 329.9 $[M+H]^+$.

Synthesis of *tert*-butyl (*S*)-2-(biphenyl-4-ylmethylamino)-1-((*S*)-3-bromo-4,5-dihydroisoxazol-5-yl)-2-oxoethylcarbamate [(*S*,*S*)-81]

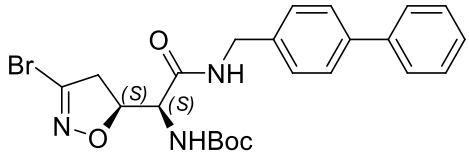

(*S*,*S*)-**81**

4-Phenylbenzylamine (**77**) (59 mg, 0.322 mmol), EDC hydrochloride (62 mg, 0.322 mmol) and HOBt (22 mg, 0.161 mmol) were added to a solution of (*S*,*S*)-**41** (104 mg, 0.322 mmol) in dry THF (12 mL). The reaction mixture was stirred at room temperature for 2 h, then the solvent was removed under reduced pressure and the crude product was purified by flash chromatography on silica gel (cyclohexane/EtOAc, 8:2) obtaining *tert*-butyl (*S*)-2-(biphenyl-4-ylmethylamino)-1-((*S*)-3-bromo-4,5-dihydroisoxazol-5-yl)-2-oxoethylcarbamate [(*S*,*S*)-**81**] as a brown oil (127 mg, 81% yield).

R_f= 0.42 (cyclohexane/EtOAc, 7:3).

^{1}H-NMR (300 MHz, $CDCl_3$): δ= 7.55 (m, 4H), 7.43 (t, *J*= 7.3 Hz, 2H), 7.34 (m, 3H), 6.70 (t, *J*= 5.4 Hz, 1H), 5.53 (d, *J*= 6.9 Hz, 1H), 4.77 (ddd, *J*= 6.6, 7.8, 10.5 Hz, 1H), 4.50 (d, *J*= 5.4 Hz, 2H), 4.31 (dd, *J*= 6.9, 7.8 Hz, 1H), 3.52 (dd, *J*= 6.6, 17.7 Hz, 1H), 3.31 (dd, *J*= 10.5, 17.7 Hz, 1H), 1.44 (s, 9H).

^{13}C-NMR (75 MHz, $CDCl_3$): δ= 168.7, 155.9, 140.7, 140.3, 138.5, 136.7, 128.8, 128.0, 127.4, 127.0, 81.8, 80.7, 55.8, 44.0, 43.4, 20.3.

$[\alpha]_D^{20}$= + 150.9° (c= 0.50, $CHCl_3$).

Synthesis of (*S*)-2-amino-*N*-(biphenyl-4-ylmethyl)-2-((*S*)-3-bromo-4,5-dihydroisoxazol-5-yl)acetamide [(*S*,*S*)-67]

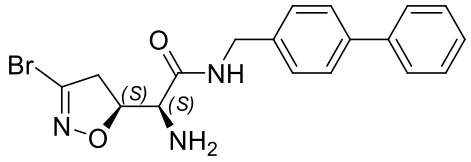

(*S*,*S*)-**67**

TFA (296 µL, 2.60 mmol) was added at 0 °C to a solution of (*S*,*S*)-**81** (127 mg, 0.260 mmol) in DCM (1.3 mL). The reaction mixture was stirred at room temperature for 4 h, then DCM was added and the acid was quenched with 5% aq. $NaHCO_3$. Phases were separated and the aqueous phase was extracted with DCM. The pooled organic layers were dried over anhydrous Na_2SO_4, filtered and the solvent was removed under reduced pressure. The crude product was purified by flash chromatography on silica gel (EtOAc, 100%) obtaining (*S*)-2-amino-*N*-(biphenyl-4-ylmethyl)-2-((*S*)-3-bromo-4,5-dihydroisoxazol-5-yl)acetamide [(*S*,*S*)-**67**] as a pink solid (84 mg, 83% yield) (decomposes at T> 155 °C).

R_f= 0.43 (EtOAc, 100%).

^{1}H-NMR (300 MHz, DMSO-d_6): δ= 8.53 (t, *J*= 6.0 Hz, 1H), 7.60 (m, 4H), 7.42 (t, *J*= 7.6 Hz, 2H), 7.33 (m, 3H), 4.77 (dt, *J*= 5.7, 9.3 Hz, 1H), 4.30 (d, *J*= 6.0 Hz, 2H), 3.45 (d, *J*= 5.7 Hz, 1H), 3.29 (d, *J*=9.3 Hz, 2H), 2.23 (bs, 2H)

^{13}C-NMR (75 MHz, DMSO-d_6): δ= 171.9, 140.4, 139.2, 138.9, 138.7, 129.4, 128.2, 127.8, 127.0, 83.6, 56.8, 42.5, 42.2.

$[\alpha]_D^{20}$= + 84.2° (c= 0.55, $CHCl_3$).

MS(ESI): *m/z* calcd for $C_{18}H_{18}{}^{79}BrN_3O_2$: 387.1; found: 388.2 $[M+H]^+$.

Synthesis of *tert*-butyl (*S*)-1-((*S*)-3-bromo-4,5-dihydroisoxazol-5-yl)-2-(4-methoxybenzylamino)-2-oxoethylcarbamate [(*S*,*S*)-82]

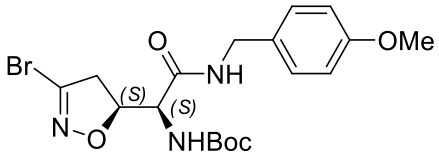

(*S*,*S*)-**82**

4-Methoxybenzylamine (**78**) (34 µL, 0.309 mmol), EDC hydrochloride (59 mg, 0.309 mmol) and HOBt (21 mg, 0.154 mmol) were added to a solution of (*S*,*S*)-**41** (100 mg, 0.309 mmol) in dry THF (12 mL). The reaction mixture was stirred at room temperature for 2 h, then the solvent was removed under reduced pressure and the crude product was purified by flash chromatography on silica gel (cyclohexane/EtOAc, 8:2 to 7:3) obtaining *tert*-butyl (*S*)-1-((*S*)-3-bromo-4,5-dihydroisoxazol-5-yl)-2-(4-methoxybenzylamino)-2-oxoethylcarbamate [(*S*,*S*)-**82**] as a white foam (93 mg, 68% yield).

R_f= 0.30 (cyclohexane/EtOAc, 7:3).

^{1}H-NMR (300 MHz, $CDCl_3$): δ= 7.20 (m, 2H), 6.86 (m, 2H), 6.47 (t, *J*= 5.7 Hz, 1H), 5.47 (d, *J*= 8.4 Hz, 1H), 4.72 (ddd, *J*= 6.6, 7.5, 10.5 Hz, 1H), 4.40 (d, *J*= 5.7 Hz, 2H), 4.24 (dd, *J*= 7.5, 8.4 Hz, 1H), 3.79 (s, 3H), 3.51 (dd, *J*= 6.6, 17.6 Hz, 1H), 3.31 (dd, *J*= 10.5, 17.6 Hz, 1H), 1.43 (s, 9H).

^{13}C-NMR (75 MHz, $CDCl_3$): δ= 168.4, 159.0, 155.8, 138.6, 129.6, 129.0, 114.1, 81.8, 80.7, 55.7, 55.3, 44.1, 43.2, 28.2.

$[\alpha]_D^{20}$= + 135.8° (c= 0.50, $CHCl_3$).

Synthesis and (*S*)-2-amino-2-((*S*)-3-bromo-4,5-dihydroisoxazol-5-yl)-*N*-(4-methoxybenzyl)acetamide [(*S*,*S*)-68]

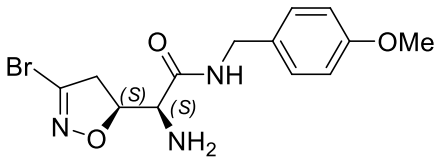

(*S*,*S*)-**68**

TFA (154 µL, 2.01 mmol) was added at 0 °C to a solution of (*S*,*S*)-**82** (89 mg, 0.201 mmol) in DCM (0.87 mL). The reaction mixture was stirred at room temperature for 4 h, then DCM was added and the acid was quenched with 5% aq. $NaHCO_3$. Phases were separated and the aqueous phase was extracted with DCM. The pooled organic layers were dried over anhydrous Na_2SO_4, filtered and the solvent was removed under reduced pressure. The crude product was purified by flash chromatography on silica gel (EtOAc, 100%) obtaining (*S*)-2-amino-2-((*S*)-3-bromo-4,5-dihydroisoxazol-5-yl)-*N*-(4-methoxybenzyl)acetamide [(*S*,*S*)-**82**] as a colourless solid (58 mg, 84% yield) which recrystallizes from 1:3 *i*PrOH/*n*-hexane as colourless needles (m.p.= 118.0-118.8 °C).

R_f= 0.31 (EtOAc, 100%).

^{1}H-NMR (300 MHz, CD_3OD): δ= 7.22 (d, *J*= 8.1 Hz, 2H), 6.86 (d, *J*= 8.1 Hz, 2H), 4.32 (s, 2H), 3.76 (s, 3H), 3.55 (d, *J*= 5.7 Hz, 1H).

^{13}C-NMR (75 MHz, CD_3OD): δ= 171.9, 159.0, 138.0, 130.1, 128.5, 113.5, 83.0, 56.5, 54.3, 42.2.

$[\alpha]_D^{20}$= + 143.0° (c= 0.50, MeOH).

MS(ESI): *m/z* calcd for $C_{13}H_{16}{}^{79}BrN_3O_3$: 341.1; found: 342.1 $[M+H]^+$.

Synthesis of (*S*)-2-(*tert*-butoxycarbonylamino)but-3-enyl methanesulfonate [(*S*)-85]

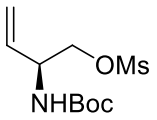

(*S*)-**85**

MsCl (83 µL, 1.07 mmol) was added at 0 °C to a solution of (*S*)-**24** (200 mg, 1.07 mmol) was dissolved in dry DCM (2 mL). TEA (194 µL, 1.39 mmol) and DMAP (13 mg, 0.107 mmol). The reaction mixture was stirred at 0 °C for 15 min, then it was diluted with DCM, washed with 1 M aq. HCl and sat. aq. $NaHCO_3$. The organic phase was dried over anhydrous Na_2SO_4, filtered and the solvent was removed under reduced pressure, obtaining (*S*)-2-(*tert*-butoxycarbonylamino)but-3-enyl methanesulfonate [(*S*)-**85**] as a yellow oil (256 mg, 90% yield).

R_f= 0.51 (cyclohexane/EtOAc, 6:4).

^{1}H-NMR (300 MHz, $CDCl_3$): δ= 5.80 (ddd, *J*= 6.0, 10.5, 17.1 Hz, 1H), 5.31 (d, *J*= 17.1 Hz, 1H), 5.27 (d, *J*= 10.5 Hz, 1H), 4.82 (m, 1H), 4.45 (m, 1H), 4.29 (dd, *J*= 4.5, 10.2 Hz, 1H), 4.21 (dd, *J*= 5.3, 10.2 Hz, 1H), 3.02 (s, 3H), 1.44 (s, 9H).

^{13}C-NMR (75 MHz, $CDCl_3$): δ= 155.0, 133.6, 117.8, 80.2, 70.5, 51.7, 37.5, 28.3.

$[\alpha]_D^{20}$= - 33.7° (c= 0.50, $CHCl_3$).

Synthesis of (*S*)-*tert*-butyl 1-(benzylthio)but-3-en-2-ylcarbamate [(*S*)-86]

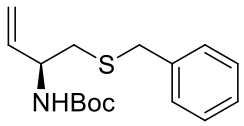

(*S*)-**86**

Phenylmethanethiol (113 µL, 0.965 mmol) and DBU (217 µL, 1.45 mmol) were added to a solution of (*S*)-**86** (256 mg, 0.965 mmol) in benzene (1.2 mL). Reaction mixture was stirred at room temperature for 1 h and additional phenylmethanethiol (23 µL, 0.193 mmol) was added. The reaction mixture was stirred for 30 min then Et_2O was added and washed two times with 0.2 M aq. NaOH. The aqueous phase was extracted with Et_2O and the pooled organic phases were washed with brine, dried over anhydrous Na_2SO_4, filtered and the solvent was removed under reduced pressure. The crude product was purified by flash chromatography on silica gel (cyclohexane/EtOAc, 95:5 to 9:1) obtaining (*S*)-*tert*-butyl 1-(benzylthio)but-3-en-2-ylcarbamate [(*S*)-**86**] as a colourless oil (226 mg, 80% yield).

R_f= 0.32 (cyclohexane/EtOAc, 9:1).

^{1}H-NMR (300 MHz, $CDCl_3$,): δ= 7.35-7.19 (m, 5H), 5.78 (ddd, *J*= 5.4, 11.1, 17.1 Hz, 1H), 5.19 (d, *J*= 17.1 Hz, 1H), 5.14 (d, *J*= 11.1 Hz, 1H), 4.74 (m, 1H), 4.33 (m, 1H), 3.73 (s, 2H), 2.59 (d, *J*= 6.3 Hz, 2H), 1.45 (s, 9H).

^{13}C-NMR (75 MHz, $CDCl_3$): δ= 155.2, 138.0, 137.4, 128.9, 128.5, 127.1, 115.5, 79.6, 51.7, 36.7, 36.4, 28.4.

$[\alpha]_D^{20}$= - 11.8° (c= 1.00, $CHCl_3$).

Synthesis of *tert*-butyl (*S*)-2-(benzylthio)-1-((*R*)-3-bromo-4,5-dihydroisoxazol-5-yl)ethylcarbamate [(*R,S*)-87] and *tert*-butyl (*S*)-2-(benzylthio)-1-((*S*)-3-bromo-4,5-dihydroisoxazol-5-yl)ethylcarbamate [(*S,S*)-88]

DBU (187 mg, 0.924 mmol) and $NaHCO_3$ (388 mg, 4.62 mmol) were added to a solution of (*S*)-**GC86** (226 mg, 0.770 mmol) in EtOAc (4 mL). The reaction mixture was vigorously stirred at room temperature until consumption of (*S*)-**86**. EtOAc was added, washed with water, dried over anhydrous Na_2SO_4, filtered and the solvent was removed under reduced pressure. The crude product was purified by flash chromatography on silica gel (cyclohexane/EtOAc, 9:1 to 85:15).

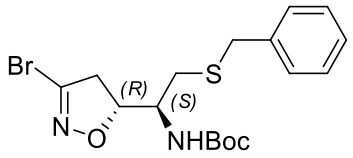

(*R,S*)-**87**

tert-Butyl (*S*)-2-(benzylthio)-1-((*R*)-3-bromo-4,5-dihydroisoxazol-5-yl)ethylcarbamate [(*R,S*)-**87**] was obtained as a white solid (164 mg, 51% yield) which recrystallizes from diisopropylether as white needles (m.p.= 106.5-107.3 °C).

R_f= 0.22 (cyclohexane/EtOAc, 9:1).

^{1}H-NMR (300 MHz, $CDCl_3$): δ= 7.37-7.20 (m, 5H), 4.98 (ddd, *J*= 1.8, 8.4, 11.1 Hz, 1H), 4.66 (d, *J*= 9.9 Hz, 1H), 3.87 (dt, *J*= 7.8, 8.4 Hz, 1H), 3.73 (s, 2H), 3.25 (dd, *J*= 11.1, 17.4 Hz, 1H), 3.10 (dd, *J*= 8.4, 17.4 Hz, 1H), 2.57 (d, *J*= 7.8 Hz, 2H), 1.45 (s, 9H).

^{13}C-NMR (75 MHz, $CDCl_3$): δ= 156.0, 138.2, 137.8, 129.0, 128.5, 127.2, 81.0, 80.2, 52.2, 44.0, 36.1, 33.0, 28.3.

$[\alpha]_D^{20}$= - 85.5° (c= 1.00, $CHCl_3$).

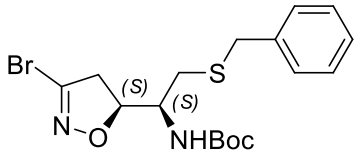

(*S*,*S*)-**88**

tert-Butyl (*S*)-2-(benzylthio)-1-((*S*)-3-bromo-4,5-dihydroisoxazol-5-yl)ethylcarbamate [(*S*,*S*)-**88**] was obtained as a green oil (138 mg, 43% yield) which solidifies upon cooling at - 20 °C.

R_f= 0.15 (cyclohexane/EtOAc, 9:1).

^{1}H-NMR (300 MHz, $CDCl_3$): δ= 7.35-7.20 (m, 5H), 4.79 (d, *J*= 9.3 Hz, 1H), 4.65 (ddd, *J*= 7.6, 7.8, 10.2 Hz, 1H), 3.83 (m, 1H), 3.73 (s, 2H), 3.23 (dd, *J*= 10.2, 17.7 Hz, 1H), 3.11 (dd, *J*= 7.6, 17.7 Hz, 1H), 2.67 (d, *J*= 5.7 Hz, 2H), 1.45 (s, 9H).

^{13}C-NMR (75 MHz, $CDCl_3$): δ= 155.5, 137.7, 137.7, 129.0, 128.6, 127.3, 82.3, 80.2, 52.3, 44.4, 36.8, 32.2, 28.3.

$[\alpha]_D^{20}$= + 84.6° (c= 1.05, $CHCl_3$).

Synthesis of *tert*-butyl (*S*)-2-(benzylsulfonyl)-1-((*R*)-3-bromo-4,5-dihydroisoxazol-5-yl)ethylcarbamate [(*R,S*)-89]

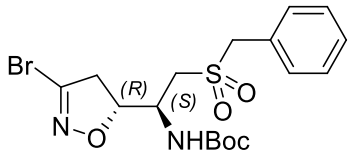

(*R,S*)-**89**

*m*CPBA (131 mg, ≥77% purity, 0.583 mmol) was added at 0 °C to a solution of (*R,S*)-**87** (110 mg, 0.265 mmol) in $CHCl_3$ (3.3 mL). Reaction mixture was stirred at room temperature for 10 min then DCM was added and washed with sat. aq. $NaHCO_3$. The organic phase was dried over anhydrous Na_2SO_4, filtered and the solvent was removed under reduced pressure, obtaining *tert*-butyl (*S*)-2-(benzylsulfonyl)-1-((*R*)-3-bromo-4,5-dihydroisoxazol-5-yl)ethylcarbamate [(*R,S*)-**89**] as a white solid (118 mg, quantitative yield) which recrystallizes from 1:3 $CHCl_3$/EtOH as white needles (decomposes at T> 180 °C).

R_f= 0.39 (cyclohexane/EtOAc, 7:3).

^{1}H-NMR (300 MHz, $CDCl_3$): δ= 7.46-7.37 (m, 5H), 5.00 (t, *J*= 9.4 Hz, 1H), 4.80 (d, *J*= 10.2 Hz, 1H), 4.42 (m, 1H), 4.34 (d, *J*= 14.2 Hz, 1H), 4.27 (d, *J*= 14.2 Hz, 1H), 3.33 (dd, *J*= 10.8, 17.7 Hz, 1H), 3.19-3.02 (m, 3H), 1.46 (s, 9H).

^{13}C-NMR (75 MHz, $CDCl_3$): δ= 155.5, 138.3, 130.7, 129.2, 129.1, 127.5, 81.9, 81.0, 60.1, 52.4, 48.4, 43.8, 28.2.

$[\alpha]_D^{20}$= - 108.5° (c= 0.55, $CHCl_3$).

Synthesis of (*S*)-2-(benzylsulfonyl)-1-((*R*)-3-bromo-4,5-dihydroisoxazol-5-yl)ethanamine [(*R*,*S*)-83]

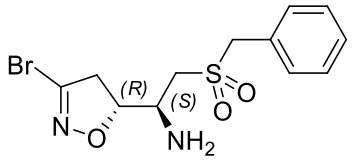

(*R*,*S*)-**83**

TFA (432 µL, 5.64 mmol) was added at 0 °C to a solution of (*R*,*S*)-**89** (126 mg, 0.282 mmol) in DCM (2.4 mL). Reaction mixture was stirred at room temperature for 1 h then it was diluted with DCM and sat. aq. $NaHCO_3$ was added. Phases were separated and the organic phase was dried over anhydrous Na_2SO_4, filtered and the evaporated. The crude product was purified by flash chromatography on silica gel (cyclohexane/EtOAc, 3:7) obtaining (*S*)-2-(benzylsulfonyl)-1-((*R*)-3-bromo-4,5-dihydroisoxazol-5-yl)ethanamine [(*R*,*S*)-**83**] as a white solid (67 mg, 68% yield) which recrystallizes from *i*PrOH as colorless needles (m.p.= 144.6-145.5 °C).

R_f= 0.46 (cyclohexane/EtOAc, 3:7).

^{1}H-NMR (300 MHz, CD_3OD): δ= 7.49-7.38 (m, 5H), 4.73 (ddd, *J*= 4.0, 8.2, 10.5 Hz, 1H), 4.51 (s, 2H), 3.42 (ddd, *J*= 3.9, 4.0, 8.7 Hz, 1H), 3.34 (dd, *J*= 10.5, 17.4 Hz, 1H), 3.21 (dd, *J*= 8.6, 17.4 Hz, 1H), 3.21 (dd, *J*= 3.9, 14.7 Hz, 1H), 3.12 (dd, *J*= 8.7, 14.7 Hz, 1H).

^{13}C-NMR (75 MHz, CD_3OD): δ= 138.0, 130.9, 128.5, 128.4, 128.0, 83.8, 59.7, 54.4, 48.8, 42.8.

$[\alpha]_D^{20}$= - 111.9° (c= 0.50, MeOH).

MS(ESI): *m/z* calcd for $C_{12}H_{15}{}^{79}BrN_2O_3S$: 346.0; found: 347.0 $[M+H]^+$.

Synthesis of *tert*-butyl (*S*)-2-(benzylsulfonyl)-1-((*S*)-3-bromo-4,5-dihydroisoxazol-5-yl)ethylcarbamate [(*S,S*)-90]

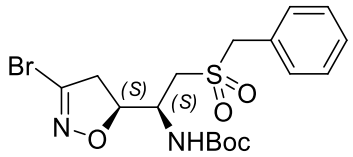

(*S,S*)-**90**

*m*CPBA (214 mg, ≥77% purity, 0.953 mmol) was added at 0 °C to a solution of [(*S,S*)-**88**] (180 mg, 0.433 mmol) in $CHCl_3$ (5.3 mL). Reaction mixture was stirred at room temperature for 10 min then DCM was added and washed with sat. aq. $NaHCO_3$. The organic phase was dried over anhydrous Na_2SO_4, filtered and the solvent was removed under reduced pressure. The crude was decanted from 1:1 cyclohexane/EtOAc as eluent, obtaining *tert*-butyl (*S*)-2-(benzylsulfonyl)-1-((*S*)-3-bromo-4,5-dihydroisoxazol-5-yl)ethylcarbamate [(*S,S*)-**90**] as a white solid (127 mg, 65% yield) (decomposes at T> 170 °C).

R_f= 0.54 (cyclohexane/EtOAc, 6:4).

^{1}H-NMR (300 MHz, DMSO-d_6): δ= 7.45-7.33 (m, 5H), 7.20 (d, *J*= 9.0 Hz, 1H), 4.59 (m, 1H), 4.46 (s, 2H), 4.14 (m, 1H), 3.41 (dd, *J*= 10.5, 17.4 Hz, 1H), 3.27-3.16 (m, 2H), 3.10 (dd, *J*= 6.4, 17.4 Hz, 1H), 1.36 (s, 9H).

^{13}C-NMR (75 MHz, DMSO-d_6): δ= 155.6, 138.8, 131.5, 129.0, 128.9, 128.6, 82.4, 79.1, 59.2, 52.1, 47.6, 43.1, 28.6.

$[\alpha]_D^{20}$= + 101.5° (c= 0.55, DMSO).

Synthesis of (*S*)-2-(benzylsulfonyl)-1-((*S*)-3-bromo-4,5-dihydroisoxazol-5-yl)ethanamine [(*S*,*S*)-84]

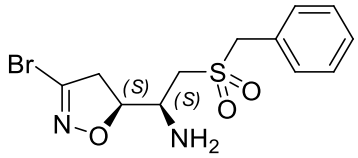

(*S*,*S*)-**84**

TFA (341 µL, 4.46 mmol) was added at 0 °C to a suspension of [(*S*,*S*)-**90**] (100 mg, 0.223 mmol) in DCM (1.9 mL). Reaction mixture was stirred at room temperature for 1 h, then it was diluted with DCM and sat. aq. $NaHCO_3$ was added. Phases were separated and the organic phase was dried over anhydrous Na_2SO_4, filtered and the solvent was removed under reduced pressure. The crude product was purified by flash chromatography on silica gel (cyclohexane/EtOAc, 4:6) obtaining (*S*)-2-(benzylsulfonyl)-1-((*S*)-3-bromo-4,5-dihydroisoxazol-5-yl)ethanamine [(*S*,*S*)-**84**] as a pale orange solid (54 mg, 70% yield) (m.p.= 132.8-134.0 °C).

R_f= 0.38 (cyclohexane/EtOAc, 4:6).

^{1}H-NMR (300 MHz, $CDCl_3$): δ= 7.42-7.38 (m, 5H), 4.55 (m, 1H), 4.33 (s, 2H), 3.55 (m, 1H), 3.25 (dd, *J*= 9.9, 17.4 Hz, 1H), 3.20 (dd, *J*= 8.1, 17.4 Hz, 1H), 3.13 (dd, *J*= 1.8, 14.1 Hz, 1H), 2.86 (dd, *J*= 9.3, 14.1 Hz, 1H), 2.18 (bs, 2H).

^{13}C-NMR (75 MHz, $CDCl_3$): δ= 137.9, 130.8, 129.2, 129.2, 127.5, 83.7, 60.9, 53.7, 49.0, 43.3.

$[\alpha]_D^{20}$= + 116.3° (c= 0.50, $CHCl_3$).

MS(ESI): *m/z* calcd for $C_{12}H_{15}{}^{79}BrN_2O_3S$: 346.0; found: 347.1 $[M+H]^+$.

Synthesis of *tert*-butyl 5-(5-((3a*S*,4*S*,6a*R*)-2-oxohexahydro-1*H*-thieno[3,4-*d*]imidazole-4-yl)pentanamido) pentylcarbamate [(*S*,*S*,*R*)-94]

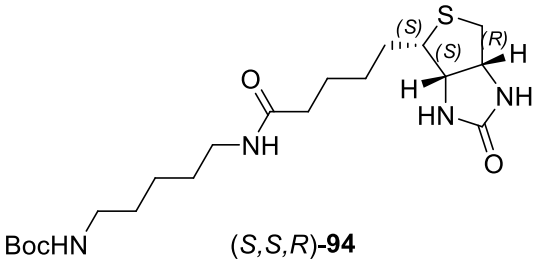

(*S*,*S*,*R*)-**94**

EDC hydrochloride (88.6 mg, 0.462 mmol), HOBt (62.4 mg, 0.462 mmol) and TEA (114 µL, 0.818 mmol) were added at 0 °C to a suspension of (*S*,*S*,*R*)-**93** (100 mg, 0.409 mmol) in dry DMF (2.2 mL). The mixture was stirred at 0 °C for 10 min then **92** (85.3 µL, 0.409 mmol) was added at 0 °C. The reaction mixture was stirred at room temperature for 24 h protected from light. DMF was removed under reduced pressure, water was added and the precipitate filtered and washed with water (10 mL) and *n*-hexane (8 ml). The obtained white solid was purified by flash chromatography on silica gel (DCM/MeOH, 9:1) as eluent, obtaining *tert*-butyl 5-(5-((3a*S*,4*S*,6a*R*)-2-oxohexahydro-1*H*-thieno[3,4-*d*]imidazole-4-yl)pentanamido)pentylcarbamate [(*S*,*S*,*R*)-**94**] as a white solid (135 mg, 80% yield) (m.p.= 134.6-135.5 °C).

R_f= 0.43 (DCM/MeOH, 9:1).

^{1}H-NMR (300 MHz, CD_3OD): δ= 4.48 (dd, *J*= 4.8, 7.8 Hz, 1H), 4.29 (dd, *J*= 4.4, 7.8 Hz, 1H), 3.20 (m, 1H), 3.16 (t, *J*= 7.0 Hz, 2H), 3.02 (t, *J*= 6.7 Hz, 2H), 2.92 (dd, *J*= 4.8, 12.3 Hz, 1H), 2.92 (d, *J*= 12.3 Hz, 1H), 2.19 (t, *J*= 7.4 Hz, 2H), 1.80-1.26 (m, 21H).

^{13}C-NMR (75 MHz, CD_3OD): δ= 175.8, 175.7, 165.7, 158.2, 79.8, 79.3, 78.8, 78.4, 63.1, 61.4, 56.8, 41.1, 41.0, 40.3, 40.2, 36.7, 30.4, 29.9, 29.6, 29.2, 28.9, 26.7, 25.0.

$[\alpha]_D^{20}$= + 44.9° (c= 0.55, CH_3OH).

Synthesis of *tert*-butyl (*S*)-1-((*S*)-3-bromo-4,5-dihydroisoxazol-5-yl)-2-oxo-2-(5-(5-((3a*S*,4*S*,6a*R*)-2-oxohexahydro-1*H*-thieno[3,4-*d*]imidazol-4-yl)pentanamido)pentylamino)ethylcarbamate [(*S*,*S*,*S*,*S*,*R*)-96]

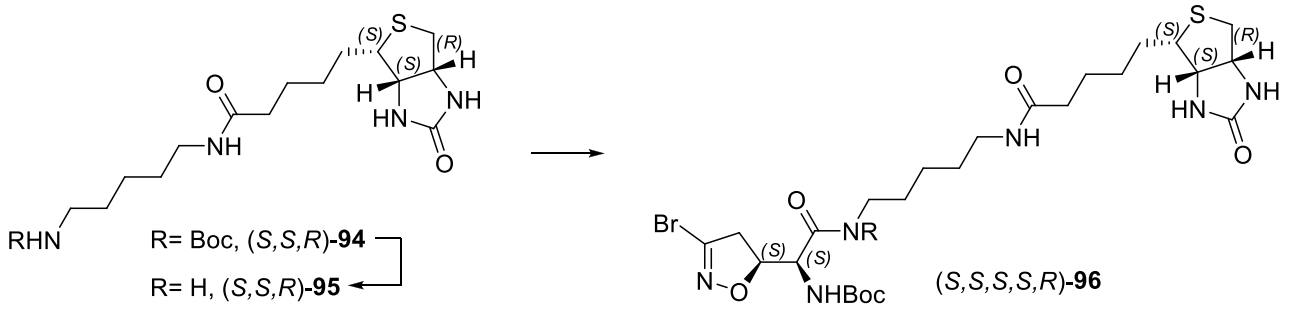

30% TFA/DCM (1.80 mL) was added at 0 °C to (*S*,*S*,*R*)-**94** (135 mg, 0.315 mmol). Reaction mixture was stirred at room temperature for 16 h. Solvent was evaporated and the residue was dissolved in 1:1 $CHCl_3$/MeOH (6.5 mL) and neutralized with solid $KHCO_3$. The solid was filtered and the filtrate was evaporated, obtaining *N*-(5-aminopentyl)-5-((3a*S*,4*S*,6a*R*)-2-oxohexahydro-1*H*-thieno[3,4-*d*]imidazol-4-yl)pentanamide [(*S*,*S*,*R*)-**95**] as a white fluffy solid (103 mg, quantitative yield) that was subsequently used without characterization.

EDC hydrochloride (66.1 mg, 0.345 mmol), HOBt (46.6 mg, 0.345 mmol) and TEA (131 µL, 0.942 mmol) were added at 0 °C to a solution of (*S*,*S*)-**41** (101 mg, 0.314 mmol) in dry DCM (1 mL). The mixture was stirred at 0 °C for 10 min, then a solution of (*S*,*S*,*R*)-**95** (103 mg, 0.314 mmol) in dry DMF (3.3 mL) was added at 0 °C. The reaction mixture was stirred at room temperature for 24 h. Water (5 mL) was added and it was extracted with 1:1 $CHCl_3$/MeOH (10 mL). The organic layer was washed with brine, dried over anhydrous Na_2SO_4, filtered and the solvent was removed under reduced pressure. The crude product was purified by flash chromatography on silica gel (DCM/MeOH, 95:5 to 9:1) obtaining *tert*-butyl (*S*)-1-((*S*)-3-bromo-4,5-dihydroisoxazol-5-yl)-2-oxo-2-(5-(5-((3a*S*,4*S*,6a*R*)-2-oxohexahydro-1*H*-thieno[3,4-*d*]imidazol-4-yl)pentanamido)pentylamino)ethylcarbamate [(*S*,*S*,*S*,*S*,*R*)-**96**] as a yellow solid (31 mg, 16% yield) (decomposes at T> 70 °C).

R_f= 0.36 (DCM/MeOH, 9:1).

^{1}H-NMR (300 MHz, CD_3OD): δ= 4.87 (m, 1H), 4.49 (dd, *J*= 4.8, 7.8 Hz, 1H), 4.30 (dd, *J*= 4.8, 7.8 Hz, 1H), 4.22 (d, *J*= 6.6 Hz, 1H), 3.41 (dd, *J*= 10.5, 17.7 Hz, 1H), 3.26-3.12 (m, 5H), 2.92 (dd, *J*= 4.8, 12.3 Hz, 1H), 2.70 (d, *J*= 12.3 Hz, 1H), 2.19 (t, *J*= 7.1 Hz, 2H), 1.80-1.26 (m, 12H), 1.44 (s, 9H).

^{13}C-NMR (75 MHz, CD_3OD): δ= 174.5, 169.7, 164.7, 156.2, 138.0, 81.2, 79.7, 62.0, 60.2, 55.6, 53.4, 43.3, 39.6, 38.9, 38.8, 35.4, 28.6, 28.5, 28.4, 28.1, 27.2, 25.5, 23.7.

$[\alpha]_D^{20}$= + 60.9° (c= 0.30, CH_3OH).

Synthesis of (*S*)-1-((*S*)-3-bromo-4,5-dihydroisoxazol-5-yl)-2-oxo-2-(5-(5-((3a*S*,4*S*,6a*R*)-2-oxohexahydro-1*H*-thieno[3,4-*d*]imidazol-4-yl)pentanamido)pentylamino)ethanaminium 2,2,2-trifluoroacetate [(*S*,*S*,*S*,*S*,*R*)-91*TFA]

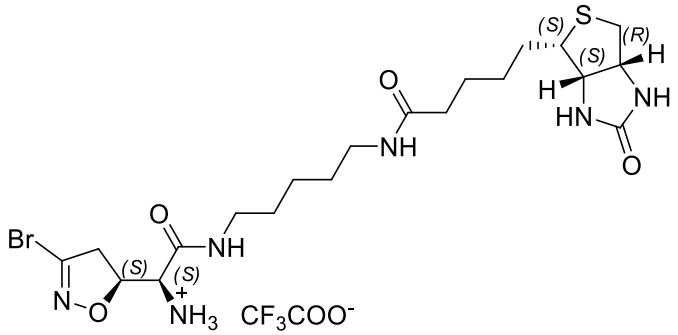

(*S*,*S*,*S*,*S*,*R*)-**91*TFA**

30% TFA/DCM (1.1 mL) was added at 0 °C to (*S*,*S*,*S*,*S*,*R*)-**96** (31 mg, 0.0489 mmol). The reaction mixture was stirred at room temperature for 3.5 h. The solvent was removed at reduced pressure, obtaining (*S*)-1-((*S*)-3-bromo-4,5-dihydroisoxazol-5-yl)-2-oxo-2-(5-(5-((3a*S*,4*S*,6a*R*)-2-oxohexahydro-1*H*-thieno[3,4-*d*]imidazol-4-yl)pentanamido)pentylamino)ethanaminium 2,2,2-trifluoroacetate [(*S*,*S*,*S*,*S*,*R*)-**91*TFA**] as a red solid (31 mg, quantitative yield) (decomposes at T> 70 °C).

^{1}H-NMR (300 MHz, CD_3OD): δ= 5.11 (ddd, *J*= 4.5, 8.7, 10.5 Hz, 1H), 4.49 (dd, *J*= 4.8, 8.0 Hz, 1H), 4.30 (dd, *J*= 4.3, 8.0 Hz, 1H), 4.18 (d, *J*=4.8 Hz, 1H), 3.50 (dd, *J*= 10.5, 18.3 Hz, 1H), 3.40 (dd, *J*= 8.7, 18.3 Hz, 1H), 3.27-3.11 (m, 5H), 2.93 (dd, *J*= 4.8, 12.9 Hz, 1H), 2.70 (d, *J*= 12.9 Hz, 1H), 2.20 (t, *J*= 7.2 Hz, 2H), 1.81-1.26 (m, 12H).

^{13}C-NMR (75 MHz, CD_3OD): δ= 174.6, 164.7, 164.5, 138.5, 79.0, 62.0, 60.2, 55.6, 53.8, 41.6, 39.6, 39.3, 38.7, 35.4, 28.6, 28.3, 28.3, 28.1, 25.5, 23.7 (TFA signals are too low to detect).

$[\alpha]_D^{20}$= + 53.1° (c= 0.54, CH_3OH).

MS(ESI): *m/z* calcd for $C_{22}H_{34}{}^{79}BrF_3N_6O_6S$: 532.1 (M-TFA); found: 533.3 $[M\text{-}TFA+H]^+$.

Synthesis of (±)-3-bromo-4,5,6,6a-tetrahydro-3a*H*-pyrrolo[3,4-*d*]isoxazole [(±)-148]

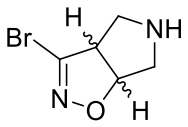

(±)-**148**

TFA (264 µL, 3.43 mmol) was added at 0 °C to a solution of (±)-**6** (100 mg, 0.343 mmol) in DCM (0.88 mL). The reaction was stirred at room temperature for 4 h, then the solvent was removed under reduced pressure. The residue was dissolved in EtOAc and washed with 5% aq. $NaHCO_3$. The organic phase was dried over anhydrous Na_2SO_4, filtered and the solvent was removed under vacuum. The crude product was purified by flash chromatography on silica gel (EtOAc/MeOH, 9:1) obtaining (±)-3-bromo-4,5,6,6a-tetrahydro-3a*H*-pyrrolo[3,4-*d*]isoxazole [(±)-**148**] as a white solid (55 mg, 84% yield).

R_f= 0.22 (EtOAc/MeOH, 9:1).

^{1}H-NMR (300 MHz, $CDCl_3$): δ= 5.25 (dd, *J*= 3.8, 8.2 Hz, 1H), 3.82 (dd, *J*= 7.4, 8.2 Hz, 1H), 3.48 (d, *J*= 13.5 Hz, 1H), 3.36 (d, *J*= 12.6 Hz, 1H), 2.88 (dd, *J*= 7.4, 12.6 Hz, 1H), 2.84 (dd, *J*= 3.8, 13.5 Hz, 1H), 1.84 (bs, 1H).

^{13}C-NMR (75 MHz, $CDCl_3$): δ= 139.5, 88.2, 60.1, 57.4, 52.3.

Following the same procedure starting from (*R*,*R*)-**6** or (*S*,*S*)-**6** the single enantiomers were obtained.

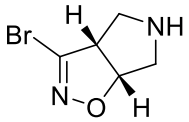

(***R*,*R***)-**148**

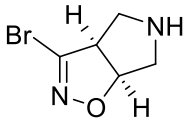

(***S*,*S***)-**148**

(3a*R*,6a*R*)-3-bromo-4,5,6,6a-tetrahydro-3a*H*-pyrrolo[3,4-*d*]isoxazole [(*R*,*R*)-148]

$[\alpha]_D^{20}$= - 179.8° (c= 0.60, $CHCl_3$).

(3a*S*,6a*S*)-3-bromo-4,5,6,6a-tetrahydro-3a*H*-pyrrolo[3,4-*d*]isoxazole [(*S*,*S*)-148]

$[\alpha]_D^{20}$= + 180.0° (c= 0.61, $CHCl_3$).

General procedure for carbamates (*S*)-100-111 synthesis

Method A

The required chloroformate (1.5 eq.) was added dropwise at 0 °C to a solution of compound (*S*)-**97**, (*S*)-**98** or (*S*)-**99** (1 eq.) in 7:3 sat. aq. $NaHCO_3$/dioxane (30 mL). The reaction mixture was stirred at room temperature for 12 h. Dioxane was evaporated and the reaction mixture was diluted with EtOAc, washed with 3 M aq. HCl, dried over anhydrous Na_2SO_4, filtered and the solvent was removed under reduced pressure. The crude product was purified by flash column chromatography on silica gel (light petroleum/EtOAc, 6:4) to afford pure carbamates.

Method B

TEA (1.5 eq.) and $(Boc)_2O$ (1.2 eq.) were added at 0 °C to a solution of compound (*S*)-**97**, (*S*)-**98** or (*S*)-**99** (1 equiv) in dry DCM. The reaction mixture was stirred at room temperature for 12 h, then it was diluted with EtOAc, washed with 3 M aq. HCl, dried over anhydrous Na_2SO_4, filtered and the solvent was removed under reduced pressure. The crude product was purified by flash column chromatography on silica gel (light petroleum/EtOAc, 6:4) to afford pure carbamates.

The products have been used in the following step without characterization.

General procedure for esters (*S*)-100-123 hydrolysis

The synthesis of compounds (*S*)-**100-123** was performed following the reported procedure [48] which is reported below.

LiOH (2 eq.) was added at 0 °C to a solution carbamate (1 eq.) in 1:1 methanol/water. The reaction mixture was stirred at room temperature until disappearance of the starting material. The reaction mixture was concentrated under vacuum, treated with 10% aq. citric acid and extracted with EtOAc. The pooled organic extracts were dried over anhydrous Na_2SO_4, filtered and the solvent was removed under reduced pressure to afford the pure carboxylic acids [(*S*)-**112-123**].

General procedure for the coupling of acids (*S*)-112-123 and amine (±)-148

HOBt (1.2 eq.), EDC (1.2 eq.), amine (±)-**148**, (*R*,*R*)-**148** or (*S*,*S*)-**148**, (1 eq.) and DIPEA (1.5 eq.) were added at 0 °C to a solution of the desired acid (1 eq.) in 1:1 DMF/DCM (1:1). The reaction mixture was stirred at room temperature for 15 h, then it was diluted with EtOAc and washed with sat. aq. $NaHCO_3$. The organic phase dried over anhydrous Na_2SO_4, filtered and the solvent was removed under vacuum. The crude product was purified by flash column chromatography on silica gel (light petroleum/EtOAc, 4:6) to afford the desired product. When racemic (±)-**148** was used, the product was obtained as a mixture of diastereoisomers. When enantiopure amines (*R*,*R*)-**148** or (*S*,*S*)-**148** were used, the product was obtained as a single diastereoisomer.

The following characterizations are in keeping with the literature. [48]

Synthesis of *n*-propyl (*S*)-1-((3a*S*,6a*S*)-3-bromo-3a,4,6,6a-tetrahydropyrrolo[3,4-*d*]isoxazol-5-yl)-4-methyl-1-oxopentan-2-ylcarbamate [(*S*,*S*,*S*)-124] and *n*-propyl (*S*)-1-((3a*R*,6a*R*)-3-bromo-3a,4,6,6a-tetrahydropyrrolo[3,4-*d*]isoxazol-5-yl)-4-methyl-1-oxopentan-2-ylcarbamate [(*S*,*R*,*R*)-125]

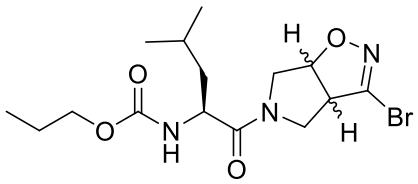

(*S*,*S*,*S*)-**124**/(*S*,*R*,*R*)-**125**

86% yield. R_f= 0.50 (light petroleum/EtOAc, 4:6).

^{1}H-NMR (300 MHz, $CDCl_3$): δ= 5.44-5.19 (m, 2H), 4.61-4.39 (m, 1H), 4.21 (d, *J*= 13.4 Hz, 1H), 4.15-3.87 (m, 4H), 3.84-3.47 (m, 2H), 1.80-1.48 (m, 5H), 1.02 (t, *J*= 7.4 Hz, 3H), 0.96 (d, *J*= 7.3 Hz, 3H), 0.91 (d, *J*= 7.5 Hz, 3H).

MS(ESI): *m/z* calcd for $C_{15}H_{24}{}^{79}BrN_3O_4$: 389.1; found: 390.1 $[M+H]^+$.

Synthesis of allyl (*S*)-1-((3a*S*,6a*S*)-3-bromo-3a,4,6,6a-tetrahydropyrrolo[3,4-*d*]isoxazol-5-yl)-4-methyl-1-oxopentan-2-ylcarbamate [(*S*,*S*,*S*)-126]

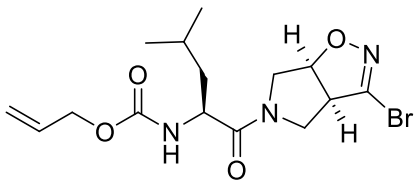

(*S*,*S*,*S*)-**126**

87% yield. R_f= 0.48 (light petroleum/EtOAc, 4:6).

^{1}H-NMR (300 MHz, $CDCl_3$): δ= 5.99-5.82 (m, 1H), 4.63-4.51 (m, 2H), 5.51–5.32 (m, 2H), 5.25 (m, 2H), 4.50-4.39 (m, 1H), 4.28–4.15 (m, 1H), 4.19 (d, *J*= 12.2 Hz, 1H), 4.03-3.90 (m, 1H), 3.99 (d, *J*= 12.2 Hz, 1H), 3.51 (m, 1H), 1.77–1.63 (m, 1H), 1.62–1.38 (m, 2H), 0.99 (d, *J*= 6.1 Hz, 3H), 0.94 (d, *J*= 6.5 Hz, 3H).

^{13}C-NMR (75 MHz, $CDCl_3$): δ= 172.1, 157.4, 139.6, 134.9, 119.1, 84.1, 65.9, 57.9, 53.7, 51.6, 47.9, 44.2, 26.5, 23.8, 21.7.

$[\alpha]_D^{20}$= + 62.2° (c= 0.36, DCM).

MS(ESI): *m/z* calcd for $C_{15}H_{22}{}^{79}BrN_3O_4$: 387.1; found: 388.3 $[M+H]^+$.

Synthesis of allyl (*S*)-1-((3a*R*,6a*R*)-3-bromo-3a,4,6,6a-tetrahydropyrrolo[3,4-*d*]isoxazol-5-yl)-4-methyl-1-oxopentan-2-ylcarbamate [(*S*,*R*,*R*)-127]

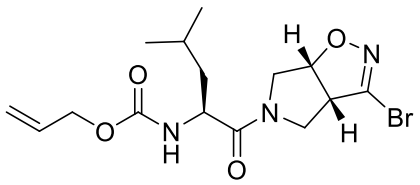

(*S*,*R*,*R*)-**127**

93% yield. R_f= 0.48 (light petroleum/EtOAc, 4:6).

^{1}H-NMR (300 MHz, $CDCl_3$): δ= 5.98-5.82 (m, 1H), 5.49 (d, *J*= 8.1 Hz, 1H), 5.42-5.24 (m, 1H), 5.24 (m, 2H), 4.62-4.50 (m, 2H), 4.50-4.41 (m, 1H), 4.17 (d, *J*= 14.1 Hz, 1H), 4.11-3.96 (m, 1H), 4.00 (d, *J*= 14.1 Hz, 1H), 3.82-3.67 (m, 1H), 3.58 (m, 1H), 1.81-1.64 (m, 1H), 1.62-1.44 (m, 1H), 1.45-1.31 (m, 1H), 1.01 (d, *J*= 6.7 Hz, 3H), 0.94 (d, *J*= 6.5 Hz, 3H).

^{13}C-NMR (75 MHz, $CDCl_3$): δ= 172.2, 157.4, 139.7, 134.9, 119.1, 84.1, 65.9, 58.0, 53.7, 51.6, 47.9, 44.2, 26.5, 23.8, 21.7.

$[\alpha]_D^{20}$= - 79.3° (c= 0.75, DCM);

MS(ESI): *m/z* calcd for $C_{15}H_{22}{}^{79}BrN_3O_4$: 387.1; found: 388.3 $[M+H]^+$.

Synthesis of *tert*-butyl (*S*)-1-((3a*S*,6a*S*)-3-bromo-3a,4,6,6a-tetrahydropyrrolo[3,4-*d*]isoxazol-5-yl)-4-methyl-1-oxopentan-2-ylcarbamate [(*S*,*S*,*S*)-128] and *tert*-butyl (*S*)-1-((3a*R*,6a*R*)-3-bromo-3a,4,6,6a-tetrahydropyrrolo[3,4-*d*]isoxazol-5-yl)-4-methyl-1-oxopentan-2-ylcarbamate [(*S*,*R*,*R*)-129]

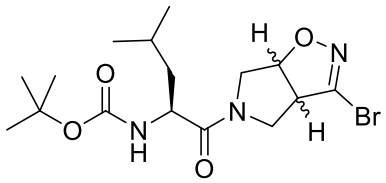

(*S*,*S*,*S*)-**128**/(*S*,*R*,*R*)-**129**

93% yield. R_f= 0.58 (light petroleum/EtOAc, 4:6).

^{1}H-NMR (300 MHz, $CDCl_3$): δ= 5.20 (d, *J*= 7.9 Hz, 1H), 5.20-5.06 (m, 1H), 4.55-4.36 (m, 1H), 4.21 (d, *J*= 14.9 Hz, 1H), 4.12-3.91 (m, 3H), 3.69-3.59 (m, 0.5H), 3.59-3.46 (m, 0.5H), 1.79-1.66 (m, 1H), 1.67-1.54 (m, 2H), 1.45 (s, 9H), 1.00 (d, *J*= 7.4 Hz, 3H), 0.96 (d, *J*= 6.7 Hz, 3H).

MS(ESI): *m/z* calcd for $C_{16}H_{26}{}^{79}BrN_3O_4$: 403.1; found: 404.1 $[M+H]^+$.

Synthesis of benzyl (*S*)-1-((3a*S*,6a*S*)-3-bromo-3a,4,6,6a-tetrahydropyrrolo[3,4-*d*]isoxazol-5-yl)-4-methyl-1-oxopentan-2-ylcarbamate [(*S*,*S*,*S*)-130] and benzyl (*S*)-1-((3a*R*,6a*R*)-3-bromo-3a,4,6,6a-tetrahydropyrrolo[3,4-*d*]isoxazol-5-yl)-4-methyl-1-oxopentan-2-ylcarbamate [(*S*,*R*,*R*)-131]

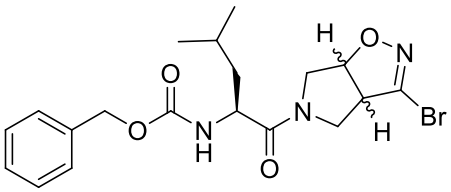

(*S*,*S*,*S*)-**130**/(*S*,*R*,*R*)-**131**

83% yield. R_f= 0.56 (light petroleum/EtOAc, 4:6).

^{1}H-NMR (300 MHz, $CDCl_3$): δ= 7.47-7.30 (m, 5H), 5.52-5.27 (m, 2H), 5.11 (s, 2H), 4.63-4.42 (m, 1H), 4.21 (d, *J*= 13.8 Hz, 1H), 4.13-3.86 (m, 2H), 3.84-3.71 (m, 1H), 3.68-3.55 (m, 0.5H), 3.54-3.42 (m, 0.5H), 1.80-1.66 (m, 1H), 1.59-1.46 (m, 2H), 1.01 (d, *J*= 6.7 Hz, 3H), 0.96 (d, *J*= 6.5 Hz, 3H).

MS(ESI): *m/z* calcd for $C_{19}H_{24}{}^{79}BrN_3O_4$: 437.1; found: 438.1 $[M+H]^+$.

Synthesis of *n*-propyl (*S*)-1-((3a*S*,6a*S*)-3-bromo-3a,4,6,6a-tetrahydropyrrolo[3,4-*d*]isoxazol-5-yl)-1-oxo-3-phenylpropan-2-ylcarbamate [(*S*,*S*,*S*)-132] and *n*-propyl (*S*)-1-((3a*R*,6a*R*)-3-bromo-3a,4,6,6a-tetrahydropyrrolo[3,4-*d*]isoxazol-5-yl)-1-oxo-3-phenylpropan-2-ylcarbamate [(*S*,*R*,*R*)-133]

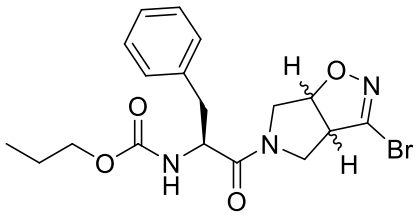

(*S*,*S*,*S*)-**132**/(*S*,*R*,*R*)-**133**

84% yield. R_f= 0.39 (light petroleum/EtOAc, 4:6).

^{1}H-NMR (300 MHz, $CDCl_3$): δ= 7.33-7.11 (m, 5H), 5.42 (d, *J*= 7.4 Hz, 1H), 5.26-5.17 (m, 1H), 4.68-4.52 (m, 1H), 4.17 (d, *J*= 13.8 Hz, 0.5H), 4.10 (d, *J*= 13.8 Hz, 0.5H), 4.09-3.99 (m, 1H), 3.97 (t, *J*= 7.0 Hz, 2H), 3.84-3.61 (m, 2H), 3.56-3.46 (m, 0.5H), 3.46-3.37 (m, 0.5H), 3.15-3.02 (m, 1H), 3.02-2.88 (m, 1H), 1.68-1.55 (m, 2H), 0.93 (t, *J*= 8.0 Hz, 3H).

MS(ESI): *m/z* calcd for $C_{18}H_{22}{}^{79}BrN_3O_4$: 423.1; found: 424.1 $[M+H]^+$.

Synthesis of allyl (*S*)-1-((3a*S*,6a*S*)-3-bromo-3a,4,6,6a-tetrahydropyrrolo[3,4-*d*]isoxazol-5-yl)-1-oxo-3-phenylpropan-2-ylcarbamate [(*S*,*S*,*S*)-134]

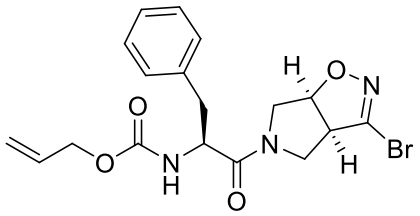

(*S*,*S*,*S*)-**134**

92% yield. R_f= 0.40 (light petroleum/EtOAc, 4:6).

^{1}H-NMR (300 MHz, $CDCl_3$): δ= 7.36-7.13 (m, 5H), 6.00-5.82 (m, 1H), 5.51 (d, *J*= 7.6 Hz, 1H), 5.37-5.19 (m, 3H), 4.72-4.51 (m, 3H), 4.07 (d, *J*= 12.3 Hz, 1H), 3.96-3.73 (m, 2H), 3.54 (m, 1H), 3.34 (d, *J*= 12.3 Hz, 1H), 3.16-2.83 (m, 2H).

^{13}C-NMR (75 MHz, $CDCl_3$): δ= 171.8, 155.8, 137.2, 136.1, 134.1, 129.5, 129.1, 128.8, 118.4, 85.4, 66.8, 57.5, 55.8, 53.4, 48.7, 40.4.

$[\alpha]_D{}^{20}$= + 42.7° (c= 0.18, DCM).

MS(ESI): *m/z* calcd for $C_{18}H_{20}{}^{79}BrN_3O_4$: 421.1; found: 422.2 $[M+H]^+$.

Synthesis of allyl (*S*)-1-((3a*R*,6a*R*)-3-bromo-3a,4,6,6a-tetrahydropyrrolo[3,4-*d*]isoxazol-5-yl)-1-oxo-3-phenylpropan-2-ylcarbamate [(*S*,*R*,*R*)-135]

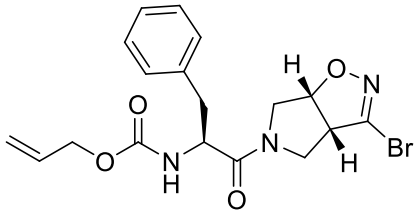

(*S*,*R*,*R*)-**135**

89% yield. R_f= 0.40 (light petroleum/EtOAc, 4:6).

^{1}H-NMR (300 MHz, $CDCl_3$): δ= 7.38-7.13 (m, 5H), 6.00-5.81 (m, 1H), 5.58 (d, *J*= 8.8 Hz, 1H), 5.30 (m, 1H), 5.22 (m, 2H), 4.69-4.51 (m, 3H), 4.19 (d, *J*= 11.8 Hz, 1H), 4.03-3.88 (m, 1H), 3.85-3.67 (m, 1H), 3.38 (d, *J*= 11.8 Hz, 1H), 3.27 (m, 1H), 3.19-2.86 (m, 2H).

^{13}C-NMR (75 MHz, $CDCl_3$): δ= 171.8, 155.8, 137.2, 136.0, 134.0, 129.5, 129.0, 128.8, 118.4, 85.4, 66.8, 57.5, 55.9, 53.4, 48.7, 40.4.

$[\alpha]_D^{20}$= - 51.2° (c= 0.40, DCM).

MS(ESI): *m/z* calcd for C18H20BrN3O4: 421.1; found: 422.2 $[M+H]^+$.

Synthesis of *tert*-butyl (*S*)-1-((3a*S*,6a*S*)-3-bromo-3a,4,6,6a-tetrahydropyrrolo[3,4-*d*]isoxazol-5-yl)-1-oxo-3-phenylpropan-2-ylcarbamate [(*S*,*S*,*S*)-136] and tert-butyl (*S*)-1-((3a*R*,6a*R*)-3-bromo-3a,4,6,6a-tetrahydropyrrolo[3,4-*d*]isoxazol-5-yl)-1-oxo-3-phenylpropan-2-ylcarbamate [(*S*,*R*,*R*)-137]

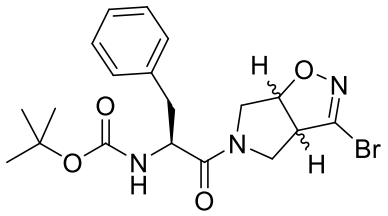

(*S*,*S*,*S*)-**136**/(*S*,*R*,*R*)-**137**

90% yield. R_f= 0.46 (light petroleum/EtOAc, 4:6).

^{1}H-NMR (300 MHz, $CDCl_3$): δ= 7.41-7.12 (m, 5H), 5.37 (bs, 1H), 5.31-5.19 (m, 1H), 4.69-4.50 (m, 1H), 4.19 (d, *J*= 15.3 Hz, 0.5H), 4.06 (d, *J*= 15.3 Hz, 0.5H), 4.00-3.62 (m, 3H), 3.54 (m, 0.5H), 3.49-3.38 (m, 0.5H), 3.17-2.86 (m, 2H), 1.44 (s, 9H).

MS(ESI): *m/z* calcd for $C_{19}H_{24}{}^{79}BrN_3O_4$: 437.1; found: 438.1 $[M+H]^+$.

Synthesis of benzyl (*S*)-1-((3a*S*,6a*S*)-3-bromo-3a,4,6,6a-tetrahydropyrrolo[3,4-*d*]isoxazol-5-yl)-1-oxo-3-phenylpropan-2-ylcarbamate [(*S*,*S*,*S*)-138] and benzyl (*S*)-1-((3a*R*,6a*R*)-3-bromo-3a,4,6,6a-tetrahydropyrrolo[3,4-*d*]isoxazol-5-yl)-1-oxo-3-phenylpropan-2-ylcarbamate [(*S*,*R*,*R*)-139]

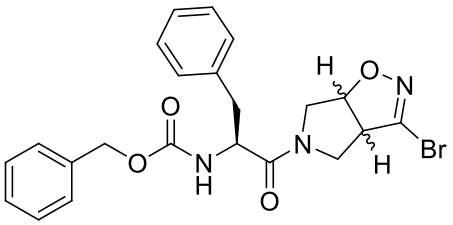

(*S*,*S*,*S*)-**138**/(*S*,*R*,*R*)-**139**

92% yield. R_f= 0.42 (light petroleum/EtOAc, 4:6).

^{1}H-NMR (300 MHz, $CDCl_3$): δ= 7.46-7.10 (m, 10H), 5.54 (d, *J*= 7.4 Hz, 1H), 5.29-5.18 (m, 0.5H), 5.14 (s, 2H), 5.12-5.05 (m, 0.5H), 4.73-4.57 (m, 1H), 4.19 (d, *J*= 12.1 Hz, 0.5H), 4.07 (d, *J*= 12.1 Hz, 0.5H), 3.99-3.86 (m, 1H), 3.84-3.66 (m, 1H), 3.60-3.46 (m, 0.5H), 3.38 (d, *J*= 12.1 Hz, 0.5H), 3.30 (d, *J*= 12.1 Hz, 0.5H), 3.34-3.23 (m, 0.5H), 3.18-2.89 (m, 2H).

MS(ESI): *m/z* calcd for $C_{22}H_{22}{}^{79}BrN_3O_4$: 471.1; found: 472.1 $[M+H]^+$.

Synthesis of *n*-propyl (*S*)-1-((3a*S*,6a*S*)-3-bromo-3a,4,6,6a-tetrahydropyrrolo[3,4-*d*]isoxazol-5-yl)-1-oxo-4-phenylbutan-2-ylcarbamate [(*S*,*S*,*S*)-140] and *n*-propyl (*S*)-1-((3a*R*,6a*R*)-3-bromo-3a,4,6,6a-tetrahydropyrrolo[3,4-*d*]isoxazol-5-yl)-1-oxo-4-phenylbutan-2-ylcarbamate [(*S*,*R*,*R*)-141]

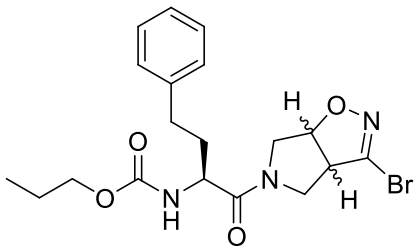

(*S*,*S*,*S*)-**140**/(*S*,*R*,*R*)-**141**

88% yield. R_f= 0.45 (light petroleum/EtOAc, 4:6).

^{1}H-NMR (300 MHz, $CDCl_3$): δ= 7.39-7.17 (m, 5H), 5.41 (bs, 1H), 5.34-5.22 (m, 1H), 4.49-4.33 (m, 1H), 4.30-4.16 (m, 1H), 4.03 (t, *J*= 7.5 Hz, 2H), 3.99-3.90 (m, 1H), 3.76-3.59 (m, 2H), 3.52-3.42 (m, 0.5H), 3.42-3.31 (m, 0.5H), 2.77-2.65 (m, 2H), 2.07-1.89 (m, 2H), 1.71-1.59 (m, 2H), 0.96 (t, *J*= 8.0 Hz, 3H).

MS(ESI): *m/z* calcd for $C_{19}H_{24}{}^{79}BrN_3O_4$: 437.1; found: 438.1 $[M+H]^+$.

Synthesis of allyl (*S*)-1-((3a*S*,6a*S*)-3-bromo-3a,4,6,6a-tetrahydropyrrolo[3,4-*d*]isoxazol-5-yl)-1-oxo-4-phenylbutan-2-ylcarbamate [(*S*,*S*,*S*)-142]

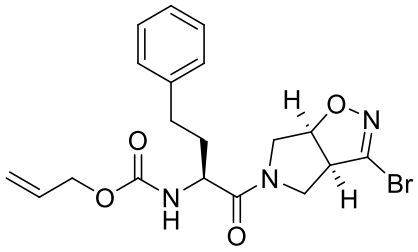

(*S*,*S*,*S*)-**142**

85% yield. R_f= 0.46 (light petroleum/EtOAc, 4:6).

^{1}H-NMR (300 MHz, $CDCl_3$): δ= 7.38-7.15 (m, 5H), 6.01-5.85 (m, 1H), 5.60 (d, *J*= 7.7 Hz, 1H), 5.39-5.20 (m, 3H), 4.63-4.55 (m, 2H), 4.45-4.33 (m, 1H), 4.21 (d, *J*= 13.0 Hz, 1H), 3.94 (m, 1H), 3.72-3.60 (m, 2H), 3.46 (m, 1H), 2.78-2.63 (m, 2H), 2.13-1.88 (m, 2H).

^{13}C-NMR (75 MHz, $CDCl_3$): δ= 171.8, 156.6, 141.3, 139.2, 133.1, 129.4, 128.6, 125.8, 117.3, 84.5, 66.1, 55.7, 53.1, 51.4, 47.9, 31.8, 29.6.

$[\alpha]_D^{20}$= + 60.4° (c= 0.22, DCM).

MS(ESI): *m/z* calcd for $C_{19}H_{22}{}^{79}BrN_3O_4$: 435.1; found: 436.1 $[M+H]^+$.

Synthesis of allyl (*S*)-1-((3a*R*,6a*R*)-3-bromo-3a,4,6,6a-tetrahydropyrrolo[3,4-*d*]isoxazol-5-yl)-1-oxo-4-phenylbutan-2-ylcarbamate [(*S*,*R*,*R*)-143]

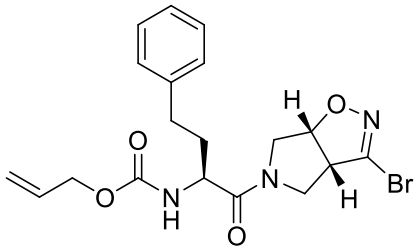

(*S*,*R*,*R*)-**143**

81% yield. R_f= 0.46 (light petroleum/EtOAc, 4:6).

^{1}H-NMR (300 MHz, $CDCl_3$): δ= 7.38-7.17 (m, 5H), 6.01-5.85 (m, 1H), 5.62 (d, *J*= 8.1 Hz, 1H), 5.32-5.20 (m, 1H), 5.28 (m, 2H), 4.66-4.54 (m, 2H), 4.55-4.39 (m, 1H), 4.13 (d, *J*= 13.4 Hz, 1H), 4.05-3.88 (m, 1H), 3.77-3.57 (m, 1H), 3.68 (d, *J*= 13.4 Hz, 1H), 3.42 (m, 1H), 2.82-2.60 (m, 2H), 2.06-1.87 (m, 2H).

^{13}C-NMR (75 MHz, $CDCl_3$): δ= 171.8, 156.6, 141.3, 139.2, 133.1, 129.3, 128.7, 125.9, 117.2, 84.4, 66.1, 55.6, 53.1, 51.4, 47.9, 31.7, 29.5.

$[\alpha]_D^{20}$= - 70.5° (c= 0.39, DCM);

MS(ESI): *m/z* calcd for $C_{19}H_{22}{}^{79}BrN_3O_4$: 435.1; found: 436.1 $[M+H]^+$.

Synthesis of *tert*-butyl (*S*)-1-((3a*S*,6a*S*)-3-bromo-3a,4,6,6a-tetrahydropyrrolo[3,4-*d*]isoxazol-5-yl)-1-oxo-4-phenylbutan-2-ylcarbamate [(*S*,*R*,*R*)-144] and *tert*-butyl (*S*)-1-((3a*R*,6a*R*)-3-bromo-3a,4,6,6a-tetrahydropyrrolo[3,4-*d*]isoxazol-5-yl)-1-oxo-4-phenylbutan-2-ylcarbamate [(*S*,*R*,*R*)-145]

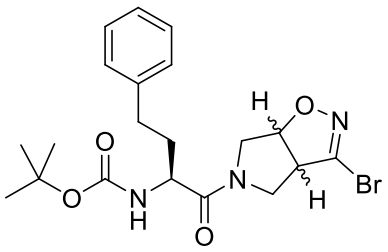

(*S*,*S*,*S*)-**144**/(*S*,*R*,*R*)-**145**

96% yield. R_f= 0.48 (light petroleum/EtOAc, 4:6).

^{1}H-NMR (300 MHz, $CDCl_3$): δ= 7.37-7.17 (m, 5H), 5.37 (bs, 1H), 5.33-5.18 (m, 1H), 4.53-4.26 (m, 1H), 4.26-4.11 (m, 1H), 4.06-3.88 (m, 1H), 3.79-3.56 (m, 2H), 3.54-3.42 (m, 0.5H), 3.42-3.32 (m, 0.5H), 2.84-2.61 (m, 2H), 2.11-1.83 (m, 2H), 1.46 (s, 9H).

MS(ESI): *m/z* calcd for $C_{20}H_{26}{}^{79}BrN_3O_4$: 451.1; found: 452.1 $[M+H]^+$.

Synthesis of benzyl (*S*)-1-((3a*S*,6a*S*)-3-bromo-3a,4,6,6a-tetrahydropyrrolo[3,4-*d*]isoxazol-5-yl)-1-oxo-4-phenylbutan-2-ylcarbamate [(*S*,*S*,*S*)-146] and benzyl (*S*)-1-((3a*R*,6a*R*)-3-bromo-3a,4,6,6a-tetrahydropyrrolo[3,4-*d*]isoxazol-5-yl)-1-oxo-4-phenylbutan-2-ylcarbamate [(*S*,*R*,*R*)-147]

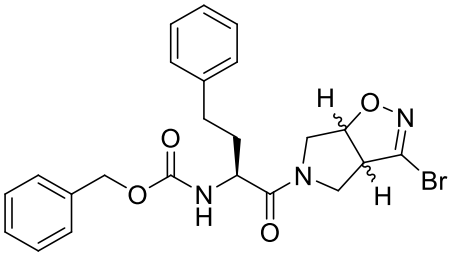

(*S*,*S*,*S*)-**146**/(*S*,*R*,*R*)-**147**

87% yield. R_f= 0.42 (light petroleum/EtOAc, 4:6).

^{1}H-NMR (300 MHz, $CDCl_3$): δ= 7.46–7.16 (m, 10H), 5.52 (bs, 1H), 5.33-5.22 (m, 1H), 5.14 (s, 2H), 4.60-4.36 (m, 1H), 4.26-4.10 (m, 1H), 4.04-3.86 (m, 1H), 3.74-3.59 (m, 2H), 3.53-3.42 (m, 0.5H), 3.42-3.30 (m, 0.5H), 2.87-2.62 (m, 2H), 2.13-1.88 (m, 2H).

MS(ESI): *m/z* calcd for $C_{23}H_{24}{}^{79}BrN_3O_4$: 485.1; found: 486.1 $[M+H]^+$.

Synthesis of ethyl 4-(3-(2,4-diamino-6-hydroxypyrimidin-5-yl)ureido)benzoate (153)

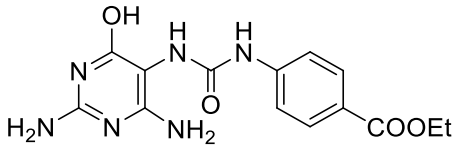

153

1 M aq. NaOH (11.4 mL) was added to a suspension of 4-hydroxy-2,5,6-triaminopyrimidine sulfate salt (**150*H_2SO_4**) (910 mg, 3.80 mmol) in water (2.0 mL). A solution of ethyl 4-isocyanatebenzoate (**151**) (726 mg, 3.80 mmol) in MeCN (6.0 mL) was slowly added. The reaction mixture was vigorously stirred at room temperature for 2.5 h, then it was neutralized with 1 M aq. HCl (11.4 mL). The precipitate was filtered, washed with water (50 mL), ethanol (30 mL) and Et_2O (30 mL) obtaining ethyl 4-(3-(2,4-diamino-6-hydroxypyrimidin-5-yl)ureido)benzoate (**153**) as a pale orange solid (950 mg, 75% yield) (decomposes at T> 180 °C).

^{1}H-NMR (300 MHz, DMSO-d_6): δ= 10.0 (bs, 1H), 8.98 (bs, 1H), 7.84 (d, *J*= 8.4 Hz, 2H), 7.57 (d., *J*= 8.4 Hz, 2H), 6.76 (s, 1H), 6.16 (bs, 2H), 5.96 (bs, 2H), 4.26 (q, *J*= 7.0 Hz, 2H), 1.31 (t, *J*= 7.0 Hz, 3H).

^{13}C-NMR (75 MHz, DMSO-d_6): δ= 166.2, 162.4, 161.0, 155.3, 154.0, 145.9, 130.9, 122.6, 117.6, 89.9, 60.8, 14.9.

Synthesis of 4-(3-(2,4-diamino-6-hydroxypyrimidin-5-yl)ureido)benzoic acid (154)

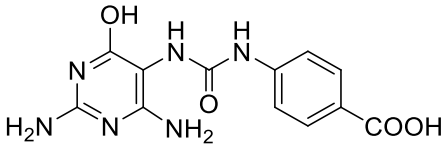

154

1 M aq. NaOH (28.6 mL) was added to a suspension of **153** (950 mg, 2.86 mmol) in water (25 mL). The reaction mixture was stirred at room temperature for 3 h, then it was neutralized with 1 M aq. HCl (28.6 mL). The precipitate was centrifuged (5000 rpm, 3 min) and washed with water (20 mL), ethanol (20 mL) and Et_2O (20 mL) obtaining 4-(3-(2,4-diamino-6-hydroxypyrimidin-5-yl)ureido)benzoic acid (**154**) as a pale orange solid (800 mg, 92% yield) (decomposes at T> 240 °C).

^{1}H-NMR (300 MHz, DMSO-d_6): δ= 12.50 (bs, 1H), 9.98 (bs, 1H), 8.90 (bs, 1H), 7.80 (d, *J*= 7.6 Hz, 2H), 7.52 (d, *J*= 7.6 Hz, 2H), 6.71 (s, 1H), 6.18 (bs, 2H), 5.88 (bs, 2H).

^{13}C-NMR (75 MHz, DMSO-d_6): δ= 167.8, 162.2, 160.9, 155.3, 154.0, 145.6, 131.1, 123.5, 117.5, 90.0.

General procedure for the esterification of amino acids

$SOCl_2$ (2.2 eq.) was added dropwise at 0 °C to a suspension of amino acid in methanol or ethanol (0.75 mol/L). The reaction mixture was stirred at room temperature for 24 h, then the solvent was removed under reduced pressure obtaining the diester hydrochloride product.

Synthesis (*S*)-1,5-diethoxy-1,5-dioxopentan-2-aminium chloride [(*S*)-158]

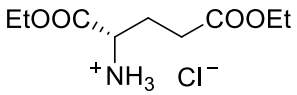

158

The product was synthesized following the general procedure for the esterification of amino acids, and it was obtained as a white solid (99% yield) (m.p.= 108-110 °C) (lit. m.p.= 109-110 °C). [77]

^{1}H-NMR (300 MHz, D_2O): δ= 4.20 (q, *J*= 7.3 Hz, 2H), 4.13-4.04 (m, 3H), 2.53 (dt, *J*= 1.8, 7.3 Hz, 2H), 2.25-2.05 (m, 2H), 1.21 (t, *J*= 7.3 Hz, 3H), 1.16 (t, *J*= 7.3 Hz, 3H).

^{13}C-NMR (75 MHz, D_2O): δ= 174.6, 169.9, 63.9, 62.3, 52.3, 29.8, 25.0, 13.5, 13.4.

Synthesis of (*S*)-1,4-dimethoxy-1,4-dioxobutan-2-aminium chloride [(*S*)-162]

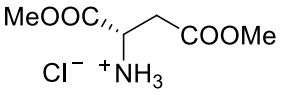

162

The product was synthesized following the general procedure for the esterification of amino acids, and it was obtained as a white solid (98% yield) (m.p.= 115.7-116.5 °C) (lit. m.p.= 115-116 °C). [78]

^{1}H-NMR (300 MHz, DMSO-d_6): δ= 8.68 (bs, 3H), 4.33 (t, *J*= 6.2 Hz, 1H), 3.72 (s, 3H), 3.64 (s, 3H), 2.99 (m, 2H).

^{13}C-NMR (75 MHz, DMSO-d_6): δ= 169.6, 168.7, 53.0, 52.2, 48.4, 34.0.

Synthesis of (*S*)-1,6-dimethoxy-1,6-dioxohexan-2-aminium chloride [(*S*)-163]

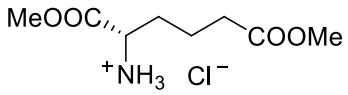

163

The product was synthesized following the general procedure for the esterification of amino acids, and it was obtained as a colourless oil (quantitative yield).

^{1}H-NMR (300 MHz, D_2O): δ= 4.05 (t, *J*= 6.3 Hz, 1H), 3.74 (s, 3H), 3.58 (s, 3H), 2.36 (t, *J*= 7.1, 7.7 Hz, 2H), 1.97-1.75 (m, 2H), 1.73-1.48 (m, 2H).

^{13}C-NMR (75 MHz, D_2O): δ= 169.6, 168.7, 53.0, 52.2, 48.4, 34.0.

Synthesis of 4-methoxy-4-oxobutan-1-aminium chloride (164)

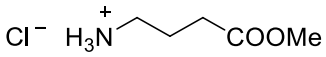

164

The product was synthesized following the general procedure for the esterification of amino acids, and it was obtained as a white solid (90% yield) (m.p.= 122.5-123.2 °C) (lit. m.p.= 120.0 °C). [79]

^{1}H-NMR (300 MHz, CD_3OD): δ= 3.68 (s, 3H), 2.98 (t, *J*= 7.7 Hz, 2H), 2.48 (t, *J*= 7.1 Hz, 2H), 1.93 (tt, *J*= 7.1, 7.7 Hz, 2H).

^{13}C-NMR (75 MHz, DMSO-d_6): δ= 174.5, 52.3, 40.0, 31.4, 23.7.

General procedure for the coupling of 154 with amino esters

NMM (4 eq.) and CDMT (4 eq.) were added to a suspension of **154** (1 eq.) in dry DMF (47 mmol/L). The reaction mixture was stirred at 35 °C for 5 h, then the amino ester hydrochloride (4 eq.) and NMM (4 eq.) were added. The reaction mixture was stirred at 30 °C for 18 h, then the solvent was removed at reduced pressure, ethanol was added and the precipitate was filtered, washed with ethanol and Et_2O, obtaining the desired product.

Synthesis of (*S*)-diethyl 2-(4-(3-(2,4-diamino-6-oxo-1,6-dihydropyrimidin-5-yl)ureido)benzamido)pentanedioate [(*S*)-155]

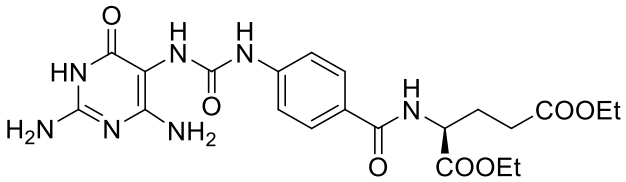

(*S*)-**155**

The product was synthesized following the general procedure for the coupling of **154** with amino esters, and it was obtained as a pale orange solid (65% yield) (decomposes at T> 180 °C).

^{1}H-NMR (300 MHz, DMSO-d_6): δ= 9.95 (bs, 1H), 8.82 (bs, 1H), 8.48 (d, *J*= 7.0 Hz, 1H), 7.80 (d, *J*= 8.8 Hz, 2H), 7.50 (d, *J*= 8.8 Hz, 2H), 6.70 (s, 1H), 6.18 (bs, 2H), 5.88 (bs, 2H), 4.40-4.37 (m, 1H), 4.07 (q, *J*= 7.3 Hz, 2H), 4.00 (q, *J*= 7.3 Hz, 2H), 2.45-2.38 (m, 2H), 2.17-1.95 (m, 2H), 1.17 (t, *J*= 7.3 Hz, 3H), 1.13 (t, *J*= 7.3 Hz, 3H).

^{13}C-NMR (75 MHz, DMSO-d_6): δ= 172.9, 172.7, 167.0, 162.2, 160.9, 155.4, 153.9, 144.4, 129.1, 126.6, 117.4, 90.1, 61.2, 60.6, 52.6, 30.9, 26.5, 14.8.

Synthesis of (*S*)-dimethyl 2-(4-(3-(2,4-diamino-6-oxo-1,6-dihydropyrimidin-5-yl)ureido)benzamido)succinate [(*S*)-168]

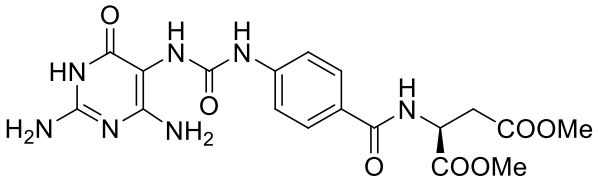

(*S*)-**168**

The product was synthesized following the general procedure for the coupling of **154** with amino esters, and it was obtained as a pale orange solid (72% yield) (decomposes at T> 178 °C).

^{1}H-NMR (300 MHz, DMSO-d_6): δ= 10.06 (bs, 1H), 8.82 (bs, 1H), 8.70 (d, *J*= 7.7 Hz, 1H), 7.75 (d, *J*= 8.8 Hz, 2H), 7.51 (d, *J*= 8.8 Hz, 2H), 6.72 (s, 1H), 6.25 (bs, 2H), 5.96 (bs, 2H), 4.79 (ddd, *J*= 6.3, 7.7, 7.9 Hz, 1H), 3.62 (s, 3H), 3.60 (s, 3H), 2.93 (dd, *J*= 6.3, 16.5 Hz, 1H), 2.79 (dd, *J*= 7.9, 16.5Hz, 1H).

^{13}C-NMR (75 MHz, DMSO-d_6): δ= 172.2, 171.3, 166.5, 161.8, 160.9, 155.3, 153.8, 144.5, 129.0, 126.3, 117.4, 90.0, 52.9, 52.4, 49.8, 36.1.

Synthesis of (*S*)-dimethyl 2-(4-(3-(2,4-diamino-6-oxo-1,6-dihydropyrimidin-5-yl)ureido)benzamido)hexanedioate [(*S*)-169]

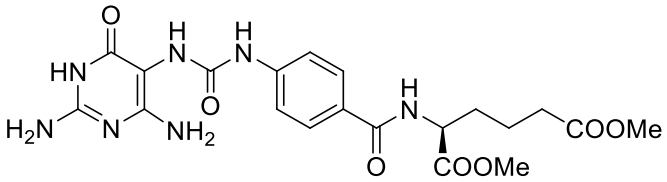

(*S*)-**169**

The product was synthesized following the general procedure for the coupling of **154** with amino esters, and it was obtained as a pale orange solid (61% yield) (decomposes at T> 190 °C).

^{1}H-NMR (300 MHz, DMSO-d_6): δ= 9.96 (bs, 1H), 8.82 (bs, 1H), 8.50 (d, *J*= 7.4 Hz, 1H), 7.77 (d, *J*= 8.8 Hz, 2H), 7.50 (d, *J*= 8.8 Hz, 2H), 6.69 (s, 1H), 6.14 (bs, 2H), 5.88 (bs, 2H), 4.38 (dt, 1H, *J* = 6.9, 7.4 Hz, 1H), 3.62 (s, 3H), 3.56 (s, 3H), 2.32 (t, *J*= 7.3 Hz, 2H), 1.89-1.72 (m, 2H), 1.68-1.53 (m, 2H).

^{13}C-NMR (75 MHz, DMSO-d_6): δ= 173.8, 173.4, 166.9, 162.3, 160.9, 155.4, 154.0, 144.4, 129.1, 126.5, 117.3, 90.0, 53.0, 52.5, 51.9, 33.5, 30.5, 22.0.

Synthesis of methyl 4-(4-(3-(2,4-diamino-6-oxo-1,6-dihydropyrimidin-5-yl)ureido)benzamido)butanoate (170)

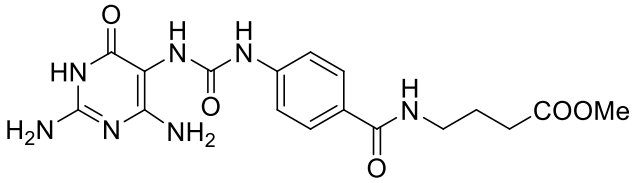

170

The product was synthesized following the general procedure for the coupling of **154** with amino esters, and it was obtained as a pale orange solid (63% yield) (decomposes at T> 210 °C).

^{1}H-NMR (300 MHz, DMSO-d_6): δ= 9.98 (bs, 1H), 8.77 (bs, 1H), 8.26 (t, *J*= 5.5 Hz, 1H), 7.71 (d, *J*= 8.5 Hz, 2H), 7.47 (d, *J*= 8.5 Hz, 2H), 6.69 (s, 1H), 6.16 (bs, 2H), 5.88 (bs, 2H), 3.56 (s, 3H) 3.23 (dt, *J*= 5.5, 6.6 Hz, 2H), 2.34 (t, *J*= 7.1 Hz, 2H), 1.75 (tt, *J*= 6.6, 7.1 Hz, 2H).

^{13}C-NMR (75 MHz, DMSO-d_6): δ= 173.9, 166.6, 162.3, 160.9, 155.4, 154.0, 143.9, 128.6, 127.5, 117.4, 90.1, 51.9, 39.1, 31.5, 25.3.

Synthesis of (*S*)-methyl 2-(4-(3-(2,4-diamino-6-oxo-1,6-dihydropyrimidin-5-yl)ureido)benzamido)propanoate [(*S*)-171]

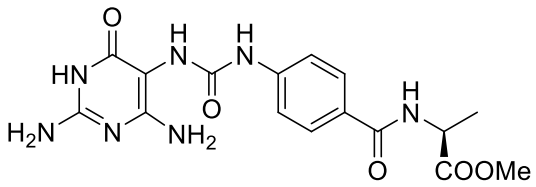

(*S*)-**171**

The product was synthesized following the general procedure for the coupling of **154** with amino esters, and it was obtained as a pale orange solid (69% yield) (decomposes at T> 172 °C).

^{1}H-NMR (300 MHz, DMSO-d_6): δ= 9.98 (bs, 1H), 8.82 (bs, 1H,), 8.55 (d, *J*= 6.9 Hz, 1H), 7.77 (d, *J*= 8.7 Hz, 2H), 7.50 (d, *J*= 8.7 Hz, 2H), 6.70 (s, 1H), 6.17 (bs, 2H), 5.89 (bs, 2H), 4.43 (dq, *J*= 6.9, 7.1 Hz, 1H), 3.62 (s, 3H), 1.37 (d, *J*= 7.1 Hz, 3H).

^{13}C-NMR (75 MHz, DMSO-d_6): δ= 174.1, 166.5, 162.2, 160.9, 155.4, 153.9, 144.3, 129.0, 126.5, 117.3, 90.0, 52.5, 48.9, 17.5.

Synthesis of methyl 3-(4-(3-(2,4-diamino-6-oxo-1,6-dihydropyrimidin-5-yl)ureido)benzamido)propanoate (172)

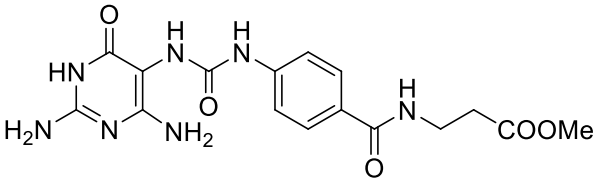

172

The product was synthesized following the general procedure for the coupling of **154** with amino esters, and it was obtained as a pale orange solid (63% yield) (decomposes at T> 180 °C).

^{1}H-NMR (300 MHz, DMSO-d_6): δ= 9.98 (bs, 1H), 8.77 (bs, 1H), 8.33 (t, *J*= 5.5 Hz, 1H), 7.70 (d, *J*= 8.8 Hz, 2H), 7.47 (d, *J*= 8.8 Hz, 2H), 6.69 (s, 1H), 6.16 (bs, 2H), 5.89 (bs, 2H), 3.59 (s, 3H), 3.44 (dt, *J*= 5.5, 6.9 Hz, 2H), 2.56 (t, *J*= 6.9 Hz, 2H).

^{13}C-NMR (75 MHz, DMSO-d_6): δ= 172.5, 166.6, 162.3, 160.9, 155.4, 154.0, 144.1, 128.7, 127.2, 117.4, 90.1, 52.1, 36.1, 34.4.

Synthesis of (*S*)-methyl 2-(4-(3-(2,4-diamino-6-oxo-1,6-dihydropyrimidin-5-yl)ureido)benzamido)-3-phenylpropanoate [(*S*)-173]

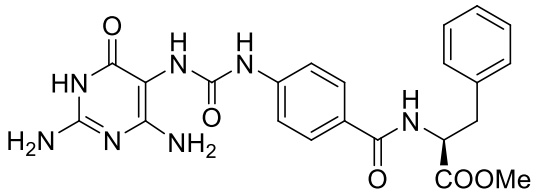

(*S*)-**173**

The product was synthesized following the general procedure for the coupling of **154** with amino esters, and it was obtained as a pale orange solid (58% yield) (decomposes at T> 180 °C).

^{1}H-NMR (300 MHz, DMSO-d_6): δ= 9.98 (bs, 1H), 8.81 (bs, 1H), 8.61 (d, *J*= 7.0 Hz,1H), 7.70 (d, *J*= 8.8 Hz, 2H), 7.48 (d, *J*= 8.8 Hz, 2H), 7.30-7.21 (m, 4H), 7.20-7.13 (m, 1H), 6.70 (s, 1H), 6.16 (bs, 2H), 5.89 (bs, 2H), 4.60 (ddd, *J*= 6.0, 8.0, 9.1 Hz, 1H), 3.61 (s, 3H) 3.17-3.04 (m, 2H).

^{13}C-NMR (75 MHz, DMSO-d_6): δ= 173.1, 166.7, 162.3, 160.9, 155.3, 154.0, 144.4, 138.5, 129.7, 129.0, 128.9, 127.1, 126.5, 117.3, 90.0, 54.7, 52.6, 37.0.

Synthesis of (*S*)-methyl 2-(4-(3-(2,4-diamino-6-oxo-1,6-dihydropyrimidin-5-yl)ureido)benzamido)-3-(4-hydroxyphenyl)propanoate [(*S*)-174]

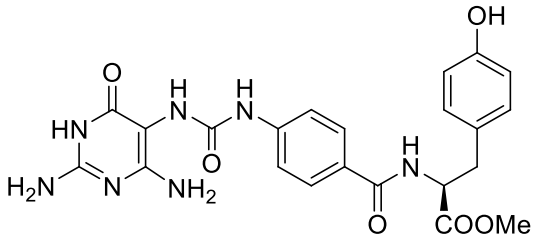

(*S*)-**174**

The product was synthesized following the general procedure for the coupling of **154** with amino esters, and it was obtained as a pale orange solid (59% yield) (decomposes at T> 175 °C).

^{1}H-NMR (300 MHz, DMSO-d_6): δ= 9.97 (bs, 1H), 9.19 (s, 1H), 8.83 (bs, 1H), 8.55 (d, *J*= 7.8 Hz, 1H), 7.70 (d, *J*= 8.7 Hz, 2H), 7.48 (d, *J*= 8.7 Hz, 2H), 7.06 (d, *J*= 8.4 Hz, 2H), 6.71 (s, 1H), 6.63 (d, *J*= 8.4 Hz, 2H), 6.15 (bs, 2H), 5.89 (bs, 2H), 4.56−4.45 (m, 1H), 3.60 (s, 3H), 3.05−2.87 (m, 2H).

^{13}C-NMR (75 MHz, DMSO-d_6): δ= 173.3, 166.7, 162.3, 160.9, 156.6, 155.4, 154.0, 144.3, 130.7, 129.0, 128.4, 126.5, 117.3, 115.7, 90.0, 55.4, 52.5, 36.3.

General procedure for the synthesis of (*S*)-156 and analogues

The coupling product (1 eq.) was dissolved in 1 M aq. NaOH (2 or 4 eq.). The reaction mixture was stirred at room temperature for 5 h, then it was neutralized with 1 M aq. HCl (2 or 4 eq.). The precipitate was filtered and washed with water, ethanol and Et_2O, obtaining the desired product.

Synthesis of (*S*)-2-(4-(3-(2,4-diamino-6-oxo-1,6-dihydropyrimidin-5-yl)ureido)benzamido)pentanedioic acid [(*S*)-156]

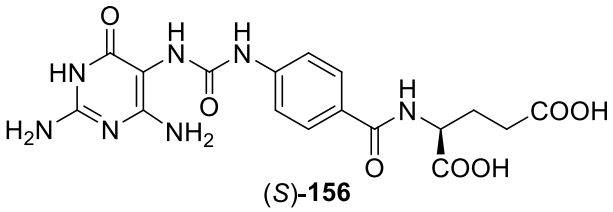

(*S*)-**156**

The product was synthesized following the general procedure for the synthesis of (*S*)-**156** and analogues, and it was obtained as a pale orange solid (88% yield) (decomposes at T> 190 °C).

^{1}H-NMR (300 MHz, DMSO-d_6): δ= 12.35 (bs, 2H), 9.98 (bs, 1H), 8.82 (bs, 1H), 8.38 (d, *J*= 6.6 Hz, 1H), 7.79 (d, *J* = 8.0 Hz, 2H), 7.50 (d, *J*= 8.0 Hz, 2H), 6.68 (s, 1H), 6.18 (bs, 2H), 5.90 (bs, 2H), 4.40-4.30 (m, 1H), 2.38-2.30 (m, 2H), 2.10-2.00 (m, 1H), 2.00-1.90 (m, 1H).

^{13}C-NMR (75 MHz, DMSO-d_6): δ= 174.6, 174.3, 166.8, 162.3, 160.9, 155.4, 154.0, 144.3, 129.0, 126.8, 117.4, 90.1, 52.5, 31.1, 26.7.

MS(ESI): *m/z* calcd for $C_{17}H_{19}N_7O_7$: 433.1; found: 434.1 $[M+H]^+$.

Synthesis of (*S*)-2-(4-(3-(2,4-diamino-6-oxo-1,6-dihydropyrimidin-5-yl)ureido)benzamido)succinic acid [(*S*)-175]

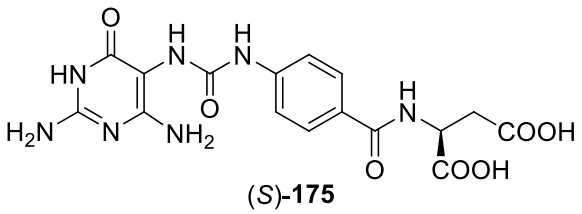

(*S*)-**175**

The product was synthesized following the general procedure for the synthesis of (*S*)-**156** and analogues, and it was obtained as a pale orange solid (80% yield) (decomposes at T> 230 °C).

^{1}H-NMR (300 MHz, DMSO-d_6): δ= 12.48 (bs, 2H), 9.96 (bs, 1H), 8.81 (bs, 1H), 8.48 (d, *J*= 7.4 Hz, 1H), 7.74 (d, *J*= 8.5 Hz, 2H), 7.50 (d, *J*= 8.5 Hz, 2H), 6.69 (s, 1H), 6.14 (bs, 2H), 5.88 (bs, 2H), 4.70 (ddd, *J*= 6.1, 7.4, 7.8 Hz, 1H), 2.81 (dd, *J*= 6.1, 16.4 Hz, 1H), 2.66 (dd, *J*= 7.8, 16.4 Hz, 1H).

^{13}C-NMR (75 MHz, DMSO-d_6): δ= 173.5, 172.6, 166.3, 162.3, 160.9, 155.4, 154.0, 144.3, 128.9, 126.7, 117.4, 90.0, 49.9, 36.9.

MS(ESI): *m/z* calcd for $C_{16}H_{17}N_7O_7$: 419.1; found: 420.1 $[M+H]^+$.

Synthesis of (*S*)-2-(4-(3-(2,4-diamino-6-oxo-1,6-dihydropyrimidin-5-yl)ureido)benzamido)hexanedioic acid [(*S*)-176]

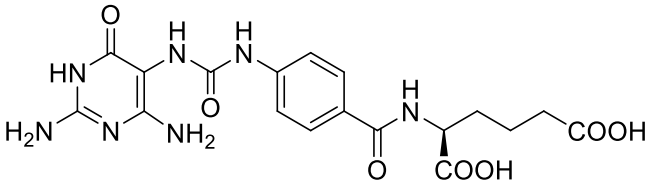

(*S*)-**176**

The product was synthesized following the general procedure for the synthesis of (*S*)-**156** and analogues, and it was obtained as a pale orange solid (79% yield) (decomposes at T> 205 °C).

^{1}H-NMR (300 MHz, DMSO-d_6): δ= 12.26 (bs, 2H), 9.97 (bs, 1H), 8.80 (bs, 1H), 8.35 (d, *J*= 7.7 Hz, 1H), 7.78 (d, *J*= 8.7 Hz, 2H), 7.50 (d, *J*= 8.7 Hz, 2H), 6.69 (s, 1H), 6.14 (bs, 2H), 5.87 (bs, 2H), 4.31 (dt, *J*= 5.1, 7.7 Hz, 1H), 2.22 (t, *J*= 7.4 Hz, 2H), 1.89-1.68 (m, 2H), 1.68-1.49 (m, 2H).

^{13}C-NMR (75 MHz, DMSO-d_6): δ= 175.0, 174.5, 166.7, 162.3, 160.9, 155.4, 154.0, 144.2, 129.0, 126.9, 117.3, 90.1, 53.1, 34.0, 30.9, 22.1.

MS(ESI): *m/z* calcd for $C_{18}H_{21}N_7O_7$: 447.1; found: 448.1 $[M+H]^+$.

Synthesis of 4-(4-(3-(2,4-diamino-6-oxo-1,6-dihydropyrimidin-5-yl)ureido)benzamido)butanoic acid (177)

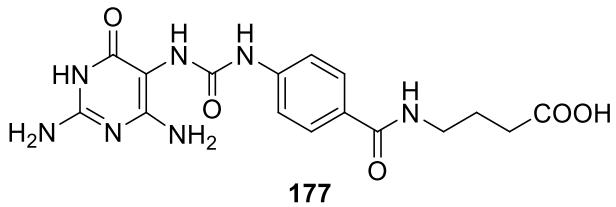

177

The product was synthesized following the general procedure for the synthesis of (*S*)-**156** and analogues, and it was obtained as a pale orange solid (79% yield) (dec. T> 205 °C).

^{1}H-NMR (300 MHz, DMSO-d_6): δ= 12.02 (bs, 1H), 9.97 (bs, 1H), 8.78 (bs, 1H), 8.25 (t, *J*= 5.8 Hz, 1H), 7.72 (d, *J*= 8.8 Hz, 2H), 7.47 (d, *J*= 8.8 Hz, 2H), 6.68 (s, 1H), 6.13 (bs, 2H), 5.86 (bs, 2H), 3.23 (dt, *J*= 5.8, 6.6 Hz, 2H), 2.25 (t, *J*= 7.4 Hz, 2H), 1.72 (tt, *J*= 5.8, 6.6 Hz, 2H).

^{13}C-NMR (75 MHz, DMSO-d_6): δ= 175.0, 166.6, 162.2, 160.9, 155.4, 154.0, 143.9, 128.6, 127.6, 117.4, 90.2, 39.2, 31.9, 25.4.

MS(ESI): *m/z* calcd for $C_{16}H_{19}N_7O_5$: 389.1; found: 390.1 $[M+H]^+$.

Synthesis of (*S*)-2-(4-(3-(2,4-diamino-6-oxo-1,6-dihydropyrimidin-5-yl)ureido)benzamido)propanoic acid [(*S*)-178]

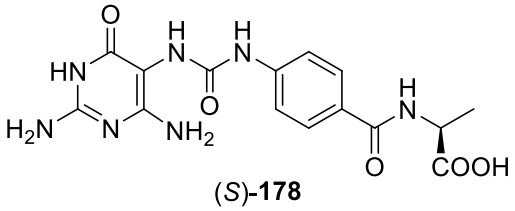

(*S*)-**178**

The product was synthesized following the general procedure for the synthesis of (*S*)-**156** and analogues, and it was obtained as a pale orange solid (70% yield) (decomposes at T> 195 °C).

^{1}H-NMR (300 MHz, DMSO-d_6): δ= 12.44 (bs, 1H), 9.98 (bs, 1H), 8.82 (bs, 1H), 8.40 (d, *J*= 7.1 Hz, 1H), 7.77 (d, *J*= 8.8 Hz, 2H), 7.49 (d, *J*= 8.8 Hz, 2H), 6.69 (s, 1H), 6.13 (bs, 2H), 5.87 (bs, 2H), 5.74 (s, 1H), 4.37 (dq, *J*= 7.1, 7.4 Hz, 1H), 1.36 (d, *J*= 7.4 Hz, 3H).

^{13}C-NMR (75 MHz, DMSO-d_6): δ= 175.1, 166.3, 162.3, 160.9, 155.4, 154.0, 144.2, 128.9, 126.9, 117.3, 90.1, 48.8, 17.8.

MS(ESI): *m/z* calcd for $C_{15}H_{17}N_7O_5$: 375.1; found: 376.1 $[M+H]^+$.

Synthesis of 3-(4-(3-(2,4-diamino-6-oxo-1,6-dihydropyrimidin-5-yl)ureido)benzamido)propanoic acid (179)

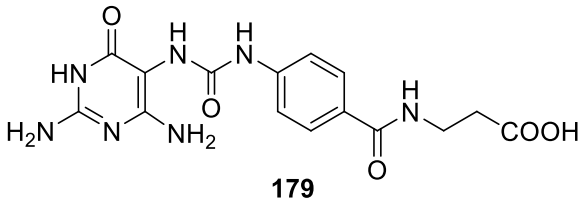

179

The product was synthesized following the general procedure for the synthesis of (*S*)-**156** and analogues, and it was obtained as a pale orange solid (82% yield) (dec. T> 220 °C).

^{1}H-NMR (300 MHz, DMSO-d_6): δ= 12.19 (bs, 1H), 9.97 (bs, 1H), 8.78 (bs, 1H), 8.30 (t, *J*= 5.3 Hz, 1H), 7.71 (d, *J*= 8.8 Hz, 2H), 7.47 (d, *J*= 8.8 Hz, 2H), 6.69 (s, 1H), 6.14 (bs, 2H), 5.87 (bs, 2H), 3.41 (dt, *J*= 5.3, 6.7 Hz, 2H), 2.43 (t, *J*= 6.7 Hz, 2H).

^{13}C-NMR (75 MHz, DMSO-d_6): δ= 173.6, 166.6, 162.3, 160.9, 155.4, 154.0, 144.0, 128.7, 127.3, 117.4, 90.1, 36.2, 34.6.

MS(ESI): *m/z* calcd for $C_{15}H_{17}N_7O_5$: 375.1; found: 376.1 $[M+H]^+$.

Synthesis of (*S*)-2-(4-(3-(2,4-diamino-6-oxo-1,6-dihydropyrimidin-5-yl)ureido)benzamido)-3-phenylpropanoic acid [(*S*)-180]

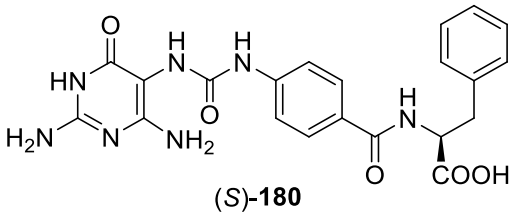

(*S*)-**180**

The product was synthesized following the general procedure for the synthesis of (*S*)-**156** and analogues, and it was obtained as a pale orange solid (72% yield) (decomposes at T> 180 °C).

^{1}H-NMR (300 MHz, DMSO-d_6): δ= 12.76 (bs, 1H), 9.97 (bs, 1H), 8.79 (bs, 1H), 8.46 (d, *J*= 8.2 Hz,1H), 7.69 (d, *J*= 8.8 Hz, 2H), 7.48 (d, *J*= 8.8 Hz, 2H), 7.33-7.21 (m, 4H), 7.19-7.12 (m, 1H), 6.69 (s, 1H), 6.14 (bs, 2H), 5.87 (bs, 2H), 4.56 (ddd, *J*= 4.6, 8.2, 10.5 Hz, 1H), 3.15 (dd, *J*= 4.6, 13.8 Hz, 1H), 3.04 (dd, *J*= 10.5, 13.8 Hz, 1H).

^{13}C-NMR (75 MHz, DMSO-d_6): δ= 174.1, 166.6, 162.3, 160.9, 155.3, 154.0, 144.2, 139.0, 129.7, 128.9, 128.8, 127.0, 126.8, 117.3, 90.1, 54.9, 37.0.

MS(ESI): *m/z* calcd for $C_{21}H_{21}N_7O_5$: 451.2; found: 452.2 $[M+H]^+$.

Synthesis of (*S*)-2-(4-(3-(2,4-diamino-6-oxo-1,6-dihydropyrimidin-5-yl)ureido)benzamido)-3-(4-hydroxyphenyl)propanoic acid [(*S*)-181]

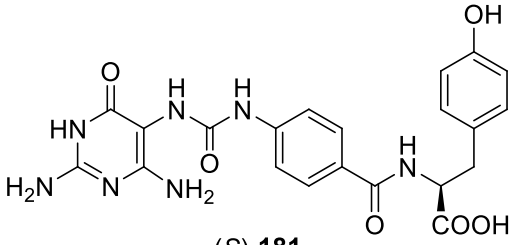

(*S*)-**181**

The product was synthesized following the general procedure for the synthesis of (*S*)-**156** and analogues, and it was obtained as a pale orange solid (76% yield) (decomposes at T> 198 °C).

^{1}H-NMR (300 MHz, DMSO-d_6): δ= 12.61 (bs, 1H), 9.96 (bs, 1H), 9.16 (s, 1H), 8.81 (bs, 1H), 8.39 (d, *J*= 8.2 Hz, 1H), 7.69 (d, *J*= 8.8 Hz, 2H), 7.47 (d, *J*= 8.8 Hz, 2H), 7.07 (d, *J*= 8.4 Hz, 2H), 6.69 (s, 1H), 6.62 (d, *J*= 8.4 Hz, 2H), 6.15 (bs, 2H), 5.89 (bs, 2H), 4.53−4.41 (m, 1H), 3.02 (dd, 1H, *J*= 4.5, 13.8 Hz, 1H), 2.91 (dd, *J*= 10.1, 13.8 Hz, 1H).

^{13}C-NMR (75 MHz, DMSO-d_6): δ= 174.2, 166.6, 162.3, 160.9, 156.5, 155.4, 154.0, 144.2, 130.7, 129.0, 126.9, 126.8, 117.3, 115.6, 90.0, 55.2, 36.2.

MS(ESI): *m/z* calcd for $C_{21}H_{21}N_7O_6$: 467.2; found: 468.2 $[M+H]^+$.

Synthesis of (±)-ethyl 2-methyldodecanoate [(±)-187]

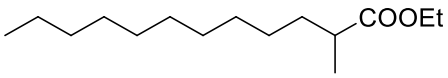

(±)-**187**

Ethyl laurate (**186**) (174 µL, 0.657 mmol) was added at -78 °C to a freshly prepared solution of LDA [*n*BuLi (341 µL, 2.5 M in hexanes, 0.854 mmol) was added to diisopropylamine (138 µL, 0.985 mmol) in 1.0 mL of dry THF at -78 °C, then the reaction mixture was stirred at 0 °C for 15 min]. The solution was stirred for 1 h, then MeI (82 µL, 1.31 mmol) was added. The reaction mixture was stirred at -78 °C for 1 h, then the solution was allowed to warm to room temperature and stirred overnight. The reaction was quenched with water and extracted twice with Et_2O. The pooled organic phases were dried over anhydrous Na_2SO_4, filtered and the solvent was removed under reduced pressure. The crude product was purified by column chromatography on silica gel (*n*-hexane/EtOAc, 20:1) obtaining (±)-ethyl 2-methyldodecanoate [(±)-**187**] as colourless oil (152 mg, 96% yield).

R_f= 0.37 (*n*-hexane/EtOAc, 20:1).

^{1}H-NMR (400 MHz, $CDCl_3$): δ= 4.11 (q, *J*= 7.1 Hz, 2H), 2.40 (sex, *J*= 7.0 Hz, 1H), 1.68-1.58 (m, 1H), 1.43-1.34 (m, 1H), 1.32-1.21 (m, 19H), 1.12 (d, *J*= 7.0 Hz, 3H), 0.87 (m, 3H).

^{13}C-NMR (100 MHz, $CDCl_3$): δ= 177.0, 60.0, 39.6, 33.8, 31.9, 29.6, 29.5, 29.5, 29.3, 27.2, 22.7, 17.1, 14.3, 14.1.

Synthesis of (±)-2-methyldodecanoic acid [(±)-188]

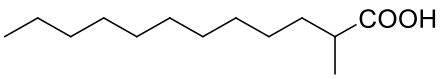

(±)-**188**

(±)-**187** (152 mg, 0.627 mmol) was added to 1.25 M aq. LiOH (1 mL) and the reaction mixture was stirred under reflux for 24 h. The reaction was quenched with 1 M aq. HCl and it was extracted twice with Et_2O. The pooled organic extracts were dried over anhydrous Na_2SO_4, filtered and the solvent was removed under reduced pressure. The crude product was purified by column chromatography on silica gel (*n*-hexane/EtOAc, 20:1 to 5:1) obtaining (±)-2-methyldodecanoic acid [(±)-**188**] as colourless oil (80 mg, 60% yield).

R_f= 0.25 (*n*-hexane/EtOAc, 5:1).

^{1}H-NMR (400 MHz, $CDCl_3$): δ= 11.74 (bs, 1H), 2.45 (sex, *J*= 7.0 Hz, 1H), 1.74-1.62 (m, 1H), 1.48-1.37 (m, 1H), 1.36-1.21 (m, 18H), 1.17 (d, *J*= 7.0 Hz, 3H), 0.88 (m, 3H).

^{13}C-NMR (100 MHz, $CDCl_3$): δ= 183.8, 39.4, 33.5, 31.9, 29.6, 29.5, 29.5, 29.3, 27.1, 22.7, 16.8, 14.1.

Synthesis of 2,4,6-trimethoxyaniline (189)

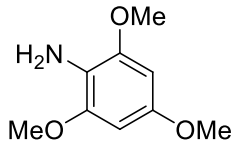

189

1,3,5-Trimethoxy-2-nitrobenzene (**190**) (500 mg, 2.34 mmol) and zinc dust (765 mg, 11.7 mmol) were suspended in ethanol (2.5 mL). The reaction mixture was cooled to 0 °C and acetic acid (2.5 mL) was slowly added. The reaction was stirred at room temperature overnight, then it was quenched with sat. aq. $NaHCO_3$. Et_2O was added, phases were separated and the aqueous phase was extracted with Et_2O. The pooled organic phases were dried over anhydrous Na_2SO_4, filtered and the solvent was removed under vacuum. The crude product was purified by column chromatography on silica gel (*n*-hexane/EtOAc, 1:1) obtaining 2,4,6-trimethoxyaniline(**189**) as a brown oil (429 mg, quantitative yield).

R_f= 0.37 (*n*-hexane/EtOAc, 2:1).

^{1}H-NMR (400 MHz, $CDCl_3$): δ= 6.17 (s, 2H), 3.83 (s, 6H), 3.77 (s, 3H), 3.49 (bs, 2H).

^{13}C-NMR (100 MHz, $CDCl_3$): δ= 152.5, 148.1, 119.0, 91.4, 55.8.

MS (ESI): *m/*z calcd for $C_9H_{13}NO_3$: 183.1; found: 184.1 $[M+H]^+$.

Synthesis of (±)-2-methyl-*N*-(2,4,6-trimethoxyphenyl)dodecanamide [(±)-183]

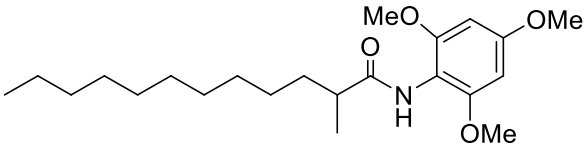

(±)-**183**

1,1'-Carbonyldiimidazole (92 mg, 0.559 mmol) was added at 0 °C to a suspension of (±)-**188** (80 mg, 0.373 mmol) in dry THF (1.5 mL) and the reaction mixture was stirred at room temperature for 1 h. A solution of **189** (102 mg, 0.559 mmol) in dry THF (1 mL) was added and the reaction mixture was stirred at 45 °C overnight. Et_2O was added and washed with water. The organic phase was dried over anhydrous Na_2SO_4, filtered and the solvent was removed under reduced pressure. The crude product was purified by column chromatography on silica gel (*n*-hexane/EtOAc, 2:1 to 1:1) obtaining 2-methyl-*N*-(2,4,6-trimethoxyphenyl)dodecanamide [(±)-**183**] as a white amorphous solid (81 mg, 57% yield).

R_f= 0.34 (*n*-hexane-EtOAc, 1:1).

^{1}H-NMR (400 MHz, $CDCl_3$): δ= 6.41 (bs, 1H), 6.13 (s, 2H), 3.80 (m, 3H), 3.78 (s, 6H), 2.45-2.32 (m, 1H), 1.79-1.65 (m, 1H), 1.50-1.35 (m, 1H), 1.34-1.15 (m, 18H), 0.87 (m, 3H).

^{13}C-NMR (100 MHz, $CDCl_3$): δ= 175.6, 159.7, 156.4, 107.7, 91.1, 55.9, 55.5, 41.7, 34.7, 31.9, 29.8, 29.7, 29.6, 29.3, 27.4, 22.7, 18.1, 14.1.

MS (ESI): *m/z* calcd for $C_{22}H_{37}NO_4$: 379.3; found: 380.2 $[M+H]^+$.

HRMS (ESI): *m/z* calcd for $C_{22}H_{38}NO_4^+$: 380.2795; found: 380.2793 (Δ= - 0.6 ppm).

Synthesis of (±)-*N*-(2,4,6-trimethoxyphenyl)dodecanamide [(±)-184]

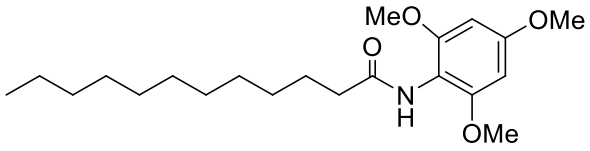

(±)-**184**

1,1'-Carbonyldiimidazole (121 mg, 0.748 mmol) was added at 0 °C to a suspension of lauric acid (**191**) (100 mg, 0.499 mmol) in dry THF (2.0 mL) and the reaction mixture was stirred at room temperature for 1 h. A solution of **189** (137 mg, 0.748 mmol) in dry THF (1.0 mL) was added and the reaction mixture was stirred at 45 °C for 4 h. Et_2O was added and washed with water. The organic phase was dried over anhydrous Na_2SO_4, filtered and the solvent was removed under reduced pressure. The crude product was purified by column chromatography on silica gel (*n*-hexane/EtOAc, 2:1 to 3:7) obtaining (±)-*N*-(2,4,6-trimethoxyphenyl)dodecanamide [(±)-**184**] as a white solid (160 mg, 88% yield).

R_f= 0.28 (*n*-hexane/EtOAc, 1:1).

^{1}H-NMR (400 MHz, $CDCl_3$, mixture of conformers): δ= 6.43 (bs, 1H), 6.13 (s, 2H), 3.78 (s, 9H), 2.41-2.30 (m, 2H), 1.78-1.66 (m, 2H), 1.45-1.14 (m, 16H), 0.87 (m, 3H).

^{13}C-NMR (100 MHz, $CDCl_3$): δ= 172.3, 159.8, 156.4, 107.7, 91.1, 56.0, 55.5, 36.8, 31.9, 29.7, 29.6, 29.6, 29.4, 29.3, 29.2, 25.9, 22.7, 14.1.

MS (ESI): *m/z* calcd for $C_{21}H_{35}NO_4$: 365.3; found: 366.3 $[M+H]^+$.

HRMS (ESI): *m/z* calcd for $C_{21}H_{36}NO_4^+$: 366.2639; found: 366.2638 (Δ= - 0.2 ppm).

Synthesis of (±)-ethyl 2,2-difluoro-3-hydroxydodecanoate [(±)-194]

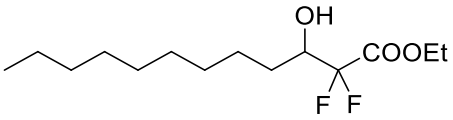

(±)-**194**

TMSCl (113 µL, 0.891 mmol) was added to a suspension of zinc dust (583 mg, 8.91 mmol) in dry THF (10 mL) and the mixture was gently heated for 5 min. After additional 15 min, decyl aldehyde (**192**) (500 µL, 2.65 mmol) and ethyl bromodifluoroacetate (**193**) (680 µL, 5.30 mmol) were added. The reaction mixture was vigorously stirred at room temperature for 3 h, then it was quenched with sat. aq. NH_4Cl. EtOAc was added, the phases were separated and the aqueous phase was extracted with ethyl acetate. The pooled organic extracts were washed with brine, dried over anhydrous Na_2SO_4, filtered and the solvent was removed under reduced pressure. The crude product was purified by column chromatography on silica gel (*n*-hexane/EtOAc, 10:1) obtaining (±)-ethyl 2,2-difluoro-3-hydroxydodecanoate [(±)-**194**] as a colourless oil (734 mg, 99% yield).

R_f= 0.50 (*n*-hexane/EtOAc, 5:1).

^{1}H-NMR (400 MHz, $CDCl_3$): δ= 4.37 (q, *J*= 7.7 Hz, 2H), 4.08-3.97 (m, 1H), 2.13 (d, *J*= 7.1 Hz, 1H), 1.72-1.49 (m, 2H), 1.36 (t, *J*= 7.7 Hz, 3H), 1.40-1.25 (m, 14H), 0.88 (m, 3H).

These NMR data are in keeping with the literature. [61]

Synthesis of (±)-ethyl 3-(1*H*-imidazole-1-carbonothioyloxy)-2,2-difluorododecanoate [(±)-195]

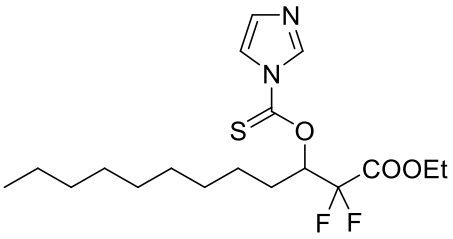

(±)-**195**

DMAP (19 mg, 0.159 mmol) and 1,1'-thiocarbonyldiimidazole (453 mg, 2.54 mmol) were added at 0 °C to a solution of (±)-**194** (446 mg, 1.59 mmol) in dry DCM (7.0 mL). The reaction mixture was stirred at room temperature for 1 h. The solvent was removed under reduced pressure and the crude product was purified by column chromatography on silica gel (*n*-hexane/EtOAc, 5:1) obtaining (±)-ethyl 3-(1*H*-imidazole-1-carbonothioyloxy)-2,2-difluorododecanoate [(±)-**195**] as a colourless oil (572 mg, 92% yield).

R_f= 0.25 (*n*-hexane/EtOAc, 5:1).

^{1}H-NMR (400 MHz, $CDCl_3$): δ= 8.31 (1H, m), 7.60 (1H, m), 7.04 (m, 1H), 6.13 (m, 1H), 4.28 (q, *J*= 7.1 Hz, 2H), 1.93 (m, 2H), 1.49-1.18 (m, 17H), 0.85 (m, 3H).

^{13}C-NMR (100 MHz, $CDCl_3$): δ= 183.1, 162.1 (t, J_{C-F}= 31.3 Hz), 137.1, 131.2, 118.1, 112.6 (dd, J_{C-F}= 253.7, 257.5 Hz), 79.4 (dd, J_{C-F}= 25.2, 30.0 Hz), 63.6, 31.8, 29.4, 29.2, 29.2, 27.5, 24.6, 22.6, 14.0, 13.8.

^{19}F-NMR (376.45 MHz, $CDCl_3$): δ= - 113.1 (dd, *J*= 7.9, 266.2 Hz, 1F), - 117.4 (dd, *J*= 13.7, 266.2 Hz, 1F).

^{19}F-CPD-NMR (376.45 MHz, $CDCl_3$): δ= - 113.1 (d, *J*= 266.2 Hz, 1F), - 117.4 (d, *J*= 266.2 Hz, 1F).

Synthesis of ethyl 2,2-difluorododecanoate (196)

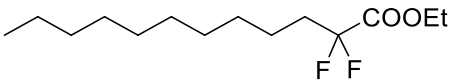

196

(±)-**195** (685 mg, 1.75 mmol) in dry toluene (5.0 mL) was added dropwise to a refluxing solution of tributyltin hydride (941 µL, 3.50 mmol) in toluene (18 mL). The reaction mixture was stirred under reflux for 30 min, then the solvent was removed under reduced pressure. The crude product was purified by column chromatography on silica gel (*n*-hexane, 100% to *n*-hexane/EtOAc, 20:1) obtaining ethyl 2,2-difluorododecanoate (**196**) as a colourless oil (430 mg, 93% yield).

R_f= 0.25 (*n*-hexane/EtOAc, 20:1).

^{1}H-NMR (400 MHz, $CDCl_3$): δ= 4.32 (q, *J*= 7.2 Hz, 2H), 2.04 (m, 2H), 1.51-1.40 (m, 2H), 1.39-1.19 (m, 17H), 0.88 (m, 3H).

^{13}C-NMR (100 MHz, $CDCl_3$): δ = 164.4 (t, $J_{C\text{-}F}$= 32.9 Hz), 116.4 (t, $J_{C\text{-}F}$= 248.3 Hz), 62.6, 34.5 (t, $J_{C\text{-}F}$= 23.0 Hz), 31.9, 29.5, 29.4, 29.3, 29.2, 29.0, 22.6, 21.4 (t, $J_{C\text{-}F}$= 4.3 Hz), 14.0, 13.9.

^{19}F-NMR (376.45 MHz, $CDCl_3$): δ = - 105.9 (t, $J_{F\text{-}H}$= 16.8 Hz, 2F).

^{19}F-CPD-NMR (376.45 MHz, $CDCl_3$): δ = - 105.9 (s, 2F).

MS (ESI): *m/*z calcd for $C_{14}H_{26}F_2O_2$: 264.2; found: 287.1 $[M+Na]^+$.

Synthesis of 2,2-difluoro-*N*-(2,4,6-trimethoxyphenyl)dodecanamide (185)

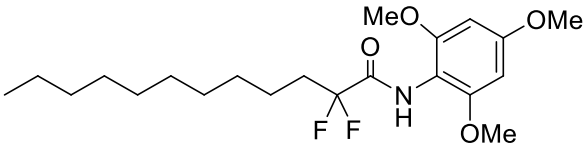

185

LiHMDS (568 µL, 1.0 M in THF) was added at 0 °C to a solution of **196** (75 mg, 0.284 mmol) and **189** (78 mg, 0.426 mmol) in dry THF (2.6 mL). The reaction mixture was stirred at room temperature for 1 h and then quenched at 0 °C with sat. aq. NH_4Cl. EtOAc was added and the phases were separated. The organic phase was washed with 1 M aq. HCl, 5% aq. $NaHCO_3$, dried over anhydrous Na_2SO_4, filtered and the solvent was removed under vacuum. The crude product was purified by column chromatography on silica gel (*n*-hexane/EtOAc, 10:1) obtaining 2,2-difluoro-*N*-(2,4,6-trimethoxyphenyl)dodecanamide (**185**) as a brown solid (92 mg, 81% yield) which recrystallizes as brown needles from *n*-hexane (m.p.= 63.3-63.9 °C).

R_f= 0.27 (*n*-hexane/EtOAc, 3:1).

^{1}H-NMR (400 MHz, $CDCl_3$): δ= 7.27 (bs, 1H), 6.16 (s, 2H), 3.81 (s, 3H), 3.81 (s, 6H), 2.23-2.08 (m, 2H), 1.60-1.49 (m, 2H), 1.41-1.20 (m, 14H), 0.88 (m, 3H).

^{13}C-NMR (100 MHz, $CDCl_3$): δ = 163.0 (t, J_{C-F}= 28.3 Hz), 160.5, 156.2, 118.9 (t, J_{C-F}= 251.0 Hz), 105.2, 91.0, 55.9, 55.4, 34.4 (t, J_{C-F}= 23.0 Hz), 31.9, 29.6, 29.4, 29.4, 29.3, 29.2, 22.7, 21.7 (t, J_{C-F}= 4.2 Hz), 14.1.

^{19}F-NMR (376.45 MHz, $CDCl_3$): δ= - 105.6 (dt, J_{F-H} = 2.4, 17.0 Hz, 2F).

^{19}F-CPD-NMR (376.45 MHz, $CDCl_3$): δ= - 105.6 (s, 2F).

MS (ESI): *m/*z calcd for $C_{21}H_{33}F_2NO_4$: 401.2; found: 402.2 $[M+H]^+$.

HRMS (ESI): *m/z* calcd for $C_{21}H_{34}F_2NO_4^+$: 402.2450; found: 402.4422 (Δ= - 2.1 ppm).

General procedure for the alkylation of cycloalkane esters 200-202

The desired cycloalkane ester (1.0 eq.) was added at -78 °C to a freshly prepared solution of LDA [*n*BuLi (1.3 eq.) was added to diisopropylamine (1.5 eq.) in dry THF (1.0 mL/mmol of cycloalkane ester) at -78 °C, then the reaction mixture was stirred at 0 °C for 15 min]. The reaction mixture was stirred at -78 °C for 1 h, then 1-bromodecane (**203**) (3.0 eq.) was added. After another hour at -78 °C, the solution was allowed to warm to room temperature and was stirred overnight. The reaction mixture was quenched with water and extracted twice with Et_2O. The pooled organic extracts were dried over anhydrous Na_2SO_4, filtered and the solvent was removed under reduced pressure. The crude product was purified by column chromatography on silica gel (*n*-hexane, 100% to *n*-hexane/EtOAc, 20:1) obtaining the desired product.

Synthesis of ethyl 1-decylcyclobutanecarboxylate (204)

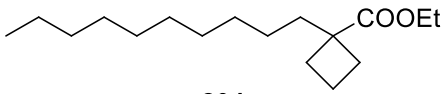

204

The product was synthesized following the general procedure for the alkylation of cycloalkane esters **200**-**202**, and it was obtained as colourless oil (43% yield).

R_f= 0.39 (*n*-hexane/EtOAc, 20:1).

^{1}H-NMR (400 MHz, $CDCl_3$): δ= 4.14 (q, *J*= 7.1 Hz, 2H), 2.43-2.34 (m, 2H), 1.91-1.82 (m, 4H), 1.77-1.70 (m, 2H), 1.33-1.21 (m, 17H), 1.20-1.11 (m, 2H), 0.88 (m, 3H).

^{13}C-NMR (100 MHz, $CDCl_3$): δ= 177.4, 60.1, 47.7, 38.1, 31.9, 30.0, 29.9, 29.6, 29.6, 29.5, 29.3, 24.8, 22.7, 15.6, 14.3, 14.1.

Synthesis of methyl 1-decylcyclopentanecarboxylate (205)

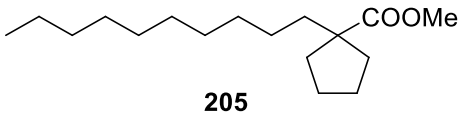

205

The product was synthesized following the general procedure for the alkylation of cycloalkane esters **200**-**202**, and it was obtained as a yellow oil (63% yield).

R_f= 0.38 (*n*-hexane/EtOAc, 20:1).

^{1}H-NMR (400 MHz, $CDCl_3$): δ= 3.66 (s, 3H), 2.15-2.05 (m, 2H), 1.64-1.54 (m, 6H), 1.50-1.41 (m, 2H), 1.33-1.12 (m, 16H), 0.88 (m, 3H).

^{13}C-NMR (100 MHz, $CDCl_3$): δ= 178.5, 54.2, 51.6, 39.4, 36.0, 31.9, 30.1, 29.6, 29.6, 29.5, 29.3, 26.0, 24.9, 22.7, 14.1.

Synthesis of methyl 1-decylcyclohexanecarboxylate(206)

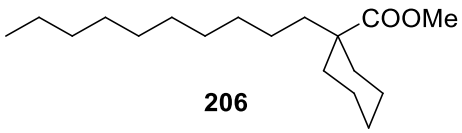

206

The product was synthesized following the general procedure for the alkylation of cycloalkane esters **200**-**202**, and it was obtained as a yellow oil (48% yield).

R_f= 0.42 (*n*-hexane/EtOAc, 20:1).

^{1}H-NMR (400 MHz, $CDCl_3$): δ= 3.66 (s, 3H), 2.09-2.00 (m, 2H), 1.60-1.50 (m, 3H), 1.48-1.41 (m, 2H), 1.36-1.11 (m, 21H), 0.87 (m, 3H).

^{13}C-NMR (100 MHz, $CDCl_3$): δ= 177.5, 51.3, 47.1, 40.7, 34.2, 31.9, 30.1, 29.6, 29.5, 29.3, 26.0, 24.0, 23.3, 22.7, 14.1.

General procedure for the synthesis of compounds 197-199

LiHMDS (1.0 M in THF, 2.0 eq.) was added at 0 °C to a solution of compound **204**, **205** or **206** (1.0 eq.) and **189** (1.5 eq.) in dry THF (8.0 mL/mmol of ester). The reaction mixture was stirred at room temperature overnight, then it was quenched at 0 °C with sat. aq. NH_4Cl. EtOAc was added and the phases were separated. The organic phase was washed with 1 M aq. HCl, 5% aq. $NaHCO_3$, dried over anhydrous Na_2SO_4, filtered and the solvent was removed under vacuum. The crude product was purified by column chromatography on silica gel (*n*-hexane/EtOAc) obtaining the desired product.

Synthesis of 1-decyl-*N*-(2,4,6-trimethoxyphenyl)cyclobutanecarboxamide (197)

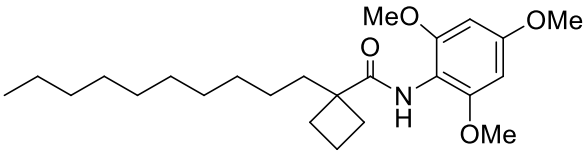

197

The product was synthesized following the general procedure for the synthesis of compounds **197**-**199**, and it was obtained as an orange solid (56% yield) which recrystallizes as orange needles from *n*-hexane (m.p.= 94.3-95.5 °C).

R_f= 0.44 (*n*-hexane/EtOAc, 1:1).

^{1}H-NMR (400 MHz, $CDCl_3$): δ= 6.36 (bs, 1H), 6.14 (s, 2H), 3.79 (s, 3H), 3.78 (s, 6H), 2.55-2.46 (m, 2H), 1.97-1.78 (m, 6H), 1.43-1.20 (m, 16H), 0.87 (m, 3H).

^{13}C-NMR (100 MHz, $CDCl_3$): δ= 176.3, 159.6, 156.3, 107.7, 91.1, 55.9, 55.5, 48.8, 39.6, 31.9, 30.2, 30.2, 29.7, 29.7, 29.4, 24.6, 22.7, 15.3, 14.1.

MS (ESI): *m/*z calcd for $C_{24}H_{39}NO_4$: 405.3; found: 428 $[M+Na]^+$.

HRMS (ESI): *m/z* calcd for $C_{24}H_{40}NO_4^+$: 406.2952; found: 406.2944 (Δ= - 1.9 ppm).

Synthesis of 1-decyl-*N*-(2,4,6-trimethoxyphenyl)cyclopentanecarboxamide (198)

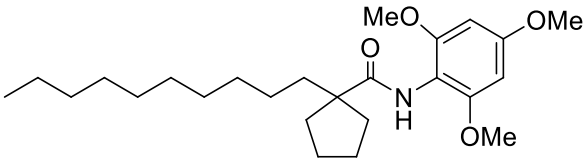

198

The product was synthesized following the general procedure for the synthesis of compounds **197**-**199**, and it was obtained as a purple solid (55% yield) which recrystallizes as colourless needles from *n*-hexane (m.p.= 77.4-78.6 °C).

R_f= 0.29 (*n*-hexane/EtOAc, 2:1).

^{1}H-NMR (400 MHz, $CDCl_3$): δ= 6.53 (bs, 1H), 6.13 (s, 2H), 3.79 (s, 3H), 3.77 (s, 6H), 2.26-2.17 (m, 2H), 1.76-1.61 (m, 2H), 1.58-1.48 (m, 2H), 1.47-1.37 (m, 2H), 1.34-1.19 (m, 14H), 0.87 (m, 3H).

^{13}C-NMR (100 MHz, $CDCl_3$): δ= 176.3, 159.6, 156.3, 108.0, 91.0, 55.9, 55.5, 55.1, 40.6, 36.2, 31.9, 30.4, 29.7, 29.7, 29.7, 29.3, 25.7, 24.6, 22.7, 14.1.

MS (ESI): *m/z* calcd for $C_{25}H_{41}NO_4$: 419.3; found: 442 $[M+Na]^+$.

HRMS (ESI): *m/z* calcd for $C_{25}H_{42}NO_4^+$: 420.3108; found: 420.3100 (Δ= - 2.0 ppm).

Synthesis of 1-decyl-*N*-(2,4,6-trimethoxyphenyl)cyclohexanecarboxamide (199)

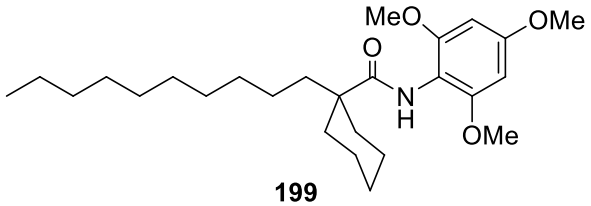

199

The product was synthesized following the general procedure for the synthesis of compounds **197**-**199**, and it was obtained as an orange solid (57% yield) which recrystallizes as colourless scales from *n*-hexane (m.p.= 74.8-76.0 °C).

R_f= 0.31 (*n*-hexane/EtOAc, 2:1).

^{1}H-NMR (400 MHz, $CDCl_3$): δ= 6.63 (bs, 1H), 6.13 (s, 2H), 3.78 (s, 3H), 3.76 (s, 6H), 2.14-2.06 (m, 2H), 1.64-1.54 (m, 5H), 1.54-1.47 (m, 2H), 1.45-1.35 (m, 2H), 1.35-1.19 (m, 17H), 0.87 (m, 3H).

^{13}C-NMR (100 MHz, $CDCl_3$): δ= 175.1, 159.6, 156.3, 108.0, 91.0, 55.9, 55.5, 46.9, 41.9, 35.0, 31.9, 30.5, 29.8, 29.7, 29.7, 29.3, 26.4, 23.8, 23.0, 22.7, 14.1.

MS (ESI): *m/*z calcd for $C_{26}H_{43}NO_4$: 433.3; found: 456 $[M+Na]^+$.

HRMS (ESI): *m/z* calcd for $C_{26}H_{44}NO_4^+$: 434.3265; found: 434.3258 (Δ= - 1.6 ppm).

Synthesis of methyl 2,2-dimethyldodecanoate (210)

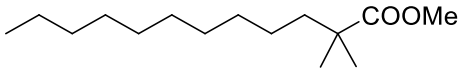

210

Methyl isobutyrate (**209**) (236 µL, 2.06 mmol) was added at -78 °C to a freshly prepared solution of LDA [*n*BuLi (1.07 µL, 2.5 M in hexanes, 2.68 mmol) was added to diisopropylamine (433 µL, 3.09 mmol) in 3 mL of dry THF at -78 °C and the reaction mixture was stirred at 0 °C for 15 min]. The reaction mixture was stirred for 1 h, then 1-bromodecane (**203**) (1.28 µL, 6.18 mmol) was added. After another hour at -78 °C, the reaction mixture was allowed to warm to room temperatur and stirred overnight. The reaction was quenched with water and extracted twice with Et_2O. The pooled organic extracts were dried over anhydrous Na_2SO_4, filtered and the solvent was removed under reduced pressure. The crude product was purified by column chromatography on silica gel (*n*-hexane, 100% to *n*-hexane/EtOAc, 10:1) obtaining methyl 2,2-dimethyldodecanoate (**210**) as a colourless oil (500 mg, quantitative yield).

R_f= 0.32 (*n*-hexane/EtOAc, 20:1).

^{1}H-NMR (400 MHz, $CDCl_3$): δ= 3.65 (s, 3H), 1.52-1.46 (m, 2H), 1.33-1.17 (m, 16H), 1.15 (s, 6H), 0.87 (m, 3H).

^{13}C-NMR (100 MHz, $CDCl_3$): δ= 178.6, 51.6, 42.3, 40.8, 31.9, 30.1, 29.6, 29.5, 29.3, 25.2, 24.9, 22.7, 14.1.

MS (ESI): *m/z* calcd for $C_{15}H_{30}O_2$: 242.2; found: 265.2 $[M+Na]^+$.

General procedure for the synthesis of 182 analogues

LiHMDS 1.0 M in THF (2.0 eq.) was added at 0 °C to a solution of **210** (1.0 eq.) and desired aniline (1.5 eq.) in dry THF (12 mL/mmol of ester). The reaction mixture was stirred at room temperature until consumption of **210**, then it was quenched at 0 °C with sat. aq. NH_4Cl. EtOAc was added and the phases were separated. The organic phase was washed with 1 M aq. HCl, 5% aq. $NaHCO_3$, dried over Na_2SO_4, filtered and the solvent was removed under vacuum. The crude product was purified by column chromatography on silica gel (*n*-hexane/EtOAc, 10:1) obtaining the desired product.

Synthesis of *N*-(4-chloro-3-fluorophenyl)-2,2-dimethyldodecanamide (211)

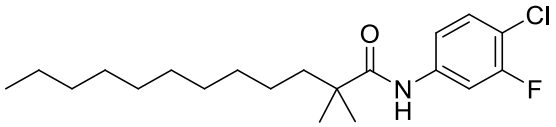

211

The product was synthesized following the general procedure for the synthesis of **182** analogues, and it was obtained as a colourless solid (80% yield) (m.p.= 73.3-73.7 °C).

R_f= 0.32 (*n*-hexane/EtOAc, 10:1).

^{1}H-NMR (400 MHz, $CDCl_3$): δ= 7.64 (dd, *J*= 2.0, 11.1 Hz, 1H), 7.38 (bs, 1H), 7.27 (t, *J*= 8.3 Hz, 1H), 7.09 (ddd, *J*= 1.0, 2.2, 8.7 Hz, 1H), 1.61-1.53 (m, 2H), 1.32-1.18 (m, 22H), 0.86 (m, 3H).

^{13}C-NMR ($CDCl_3$): δ= 176.3, 158.0 (d, J_{C-F}= 245.8 Hz), 138.0 (d, J_{C-F}= 9.9 Hz), 130.3, 115.9 (m), 115.5 (d, J_{C-F}= 18.1 Hz), 108.7 (d, J_{C-F}= 25.9 Hz), 43.2, 41.4, 31.9, 30.1, 29.6, 29.6, 29.5, 29.3, 25.4, 24.8, 22.7, 14.1.

^{19}F-NMR (376.45 MHz, $CDCl_3$): δ= -113.4 (m, 1F).

MS (ESI): *m/*z calcd for $C_{20}H_{31}{}^{35}ClFNO$: 355.2; found: 356.2$[M+H]^+$.

HRMS (ESI): *m/z* calcd for $C_{20}H_{32}{}^{35}ClFNO^+$: 356.2151; found: 356.2151 (Δ= 0.0 ppm).

Synthesis of 2,2-dimethyl *N*-phenyldodecanamide (212)

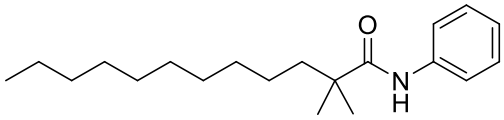

212

The product was synthesized following the general procedure for the synthesis of **182** analogues, and it was obtained as a colourless solid (62% yield) (m.p.= 58.7-59.3 °C);

R_f= 0.39 (*n*-hexane/EtOAc, 10:1).

^{1}H-NMR (400 MHz, $CDCl_3$): δ= 7.52 (m, 2H), 7.36 (bs, 1H), 7.30 (m, 2H), 7.09 (m, 1H), 1.62-1.55 (m, 2H), 1.33-1.21 (m, 22H), 0.88 (m, 3H).

^{13}C-NMR (100 MHz, $CDCl_3$): δ= 176.1, 138.0, 128.9, 124.1, 120.1, 43.0, 41.6, 31.9, 30.2, 29.6, 29.6, 29.5, 29.3, 25.5, 24.9, 22.7, 14.1.

MS (ESI): *m/*z calcd for $C_{20}H_{33}NO$: 303.3; found: 304.2 [M+H].

HRMS (ESI): *m/z* calcd for $C_{20}H_{34}NO^+$: 304.2635; found: 304.2629 (Δ= - 1.9 ppm).

Synthesis of *N*-(4-methoxyphenyl)-2,2-dimethyldodecanamide (213)

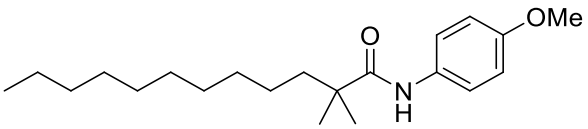

213

The product was synthesized following the general procedure for the synthesis of **182** analogues, and it was obtained as an orange solid (98% yield) (m.p.= 79.5-80.7 °C).

R_f= 0.30 (*n*-hexane-EtOAc, 10:1).

^{1}H-NMR (400 MHz, $CDCl_3$): δ= 7.41 (m, 2H), 7.20 (bs, 1H), 6.85 (m, 2H), 3.78 (s, 3H), 1.61-1.53 (m, 2H), 1.32-1.19 (m, 22H), 0.87 (m, 3H).

^{13}C-NMR ($CDCl_3$): δ= 175.9, 156.4, 131.1, 121.9, 114.1, 55.5, 42.8, 41.6, 31.9, 30.2, 29.6, 29.6, 29.5, 29.3, 25.5, 24.9, 22.7, 14.1.

MS (ESI): *m/*z calcd for $C_{21}H_{35}NO_2$: 333.3; found: 334.3 [M+H].

HRMS (ESI): *m/z* calcd for $C_{21}H_{36}N_2O^+$: 334.2741; found: 334.2737 (Δ= - 1.1 ppm).

General procedure for the synthesis of 185 analogues

LiHMDS (568 µL, 1.0 M in THF) was added at 0 °C to a solution of **196** (1.0 eq) and desired aniline (1.5 eq.) in dry THF (10 mL/mmol of ester). The reaction mixture was stirred at room temperature for 1 h and then quenched at 0 °C with sat. aq. NH_4Cl. EtOAc was added and the phases were separated separated. The organic phase was washed with 1 M aq. HCl, 5% aq. $NaHCO_3$, dried over Na_2SO_4, filtered and the solvent was removed under vacuum. The crude product was purified by column chromatography on silica gel (*n*-hexane/EtOAc, 10:1) obtaining the desired product.

Synthesis of *N*-(4-chloro-3-fluorophenyl)-2,2-difluorododecanamide (214)

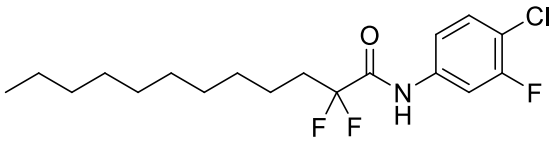

214

The product was synthesized following the general procedure for the synthesis of **185** analogues, and it was obtained as a white solid (85% yield).

R_f= 0.36 (*n*-hexane/EtOAc, 10:1).

^{1}H-NMR (400 MHz, $CDCl_3$): δ= 8.03 (bs, 1H), 7.66 (dd, *J*= 2.5, 10.6 Hz, 1H), 7.37 (dd, *J*= 8.1, 8.6 Hz, 1H), 7.20 (ddd, *J*= 1.2, 2.5, 8.6 Hz, 1H), 2.24-2.08 (m, 2H), 1.54-1.44 (m, 2H), 1.40-1.19 (m, 14H), 0.88 (m, 3H).

^{13}C-NMR (100 MHz, $CDCl_3$): δ= 162.4 (t, $J_{C\text{-}F}$= 29.2 Hz), 158.1 (d, $J_{C\text{-}F}$= 247.0 Hz), 135.9 (d, $J_{C\text{-}F}$= 9.6 Hz), 130.8, 118.3 (t, $J_{C\text{-}F}$= 251.8 Hz), 117.4 (d, $J_{C\text{-}F}$= 17.8 Hz), 116.2 (d, $J_{C\text{-}F}$= 3.6 Hz), 109.0 (d, $J_{C\text{-}F}$= 26.1 Hz), 33.7 (t, $J_{C\text{-}F}$= 22.7 Hz), 31.9, 29.5, 29.4, 29.3, 29.2, 29.1, 22.7, 21.5 (t, $J_{C\text{-}F}$= 4.1 Hz), 14.1.

^{19}F-NMR (376.45 MHz, $CDCl_3$): δ= - 105.4 (dt, $J_{F\text{-}H}$= 2.9, 17.5 Hz, 2F), - 112.3 (m, 1F).

^{19}F-CPD-NMR (376.45 MHz, $CDCl_3$): δ= - 112.3 (s, 1F), - 105.4 (s, 2F).

MS (ESI): *m/z* calcd for $C_{18}H_{25}{}^{35}ClF_3NO$: 363.2; found: 386.1 $[M+Na]^+$.

HRMS (ESI): *m/z* calcd for $C_{18}H_{26}{}^{35}ClF_3NO^+$: 364.1650; found: 364.1653 (Δ= 1.0 ppm).

Synthesis of *N*-(4-chlorophenyl)-2,2-difluorododecanamide (215)

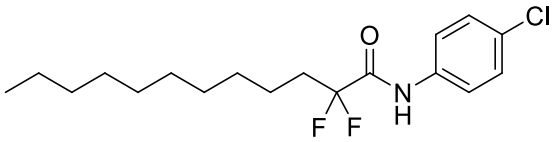

215

The product was synthesized following the general procedure for the synthesis of **185** analogues, and it was obtained as a yellow solid (85% yield).

R_f= 0.36 (*n*-hexane/EtOAc, 10:1).

^{1}H-NMR (400 MHz, $CDCl_3$): δ= 8.11 (bs, 1H), 7.53 (m, 2H), 7.31 (m, 2H), 2.23-2.07 (m, 2H), 1.54-1.43 (m, 2H), 1.39-1.19 (m, 14H), 0.88 (m, 3H).

^{13}C-NMR (100 MHz, $CDCl_3$): δ= 162.4 (t, J_{C-F}= 29.0 Hz), 134.7, 130.7, 129.2, 121.6, 118.4 (t, J_{C-F}= 251.7 Hz), 33.8 (t, J_{C-F}= 22.9 Hz), 31.9, 29.5, 29.4, 29.3, 29.2, 29.1, 22.7, 21.5 (t, J_{C-F}= 4.1 Hz), 14.1.

^{19}F-NMR (376.45 MHz, $CDCl_3$): δ= - 105.4 (dt, J_{F-H}= 3.1, 17.5 Hz, 2F).

^{19}F-CPD-NMR (376.45 MHz, $CDCl_3$): δ= - 105.4 (s, 2F).

MS (ESI): *m/z* calcd for $C_{18}H_{26}{}^{35}ClF_2NO$: 345.2; found: 368.1 $[M+Na]^+$.

HRMS (ESI): *m/z* calcd for $C_{18}H_{27}{}^{35}ClF_2NO^+$: 346.1744; found: 346.1743 (Δ= - 0.2 ppm).

Synthesis of 2,2-difluoro-*N*-phenyldodecanamide (216)

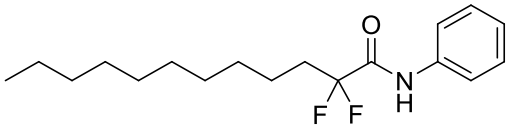

216

The product was synthesized following the general procedure for the synthesis of **185** analogues, and it was obtained as a white solid (87% yield) (m.p.= 71.8-72.4 °C).

R_f= 0.41 (*n*-hexane/EtOAc, 10:1).

^{1}H-NMR (400 MHz, $CDCl_3$): δ= 7.94 (bs, 1H), 7.58 (m, 2H), 7.38 (m, 2H), 7.20 (m, 1H), 2.26-2.10 (m, 2H), 1.56-1.45 (m, 2H), 1.41-1.19 (m, 14H), 0.88 (m, 3H).

^{13}C-NMR (100 MHz, $CDCl_3$): δ= 162.3 (t, $J_{C\text{-}F}$= 28.6 Hz), 136.1, 129.2, 125.5, 120.3, 118.5 (t, $J_{C\text{-}F}$= 251.7 Hz), 33.8 (t, $J_{C\text{-}F}$= 23.0 Hz), 31.9, 29.5, 29.4, 29.3, 29.3, 29.2, 22.7, 21.6 (t, $J_{C\text{-}F}$= 4.2 Hz), 14.1.

^{19}F-NMR (376.45 MHz, $CDCl_3$): δ= - 105.5 (dt, $J_{F\text{-}H}$= 3.1, 17.4 Hz, 2F).

^{19}F-CPD-NMR (376.45 MHz, $CDCl_3$): δ= - 105.5 (s, 2F).

MS (ESI): *m/*z calcd for $C_{18}H_{27}F_2NO$: 311.2; found: 334.1 $[M+Na]^+$.

HRMS (ESI): *m/z* calcd for $C_{18}H_{28}F_2NO^+$: 312.2133; found: 312.2134 (Δ= 0.2 ppm).

Synthesis of *N*-(2,6-diisopropylphenyl)-2,2-difluorododecanamide (217)

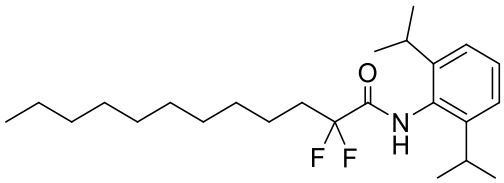

217

The product was synthesized following the general procedure for the synthesis of **185** analogues, and it was obtained as an orange solid (84% yield) (m.p.= 93.9-95.5 °C).

R_f= 0.45 (*n*-hexane/EtOAc, 10:1).

^{1}H-NMR (400 MHz, $CDCl_3$): δ= 7.60 (bs, 1H), 7.34 (t, *J*= 7.7 Hz, 1H), 7.21 (d, *J*= 7.7 Hz, 2H), 3.03 (sep, *J*= 6.8 Hz, 2H), 2.29-2.14 (m, 2H), 1.63-1.51 (m, 2H), 1.47-1.16 (m, 26H), 0.91 (m, 3H).

^{13}C-NMR (100 MHz, $CDCl_3$): δ= 163.8 (t, J_{C-F}= 28.6 Hz), 146.1, 129.0, 129.0, 123.7, 119.0 (t, J_{C-F}= 251.1 Hz), 33.8 (t, J_{C-F}= 22.8 Hz), 31.9, 29.6, 29.4, 29.4, 29.3, 29.2, 28.8, 23.5, 22.7, 21.6 (t, J_{C-F}= 4.1 Hz), 14.1.

^{19}F-NMR (376.45 MHz, $CDCl_3$): δ= - 104.4 (dt, J_{F-H}= 2.2, 17.3 Hz, 2F).

^{19}F-NMR (376.45 MHz, $CDCl_3$): δ= - 104.4 (s, 2F).

MS (ESI): *m/z* calcd for $C_{24}H_{39}F_2NO$: 395.3; found: 396.2 $[M+H]^+$.

HRMS (ESI): *m/z* calcd for $C_{24}H_{40}F_2NO^+$: 396.3072; found: 396.3070 (Δ= - 0.6 ppm).

Synthesis of 2,2-difluoro-*N*-(4-methoxyphenyl)dodecanamide(218)

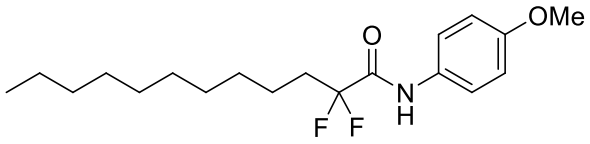

218

The product was synthesized following the general procedure for the synthesis of **185** analogues, and it was obtained as a white solid (75% yield) (m.p.= 100.4-101.1 °C).

R_f= 0.26 (*n*-hexane/EtOAc, 10:1).

^{1}H-NMR (100 MHz, $CDCl_3$): δ= 7.97 (bs, 1H), 7.48 (m, 2H), 6.88 (m, 2H), 3.79 (s, 3H), 2.24-2.08 (m, 2H), 1.55-1.44 (m, 2H), 1.40-1.19 (m, 14H), 0.88 (m, 3H).

^{13}C-NMR (100 MHz, $CDCl_3$): δ= 162.1 (t, J_{C-F}= 28.5 Hz), 157.2, 129.1, 122.0, 118.5 (t, J_{C-F}= 251.6 Hz), 114.3, 55.5, 33.9 (t, J_{C-F}= 23.0 Hz), 31.9, 29.5, 29.4, 29.3, 29.3, 29.1, 22.7, 21.6 (t, J_{C-F}= 4.1 Hz), 14.1.

^{19}F-NMR (376.45 MHz, $CDCl_3$): δ= - 105.6 (dt, J_{F-H}= 2.2, 17.4 Hz, 2F).

^{19}F-CPD-NMR (376.45 MHz, $CDCl_3$): δ= - 105.6 (s, 2F).

MS (ESI): *m/z* calcd for $C_{19}H_{29}F_2NO_2$: 341.2; found: 364.1 $[M+Na]^+$.

HRMS (ESI): *m/z* calcd for $C_{19}H_{30}F_2NO_2^+$: 342.2239; found: 342.2240 (Δ= 0.3 ppm).

Synthesis of 2,2-difluoro-*N*-(2-methoxyphenyl)dodecanamide (219)

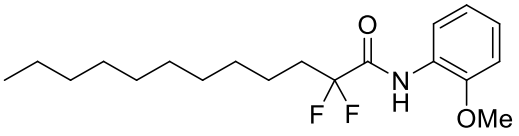

219

The product was synthesized following the general procedure for the synthesis of **185** analogues, and it was obtained as a colourless oil (81% yield).

R_f= 0.49 (*n*-hexane/EtOAc, 10:1).

^{1}H-NMR (400 MHz, $CDCl_3$): δ= 8.68 (bs, 1H), 8.38 (dd, *J*= 1.5, 8.0 Hz, 1H), 7.12 (dt, *J*= 1.5, 7.8 Hz, 1H), 6.99 (dt, *J*= 1.2, 7.8 Hz, 1H), 6.92 (dd, *J*= 1.2, 8.1 Hz, 1H), 3.91 (s, 3H), 2.26-2.10 (m, 2H), 1.57-1.46 (m, 2H), 1.41-1.19 (m, 14H), 0.89 (m, 3H).

^{13}C-NMR (100 MHz, $CDCl_3$): δ= 162.0 (t, J_{C-F}= 28.6 Hz), 148.3, 126.0, 125.1, 121.1, 119.9, 118.4 (t, J_{C-F}= 251.7 Hz), 110.1, 55.8, 33.9 (t, J_{C-F}= 23.0 Hz), 31.9, 29.5, 29.4, 29.3, 29.3, 29.2, 22.7, 21.6 (t, J_{C-F}= 4.2 Hz), 14.1.

^{19}F-NMR (376.45 MHz, $CDCl_3$): δ= - 105.7 (dt, J_{F-H}= 2.9, 17.3 Hz, 2F).

^{19}F-CPD-NMR (376.45 MHz, $CDCl_3$): δ= - 105.7 (s, 2F).

MS (ESI): *m/z* calcd for $C_{19}H_{29}F_2NO_2$: 341.2; found: 342.1 $[M+H]^+$.

HRMS (ESI): *m/z* calcd for $C_{19}H_{30}F_2NO_2^+$: 342.2239; found: 342.2238 (Δ= - 0.3 ppm).

General procedure for the synthesis of 184 analogues

Lauric acid (**191**) (300 mg, 1.50 mmol) was dissolved in dry DCM (10.0 mL) and few drops of dry DMF were added. Oxalyl chloride (3 eq.) was added at 0 °C and the reaction mixture was stirred at room temperature for 4 h, then it was concentrated under reduced pressure. The residue was dissolved in dry DCM (7.0 mL) and a solution of DMAP (0.10 eq.), TEA (2 eq.) and desired aniline (1.5 eq.) in dry DCM (3.0 mL) was slowly added at 0 °C. The reaction mixture was stirred at room temperature overnight, then it was diluted with DMC, washed with 1 M aq. HCl and sat. aq. $NaHCO_3$, dried over anhydrous Na_2SO_4 and the solvent was removed under reduced pressure. The crude product was purified by column chromatography on silica gel (*n*-hexane/EtOAc) obtaining the desired product.

Synthesis of *N*-(4-chloro-3-fluorophenyl)dodecanamide (220)

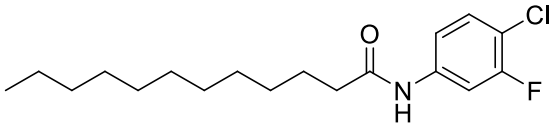

220

The product was synthesized following the general procedure for the synthesis of **184** analogues, and it was obtained as a white solid (88% yield) which recrystallizes as brown needles from *n*-hexane (m.p.= 67.5-68.4 °C).

R_f= 0.34 (*n*-hexane/EtOAc, 5:1).

^{1}H-NMR (400 MHz, $CDCl_3$): δ= 7.83 (bs, 1H), 7.61 (dd, *J* = 2.1, 11.1 Hz, 1H), 7.26 (m, 1H), 7.11 (m, 1H), 2.37 (t, *J*= 7.4 Hz, 2H), 1.70 (tt, *J*= 7.4 Hz, 2H), 1.37-1.18 (m, 16H), 0.87 (m, 3H).

^{13}C-NMR (100 MHz, $CDCl_3$): δ= 172.5, 157.9 (d, $J_{C\text{-}F}$= 245.8 Hz), 138.1 (d, $J_{C\text{-}F}$= 9.8 Hz), 130.3, 118.7 (d, $J_{C\text{-}F}$= 25.5 Hz), 116.1, 115.6 (d, $J_{C\text{-}F}$= 17.9 Hz), 37.6, 31.9, 29.6, 29.5, 29.4, 29.3, 29.3, 25.6, 22.7, 14.1.

^{19}F-NMR (376.45 MHz, $CDCl_3$): δ= - 113.4 (m, 1F).

^{19}F-CPD-NMR (376.45 MHz, $CDCl_3$): δ= - 113.4 (s, 1F).

MS (ESI): *m/z* calcd for $C_{18}H_{27}{}^{35}ClFNO$: 327.2; found: 328.2 $[M+H]^+$.

HRMS (ESI): *m/z* calcd for $C_{18}H_{28}{}^{35}ClFNO^+$: 328.1838; found: 328.1840 (Δ= 0.6 ppm).

Synthesis of *N*-(4-fluorophenyl)dodecanamide (221):

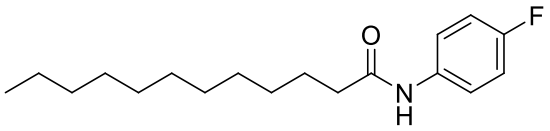

221

The product was synthesized following the general procedure for the synthesis of **184** analogues, and it was obtained as a white solid (93% yield).

^{1}H-NMR (400 MHz, $CDCl_3$): δ= 7.49 (m, 2H), 7.14 (bs, 1H), 7.03 (m, 2H), 2.36 (t, *J*= 7.5 Hz, 2H), 1.74 (tt, *J*= 7.0, 7.5 Hz, 2H), 1.44-1.23 (m, 16H), 0.90 (m, 3H).

^{13}C-NMR (100 MHz, $CDCl_3$): δ= 171.5, 159.3 (d, J_{C-F}= 243.2 Hz), 133.9 (d, J_{C-F}= 2.6 Hz), 121.7 (d, J_{C-F}= 7.9 Hz), 115.6 (d, J_{C-F}= 22.5 Hz), 37.7, 31.9, 29.6, 29.5, 29.4, 29.3, 29.3, 25.6, 22.7, 14.1.

^{19}F-NMR (376.45 MHz, $CDCl_3$): δ= - 118.2 (tt, J_{F-H}= 4.7, 8.3 Hz, 1F).

MS (ESI): *m/*z calcd for $C_{18}H_{28}FNO$: 293.2; found: 294.2 $[M+H]^+$.

Synthesis of *N*-(4-chlorophenyl)dodecanamide (222):

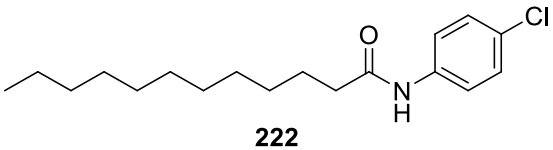

222

The product was synthesized following the general procedure for the synthesis of **184** analogues, and it was obtained as a white solid (73% yield).

^{1}H-NMR (400 MHz, $CDCl_3$): δ= 7.74-7.56 (bs, 1H), 7.49 (m, 2H), 7.27 (m, 2H), 2.35 (t, *J*= 7.5 Hz, 2H), 1.72 (tt, *J*= 6.9, 7.5 Hz, 2H), 1.42-1.21 (m, 14H), 0.90 (m, 3H).

^{13}C-NMR (100 MHz, $CDCl_3$): δ= 171.8, 136.6, 129.1, 128.9, 121.2, 37.7, 31.9, 29.6, 29.5, 29.4, 29.3, 29.3, 25.6, 22.7, 14.1.

MS (ESI): *m/*z calcd for $C_{18}H_{28}{}^{35}ClNO$: 309.2; found: 310.1 $[M+H]^+$.

Synthesis of *N*-phenyldodecanamide (223)

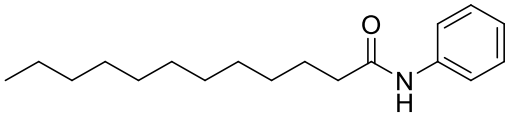

223

The product was synthesized following the general procedure for the synthesis of **184** analogues, and it was obtained as a white solid (quantitative yield) (m.p.= 81.5-82.8 °C) (lit. m.p.= 78 °C). [80]

R_f= 0.39 (*n*-hexane/EtOAc, 5:1).

^{1}H-NMR (400 MHz, $CDCl_3$): δ= 7.52 (d, *J*= 7.8 Hz, 2H), 7.47 (bs, 1H), 7.33-7.26 (m, 3H), 7.08 (t, *J*= 7.4 Hz, 1H), 2.34 (t, *J*= 7.5 Hz, 2H), 1.71 (qui, *J*= 7.5 Hz, 2H), 1.40-1.20 (m, 16H), 0.88 (m, 3H).

^{13}C-NMR (100 MHz, $CDCl_3$): δ= 171.5, 138.0, 129.0, 124.1, 119.8, 37.8, 31.9, 29.6, 29.5, 29.4, 29.3, 29.3, 25.7, 22.7, 14.1.

MS (ESI): *m/z* calcd for $C_{18}H_{29}NO$: 275.2; found: 276.2 $[M+H]^+$ (100).

HRMS (ESI): *m/z* calcd for $C_{18}H_{30}NO^+$: 276.2322; found: 276.2322 (Δ= 0.0 ppm).

Synthesis of *N*-(4-methoxyphenyl)dodecanamide (224)

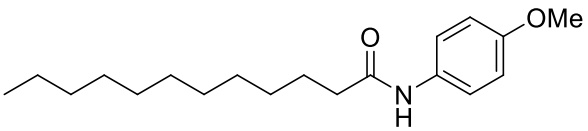

224

The product was synthesized following the general procedure for the synthesis of **184** analogues, and it was obtained as a white solid (quantitative yield).

R_f= 0.30 (*n*-hexane/EtOAc, 8:2).

^{1}H-NMR (400 MHz, $CDCl_3$): δ= 7.40 (m, 2H), 7.18 (bs, 1H), 6.84 (m, 2H), 3.78 (s, 3H), 2.32 (t, *J*= 7.5 Hz, 2H), 1.71 (qui, *J*= 7.5 Hz, 2H), 1.41-1.18 (m, 16H), 0.88 (m, 3H).

^{13}C-NMR (100 MHz, $CDCl_3$): δ= 171.3, 156.3, 131.1, 121.7, 114.1, 55.5, 37.7, 29.6, 29.5, 29.4, 29.3, 29.3, 25.7, 22.7, 14.1.

MS (ESI): *m/z* calcd for $C_{19}H_{31}NO_2$: 305.2; found: 306.2 $[M+H]^+$.

HRMS (ESI): *m/z* calcd for $C_{19}H_{32}NO_2^+$: 306.2428; found: 306.2427 (Δ= - 0.2 ppm).

Synthesis of *N*-(2-methoxyphenyl)dodecanamide (225):

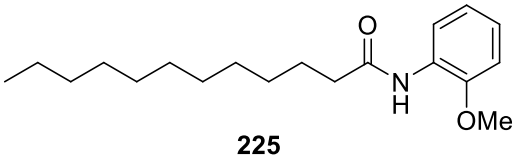

225

The product was synthesized following the general procedure for the synthesis of **184** analogues, and it was obtained as a white solid (87% yield).

^{1}H-NMR (400 MHz, $CDCl_3$): δ= 8.42 (dd, *J*= 1.1, 7.9 Hz, 1H), 7.87 (bs, 1H), 7.05 (m, 1H), 6.98 (m, 1H), 6.89 (dd, *J*= 1.4, 8.0 Hz, 1H), 3.91 (s, 3H), 2.41 (t, *J*= 7.6 Hz, 2H), 1.72 (tt, *J*= 7.0, 7.6 Hz, 2H), 1.45-1.25 (m, 14H), 0.90 (m, 3H).

^{13}C-NMR (100 MHz, $CDCl_3$): δ= 171.3, 147.6, 127.8, 123.4, 121.1, 119.7, 109.8, 55.7, 38.1, 31.9, 29.6, 29.6, 29.5, 29.4, 29.3, 29.3, 25.7, 22.7, 14.1.

MS (ESI): *m/*z calcd for $C_{19}H_{31}NO_2$: 305.2; found: 306.2 $[M+H]^+$.

Synthesis of (±)-2,2-difluoro-3-hydroxy-*N*-phenyldodecanamide [(±)-233]

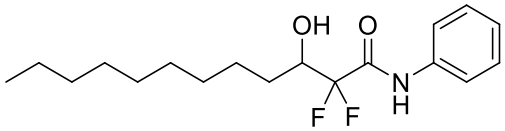

(±)-**233**

LiHMDS (1.07 mL, 1.0 M in THF) was added at 0 °C to a solution of (±)-**194** (100 mg, 0.356 mmol) and aniline (**205**) (48 µL, 0.534 mmol) in dry THF (7 mL). The reaction mixture was stirred at room temperature for 1 h, then it was quenched at 0 °C with sat. aq. NH_4Cl. EtOAc was added and the phases were separated. The organic phase was washed with 1 M aq. HCl, 5% aq. $NaHCO_3$, dried over anhydrous Na_2SO_4, filtered and the solvent was removed under vacuum. The crude product was purified by column chromatography on silica gel (*n*-hexane/EtOAc, 3:1) obtaining (±)-2,2-difluoro-3-hydroxy-*N*-phenyldodecanamide [(±)-**233**] as a white solid (90 mg, 78% yield).

R_f= 0.35 (*n*-hexane/EtOAc, 5:1).

^{1}H-NMR (400 MHz, $CDCl_3$): δ= 8.09 (bs, 1H), 7.56 (m, 2H), 7.37 (m, 2H), 7.20 (m, 1H), 4.25-4.12 (m, 1H), 2.66-2.55 (m, 1H), 1.66-1.53 (m, 2H), 1.46-1.19 (m, 14H), 0.88 (m, 3H).

^{13}C-NMR (100 MHz, $CDCl_3$): δ= 161.8 (t, J_{C-F}= 28.1 Hz), 135.8, 129.2, 125.7, 120.3, 115.6 (dd, J_{C-F}= 255.7, 258.6 Hz), 71.2 (dd, J_{C-F}= 25.5, 26.6 Hz), 31.9, 29.5, 29.4, 29.3, 29.3, 29.0 (m), 25.3, 22.7, 14.1.

^{19}F-NMR (376.45 MHz, $CDCl_3$): δ= - 113.3 (dd, J_{F-H}= 6.1 Hz, J_{F-F}= 261.3 Hz, 1F), - 122.1 (dd, J_{F-H}= 15.4 Hz, J_{F-F}= 261.3Hz, 1F).

^{19}F-CPD-NMR (376.45 MHz, $CDCl_3$): δ= - 113.3 (d, J_{F-F}= 261.3 Hz, 1F), - 122.1 (d, J_{F-F}= 261.3 Hz, 1F).

MS (ESI): *m/z* calcd for $C_{18}H_{27}F_2NO_2$: 327.2; found: 350.2 $[M+Na]^+$.

Synthesis of 2,2-difluoro-3-oxo-*N*-phenyldodecanamide (235)

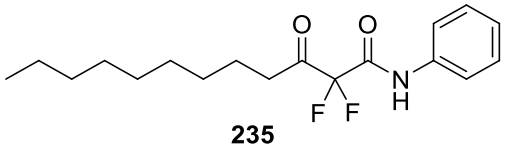

235

DMP (155 mg, 0.366 mmol) was added at 0 °C to a solution of (±)-**233** (60 mg, 0.183 mmol) in dry DCM (2 mL). The reaction mixture was stirred at room temperature for 30 min, then DCM was added and the reaction was quenched with sat. aq. $Na_2S_2O_3$ and phases were separated. The organic phase was washed with sat. aq. $NaHCO_3$, dried over anhydrous Na_2SO_4, filtered and the solvent was removed under vacuum. The crude product was purified by column chromatography on silica gel (*n*-hexane/EtOAc, 10:1 to 5:1) as eluent obtaining 2,2-difluoro-3-oxo-*N*-phenyldodecanamide (**235**) as a colourless solid (59 mg, quantitative yield) (m.p.= 106.2-107.0 °C).

R_f= 0.57 (*n*-hexane/EtOAc, 5:1).

^{1}H-NMR (400 MHz, $CDCl_3$): δ= 8.09 (bs, 1H), 7.55 (m, 2H), 7.36 (m, 2H), 7.20 (m, 2H), 2.84 (t, *J*= 7.2 Hz, 2H), 1.65 (qui, *J*= 7.2 Hz, 2H), 1.38-1.19 (m, 12H), 0.88 (m, 3H).

^{13}C-NMR (100 MHz, $CDCl_3$): δ= 198.9 (t, $J_{C\text{-}F}$= 27.0 Hz), 159.1 (t, $J_{C\text{-}F}$= 26.8 Hz), 135.6, 129.2, 126.0, 120.3, 109.2 (t, $J_{C\text{-}F}$= 265.3 Hz), 37.7, 31.8, 29.3, 29.2, 29.2, 28.8, 22.6, 22.4, 14.1.

^{19}F-NMR (376.45 MHz, $CDCl_3$): δ= - 114.5 (s, 2F).

MS (ESI): *m/z* calcd for $C_{18}H_{25}F_2NO_2$: 325.2; found: 348.1 $[M+Na]^+$.

HRMS (ESI): *m/z* calcd for $C_{18}H_{26}F_2NO_2^+$: 326.1929; found: 326.1926 (Δ= 0.9 ppm).

Synthesis of (±)-2,2-difluoro-3-hydroxy-*N*-(2,4,6-trimethoxyphenyl)dodecanamide [(±)-234]

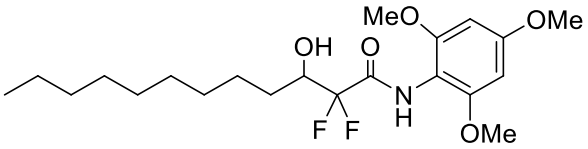

(±)-**234**

LiHMDS (800 µL, 1.0 M in THF) was added at 0 °C to a solution of (±)-**194** (75 mg, 0.267 mmol) and **189** (73 mg, 0.400 mmol) in dry THF (2.6 mL). The reaction mixture was stirred at room temperature for 1 h, then it was quenched at 0 °C with sat. aq. NH_4Cl. EtOAc was added and the phases were separated. The organic phase was washed with 2 M aq. HCl, 5% aq. $NaHCO_3$, dried over anhydrous Na_2SO_4, filtered and the solvent was removed under vacuum. The crude product was purified by column chromatography on silica gel (*n*-hexane/EtOAc, 1:1) obtaining (±)-2,2-difluoro-3-hydroxy-*N*-(2,4,6-trimethoxyphenyl)dodecanamide [(±)-**234**] as a brown waxy solid (85 mg, 77% yield).

R_f= 0.59 (*n*-hexane/EtOAc, 1:1).

^{1}H-NMR (400 MHz, $CDCl_3$): δ= 7.37 (bs, 1H), 6.16 (s, 2H), 4.18-4.05 (m, 1H), 3.81 (s, 9H), 2.72 (d, *J*= 5.8 Hz, 1H), 1.69-1.57 (m, 2H), 1.48-1.20 (m, 14H), 0.88 (m, 3H).

^{13}C-NMR (100 MHz, $CDCl_3$): δ= 162.7 (t, J_{C-F}= 27.8 Hz), 160.6, 156.1, 116.1 (t, J_{C-F}= 256.4 Hz), 104.9, 91.0, 71.6 (t, J_{C-F}= 25.7 Hz), 55.9, 55.5, 31.9, 29.6, 29.5, 29.3, 29.0, 25.4, 22.7, 14.1.

^{19}F-NMR (376.45 MHz, $CDCl_3$): δ = - 115.7 (dd, J_{F-H}= 8.3 Hz, J_{F-F}= 256.3 Hz, 1F), - 121.8 (dd, J_{F-H}= 14.4 Hz, J_{F-F}= 256.3 Hz, 1F).

^{19}F-CPD-NMR (376.45 MHz, $CDCl_3$): δ = - 115.7 (d, *J*= 256.3 Hz, 1F), - 121.8 (d, *J*= 256.3 Hz, 1F).

MS (ESI): *m/z* calcd for $C_{21}H_{33}F_2NO_5$: 417.2; found: 418.2 $[M+H]^+$.

HRMS (ESI): *m/z* calcd for $C_{21}H_{34}F_2NO_5^+$: 418.2400; found: 418.2395 (Δ= - 1.1 ppm).

Synthesis of 2,2-difluoro-3-oxo-*N*-(2,4,6-trimethoxyphenyl)dodecanamide (236)

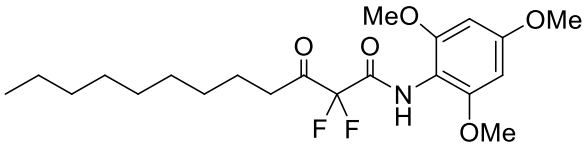

236

DMP (107 mg, 0.252 mmol) was added at 0 °C to a solution of (±)-**234** (70 mg, 0.168 mmol) in dry DCM (3.0 mL). The reaction mixture was stirred at room temperature for 30 min, then DCM was added and reaction was quenched with sat. aq. $Na_2S_2O_3$ and phases were separated. The organic phase was washed with sat. aq. $NaHCO_3$, dried over anhydrous Na_2SO_4, filtered and the solvent was removed under vacuum. The crude product was purified by column chromatography on silica gel (*n*-hexane/EtOAc, 6:4) obtaining 2,2-difluoro-3-oxo-*N*-(2,4,6-trimethoxyphenyl)dodecanamide (**236**) as a white solid (70 mg, quantitative yield).

R_f= 0.56 (*n*-hexane/EtOAc, 6:4).

^{1}H-NMR (400 MHz, $CDCl_3$): δ= 7.37 (bs, 1H), 6.12 (s, 2H), 3.78 (s, 3H), 3.78 (s, 6H), 2.82 (t, *J*= 7.2 Hz, 2H), 1.65 (qui, *J*= 7.2 Hz, 2H), 1.37-1.18 (m, 12H), 0.87 (m, 3H).

^{13}C-NMR (100 MHz, $CDCl_3$): δ= 198.1 (t, $J_{C\text{-}F}$= 26.3 Hz), 160.7, 159.7 (t, $J_{C\text{-}F}$= 26.8 Hz), 156.0, 109.8 (t, $J_{C\text{-}F}$= 263.8 Hz), 104.5, 90.9, 55.9, 55.5, 37.4, 31.8, 29.4, 29.3, 29.2, 28.8, 22.6, 22.5, 14.1.

^{19}F-NMR (376.45 MHz, $CDCl_3$): δ= - 115.3 (s, 2F).

MS (ESI): *m/z* calcd for $C_{21}H_{31}F_2NO_5$: 415.2; found: 416.2 $[M+H]^+$.

HRMS (ESI): *m/z* calcd for $C_{21}H_{32}F_2NO_5^+$: 416.2243; found: 416.2239 (Δ= - 1.0 ppm).

Synthesis of 2,2-difluoro-*N*-methyl-*N*-(2,4,6-trimethoxyphenyl)dodecanamide (237)

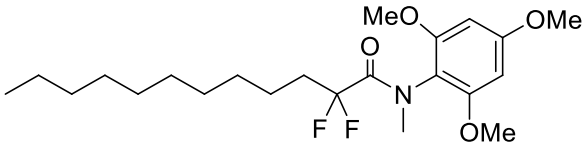

237

A solution of **185** (70 mg, 0.174 mmol) in dry THF (1.0 mL) was added at 0 °C to a suspension of NaH (15 mg, 60% in mineral oil, 0.348 mmol) in dry THF (1.0 mL). The reaction mixture was stirred at 0 °C for 30 min, then MeI (21.7 µL, 0.348 mmol) was added dropwise. The reaction mixture was stirred at room temperature overnight, then Et_2O was added, washed with water, dried over anhydrous Na_2SO_4, filtered and the solvent was removed under vacuum. The crude product was purified by column chromatography on silica gel (*n*-hexane/EtOAc, 3:1) as eluent obtaining 2,2-difluoro-*N*-methyl-*N*-(2,4,6-trimethoxyphenyl)dodecanamide (**237**) as a white solid (72 mg, quantitative yield) (m.p.= 86.4-87.1 °C).

R_f= 0.45 (*n*-hexane/EtOAc, 3:1).

^{1}H-NMR (400 MHz, $CDCl_3$): δ= 6.10 (s, 2H), 3.81 (s, 3H), 3.77 (s, 6H), 3.10 (s, 3H), 1.95-1.79 (m, 2H), 1.43-1.32 (m, 2H), 1.32-1.17 (m, 14H), 0.86 (m, 3H).

^{13}C-NMR (100 MHz, $CDCl_3$): δ= 165.3 (t, $J_{C\text{-}F}$= 28.0 Hz), 160.8, 157.0, 118.8 (t, $J_{C\text{-}F}$= 251.2 Hz), 113.0, 90.3, 55.7, 55.4, 37.2, 35.0 (t, $J_{C\text{-}F}$= 23.4 Hz), 31.9, 29.5, 29.5, 29.3, 29.3, 22.6, 21.5 (t, $J_{C\text{-}F}$= 4.2 Hz), 14.1.

^{19}F-NMR (376.45 MHz, $CDCl_3$): δ= - 102.2 (t, *J*= 17.4 Hz, 2F).

^{19}F-CPD-NMR (376.45 MHz, $CDCl_3$): δ= - 102.2 (s, 2F).

MS (ESI): *m/z* calcd for $C_{22}H_{35}F_2NO_4$: 415.2; found: 416.2 $[M+H]^+$.

HRMS (ESI): *m/z* calcd for $C_{22}H_{36}F_2NO_4^+$: 416.2607; found: 416.2600 (Δ= - 1.7 ppm).

Synthesis of *N*-benzyl-2,2-difluoro-*N*-(2,4,6-trimethoxyphenyl)dodecanamide (238)

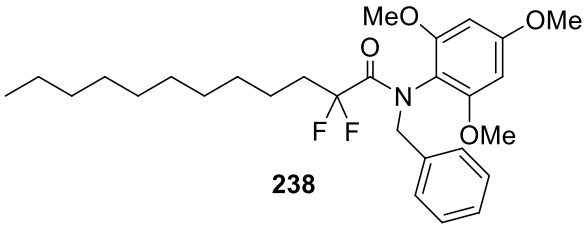

238

A solution of **185** (100 mg, 0.249 mmol) in dry THF (1 mL) was added at 0 °C to a suspension of NaH (20 mg, 60% in mineral oil, 0.498 mmol) in dry THF (2 mL) at 0 °C. The reaction mixture was stirred at 0 °C for 30 min, then benzyl bromide (59.2 µL, 0.498 mmol) was added dropwise. The reaction mixture was stirred at room temperature overnight, then Et_2O was added, washed with water, dried over anhydrous Na_2SO_4, filtered and the solvent was removed under vacuum. The crude product was purified by column chromatography on silica gel (*n*-hexane/EtOAc, 10:1 to 5:1) obtaining *N*-benzyl-2,2-difluoro-*N*-(2,4,6-trimethoxyphenyl)dodecanamide (**238**) as a colourless oil (114 mg, 93% yield).

R_f= 0.51 (*n*-hexane/EtOAc, 5:1).

^{1}H-NMR (400 MHz, $CDCl_3$): δ= 7.18 (m, 5H), 5.99 (s, 2H), 4.71 (s, 2H), 3.78 (s, 3H), 3.52 (s, 6H), 2.00-1.34 (m, 2H), 1.46-1.36 (m, 2H), 1.33-1.19 (m, 14H), 0.88 (m, 3H).

^{13}C-NMR (100 MHz, $CDCl_3$): δ= 165.5 (t, J_{C-F}= 27.9 Hz), 160.8, 157.2, 136.7, 129.9, 127.5, 127.2, 118.8 (t, J_{C-F}= 251.7 Hz), 111.2, 90.2, 55.3, 55.3, 53.4, 35.1 (t, J_{C-F}= 23.4 Hz), 31.9, 29.6, 29.5, 29.3, 29.3, 22.7, 21.5 (t, J_{C-F}= 4.0 Hz), 14.1.

^{19}F-NMR (376.45 MHz, $CDCl_3$): δ= - 102.3 (t, *J*= 17.4 Hz, 2F).

^{19}F-CPD-NMR (376.45 MHz, $CDCl_3$): δ= - 102.3 (s, 2F).

MS (ESI): *m/z* calcd for $C_{28}H_{39}F_2NO_4$: 491.3; found: 492.3 $[M+H]^+$.

HRMS (ESI): *m/z* calcd for $C_{28}H_{40}F_2NO_4^+$: 492.2920; found: 492.2915 (Δ= - 1.0 ppm).

Synthesis of (±)-ethyl 2,2-difluoro-3-hydroxy-3-phenylpropanoate [(±)-240]

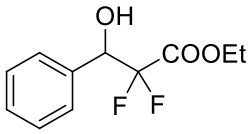

(±)-**240**

TMSCl (93.8 µL, 0.739 mmol) was added to a suspension of zinc dust (483 mg, 7.39 mmol) in dry THF (8 mL) and the reaction mixture was gently heated for 5 min. After stirring at room temperature for additional 15 min, benzaldehyde (**239**) (200 µL, 1.97 mmol) and ethyl bromodifluoroacetate (**193**) (631 µL, 4.92 mmol) were added. The reaction mixture was vigorously stirred at 55 °C until consumption of **193**, then it was quenched with sat. aq. NH_4Cl. EtOAc was added, the phases were separated and the aqueous phase was extracted with EtOAc. The pooled organic phases were washed with brine, dried over anhydrous Na_2SO_4, filtered and the solvent was removed under reduced pressure. The crude product was purified by column chromatography on silica gel (*n*-hexane/EtOAc, 5:1) obtaining (±)-ethyl 2,2-difluoro-3-hydroxy-3-phenylpropanoate [(±)-**240**] as a colourless oil (170 mg, 37% yield).

R_f= 0.24 (*n*-hexane/EtOAc, 5:1).

^{1}H-NMR (400 MHz, $CDCl_3$): δ= 7.47-7.42 (m, 2H), 7.42-7.37 (m, 3H), 5.17 (ddd, J_{H-H}= 5.3 Hz, J_{H-F}= 8.3, 15.7 Hz, 1H), 4.31 (q, *J*= 7.2 Hz, 2H), 2.69 (d, *J*= 5.3 Hz, 1H), 1.29 (t, *J*= 7.2 Hz, 3H).

^{13}C-NMR (100 MHz, $CDCl_3$): δ= 163.7 (t, J_{C-F}= 31.5 Hz), 134.6 (m), 129.2, 128.4, 127.8, 113.9 (dd, J_{C-F}= 252.7, 257.7 Hz), 73.7 (dd, J_{C-F}= 23.7, 27.5 Hz), 63.2, 13.7.

^{19}F-NMR (376.45 MHz, $CDCl_3$): δ= - 113.9 (dd, J_{F-H}= 8.3 Hz, J_{F-F} =278.6 Hz, 1F), - 120.3 (dd, J_{F-H}= 15.7 Hz, J_{F-F}= 278.6 Hz, 1F).

^{19}F-CPD-NMR (376.45 MHz, $CDCl_3$): δ= - 113.9 (d, J_{F-F}=278.6, 1F), - 120.3 (d, J_{F-F}= 278.6 Hz, 1F).

MS (ESI): *m/z* calcd for $C_{11}H_{12}F_2O_3$: 230.1; found: 253.1 $[M+Na]^+$.

Synthesis of (±)-ethyl 3-(1*H*-imidazole-1-carbonothioyloxy)-2,2-difluoro-3-phenylpropanoate [(±)-241]

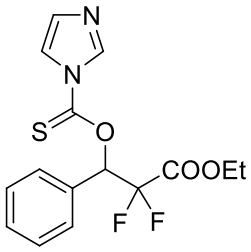

(±)-**241**

DMAP (9 mg, 73.8 μmol) and 1,1'-thiocarbonyldiimidazole (198 mg, 1.11 mmol) were added at 0 °C to a solution of (±)-**240** (170 mg, 0.738 mmol) in dry DCM (3.0 mL). The reaction mixture was stirred at room temperature for 1 h, then the solvent was removed under reduced pressure and the crude product was purified by column chromatography on silica gel (*n*-hexane/EtOAc, 3:1) obtaining (±)-ethyl 3-(1*H*-imidazole-1-carbonothioyloxy)-2,2-difluoro-3-phenylpropanoate [(±)-**241**] as a yellow oil (234 mg, 93% yield).

R_f= 0.27 (*n*-hexane/EtOAc, 3:1).

^{1}H-NMR (400 MHz, $CDCl_3$): δ= 8.37 (m, 1H), 7.65 (m, 1H), 7.47-7.42 (m, 2H), 7.42-7.37 (m, 3H), 7.05 (m, 1H), 6.81 (dd, J_{H-F}= 8.9, 14.4 Hz, 1H), 4.31-4.21 (m, 2H), 1.21 (t, *J*= 7.1 Hz, 3H).

^{13}C-NMR (100 MHz, $CDCl_3$): δ= 181.2, 161.9 (t, J_{C-F}= 31.0 Hz), 137.0, 131.3, 130.3, 129.5 (m), 128.8, 128.7, 118.0, 112.2 (dd, J_{C-F}= 254.1, 259.3 Hz), 80.7 (dd, J_{C-F}= 24.6, 29.6 Hz), 63.7, 13.8.

^{19}F-NMR (376.45 MHz, $CDCl_3$): δ= -113.2 (dd, J_{F-H}= 8.9 Hz, J_{F-F}=265.2 Hz, 1F), -115.7 (dd, J_{F-H}= 14.4 Hz, J_{F-F}= 265.2 Hz, 1H).

^{19}F-CPD-NMR (376.45 MHz, $CDCl_3$): δ= -113.2 (d, J_{F-F} =265.2 Hz, 1F), -115.7 (d, J_{F-F}= 265.2 Hz, 1H).

MS (ESI): *m/z* calcd for $C_{15}H_{14}F_2N_2O_3S$: 340.1; found: 341.0 $[M+H]^+$.

Synthesis of ethyl 2,2-difluoro-3-phenylpropanoate (242)

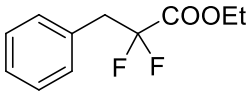

242

A solution of (±)-**241** (234 mg, 0.687 mmol) in dry toluene (2 mL) was added dropwise to a refluxing tributyltin hydride (370 µL, 1.37 mmol) solution in dry toluene (8 mL). The reaction was stirred under reflux for 1 h, then solvent was removed under reduced pressure. The crude product was purified by column chromatography on silica gel (*n*-hexane/EtOAc, 20:1 to 10:1) obtaining ethyl 2,2-difluoro-3-phenylpropanoate (**242**) as a colourless oil (40 mg, 27% yield).

R_f= 0.39 (*n*-hexane/EtOAc, 10:1).

^{1}H-NMR (400 MHz, $CDCl_3$): δ= 7.35-7.30 (m, 3H), 7.30-7.25 (m, 2H), 4.25 (q, *J*= 7.2 Hz, 2H), 3.39 (t, J_{H-F}= 16.5 Hz, 2H), 1.25 (t, *J*= 7.2 Hz, 3H).

^{13}C-NMR (100 MHz, $CDCl_3$): δ= 163.9 (t, J_{C-F}= 32.4 Hz), 130.7 (t, J_{C-F}= 4.3 Hz), 130.4, 128.5, 127.9, 115.4 (t, J_{C-F}= 250.4 Hz), 62.8, 41.0 (t, J_{C-F}= 23.6 Hz), 13.8.

^{19}F-NMR (376.45 MHz, $CDCl_3$): δ= - 104.6 (t, J_{F-H}= 16.5 Hz, 2F).

^{19}F-CPD-NMR (376.45 MHz, $CDCl_3$): δ= - 104.6 (s, 2F).

Synthesis of 2,2-difluoro-3-phenyl-*N*-(2,4,6-trimethoxyphenyl)propanamide (243)

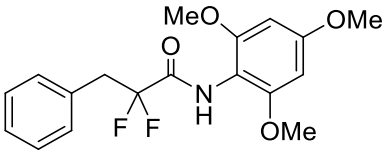

243

LiHMDS (280 µL, 1.0 M in THF) was added at 0 °C to a solution of **242** (40 mg, 0.187 mmol) and **189** (51 mg, 0.280 mmol) in dry THF (3.0 mL). The reaction mixture was stirred at room temperature for 1 h, then it was quenched at 0 °C with sat. aq. NH_4Cl. EtOAc was added and the phases were separated. The organic phase was washed with 2 M aq. HCl, 5% aq. $NaHCO_3$, dried over anhydrous Na_2SO_4, filtered and the solvent was removed under reduced pressure. The crude product was purified by column chromatography on silica gel (*n*-hexane/EtOAc, 1:1) obtaining 2,2-difluoro-3-phenyl-*N*-(2,4,6-trimethoxyphenyl)propanamide (**243**) as a white solid (53 mg, 80% yield) (m.p.= 124.1-125.3 °C).

R_f= 0.42 (*n*-hexane/EtOAc, 1:1).

^{1}H-NMR (400 MHz, $CDCl_3$): δ= 7.39-7.27 (m, 5H), 7.19 (bs, 1H), 6.11 (s, 2H), 3.78 (s, 3H), 3.73 (s, 6H), 3.50 (t, J_{H-F}= 16.8 Hz, 2H).

^{13}C-NMR (100 MHz, $CDCl_3$): δ= 162.4 (t, J_{C-F}= 27.9 Hz), 160.4, 156.1, 131.3 (t, J_{C-F}= 4.3 Hz), 130.8, 128.3, 127.5, 117.6 (t, J_{C-F}= 253.0 Hz), 105.1, 90.9, 55.9, 55.5, 40.4 (t, J_{C-F}= 23.9 Hz).

^{19}F-NMR (376.45 MHz, $CDCl_3$): δ= - 104.5 (dt, J_{F-H}= 2.4, 16.8 Hz, 2F).

^{19}F-CPD-NMR (376.45 MHz, $CDCl_3$): δ= - 104.5 (s, 2F).

MS (ESI): *m/z* calcd for $C_{18}H_{19}F_2NO_4$: 351.1; found: 352.1 $[M+H]^+$.

HRMS (ESI): *m/z* calcd for $C_{18}H_{20}F_2NO_4^+$: 352.1355; found: 352.1356 (Δ= 0.3 ppm).

12.3 Biology

***Chlamydia trachomatis* inclusion assay**

Chlamydia trachomatis L2 EBs were harvested from infected HeLa cell cultures at 37 °C with 5% CO_2, purified by discontinuous density gradient centrifugation in Renografin (Bracco Diagnostics, Princeton, NJ, USA), and titered for infectivity as measured by inclusion forming units (IFU). Cells were routinely cultivated at 37 °C with 5% CO_2 in RPMI media supplemented with 10% fetal bovine serum, 2 mM L-glutamine, and 10 μg/mL gentamicin (all from Invitrogen, Carlsbad, CA, USA). For infections, HeLa cells were plated to 85–90% confluence on 13 mm glass coverslips. On the following day, monolayers were inoculated with *C. trachomatis* serovar L2. Plates were centrifuged at 1500 rpm at 4 °C prior to a 30 min invasion step at 37 °C. Inoculum was decanted, cells were washed with PBS, and incubated for 24 h in 100 μM of the compound or the solvent DMSO (1% final concentration). The samples were fixed and permeabilized with ice-cold MeOH and stained with convalescent human sera for 2 h at room temperature, followed by staining with Alexa-594-conjugated mouse mAb anti-human IgG secondary antibody, phalloidin and DAPI for 1 h. The latter was used to visualise host cell nuclei to monitor cytotoxicity. Images were collected by fluorescence microscopy and processed using NIH ImageJ. [81]

Experimental procedures for the other assays are not reported in the present thesis because they were performed by other research groups, as indicated in the relative chapters.

13. Acknowledgments

Looking back at my PhD, I can really say that three years flew away, despite all the required energy. All the results I obtained would not be achieved without the support of several people that I want to briefly thank here.

First of all, Professor Carlo De Micheli, a wise guide in every situation, with the most appropriate words ready at the proper time (not only for chemistry). Thanks for always being a model and for establishing an equal relationship.

Thanks to Professor Paola Conti for letting me be part of these interesting projects and for creating an effective network of collaborations that allowed my work to aquire a wider scope. Thanks also for always trying to transmit me your experience in every aspect of this challenging work, despite your full agenda.

Thanks to Doctor Andrea Pinto for all the suggestions and for the support. Everyone needs a hint when facing troubles or some encouragement when problems sort out late in the evening. He knows that I have a lot of reasons to be greatful, but most of all I want to thank him for letting me walk my way with my own legs.

Thanks to Doctor Lucia Tamborini for all the kindly offered help. Especially, thanks for sustaining good ideas that jumped on my mind, even at the most umproper time (e.g. writing a review). It has been really important for my professional growth.

Thanks to Professor Matteo Zanda for hosting me in his amazing group and giving me the opportunity to follow a whole project working freely. The months I spent in Aberdeen have been fundamental for my career and for my life.

Thanks to Professor Rey Carabeo and his co-workers António Tedim Pedrosa and Ana Nogueira for the input for the project I followed at Aberdeen University and all the support for the biological side of the work.

Thanks to all the people that collaborated in these projects, in particular:
Professor Stefano Bruno, Professor Andrea Mozzarelli, Professor Donatella Taramelli and Doctor Silvia Parapini (*Pf*GAPDH project);
Doctor Roberta Ettari and Professor Tanja Schirmeister (*Tb*CatL project);
Professor Maria P. Costi, Professor William N. Hunter and Professor Anabela Cordeiro da Silva (*Tb*FolD project);
Professor Ettore Novellino and Professor Luciana Marinelli (computational studies, involved in different projects);
Dr. Leonardo Lo Presti (X-ray crystallography).

Although very exciting, the PhD absorbed most of my energies, my patience and my attention during the last three years. I am sure I have not always been the person I would like to be, so thanks to all the wonderful people that tolerated my bad moments, kept sharing happy moments with me (in the lab, having a sushi or a

beer, or hiking somewhere in Scotland), helped me overcoming the infinite obstacles of this job, and listened patiently to all my complaints (quite a few).
Firstly, many thanks to my family, especially to my beloved brother Valerio. Sometimes we can't stand each other, but it is important that you are by my side if I need you (as I do for you). Thanks also to my relatives (my grandmother Anna Maria above all) that constantly and quietly expressed all their appreciation and encouragement.

Thanks to my crazy friend Gero, the old good Dario, the tall and moustached Manuele, the sociable Fernando a.k.a. "Spagna", the beautiful Dr. Chiara, the living chemistry (and whisky) book Jimy, the kind and helpful Sergio, the always simple and smiling Samuele, the funny Monica, the coolest flatmate Patrick, the old and the young kind Federicas, the flashing red Silvia, the overtalking Jessica and his majesty Angelo.

Every people I met during this travel left me something precious, so thank you all (even if you are not mentioned here!) and I wish you can say the same about me.

Concluding, I have to make the most important acknowledgement. Thanks to all the difficulties that made me stronger, all the weird results that made me more curious and all the disappointments that made me insatiable.

14. References

[1] [Online]. Available: http://www.oxforddictionaries.com/definition/english/parasite.

[2] T. Cavalier-Smith, "A revised six-kingdom system of life," *Biological Reviews,* vol. 73, no. 3, pp. 203-266, 1998.

[3] [Online]. Available: http://www.who.int/neglected_diseases/diseases/en/.

[4] [Online]. Available: http://www.who.int/mediacentre/factsheets/fs094/en/.

[5] [Online]. Available: https://www.niaid.nih.gov/topics/Malaria/Pages/lifecycle.aspx.

[6] [Online]. Available: https://www.niaid.nih.gov/topics/Malaria/understandingMalaria/Pages/symptoms.aspx.

[7] L. Brunton, K. Parker, D. Blumenthal and I. Buxton, Goodman & Gilman. Le basi farmacologiche della terapia. Il manuale., McGraw-Hill, 2008.

[8] World Health Organization, "Malaria vaccine development," 29 January 2016. [Online]. Available: http://www.who.int/wer/2016/wer9104.pdf?ua=1. [Accessed 20 December 2016].

[9] World Health Organization, 2010. [Online]. Available: http://apps.who.int/iris/bitstream/10665/44449/1/9789241500470_eng.pdf.

[10] W. H. Organization, October 2016. [Online]. Available: http://apps.who.int/iris/bitstream/10665/250294/1/WHO-HTM-GMP-2016.11-eng.pdf?ua=1. [Accessed 27 October 2016].

[11] Nobelprize.org, "The 2015 Nobel Prize in Physiology or Medicine - Press Release," 2014. [Online]. Available: https://www.nobelprize.org/nobel_prizes/medicine/laureates/2015/press.html. [Accessed 23 October 2016].

[12] [Online]. Available: http://www.who.int/mediacentre/factsheets/fs259/en/.

[13] Drugs for Neglected Diseases initiative, August 2016. [Online]. Available: http://www.dndi.org/diseases-projects/portfolio/scyx-7158/. [Accessed 13th November 2016].

[14] Drug for Neglected Diseases initiative, August 2016. [Online]. Available: www.dndi.org/diseases-projects/portfolio/fexinidazole/. [Accessed 13th November 2016].

[15] World Health Organization, "WHO guidelines for the treatment of Chlamydia trachomatis," 2016. [Online]. Available: http://www.who.int/reproductivehealth/publications/rtis/chlamydia-treatment-guidelines/en/. [Accessed 21 11 2016].

[16] World Health Organization, "Trachoma fact sheet," July 2016. [Online]. Available: http://www.who.int/mediacentre/factsheets/fs382/en/. [Accessed 21 November 2016].

[17] T. A. Baillie, "Targeted covalent inhibitors for drug design," *Angew. Chem., Int. Ed.,* vol. 55, no. 43, pp. 13408-13421, 2016.

[18] R. A. Bauer, "Covalent inhibitors in drug discovery: from accidental discoveries to avoided liabilities and designed therapies," *Drug Discov. Today,* vol. 20, no. 9, pp. 1061-1073, 2015.

[19] R. Mah, J. R. Thomas and C. M. Shafer, "Drug discovery considerations in the development of covalent inhibitors," *Bioorg. Med. Chem. Lett.,* vol. 24, pp. 33-39, 2014.

[20] J. Singh, R. C. Petter, T. A. Baillie and A. Whitty, "The resurgence of covalent drugs," *Nat. Rev. Drug Discovery,* vol. 10, pp. 307-317, 2011.

[21] R. M. Miller, V. O. Paavilainen, S. Krishnan, I. M. Serafimova and J. Taunton, "Electrophilic fragment-based design of reversible covalent kinase inhibitors," *J. Am. Chem. Soc.,* vol. 135, pp. 5298-5301, 2013.

[22] I. M. Seramifova, M. A. Pufall, S. Krishnan, K. Duda, M. S. Cohen, R. L. Maglathlin, J. M. McGarland, R. M. Miller, M. Frödin and J. Taunton, "Reversible targeting of noncatalytic cysteines with chemically tuned electrophiles," *Nat. Chem. Biol.,* vol. 8, pp. 471-476, 2012.

[23] K. Katsuno, J. N. Burrows, K. Duncan, R. Hooft van Huijsduijnen, T. Kaneko, K. Kita, C. E. Mowbray, D. Schmatz, P. Warner and B. T. Slingsby, "Hit and lead criteria in drug discovery for infectious diseases of the developing world," *Nat. Rev. Drug Discovery,* vol. 14, no. 11, pp. 751-758, 2015.

[24] J. B. Baell and G. A. Holloway, "New substructure filters for removal of pan assay interference compounds (PAINS) from screening libraries and for their exclusion in bioassays," *J. Med. Chem.,* vol. 53, pp. 2719-2740, 2010.

[25] C. A. Lipinski, F. Lombardo, B. W. Dominy and P. J. Feeney, "Experimental and computational approaches to estimate solubility and permeability in drug discovery and development settings," *Adv. Drug Delivery Rev.,* vol. 46, pp. 3-26, 2001.

[26] K. Dalziel, N. V. McFerran and A. J. Wonacott, "Glyceraldehyde-3-phosphate dehydrogenase," *Phil. Trans. R. Soc. Lond. B,* vol. 293, pp. 105-118, 1981.

[27] M. J. Gardner, N. Hall, E. Fung, O. White, M. Berriman, R. W. Hyman, J. M. Carlton, A. Pain, K. N. Nelson, S. Bowman, I. T. Paulsen, K. James, J. A. Eisen, K. Rutherford, S. L. Salzberg, A. Craig, S. Kyes, M. Chan, V. Nene, S. J. Shallom, B. Suh, J. Peterson, S. Angiuoli, M. Pertea, J. Allen, J. Selengut, D. Haft, M. W. Mather, A. B. Vaidya, D. M. A. Martin, A. H. Fairlamb, M. J. Fraunholz, D. S. Roos, S. A. Ralph, G. I. McFadden, L. M. Cummings, M. G. Subramanian, C. Mungall, C. J. Venter, D. J. Carucci, S. L. Hoffman, C. Newbold, R. W. Davis, C. M. Fraser and B. Barrell, "Genome sequence of the human malaria parasite Plasmodium falciparum," *Nature,* vol. 419, pp. 498-511, 2002.

[28] G. S. Krasnov, A. A. Dmitriev and A. V. Snezhkina, "Deregulation of glycolysisin cancer: glyceraldehyde-3-phosphate dehydrogenase (GAPDH) as a therapeutic target," *Expert Opin. Ther. Targets,* vol. 17, no. 6, pp. 681-693, 2013.

[29] S. Ganapathy-Kanniappan, R. Kunjithapatham and J. Geschwind, "Glyceraldehyde-3-phosphate dehydrogenase: a promising target for molecular therapy in hepatocellular carcinoma," *Oncotarget,* vol. 3, no. 9, pp. 940-953, 2012.

[30] M. A. Sirover, "New insights into an old protein: the functional diversity of mammalian glyceraldehyde-3-phosphate dehydrogenase," *Biochim. Biophys. Acta,* vol. 1432, no. 2, pp. 159-194, 1999.

[31] J. Perez-Casal and A. A. Potter, "Glyceraldehyde-3-phosphate dehydrogenase as a suitable vaccine candidate for protection against bacterial and parasitic diseases," *Vaccine,* vol. 34, pp. 1012-1017, 2016.

[32] P. B. Sangolgi, C. Balaji, S. Dutta, N. Jindal and G. K. Jarori, "Cloning, expression,purification and characterization of Plasmodium spp. glyceraldehyde-3-phosphate dehydrogenase," *Protein expression purif.,* vol. 117, pp. 17-25, 2016.

[33] S. Cha, M. Kim, A. Pandey and M. Jacobs-Lorena, "Identification of GAPDH on the surface of Plasmodium sporozoites as a new candidae for targeting malaria liver invasion," *J. Exp. Med.,* 2016.

[34] M. A. Robien, J. Bosch, F. S. Buckner, W. C. E. Van Voorhis, E. A. Worthey, P. Myler, C. Mehlin, E. E. Boni, O. Kalyuzhniy, L. Anderson, A. Lauricella, S. Gulde, J. R. Luft, G. DeTitta, J. M. Caruthers, K. O. Hodgson, M. Soltis, F. Zucker, C. L. M. J. Verlinde, E. A. Merritt, L. W. Schoenfeld and W. G. J. Hol, "Crystal structure of glyceraldehyde-3-phosphate dehydrogensae from Plasmodium falciparum at 2.25 Å resolution reveals intriguing extra electron density in the active site," *Proteins: Struct., Funct., Bioinf.,* vol. 62, pp. 570-577, 2006.

[35] J. F. Satchell, R. L. Malby, C. S. Luo, A. Adisa, A. E. Alpyurek, N. Klonis, B. J. Smith, L. Tilley and P. M. Colman, "Structure of glyceraldehyde-3-phosphate dehydrogenase from Plasmodium falciparum," *Acta Cryst.,* vol. D61, pp. 1213-1221, 2005.

[36] J. Azevedo-Silva, O. Quieròs, F. Baltazar, S. Ulaszeski, A. Goffeau, Y. H. Ko, P. L. Pedersen, A. Preto and M. Casal, "The anticancer agent 3-bromopyruvate: a simple but powerful molecule taken from the lab to the bedside," *J. Bioenerg. Biomembr.,* vol. 48, pp. 349-362, 2016.

[37] A. Pinto, L. Tamborini, G. Cullia, P. Conti and C. De Micheli, "Inspired by nature: the 3-halo-4,5-dihydroisoxazole moiety as a novel molecular warhead for the design of covalent inhibitors," *ChemMedChem,* vol. 11, pp. 10-14.

[38] P. Conti, A. Pinto, P. E. Wong, L. L. Major, L. Tamborini, M. C. Iannuzzi, C. De Micheli, M. P. Barrett and T. K. Smith, "Synthesis and in vitro/in vivo evaluation of the antitrypanosomal activity of 3-bromoacivicin, a potent CTP synthetase inhibitor," *ChemMedChem,* vol. 6, pp. 329-333, 2011.

[39] L. Tamborini, A. Pinto, T. K. Smith, L. L. Major, M. C. Iannuzzi, S. Cosconati, L. Marinelli, E. Novellino, L. Lo Presti, P. E. Wong, M. P. Barrett, C. De Micheli and P. Conti, "Synthesis and biological evaluation of CTP synthetase inhibitors as potential agents for the treatment of African trypanosomiasis," *ChemMedChem,* vol. 7, pp. 1623-1634, 2012.

[40] J. S. Warmus, G. J. Dilley and A. I. Meyers, "A modified procedure for the preparation of 2,5-dihydropyrrole (3-pyrroline)," *J. Org. Chem.,* vol. 58, pp. 270-271, 1993.

[41] S. Bruno, A. Pinto, G. Paredi, L. Tamborini, C. De Micheli, V. La Pietra, L. Marinelli, E. Novellino, P. Conti and A. Mozzarelli, "Discovery of covalent inhibitors of glyceraldehyde-3-phosphate dehydrogenase, a target for the treatment of malaria," *J. Med. Chem.,* vol. 57, pp. 7465-7471, 2014.

[42] S. Bruno, M. Margiotta, A. Pinto, G. Cullia, P. Conti, C. De Micheli and A. Mozzarelli, "Selectivity of 3-bromo-isoxazoline inhibitors between human and Plasmodium falciparum glyceraldehyde 3-phosphate dehydrogenases," *Bioorg. Med. Chem.,* vol. 24, pp. 2654-2659, 2016.

[43] "ACE and JChem acidity and basicity calculator," [Online]. Available: https://epoch.uky.edu/ace/public/pKa.jsp. [Accessed 28 11 2016].

[44] ThermoFisher Scientific, "EZ-link pentylamine biotin," [Online]. Available: https://www.thermofisher.com/order/catalog/product/21345. [Accessed 28 11 2016].

[45] I. D. Kerr, P. Wu, R. Marion-Tsukamaki, Z. B. Mackey and L. S. Brinen, "Crystal structures of TbCatB and rhodesain, potential chemotherapeutic targets and major cysteine proteases of Trypanosoma brucei," *PLoS Negl. Trop. Dis.,* vol. 4, no. 6, p. e701, 2010.

[46] R. Ettari, S. Previti, L. Tamborini, G. Cullia, S. Grasso and M. Zappalà, "The inhibition of cysteine proteases rhodesain and TbCatB: a valuable approach to treat human African trypanosomiasis," *Mini-Rev. Med. Chem.,* 2016.

[47] R. Ettari, L. Tamborini, I. C. Angelo, N. Micale, A. Pinto, C. De Micheli and P. Conti, "Inhibition of rhodesain as a novel therapeutic modality for human African trypanosomiasis," *J. Med. Chem.,* vol. 56, no. 14, pp. 5637-5658, 2013.

[48] R. Ettari, A. Pinto, S. Previti, L. Tamborini, I. C. Angelo, V. La Pietra, L. Marinelli, E. Novellino, T. Schirmeister, M. Zappalà, S. Grasso, C. De Micheli and P. Conti, "Development of novel dipeptide-like rhodesain inhibitors containing the 3-bromoisoxazoline warhead in a constrained conformation," *Bioorg. Med. Chem.,* vol. 23, pp. 7053-7060, 2015.

[49] T. C. Eadsforth, A. Pinto, R. Luciani, L. Tamborini, G. Cullia, C. De Micheli, L. Marinelli, S. Cosconati, E. Novellino, L. Lo Presti, A. Cordeiro da Silva, P. Conti, W. N. Hunter and M. P. Costi, "Characterization of 2,4-diamino-6-oxo-1,6-dihydropyrimidin-5-yl ureido based inhibitors of Trypanosoma brucei FolD and testing for antiparasitic activity," *J. Med. Chem.,* vol. 58, no. 20, pp. 7938-7948, 2015.

[50] G. S. Ducker and J. D. Rabinowitz, "One-carbon metabolism in health and disease," *Cell Metab.,* vol. 25, no. 1, pp. 27-42, 2016.

[51] T. C. Eadsforth, M. Gardiner, F. V. Maluf, S. McElroy, D. James, J. Frearson, D. Gray and W. N. Hunter, "Assessment of Pseudomonas aeruginosa N5,N10-methylenetetrahydrofolate dehydrogenase-cyclohydrolase as a potential antibacterial drug target," *PLoS ONE,* vol. 7, no. 4, p. e35973, 2012.

[52] S. M. Murta, T. J. Vickers and D. A. B. S. M. Scott, "Methylene tetrahydrofolate dehydrogenase/cyclohydrolase and the synthesis of 10-CHO-THF are essential in Leishmania major," *Mol Microbiol.,* vol. 71, no. 6, pp. 1386-1401, 2009.

[53] A. Schmidt, H. Wu, R. E. MacKenzie, V. J. Chen, J. R. Bewly, J. E. Ray, J. E. Toth and M. Cygler, "Structures of three inhibitor complexes provide insight into the reaction mechanism of the human methylenetetrahydrofolate dehydrogenase/cyclohydrolase," *Biochemistry,* vol. 39, pp. 6325-6335, 2000.

[54] T. C. Eadsforth, F. V. Maluf and W. N. Hunter, "Acinetobacter baumanii FolD ligand complexes - potent inhibitors of folate metabolism and a re-evaluation of the structure of LY374571," *FEBS J.,* vol. 279, no. 23, pp. 4350-4360, 2012.

[55] S. P. Ouellette and R. A. Carabeo, "A functional slow recycling pathway of transferrin is required for growth of Chlamydia," *Front. Microbiol.,* vol. 1, 2010.

[56] B. D. Roth, C. J. Blankley, M. L. Hoefle, A. Holmes, W. H. Roark, B. K. Trivedi, A. D. Essenburg, K. A. Kieft, B. R. Krause and R. L. Stanfield, "Inhibitors of acyl-CoA:cholesterol acyltransferase. 1. Identification and structure-activity relationships of a novel series of fatty acid anilide hypocholesterolemic agents," *J. Med. Chem.,* vol. 35, no. 9, pp. 1609-1617, 1992.

[57] K. Chambers and W. J. Brown, "Characterization of a novel CI-976-sensitive lysophospholipid acyltransferase that is associated with the Golgi complex," *Biochem. Biophys. Res. Commun.,* vol. 313, pp. 681-686, 2004.

[58] D. Hollenback, L. Bonham, L. Law, E. Rossnagle, L. Romero, H. Carew, C. K. Tompkins, D. W. Leung, J. W. Singer and T. White, "Substrate specificity of lysophosphatidic acid acyltransferase β-evidence from membrane and whole cell assays," *J. Lipid Res.,* vol. 47, pp. 593-604, 2007.

[59] H. Shindou and T. Shimizu, "Acyl-CoA:lysophospholipid acyltransferases," *J. Biol. Chem.,* vol. 284, no. 1, pp. 1-5, 2009.

[60] K. Chambers, B. Judson and W. J. Brown, "A unique lysophospholipid acyltransferase (LPAT) antagonist, CI-976, affects secretory and endocytic membrane trafficking pathways," *J. Cell Sci.,* vol. 118, pp. 3061-3071, 2005.

[61] F. G. Glansdorp, G. L. Thomas, J. K. Lee, J. M. Dutton, G. P. C. Salmond, M. Welch and D. R. Spring, "Synthesis and stability of small molecule probes for Pseudomonas aeruginosa quorum sensing modulation," *Org. Biomol. Chem.,* vol. 2, pp. 3329-3336, 2004.

[62] H. W. Pinnick, Y. Chang, S. Foster and M. Govidan, "Reaction of ethyl cyclopropanecarboxylate with base," *J. Org. Chem.,* vol. 45, pp. 4505-4507, 1980.

[63] J. Coleman, "Characterization of Escherichia coli cells deficient in 1-acyl-sn-glycerol-3-phosphate acyltransferase activity," *J. Biol. Chem.,* vol. 265, no. 28, pp. 17215-17221, 1990.

[64] T. Hideshima, D. Chauhan, T. Hayashi, K. Podar, M. Akiyama, C. Mitsiades, N. Mitsiades, B. Gong, L. Bonham, P. de Vries, N. Munshi, P. G. Richardson, J. W. Singer and K. C. Anderson, "Antitumor activity of lysophosphatidic acid acyltransferase-β inhibitors, a novel class of agents, in multiple myeloma," *Cancer Res.,* vol. 63, pp. 8428-8436, 2003.

[65] D. M. Vyas, Y. Chiang and T. W. Doyle, "A short, efficient total synthesis of (±) acivicin and (±) bromo-acivicin," *Tetrahedron Lett.,* vol. 25, no. 5, pp. 487-490, 1984.

[66] M. C. Myers, J. Wang, J. A. Iera, J. Bang, T. Hara, S. Saito, G. P. Zambetti and D. H. Appella, "A new family of small molecules to probe the reactivation of mutant p53," *J. Am. Chem. Soc.,* vol. 127, no. 17, pp. 6152-6153, 2005.

[67] H. Konno, Y. Takebayashi, K. Nosaka and K. Akaji, "Synthetic studies on callipeltins: stereoselective syntheses of (3S,4R)-3,4-dimethyl-L-pyroglutamic acid and FMOC-D-allothreonine from serine derivatives," *Heterocycles,* vol. 81, no. 1, pp. 79-89, 2010.

[68] T. J. Hoffman, A. Kolleth, J. H. Rigby, S. Arseniyadis and J. Cossy, "Stereoselective synthesis of the C1-C11 and C12-C34 fragments of mycalolide A," *Org. Lett.,* vol. 12, no. 15, pp. 3348-3351, 2010.

[69] R. N. Daniels, B. J. Melancon, E. A. Wang, B. C. Crews, L. J. Marnett, G. A. Sulikowski and C. W. Lindsley, "Progress toward the total synthesis of lucentamycin A: total synthesis and biological evaluation of 8-epi-lucentamycin A," *J. Org. Chem.,* vol. 74, no. 22, p. 8852–8855, 2009.

[70] B. M. Trost, B. M. O'Boyle, W. Torres and M. K. Ameriks, "Development of a flexible strategy towards FR900482 and the mitomycins," *Chem. - Eur. J.,* vol. 17, no. 28, pp. 7890-7903, 2011.

[71] M. De Amici, C. De Micheli and V. Misani, "Nitrile oxides in medicinal chemistry-2. Synthesis of the two enantiomers of dihydromuscimol," *Tetrahedron,* vol. 46, no. 6, pp. 1975-1986, 1990.

[72] P. Conti, M. De Amici, A. Pinto, L. Tamborini, G. Grazioso, B. Frølund, C. Thomsen, B. Ebert and C. De Micheli, "Synthesis of 3-hydroxy- and 3-carboxy-Δ2-isoxazoline amino acids and evaluation of their interaction with GABA receptors and transporters," *Eur. J. Org. Chem.,* no. 24, pp. 5533-5542, 2006.

[73] R. N. Das, K. Sarma, M. G. Pathak and A. Goswami, "Silica-supported KHSO4: an efficient system for activation of aromatic terminal olefins," *Synlett,* no. 19, pp. 2908-2912, 2010.

[74] S. E. Denmark and C. R. Butler, “Vinylation of aryl bromides using an inexpensive vinylpolysiloxane,” *Org. Lett.,* vol. 8, no. 1, pp. 63-66, 2006.

[75] M. Girardin, P. G. Alsabeh, S. Lauzon, S. J. Dolman, S. G. Ouellet and G. Hughes, “Synthesis of 3-aminoisoxazoles via the addition−alimination of amines on 3-bromoisoxazolines,” *Org. Lett.,* vol. 11, no. 5, pp. 1159-1162, 2009.

[76] L. A. Carpino, “A new synthesis of unsaturated acids. I. α,β-Acetylenic acids,” *J. Am. Chem. Soc.,* vol. 80, pp. 599-601, 1958.

[77] M. Goodman, E. E. Schmitt and D. A. Yphantis, “Conformational aspects of polypeptides. III. Synthesis of oligomeric peptides derived from γ-methyl glutamate,” *J. Am. Chem. Soc.,* vol. 84, pp. 1283-1288, 1962.

[78] L. S. Fowler, D. Ellis and A. Sutherland, “Synthesis of fluorescent enone derived α-amino acids,” *Org. Biomol. Chem.,* vol. 7, no. 20, pp. 4309-4316, 2009.

[79] F. J. Dekker, M. Ghizzoni, N. van der Meer, R. Wisastra and H. J. Haisma, “Inhibition of the PCAF histone acetyl transferase and cell proliferation by isothiazolones,” *Bioorg. Med. Chem.,* vol. 17, no. 2, pp. 460-466, 2009.

[80] K. S. Keshavamurthy, Y. D. Vankar and D. N. Dhar, “Preparation of acid anhydrides, amides, and esters using chlorosulfonyl isocyanate as a dehydrating agent,” *Synthesis,* no. 6, pp. 506-508, 1982.

[81] NIH, “Image J,” [Online]. Available: https://imagej.nih.gov/ij/.